(2)

NAVAL POSTGRADUATE SCHOOL
Monterey, California

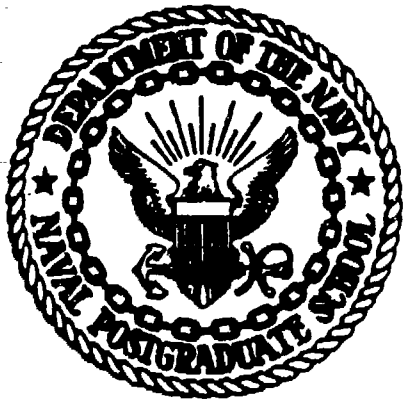

THESIS

INVESTIGATION OF USING THE WALSH TRANSFORM FOR DEINTERLEAVING SIMULATED ESM RECEIVER OUTPUT

by

Larry Wayne Ward

December 1983

Thesis Advisor: L. W. Wilson

Approved for Public Release, Distribution Unlimited

SECURITY CLASSIFICATION OF THIS PAGE (When Data Entered)

REPORT DOCUMENTATION PAGE		READ INSTRUCTIONS BEFORE COMPLETING FORM
1. REPORT NUMBER	2. GOVT ACCESSION NO. AD-A140 044	3. RECIPIENT'S CATALOG NUMBER
4. TITLE (and Subtitle) Investigation of Using the Walsh Transform for Deinterleaving Simulated ESM Receiver Output		5. TYPE OF REPORT & PERIOD COVERED Master's Thesis; December 1983
		6. PERFORMING ORG. REPORT NUMBER
7. AUTHOR(s) Larry Wayne Ward		8. CONTRACT OR GRANT NUMBER(s)
9. PERFORMING ORGANIZATION NAME AND ADDRESS Naval Postgraduate School Monterey, California 93943		10. PROGRAM ELEMENT, PROJECT, TASK AREA & WORK UNIT NUMBERS
11. CONTROLLING OFFICE NAME AND ADDRESS Naval Postgraduate School Monterey, California 93943		12. REPORT DATE December 1983
		13. NUMBER OF PAGES 229
14. MONITORING AGENCY NAME & ADDRESS(if different from Controlling Office)		15. SECURITY CLASS. (of this report)
		15a. DECLASSIFICATION/DOWNGRADING SCHEDULE

16. DISTRIBUTION STATEMENT (of this Report)

Approved for public release; distribution unlimited

17. DISTRIBUTION STATEMENT (of the abstract entered in Block 20, if different from Report)

18. SUPPLEMENTARY NOTES

19. KEY WORDS (Continue on reverse side if necessary and identify by block number)

Deinterleaving, Walsh Transform, ESM receiver

20. ABSTRACT (Continue on reverse side if necessary and identify by block number)

The Walsh Transform is investigated for its usefulness in deinterleaving the interleaved pulse stream presented to a preprocessor by an ESM receiver. After background chapters on a typical ESM system and the theory and characteristics of the Walsh Functions, a number representation of the pulse stream is described. Fast Walsh Transform and

DD FORM 1 JAN 73 1473 EDITION OF 1 NOV 65 IS OBSOLETE

S/N 0102-LF-014-6601

SECURITY CLASSIFICATION OF THIS PAGE (When Data Entered)

Block 20 Contd.

Power Spectral Densities of the pulse representations are computed and analyzed for features that could be used to recognize individual pulse trains in the interleaved representation.

Approved for public release, distribution unlimited

Investigation of Using the Walsh Transform for Deinterleaving Simulated ESM Receiver Output

by

Larry Wayne Ward
Lieutenant Commander, United States Naval Reserve
B.S., North Carolina State University, 1975

Submitted in partial fulfillment of the
requirements for the degree of

MASTER OF SCIENCE IN ELECTRICAL ENGINEERING

from the

NAVAL POSTGRADUATE SCHOOL
December, 1983

Author: Larry W. Ward

Approved by: Ronnie A. Wilson
Thesis Advisor

John M. Borsky
Second Reader

Chairman, Department of Electrical Engineering

J. M. Dyer
Dean of Science and Engineering

(Electronic Warfare Support Measures)

ABSTRACT

The Walsh Transform is investigated for its usefulness in deinterleaving the interleaved pulse stream presented to a preprocessor by an ESM receiver. After background chapters on a typical ESM system and the theory and characteristics of the Walsh Functions, a number representation of the pulse stream is described. Fast Walsh Transforms and Power Spectral Densities of the pulse representations are computed and analyzed for features that could be used to recognize individual pulse trains in the interleaved representation.

TABLE OF CONTENTS

LIST OF TABLES

LIST OF FIGURES

ACKNOWLEDGMENT

The perception and insight of Dr. Lonnie A. Wilson is sincerely acknowledged in advancing this thesis topic to me. His guidance and counseling provided the path that led to its completion.

Another NPGS Professor, Alex Gerba, provided a seemingly interested ear during a particular time in this course of instruction. He simply listened when it was needed.

Finally, this thesis could not have been completed without the interminable prodding and understanding of my wife, Sue.

I. INTRODUCTION

On a June night in 1940, a lone ANSON aircraft flew a solitary path through the skies of East Anglia, England. The wireless operator was listening for traces of signals propagating through the dark space around the aircraft. Near an important military target, a signal came through loud and clear in his earphones. First, a series of dots at the rate of sixty per minute. Then, as the ANSON droned onward, the dots disappeared into a steady tone. A little later, the steady tone broke up into a series of dashes, at the rate of sixty per minute.

This signal, known as a Lorentz beam, was transmitted from Germany and it posed a considerable threat to the high value military target. The signal was really composed of two beams, one beam of dots, and one beam of dashes, shown in Figure 1.1. By using the reception of the dots and dashes as an indication of whether they were on course, German bombers could navigate to their targets. The phasing of the dots and dashes was such that they combined into one steady tone in the overlap. Receipt of the steady tone meant the aircraft was on the course laid down by the transmitting site and receipt of dots or dashes meant the bomber was right or left of the beam overlap. With that information, the bomber crews could easily get back on course and perform their mission. [1]

The beams were ultimately countered by the British using a variety of methods, but the invaluable intelligence gained by the ANSON bomber over East Anglia was only the beginning of a wartime effort that was to save thousands of lives, both civilian and military. That brave and skillful act has been repeated hundreds of times since, in a "police action" and an undeclared war, but the priceless results have been the same, that of saving lives.

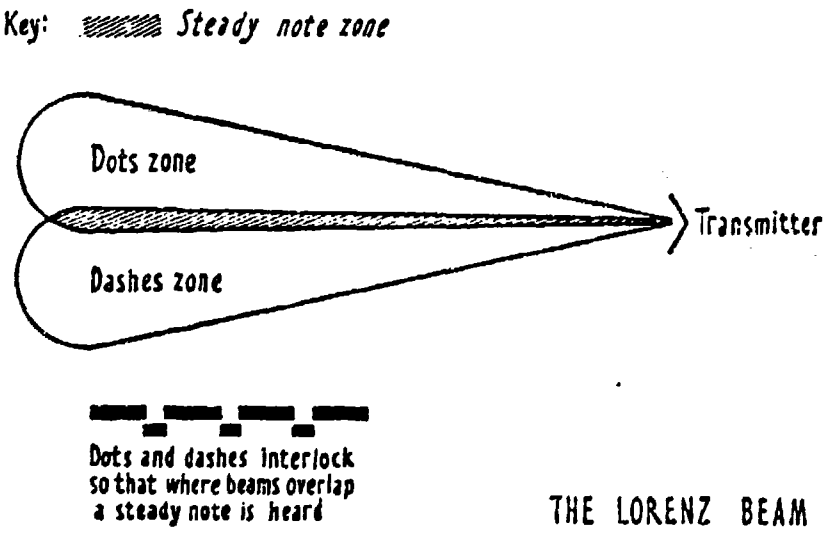

Figure 1.1. The Lorentz Beam

Since the arrival of the first electronic transmitter and receiver, man has been listening to his own radiations for communications, pleasure, and information. World War II, however, brought a new maturity to listening to his own radiations. Now he was listening to an opponent's transmissions to derive and use information about them.

About 1969, the term Electronic Support Measures (ESM) was coined [2: p.57] and now reflects the important business of obtaining and using information gained on the electromagnetic radiations of another. The alert operator aboard the lone British aircraft used his early and undefined ESM receiver to obtain knowledge that was used against the German transmitters.

A. THE ELECTRONIC WARFARE (EW) ENVIRONMENT

Of all the sensors that an enemy might use, the most important, at least as an electronic threat, is radar. This sensor is almost always the long and short range eyes and ears of the opposing force, and denial of its use gives a strategic and tactical advantage to the person capable of doing so. [2: p.7]

Consider the case of a penetrating bomber. In order to jam, deceive, or otherwise negate the effectiveness of the radars of the defense system, emissions must be detected, analyzed, and classified as to their threat. In this endeavor, the ESM receivers being used will not lack for electromagnetic sources to perform their analyses. Early warning, target detection, acquisition, and tracking, or even missile and interceptor guidance and control radars will paint the aircraft with an invisible illumination.

These electromagnetic energies will be of many frequencies, antenna scans, pulse shapes, and modulations, and even though radar systems are well understood and sometimes

easily countered, the sheer numbers and types of received signals will tax the capabilities of the ESM system.

As the bomber nears the target, the signal densities will soar because the defense is toughest close to the target. For instance, it has been reported that over 100 SAM sites were once located on the Egyptian side of the Suez Canal. As each battery transmits several signals, easily 300-500 signals could be found from this one class of weapon. When communication and radio location signals are added, the signal density problem is even further complicated. [2: pp.27-33]

Quite easily, the combat EW environment that the bomber is in will reach 500,000 pulses per second. [3: p.54]

Figure 1.2 [4] gives an indication of the pulse densities the bomber might encounter. The pulse density is dependent upon both system sensitivity and platform altitude but is not uniformly dependent on these parameters. At low sensitivities (-20 to -70 dBm) pulse density varies mostly with sensitivity and not with altitude. At high sensitivity (>-100 dBm) pulse density is almost totally altitude dependent.

The identification of various emitters and the evaluation of the possible threats they pose to the aircraft requires the sorting of these pulses. This separating or deinterleaving of signals is a difficult problem that is discussed in Chapter II.

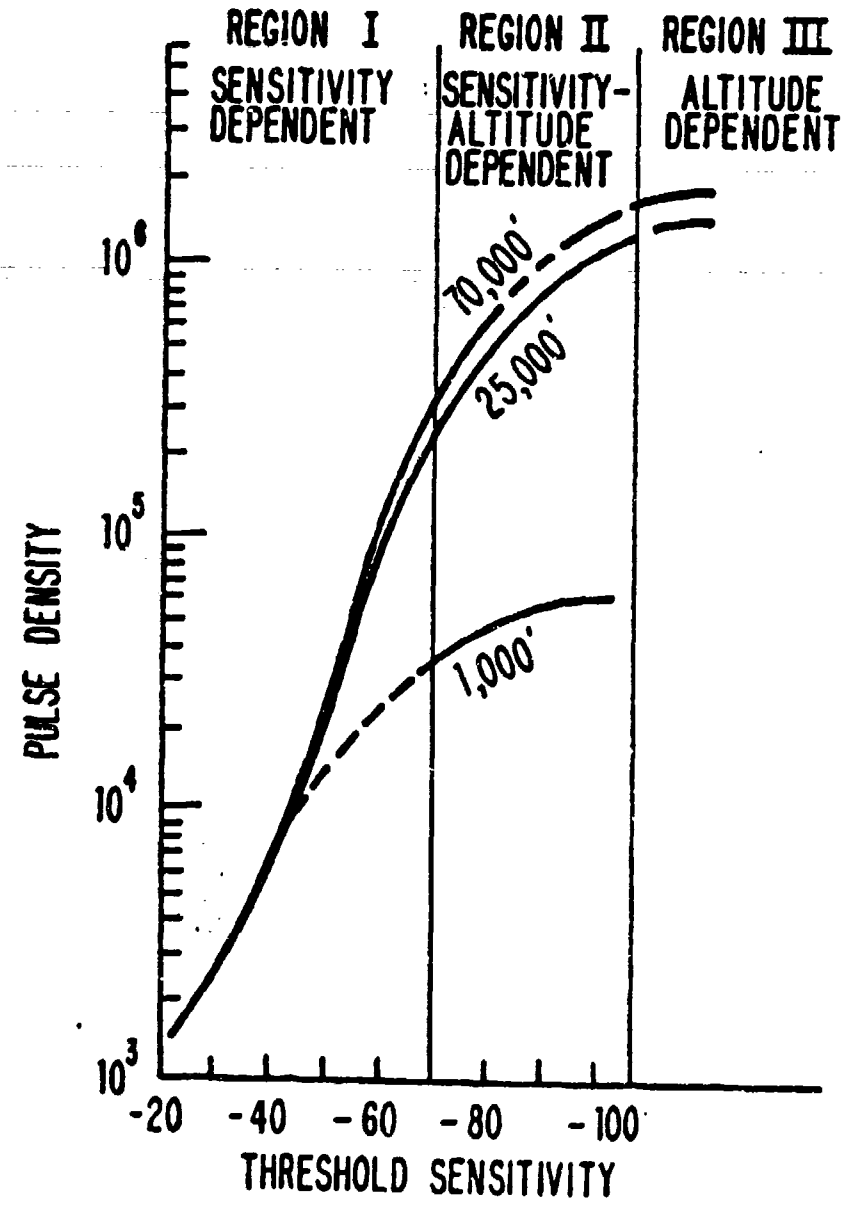

Figure 1.2. Pulse Density vs. Sensitivity and Altitude.

B. ELECTRONIC WARFARE SUPPORT MEASURES (ESM)

The broad term Electronic Warfare (EW), or sometimes referred to as Electromagnetic Warfare (EMW), is used to denote military actions that involve the friendly exploitation of the electromagnetic spectrum and the prevention of hostile use of the electromagetic spectrum. It should be realized that the electromagnetic spectrum covers from zero frequency to the infinite frequency, which includes the optical, infrared, and laser frequencies. [5] Coverage of these additions to the RF spectrum adds considerably to the problem.

EW may be divided into three major divisions:

1. Electronic Warfare Support Measures (ESM)
2. Electronic Counter Measures (ECM)
3. Electronic Counter Counter Measures (ECCM)

Electronic Support Measures, the usual shortened form of Electronic Warfare Support Measures, will be defined shortly. ECM, quite briefly, is the generation of intentional electronic interference between electronic systems for a useful purpose. ECCM , also quite briefly, is action taken to counter the detrimental effects of the opponent's ECM. [6: p.1]

This section will deal only with the ESM arena.

1. A Definition of ESM

Consider a specific definition of ESM. ESM is:

> That division of Electronics Warfare involving actions to search for, intercept, locate, record, and analyze radiated electromagnetic energy for the purpose of exploiting such radiations in support of military operations. [7: p.6]

This definition carries an underlying statement: ESM is the source of information required to carry out the other Electronic Warfare divisions as well as threat detection, warning, avoidance, target acquisition, and homing. [4: pp.3-6] In addition, by examining the individual actions specified in the definition we can gain further insight into the ESM arena.

The search for and interception of electromagnetic radiations is simply a basic part of the ESM mission. The intercepted signal must be analyzed and a determination made of its character, parameters, and location. Locating the emitter is usually a function for direction finding antennas. Recording of the signal, certainly the parameters, is usually done simultaneously with the analysis. On some missions a recording is made of the signal for postflight analysis with a mimimum of information being displayed to the operator in real time. Generally it is desired to produce this information from an ESM system with an inherent automatic processing capability that detects, classifies, and flashes a warning if need be. [2: p.36]

The information that the ESM mission provides ranges from that collected with regularly scheduled and dedicated collection excursions to debriefs of crews after completion of a routine patrol mission. To a tactical commander, this information is more extensive and useful than plain intelligence. It provides the precise state of the electronic

defense, including technical characteristics and emitter location, and becomes part of mission preflight briefings.

In obvious fact, radars not transmitting are radars that can't be intercepted and analyzed. Thus, if there are no transmissions from specific desired radars, or any at all, tactics that might provoke them into radiating are viable in the ESM scenario. Indeed, this action is included in the basic rules for Electronic Reconnaissance. [2: p.65]

2. The Role of ESM in Electronic Warfare

In general, ESM is passive electronic warfare, ECM is active electronic warfare, and ECCM may be either. These distinctions may not be clear cut, however. ESM may involve the radiation of a signal to determine the characteristics or electronic reaction of enemy equipment. ECM may involve the passive reception of enemy signals in order to decide which one to counter [2: p.3]. The latter could be the use of a tactical ESM system integrated with an ECM system for platform protection. The relationships between ESM, ECM, and ECCM are shown in Figure 1.3. [2: p.2]

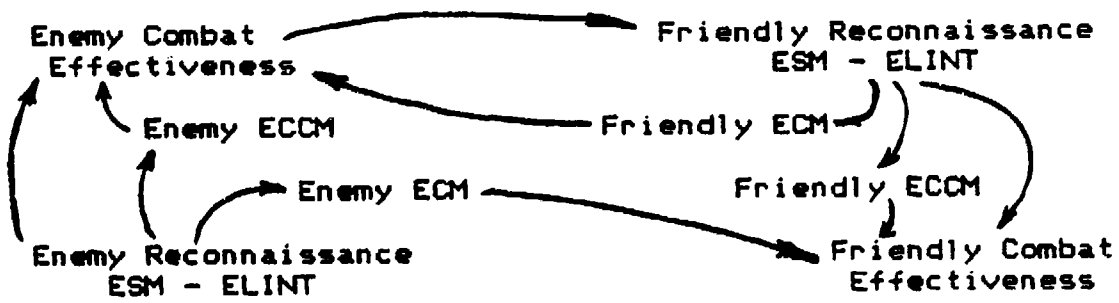

Figure 1.3. The Interactions of EW

The previous consideration of the penetrating bomber can be continued in the context of ESM's role in electronic warfare.

The bomber will almost surely face an integrated defense network. It is absolutely essential to know beforehand the technical characteristics and location of the electronic defense that will be used against the bomber. Some kind of electronic reconnaissance information is needed in order to maximize the effectiveness of ECM and ECCM equipment. Electronic intelligence (ELINT) and ESM are our sources of information.

The value of the knowledge gained from electronic reconnaissance of the defense system is proportional to its currency. The use of information from electronic intelligence which was gained from many sources and over a longer period of time is important, but the immediate needs of the tactical commander are met using ESM. This information is collected in the hours before takeoff, undergoes minimal analysis, and is used for mission planning. [2: p.37] Thus, ESM is electronic reconnaissance to determine the present state of the defense system.

ELINT, which has been subjected to extensive analysis, has been used to design and develop the ECM suite of the bomber. But the tactical commander still uses ESM to plan and accomplish the mission. Though they may share a common collection platform, the difference between them can be seen

in their operational control, end use, and time or duration of collection. ESM is used by the tactical commander today, and ELINT goes to the rear echelon for further study. [2: p.74]

Figure 1.4 [8] shows the operational role of ESM in electronic warfare. Note the central position of ESM as it "feeds" both ECM and ECCM and operational readiness.

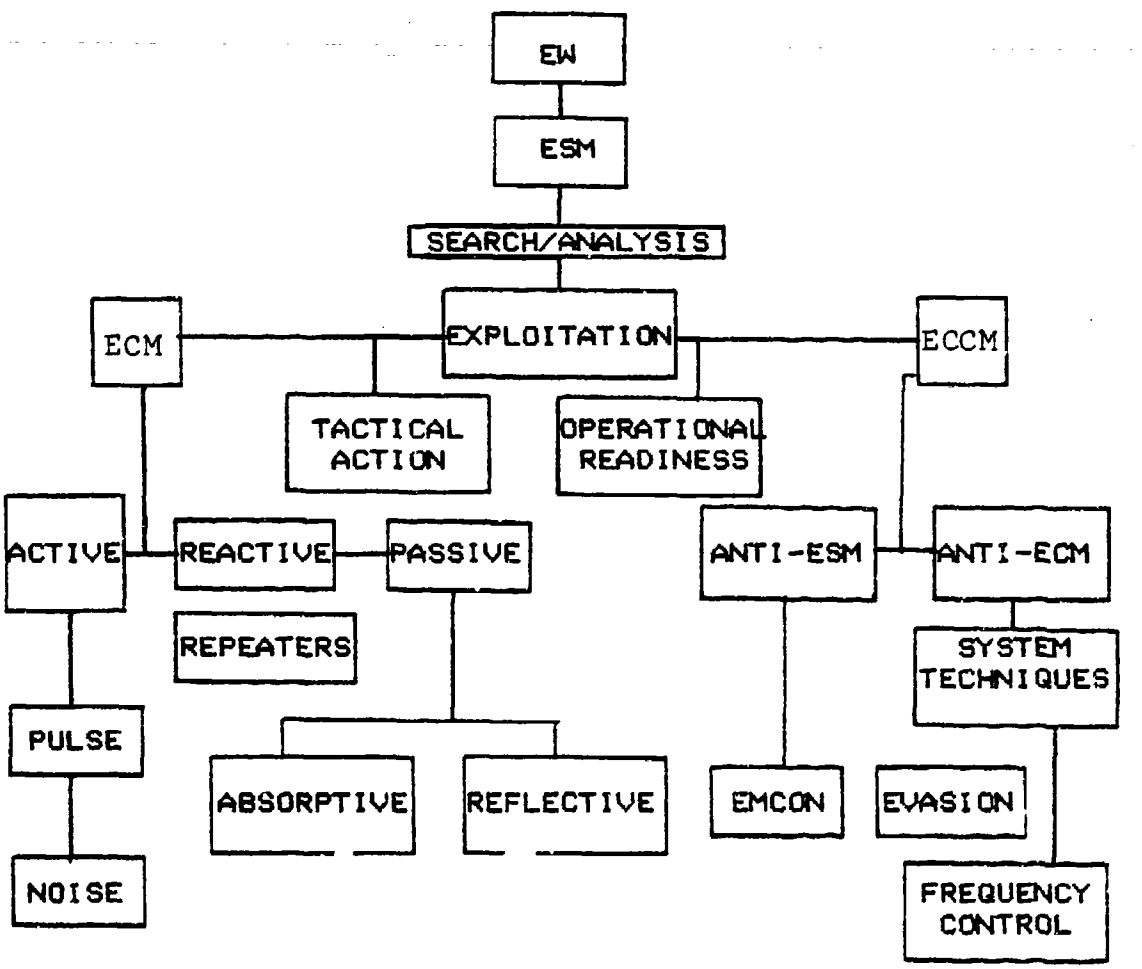

Figure 1.4. Operational Relationships in EW

C. SUMMARY

The previous sections only touch upon the vast nature of EW and ESM. They provide a general groundwork for understanding the purpose of using ESM and its role in the electromagnetic conflict.

This conflict is extremely important. New and modern weapon systems depend upon victory in the electromagnetic conflict as a prerequisite for victory in battle. [2: p.1]

Underscoring this premise are new policies and procedures by the Defense Department which will accelerate development and introduction of electronic warfare systems. The rapid escalation and introduction of new Soviet radars places current EW sytems at a disadvantage, especially in countering fire control and missile guidance radars. [9]

The future probably holds a greater integration of ESM (certainly tactical ESM) and ECM systems, with design for military aircraft leading the way. Already systems that combine ECM capability with passive warning equipment for aircraft are being sought by many NATO nations, such as the British Royal Air Force [10], the Belgian Air Force [11], as well as the United States Air Force [12]. In addition, and with considerable impact on system design, a trend toward carrying these systems internally rather than in pods hung underneath the aircraft seems to be evident [10 and 12].

In the hardware area, the use of embedded computers and microprocessors with high use of VHSIC technology will become

prevalent, along with all of the ramifications of computer use. The sophisticated signal processing needs of EW will have to be met, with verifiable, reliable, maintainable software, and the development of high capacity, non-volatile data storage. [13]

Upcoming and foreseeable developments are EW systems for space applications [2: pp.171-178]. All of the unique environmental conditions of space will generate new and different challenges for ECM and ECCM. These must be met in order for manned space stations and satellites to survive.

D. SCOPE OF THESIS

After these introductory sections Chapter II examines some of the system design requirements of an ESM system. The various components are looked at in some detail. Signal processing is addressed, beginning with basic parameter measurement, and ending with a discussion of our basic problem, that of deinterleaving received pulse trains.

The attack on the problem begins in Chapter III, with a discussion of the theory of Walsh and Rademacher Functions. Application of this theory is carried out in Chapter IV, where the Walsh transform is used on the deinterleaving problem. Finally, conclusions are developed, and listings of the programs used are given in order that follow on work can be done.

The attack on the problem using the Walsh Transform will begin with basic examples and proceed with an application of

the transform directly to an interleaved pulse train. The goal is to determine whether the Walsh Transform outputs a unique feature that can be used in a deinterleaving algorithm.

The radar pulses can be represented by time of arrival (TOA) tags, which are output by the ESM receiver to the preprocessor. A TOA tag can be thought of as merely a "mark" in time that indicates the receipt of a pulse. The stream of incoming pulses forms a string of TOA TAG's. The Transform is applied to the TOA tag string.

The Walsh Transform is easily applied to binary or two level functions, and some promise is held for its use in a deinterleaving algorithm if a PRI/PRF recognition feature exists in the transform.

With the speed and ease of computation of the Walsh Transform, a processor based on these functions should be fast and simple. Consider the programs used to compute the Walsh transforms in this thesis. They were originally written in FORTRAN, and were easily converted to BASIC for use in this thesis.

This simple, easy to use language normally brings a response that would question the use of such an "elementary" language. That response is misinformed.

BASIC is easy to learn, and easy to use. It performs well when compared to other structured languages, and has excellent mathematical and scientific processing capability. The use of the language certainly has not hindered the growth of the

computing power available in a microcomputer. The author's personal computer, the IBM Personal Computer, with 64K of RAM, has the same amount of memory that a frontline U.S. Navy P3-C Orion ASW aircraft uses to process seven tactical work stations, plus handling all the navigation, displays, and other systems.

Throughout this thesis, a microcomputer was used to compute all the results given, and only the lack of a thesis quality graphing device prevented the author from doing all work on his own personal computer. Don't underestimate a microcomputer's capabilities. The day is coming when mainframe-like computing power will be available in each office as close as the desk or table.

II. ELECTRONIC SUPPORT MEASURES SYSTEMS

The ESM system used on the modern battlefield must be able to give rapid and accurate assessments of the complex RF environment. Detection and recognition of hostile radar transmissions must take only a few seconds because to do less invites destruction or the loss of the ability to deal a decisive blow to the enemy. [3: p.54]

The design of ESM systems, in view of their importance, would seem to follow a rational and orderly path from concept to development to operational capability.

This usually isn't the case, unfortunately, as the reactive nature of EW will impede an orderly flow or development. Without perfect knowledge of an enemy's radar and EW capabilities, surprises occur which tend to drive the normal development into a "reaction" driven process. The normal process also tends to be delayed by a desire to wait until a precise definition of the threat is in hand. By the time it is, a reaction process is needed to counter the threat. [2: p.53]

As referred to in the Introduction, page 25, this design process is undergoing changes to improve the response and lessen the reaction design. Changes in the design process will not change the design requirements.

The ESM system is designed to intercept many different electromagnetic signals. Ideally, the system should be able to accomplish as quickly as possible the following tasks:

1. Intercept a transmitted signal at any frequency
2. Determine the type of modulation in the signal
3. Identify the usable intelligence carried in the signal
4. Measure the direction of arrival of the waveform for calculations that locate the transmitter.
5. Process and record the signal characteristics
6. Display to the operator and transfer to the computer for decision making

In short, the system must gather, process, and display all signals of interest. [2: p.191]

Meeting these requirements requires a lot of attention and hardware. No single tuner can cover the area of interest (usually 500 MHz to 30 GHz), so many tuners, antennas, and other system units are required.

With this equipment, an ESM system approaches the problem with these basic intents:

1. Intercept the signal. Conversion to a usable form must now take place immediately. An alarm should be given to indicate a signal has been intercepted. Some analysis or sorting must be done immediately to determine if the signal is of high threat, since signal frequency and modulation usually correlate with degree of threat. [2: p.191]

2. Analyze the signal for further information. Once it's decided there isn't an immediate threat, other parameters of the signal can be determined for recording and later decision making.

Each of these approaches has more or less importance depending upon the platforms. An airborne platform has less space to accommodate equipment for reception and analysis, but is usually exposed to more immediate threats. Therefore, an

airborne platform devotes more attention to interception and immediate analysis than the ground platform, which probably is more concerned with a full analysis and recording. Hopefully, this entire thesis has the flavor of applying to an airborne platform.

An examination of a typical airborne ESM system will begin in the next section.

A. COMPONENT SYSTEMS

Figure 2.1 [4] shows a typical ESM system. Of particular interest and discussion in this chapter will be the receiving system, the preprocessor, and the processor. The Data Files (Active Emitter and Emitter Parameters), are used by the system as records for current signals being received (Active Emitter) and comparison of parameters from processed signals with previously entered (a priori) parameters of signals of interest or expected signals (Emitter Parameters). Electronic Counter-Measures (ECM) handoff and equipment is not really a part of the ESM system, but is included as a function that could be available for manual/automatic jamming or deception of high threat signals.

1. The Receiving System

Inseparable in their functions, the antennas and the receiver form the interception and detection system that is at the forefront of the entire process. This section will cover a few of the important aspects of the antennas and receiver systems.

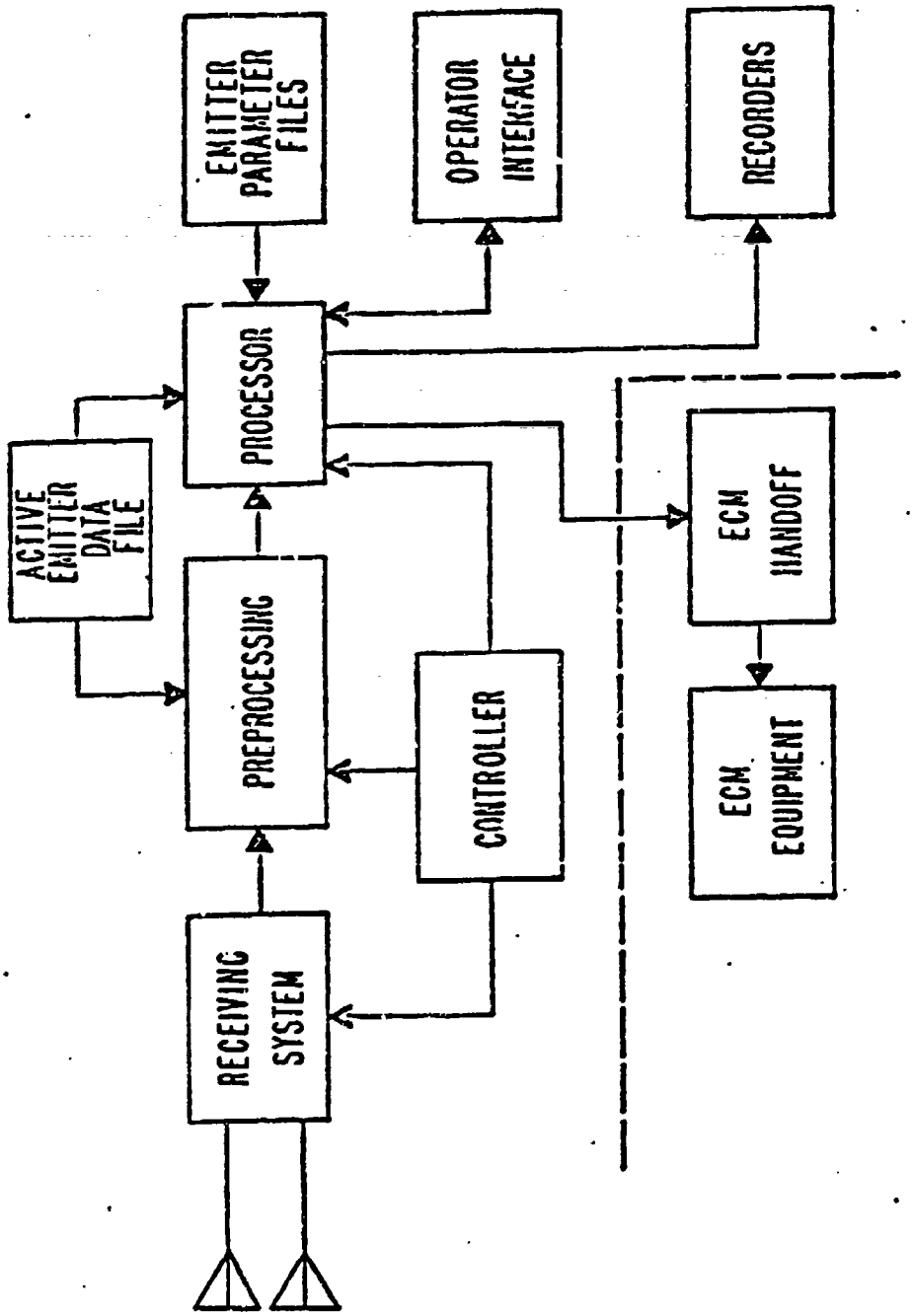

Figure 2.1. An ESM System.

a. Antennas

The energy received by any platform is a very small fraction of that transmitted. Consider Table 2.1 [14: p.9-33]. Notice the numbers in the received power column are magnitudes below one milliwatt in almost all instances.

Table 2.1. Received Power Examples.

Frequency (GHz)	Transmitter Peak Power (watts)	Transmitter Antenna Gain (dB)	Range (nm)	Received Power (dBm)
1	10^7	40	100	-7
3	2 M	30	5	+2
			200	-30
			2000	-50
10	1	30	5	-72
10	250 K	30	10	-24
			200	-50
40	100 K	35	10	-36

High sensitivity in the system is needed to use this power. Good antenna design is the starting point for reception of the signals that are desired to be analyzed, and good design is very dependent upon the application.

The basic equation that is fundamental to the amount of power available for use is:

$$P_r = P_t G_t \lambda^2 / ((4\pi)^2 R^2) \qquad (2.1)$$

where the variables and units are as indicated below:

P_r = received signal power in watts
P_t = transmitted power in watts
G_t = effective transmitting antenna gain
G_r = effective receiving antenna gain
λ = wavelength (same units as R)
R = separation between transmitter and receiver

In this age of "if you can see it, you can hit it" accuracy with guided missiles, it is not recommended that shorter ranges be used to improve the amount of power being received. Thus, the only other available factor under the designer's control (besides receiver design) is the receiving antenna gain.

Our antenna gain is affected by several factors.

$$G = 4\pi A\rho/\lambda^2 \qquad (2.2)$$

where A and ρ are defined

A = capture area
ρ = antenna efficiency

The capture area is the physical size of the antenna. The efficiency is an inherent property and a function of the type of antanna (usually between 0.5 and 0.6).

The beamwidth of the pattern that has the designer's interest also has an effect on the antenna gain [15]. It is an inverse relationship [14: p.29-3] that depends upon the current distribution across the aperture.

A typical reflector antenna, for instance, has

$$G \approx 20{,}000/(\theta_B \phi_B) \qquad (2.3)$$

where θ_B and ϕ_B are the half-power beamwidths in degrees measured in the principal planes of the pattern.

The Gain G is the power gain, and should be used in radar equations because it includes losses introduced by the antenna (Eq. 2.2). Bearing resolution and coverage functions for direction finding would lead to a consideration of the directive gain. The directive gain is more descriptive of the antenna pattern.

A useful expression for directional gain is

$$G_D = 4\pi/(\theta_B \phi_B) \qquad (2.4)$$

where θ_B and ϕ_B are the half-power beamwiths in radians. [15]

Gain must be considered in terms of signal reception. Two of the system's tasks are to receive the signals which may come from any direction (omni considerations) and locate the emitter (DF considerations). The two tasks are not necessarily complementary, so a trade-off in system performance can be accepted or 2 antennas can be used, one for each mission.

For an airborne platform, weight, space, and structural requirements may limit the size of an ESM antenna, but the altitude of the aircraft will usually offset some of these disadvantages. Dipoles, slotted monopoles, and surface wave antennas [14: p.29-30] are antennas that can be used in airborne applications.

The DF function of the system could use any of the mentioned types of antennas if the system uses amplitude or phase comparisons between two collectors. [14: p.29-31]

Loop antennas are a common amplitude sensitive DF antenna often used in a system called a goniometer [16: p. 2h-14]. Horizontal dipoles or dipoles combined with reflectors are also antenna types that are used in DF systems, as well as Adcock arrays [16: p.2h-18].

Generally, it is desired to have high gain in antennas for an ESM system, and the specific application will dictate the type and size of antenna that can be used. More often than not, an omni-directional antenna of some type is used for search, and a rotating, fixed, or multi-port highly directional antenna is used for direction finding.

b. Receivers

Most discussions on EW will address the receiver technology used to detect the signal brought in by the antenna system. Several types of receivers are in use by the Air Force, Navy, and Army, with the mission usually dictating the choice of technology.

A quick and general overview of receiver types and technologies follows in this section. Although some of the technologies have been around for some time, and some still yet to come, they are increasingly being dominated by the processing requirements and the impact of microcomputers. Cost saving and simplification of the microwave design requirements are a result of this increasing influence. In addition, combinations of receiver technologies are being used to overcome limitations of individual receiver concepts.

The future holds new technologies for the detection of signals and increases of speed and bandwidth of single receiving devices. Surface Acoustic Wave devices will certainly play an important role, as well as acousto-optic techniques. Increases in computational speed and capacity may aid or deter some technologies by eliminating some of the need for higher sensitivity in the detection scheme.

Table 2.2 [17] gives some typical ESM receiver specifications.

Table 2.2. Typical Receiver Specifications.

Frequency Range	0.5 to 18 GHz
Signal type	100 ns pulse to CW
Sensitivity	<-70 dBm
Resolution	5 MHz (pulse)
	1 MHz (CW)
Amplitude accuracy	1 dB
Bearing accuracy	5° RMS
Pulse width resolution	100 ns
Time of Arrival resolution	50 ns
Signal density	10^6 pps
Intercept probability	100%

(1) Direct Detection. Simplicity in design gives the direct detection receiver advantages in cost, reliability, size, and weight. This design is also proven, currently in use in the front end of radar warning receivers (RWR), giving a high Probability of Intercept (POI) for signals above its Minimum Discernable Signal.

Today's high density environments pose problems for the DD receivers, degrading their performance

quickly. Frequency resolution is not very high as the bandwidth is usually an octave or more in width. [18: p.26] Sensitivity is a problem, although RF amplification can provide improvements.

Quite susceptible to ECCM, the DD receiver cannot handle PRI agile signals, and does not provide frequency measurement, an important sorting parameter.

Figure 2.2 is a direct detection receiver.

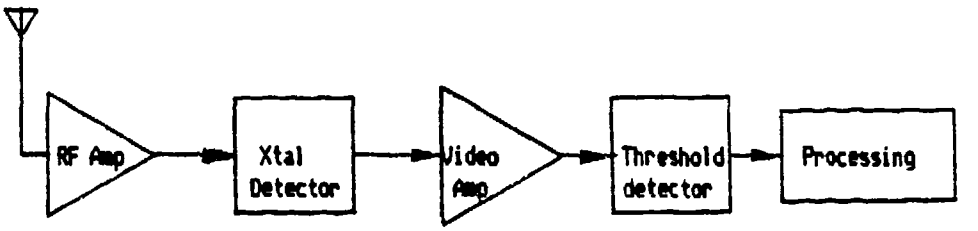

Figure 2.2. Direct Detection Receiver

(2) Instantaneous Frequency Measurement (IFM). A form of a direct detection crystal video receiver, the IFM provides frequency discrimination and measurement with a high POI. Often an output of the receiver is a polar display of amplitude versus frequency [16: p.2a-12] and the term Polar Discriminator is used in place of IFM.

The operation of the discriminator is the heart of the receiver. Note Figure 2.3(a). Input signals are divided into two parts and phase correlated after one signal is delayed by a known time. The length of the delay line is related to the amount of frequency resolution desired and the wavelength that corresponds to the desired bandwidth. By banking several discriminators and different lengths of delay line, as shown in Figure 2.3(b), a desired frequency band can be covered. This approach allows the use of practical and relatively inexpensive delays rather than attempting to use one delay line precise enough to handle the desired frequency region. The length of the longest delay becomes the frequency resolution of the bank. [18: pp.32-33]

Measurement of the frequency of the incoming signal with these analog discriminators (or current technology Digital IFM's) allows this important parameter to simplify the sorting process.

On the down side, the IFM doesn't handle high density environments very well unless a subsystem that determines when 2 pulses occur simultaneously is included. Also, the delay lines require special attention (constant temperature) and this usually increases the required input power to the system.

Working in conjunction with an analysis receiver, the IFM makes an ideal acquisition receiver by

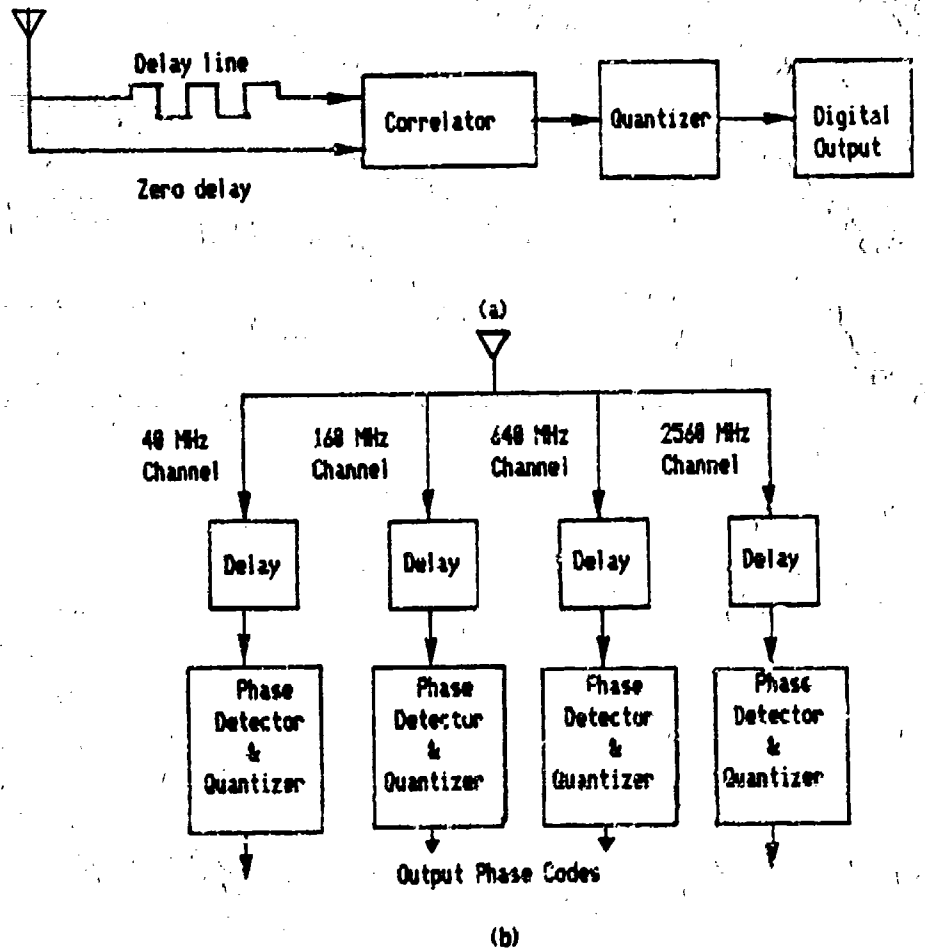

Figure 2.3. IFM Receiver Concepts.

providing the frequency of a signal of interest. Analysis receivers of another type can then be tuned to the frequency. [18: p.32-34]

(3) Superheterodyne. Most common of the receivers in current use, the superheterodyne provides high selectivity, good resistance to jamming, and is a proven design.

Drawbacks include slow time in scanning the frequency band of interest and inability to see frequency agile signals. [19: p.459]

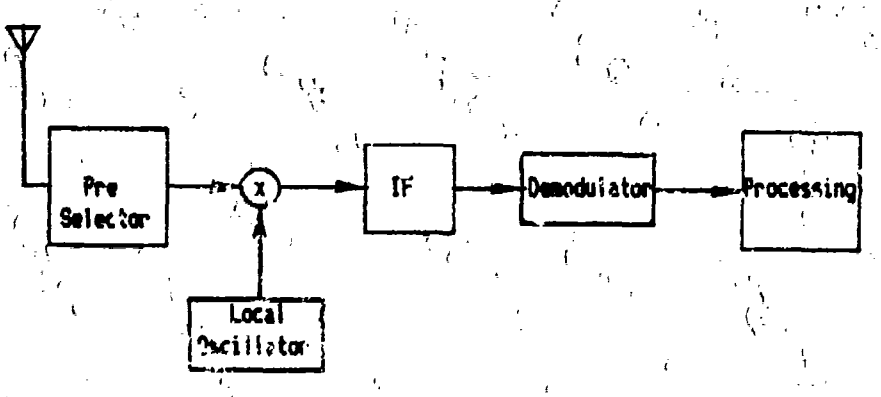

Figure 2.6. Superheterodyne Receiver.

(4) Channelized. Efforts to increase the POI of superheterodyne receivers and deal with an inability to handle high density environments led to the concept of a bank of filters followed by individual signal detectors that determine when a signal is within the filter bandwidth. The RF spectrum is simply broken into pieces. See Figure 2.5.

A key advantage of the channelized receiver is removal of pulse overlap of near simultaneous signals (only pulse frequencies that exceed the channel spacing). [17: p.105]

By following an initial bank of filters with multiplexers and fixed oscillators, then repeating the scheme with a smaller bandwidth filter, the RF input can be down converted to a final baseband frequency range with a higher frequency resolution.

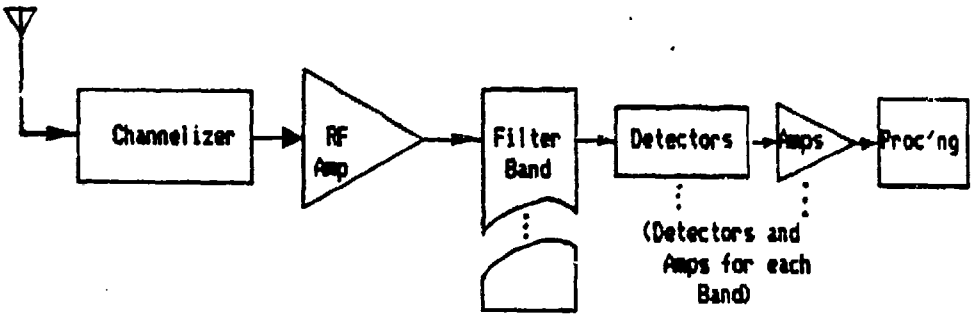

Figure 2.5. Channelized Receiver

(5) Compressive. This receiver can be characterized as a fast scanning superheterodyne receiver. Ideally, the local oscillator scans the RF bandwidth being covered in a time less than the narrowest pulse to be intercepted. Its high POI and the ability to handle wideband signals and frequency agile signals makes this receiver a good choice for an ESM receiving system. It has an excellent ability to separate signals closely spaced in frequency.

Basically, the compressive receiver provides an IF signal that is up-chirped in frequency from the RF input. The compressive filter operates in such a way that the low frequency components of the IF signal are delayed longer than the high frequency components, with the result that the shape of the output pulse of the detector is in essence the Fourier Transform of the IF signal pulse. The maximum amplitude of the detector output falls at a point in the scan time that is proportional to the frequency of the RF input. [18: pp. 30-31]

Criticality of the alignment between sweep and compressive delay makes this complex technique difficult to manage [19: p. 459]. But it is at the forefront of some of the newest technologies, with SAW's performing the delay necessary for the up and down chirp. Note Figure 2.6.

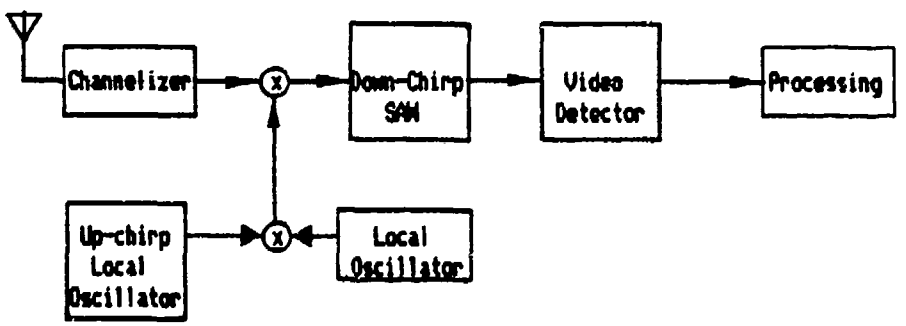

Figure 2.6. Compressive Receiver.

(6) Bragg Cell. An acousto-optic Bragg cell will interact a propagating acoustic wave with an optical beam to give a diffracted output proportional to the frequencies and

power present in the RF input signal. The acoustic wave, which varies the index of refraction of the cell material, is generated by applying the RF input to an acoustic transducer in the Bragg cell. A laser beam is deflected and modulated in intensity by the index variations which are proportional to the RF input frequency. A Fourier Transform lens collects the proportionately diffracted light which then falls on a photodetector array. The output of the detector array is similarly proportional to the RF input frequency. [18: p.28]

Having pluses for high sensitivity, high POI, and high selectivity makes this receiver a choice of the future. It doesn't handle frequency agile sources well, however, because of the time needed in determining the output of the photodetector array. Pulse width measurement is also eliminated with the use of the detector array because the array only responds to the energy contained in several pulses from the lens. [19: p.468] Figure 2.7 is the receiver.

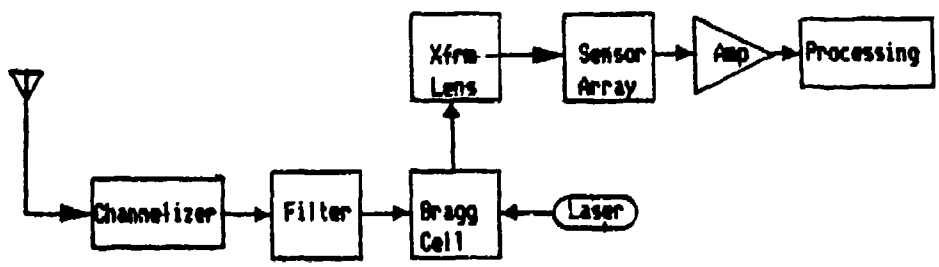

Figure 2.7. The Bragg Cell Receiver.

2. The Processing System

A steady stream of pulse descriptor words from the receiving system must be analyzed for the vital information that is contained in them. The processing system must extract this information and make decisions regarding the emitters whose signals it has processed. Information extraction, analysis and identification must be fast to avoid a mission and life threatening situation.

This section will discuss the overall purpose and general operation of preprocessors and processors in the ESM system. A more complete discussion will be found in Reference 20.

a. Preprocessor

Basically, the preprocessor must prepare the signal received from the receiving system for preliminary analysis and for advanced analysis in the main processor. Figure 2.8 is an ESM preprocessor. [20: p.8]

After digitization, the initial parameters of pulse width, time of arrival, direction of arrival, amplitude, and frequency must be measured on a pulse by pulse basis. (See Parameter Measurements in this chapter.)

The pulse data must be compared with previously received and analyzed signals to see if this signal has already been processed. Pulse data is compared with signal data in the files that contain the active emitters and the uninteresting emitters. If a match is present, then the data

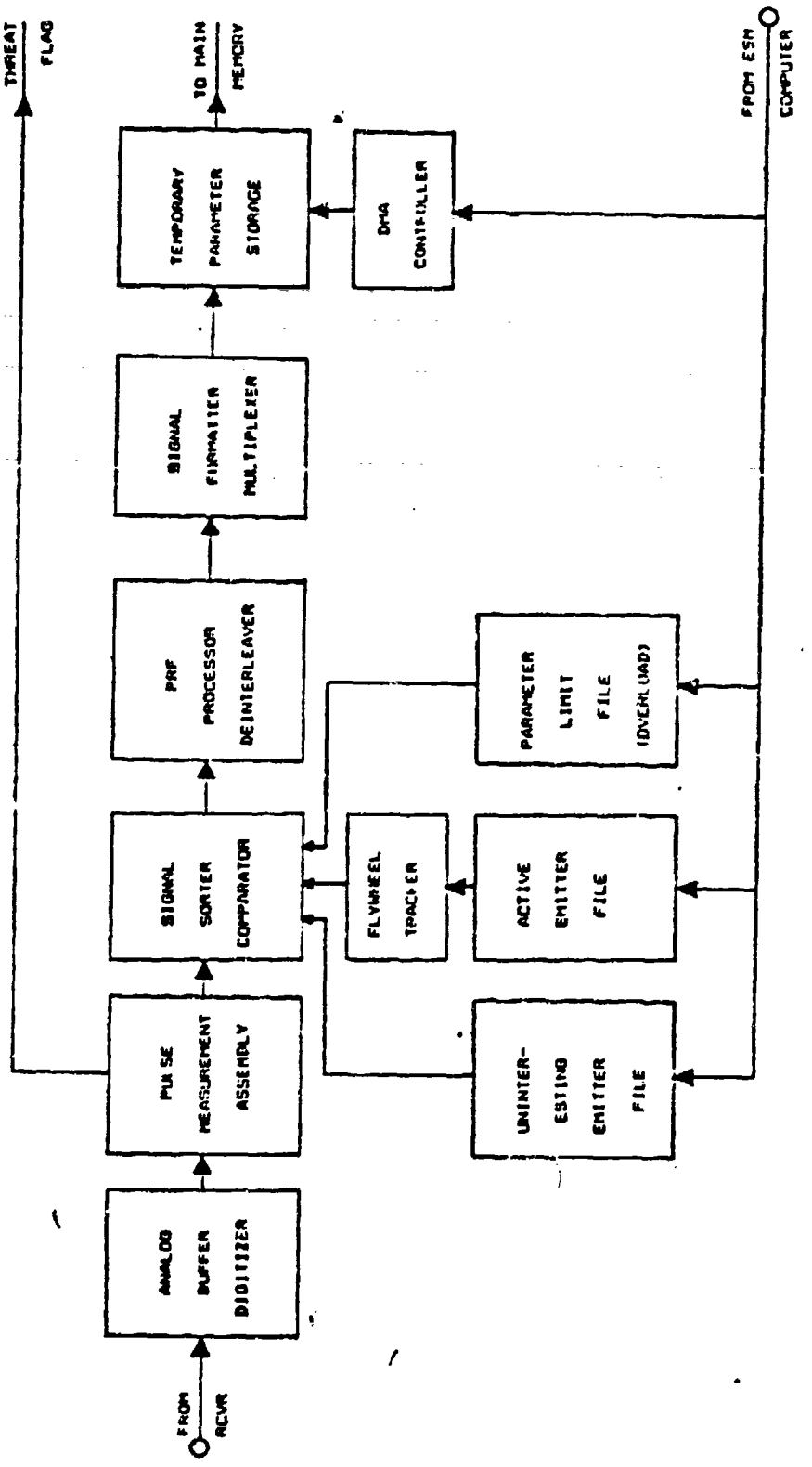

Figure 2.8. Preprocessor

can be deleted from the process. Reduction of the data stream and sorting of the signals is the purpose and result of this deletion in addition to avoiding unnecessary processing. One of the main jobs of the preprocessors is to convert the approximately 10^5 to 10^6 pulses per second being received to about 1000 pulses per second that a good main processor can handle. [21: p.164]

Unmatched or new signals must be deinterleaved (see deinterleaving in this chapter) and processed in the PRI processor section. Calculation of the PRI is usually done simply by subtracting TOA's of similar pulses. Staggered PRI's and jittered PRI's have to be handled with a more complex algorithm. [20: p. 12]

With a known PRI, TOA prediction, additional sorting, and comparison of calculated PRI's is done until a PRI is confirmed to exist in the data. This information, the newly calculated PRI and the initial parameters of the pulse, is then passed to main memory of the processor for analysis and updating of the active files so that pulses of the incoming stream can be deleted as soon as possible.

In summary, the preprocessor prepares the incoming signals for processing, measures their initial parameters, performs preliminary analysis and sorting, and passes the data information to the main processor.

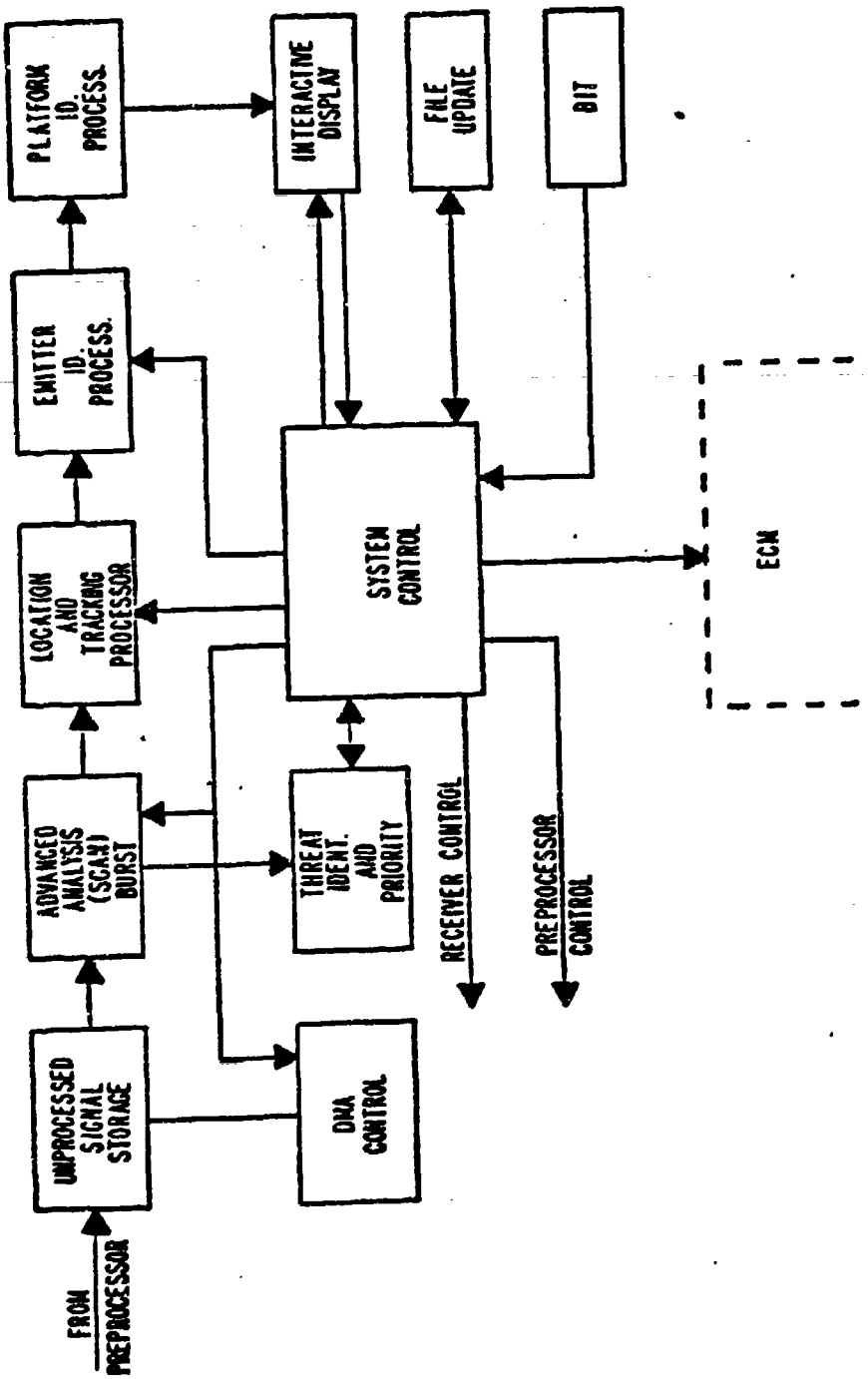

Figure 2.9. Main Processor

b. Main Processor [20: pp.13-18]

After all the action in the preprocessor and the data reduction that has been accomplished, there is still plenty to do. The functions of the main processor are:

1. Advanced analysis of the signal for scan rate and exotic emitter (such as chirp radars) identification
2. Emitter and platform identification
3. Updating the emitter files
4. System control and monitoring
5. Interfacing with the operator and ECM equipment

Since the processor is usually a general purpose computer, additional functions of navigation or routine system calculations could be added. It can also help the PRI processor handle its calculations.

Emitter identification is accomplished by comparing the measured emitter parameters with emitter parameter lists until an identification is made or the signal is tagged as unidentified. Interface with the operator for manual analysis is often the result of an unidentified signal.

3. Display System

An operator must have a visual presentation of the signal and its parameters. Almost universally CRT displays are used. CRT's usually have an intensity modulated or a deflection modulated design, with advantages and disadvantages in each one.

Multi-gun CRT displays can create a combined display that offers a pulse analyzer, presenting frequency, PRF, PW, and the presentation of an amplitude spectrum.

A warning system usually operates in conjuction with detection of high threat signals. Flashing lights and/or an aural alarm will occur, indicating immediate attention is required.

The audio system operates in parallel with the warning system. Offering not only alarms to high threat signal reception, the system usually has accomodations that allow the operator to monitor the received signal through headsets or a speaker. A trained and experienced operator can determine scan rate and analyze the scan modulation type if the signal density is low enough.

Bearings from DF equipment are usually presented on a polar display. The direction is usually indicated in relative bearings of 0 to 360° around the platform, with some output or means of determining the true bearing for plotting purposes.

Computer management of an ESM system allows for most calculations of bearing, PRF, PW, and frequency to be accomplished and shown as soon as the bearing is displayed to the operator. An excellent example of computer managed displays is the ALQ-78 ESM system on the U.S. Navy P3-C Orion. Digital readouts of the PRF, PW, and frequency are available next to the displayed bearing from the aircraft. The bearing remains on the screen and updates automatically until removed by the operator or the system. With several cross bearings, the emitter location can be obtained since the computer is not only managing the display but the navigation

of the aircraft. By "hooking" the place where the bearings cross, the operator can cause the computer to calculate the lat/long of the emitter fix.

B. ESM SIGNAL PROCESSING

The acquisition of signals is usually a design problem that is driven by the characteristics of the signals to be acquired. The designer chooses antennas and receivers to detect signals with regard to the mission, the platform, and the frequency band of interest. Generally, he desires the ESM system should have rapid acquisition, high sensitivity and frequency resolution, and wide frequency coverage.

After these signals are acquired, signal processing is the order of the day. Processing is required immediately to determine the high-threat signals (especially for tactical aircraft), and a lot of processing is required in today's dense electromagnetic environments. The signals are getting more complex also, with jittered and staggered PRF's and variable PW's in addition to frequency agility and new schemes of radiating and detecting a return.

Computational speed becomes one answer to solve these processing riddles, and the debate between digital and analog techniques fuels upon this quest for speed.

Surface Acoustic Wave (SAW) devices and Charge Coupled devices (CCD's) are being challenged by digital technology staked by the Pentagon's Very High Speed Integrated Circuits Program (VHSIC). These digital IC's are being structured to

perform high speed calculation, with a N X N matrix inversion (a N^3 operation) being a gauge of successful application. Today's analog technologies currently offer high speed also, but will require more precision and dynamic range to meet this challenge. [22: p.91]

In the end, the ESM system designer will win as new digital architectures and new device structures will yield increase in speed and throughput.

This section will discuss important signal processing parameters of the ESM system, and the techniques used to separate the signals for identification and processing from the immense amounts of pulses being received. The entire process is a continuous flow of calculations, comparisons, and decisions involving tolerances in frequencies, pulse width's (PW), pulse repetition intervals (PRI), and other parameters.

1. Parameter Measurement

Listed below are the initial parameters, as provided by the receiving system to the preprocessor. They are the basic tools that are used to deinterleave (see next section) the pulses and match them to existing tracked or not tracked emitters.

1. Direction of Arrival
2. Amplitude
3. Frequency
4. Pulse Width
5. Time of Arrival

Those that aren't matched must be analyzed further by calculating a pulse PRI and/or undergoing advanced analysis. Calculation of the PRI is done in the preprocessor. Advanced analysis is accomplished in the main processor using derived higher order parameters during the task.

A discussion of some aspects of how the initial parameters and higher order parameters are measured follows in this section. [21: p.166]

a. Direction of Arrival (DOA)

An important parameter, the DOA could be measured with a rotating DF antenna but this greatly lowers the Probability of Intercept (POI). A more usual method uses a multi-port (antennas) bearing measurement subsystem that has a high (≈100%) POI.

Phase comparison techniques can also be used, providing greater accuracy but with a tradeoff of smaller bandwidth.

b. Amplitude

Usually the amplitude is termed by the peak value of the received pulse with some tolerances included to provide for variances in emitter radiated power.

The amplitude parameter is used in the advanced analysis section of the typical processor to determine a scan pattern, but is not considered a good sorting parameter because of propagation corruption, multi-path, and other variables that influence the amplitude of the received pulse. [16: p. 2g-3]

c. Frequency

Frequency may be measured with a scanning superheterodyne receiver, but this method has a low POI for reasons similar to those of using a rotating antenna for DF. A channelized receiver provides a frequency measurement but this usually is a much more expensive system.

Most common is the IFM receiver (see section on receivers in this chapter), which has an excellent resolution and high POI.

d. Pulse Width

Pulse widths can be measured by simply noting when the pulse rises and falls through a threshold. Reflections tend to severely corrupt this method of measurement, however.

A more accurate method is to sample the pulse many times and take the PW in the distance between the 3 dB points.

e. Time of Arrival (TOA)

Threshold crossing measurement of this parameter could also be used as in the case of the PW, but a better measurement can be obtained by noting the TOA of the first 3 dB point. TOA's are used in the calculation of PRI's. Adjacent pulse TOA's are simply subtracted to find the PRI.

f. Higher Order Parameters

Parameters that are calculated from the other initial parameters are the derived or higher order parameters.

The PRI is used to link interrupted or split chains of pulses from the same emitter. It can also be used as a parameter to identify a jittered or staggered PRI.

Scan patterns can be recognized by analysis of the pulse amplitudes generated as the radar beam sweeps across the platform. Knowledge of the scan pattern can be of help in identifying the emitter since the radiation pattern can be correlated to emitter type. [21: p.167]

2. Deinterleaving

A stream of pulses from several different emitters includes different frequencies, amplitudes, and PRI's mixed together (interleaved). Separating these different pulses into chains of similar pulses for identification is the deinterleaving problem.

With high density environments, the time available for processing each pulse may be only around 1 microsecond. [21: p.168] Therefore, deinterleaving algorithms, if done digitally, must be fast. Analog equipment that sort pulses have the same requirement. This required speed is the obstacle that hinders the use of Digital FFT's for pulse sorting.

Provision must be made in algorithms for missing pulses in the data stream. Missing pulses is one of the greatest confusion factors in the system. Methods are currently in use to smooth fluctuations of the number of pulses that are input into the preprocessor. [21: p.167]

General discussions of deinterleaving methods are given in this section. The first two are digital methods, using the measured parameter of the pulse, and use of one or the other depends upon the accuracy of the ESM system. Two hardware methods are briefly covered also.

a. Cell or "Pigeon Hole" Techniques

A system that accurately measures the parameters of the pulse stream can use this technique as a fast and efficient deinterleaving scheme.

Pulse data with similar parameters are directed into cells or "pigeon holes". The cells soon contain alike parameters, such as bearing, frequency, or pulse widths that can be analyzed for emitter identification or further sorting if too wide of a variation exists.

Variations could be caused by emitter variations itself or purposeful variations such as a jittered, staggered PRI, or frequency agile radar. If variations (unmatched parameters) are present, then they are passed to a more complex algorithm for processing for the special modulations. Otherwise, a simple analysis or comparison with the active emitter file or emitter parameter file results in an emitter identification.

b. Time of Arrival Techniques [21: p.168]

When accurate computation of pulse parameters isn't available, a time slice of the pulse stream is used to simplify the data under analysis. A time slice will

contain about 8 to 512 pulses. This scheme reduces the number of pulses being considered in a high density enviroment, and forces comparison of parameters to those only in the present time slice.

The first pulse in the time slice is used as a reference and the rest of the pulses is scanned for a match. When a match is found, the TOA of the pulses is used to calculate a PRI. When a sufficient number (usually 6 or 7) of matching pulses are found, then the data is grouped as a chain and is output to the main processor. A problem generated with this technique is the splitting of chains in the pulse data stream by the time slice. Several time slices may have to be analyzed before enough matches in a slice are found to form a chain.

c. Analog Methods

A pulse sorter operating on the pulse period th[illegible] has some analogy to digital TOA methods is currently in use. [16: 2g-7 to 2g-9] Consider Figure 2.10.

The pulse stream is fed into a coincidence detector-discriminator that attempts to match the pulses with gates generated by a gating pulse generator. The gating pulses are initially generated at a PRI slightly higher than the highest pulse PRI. By gradually reducing the gate PRI, the highest PRI pulse train will be captured by the gates if the phase difference between the gates and pulses of the stream. This phase difference is used to generate an error

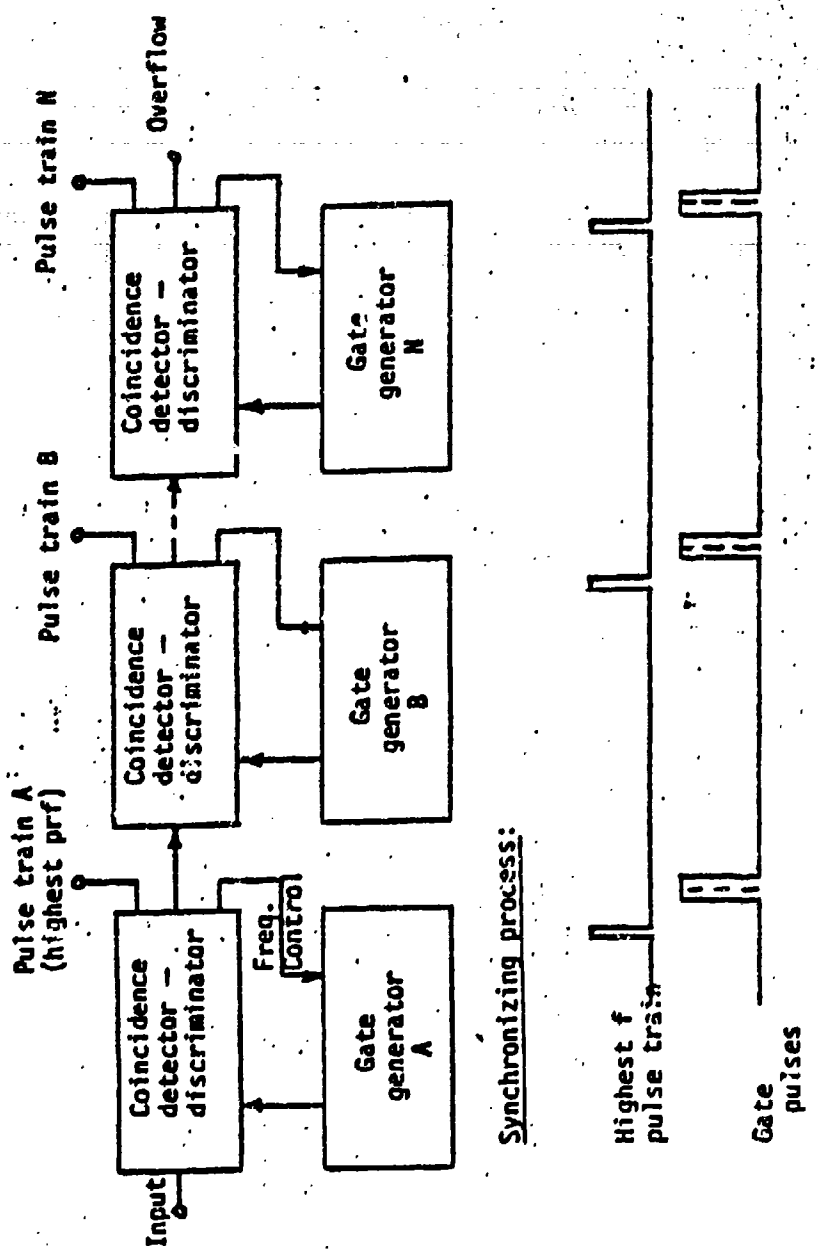

Figure 2.10. Pulse Period Sorter

signal that causes the gate PRI to decrease until synchronized with the highest PRI pulse train of the stream. The pulse train is now sorted out of the stream, and the remaining pulses are applied to a second coincidence detector-discriminator where the process is repeated.

Other methods are used on the pulses left in the stream after passing throught all the detector-discriminators. Staggered PRI's can also be handled by using two or more gate generators operating in synchronization.

d. Frequency Domain Methods

Bandpass comb filters [16: p.2g-9] can be used to pass only harmonically related frequency components. By tuning the filter with the pulse stream as an input, the filter will pass components when it is tuned to a PRI of the pulse stream. Disadvantages of this method include the low resolution of the sorted PRI's and inability to distinguish harmonic components of different PRI's.

Digital FFT's are attractive as a sorting tool, but hardware (size and cost) and computational speed have a way to go before it offers practical alternatives. VHSIC will certainly improve both the hardware and speed aspects.

III. THEORY OF WALSH AND RADEMACHER FUNCTIONS

Electrical Engineering could be said to revolve around the sine and cosine functions. They are the basis for development in many areas due in part to the inherent properties in their frequency domain representations.

The application of digital techniques and semiconductor technology, though, has brought forth uses and awareness of other orthogonal functions. These often do not have the desirable properties of sine and cosine functions for use in linear, time invariant networks, but they do have other advantages that render them useful in other applications.

The early part of this century saw the introduction of several two level orthogonal functions, or sometimes called binary functions because of their amplitudes taking only two values. Work in orthogonal matrices, by Sylvester in 1867 and Hadamard in 1893, was an early approach to these functions.

In 1910, Alfred Haar presented a complete set of rectangular functions that took only two values but yet provided complete expansion of a continuous function. These Haar functions could be made to converge uniformly and rapidly. See Reference 23 for additional information.

A German mathematician, H. Rademacher, presented another set of orthogonal functions in 1922. These were followed by

the Walsh Functions, defined in 1923 by the American mathematician J.L. Walsh. The Rademacher functions, although independently presented, were found to be an incomplete but true subset to the Walsh functions. [23: p.v-vi]

This chapter will briefly examine the Rademacher functions. They are important because products of the functions yield a certain ordering of the Walsh functions. The Walsh functions will then be examined in more detail. The reader is referred to Appendix B for a generic treatment of orthogonality and orthogonal functions.

A. RADEMACHER FUNCTIONS

These two-level orthogonal functions are represented by

$$R(n,t) \qquad (3.1)$$

$$n = 0,1,2,3,...$$

and can be seen in figure 3.1 for n = 0 to 6. [23: p.6]

Notice that they are a series of rectangular pulses or square waves and have 2^{n-1} periods over a time base from 0 to T. Mathematically they could be defined by

$$R(n,t) = \text{sign}(\sin(2^n \pi t)) \qquad (3.2)$$

The first Rademacher function, R(0,t), is equal to one for the entire interval, and subsequent Rademacher functions have odd symmetry with amplitudes of +1 and -1. All have unit mark-space ratio.

One can generate these functions with a sine function of appropriate frequency with amplification and hard limiting.

The appropriate frequency would be one with the same zero crossing positions as the Rademacher functions. [23: p.7]

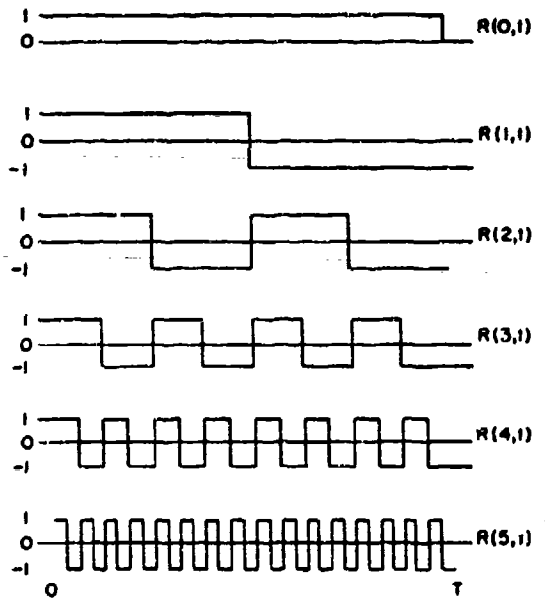

Figure 3.1. The First 6 Rademacher Functions.

B. WALSH FUNCTIONS

Of more importance than the other two-level orthogonal functions discussed are the Walsh functions. They form a set of rectangular waveforms taking only two amplitudes, +1 and -1, but do not have a unit mark-space ratio like the Rademacher functions. They are defined over a time interval T, which must be known to assign values to the functions.

Two arguments are required for complete specification of a Walsh function

$$WAL(n,t) \qquad (3.3)$$

The time base [t] of the function is usually specified as t/T, and thus normalized from 0 to 1. The number [n] is equal to the number of zero crossings a Walsh function has during the time base. [23: p.7]

Figure 3.2 shows the Walsh functions. The symmetry of the functions and the concept of sequency (next section) was used by Harmuth [24] to define another notation for each Walsh(n,t). Each WAL(n,t) is either odd or even about the midpoint. If the function is odd, then it can be referred to as SAL(k,t). If the function is even, then WAL(n,t) is also a CAL(k,t). Note the similarities between this notation and the sine-cosine functions. Relationships between [n] and [k] are

$$CAL(k,t) = WAL(2k,t) \qquad (3.4)$$

$$SAL(k,t) = WAL(2k-1,t)$$

This notation, SAL(k,t) and CAL(k,t), is seen on the right side of Figure 3.2.

1. Sequency, Ordering, and Phasing

Sequency is a term proposed by Harmuth to describe a periodic repetition rate which is independent of waveform. It is defined as "one half of the average number of zero crossings per unit time interval" and abbreviated "Zps". [23: p.13] A 100 HZ sine wave has 200 zero crossings per second, so frequency is a special measure of sequency as applied to a sinusoidal waveform.

Ordering the functions by ascending number of zero crossings (WAL(n,t) notation) is called sequency ordering.

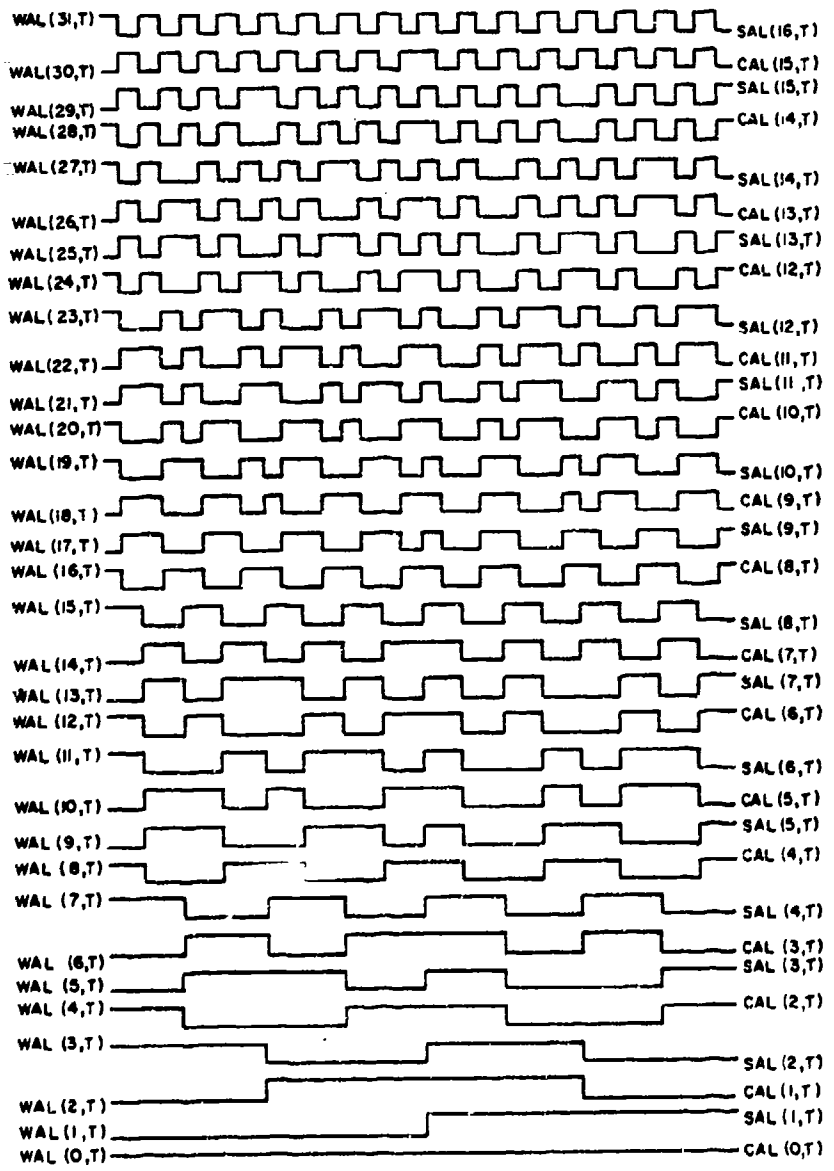

Figure 3.2. The Walsh Functions in Sequency Order.

Although [n] is not the sequency of the function, the equivalence of the WAL(n,t) with SAL(k,t) and CAL(k,t) notations automatically arranges the functions in ascending order of sequency. The value of [k] in the SAL and CAL function is the sequency for the function. Sequency ordering is the preferred ordering for spectral analysis and filtering.

The natural ordering (or Paley ordering) is obtained by generating the Walsh functions with products of Rademacher functions. Figure 3.3 shows the Walsh functions in natural order, which are referred to as

$$PAL(n,t) \qquad (3.5)$$

$$n = 0,1,2,3,...$$

because Paley [24] used this ordering. For theoretical and mathematical work, image transmission, and computational efficiency, this ordering is usually the preferred one. [23: p. 18]

A modulo-2 addition (Appendix C) relationship exists between the Walsh functions with sequency ordering and the functions with natural ordering. [23: pp.31-32] An example will illustrate the conversion between the two orderings. Consider $WAL(n_w,t) = WAL(13,t)$.

Here $n_w = 13 = 1101_2$. To find the equivalent natural order function, $PAL(n_p,t)$, first add a zero (base 2) as the leftmost digit to base 2 n_w. Then generate the value of n_p in base 2 by doing modulo-2 addition between consecutive zeroes and ones of base 2 n_w, starting with the

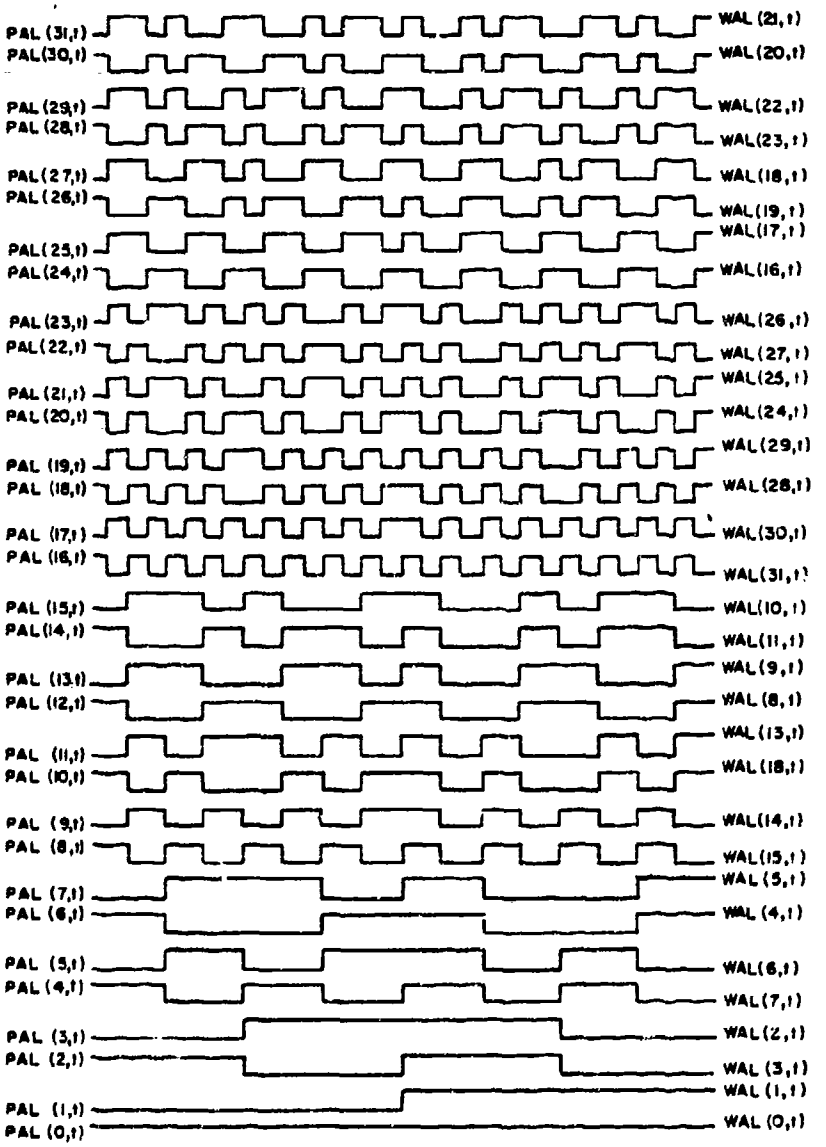

Figure 3.3. The Walsh Functions in Natural Order.

leftmost digit (the zero that was added on to base 2 n_w). Following these rules, $n_w = 13 = 1101_2 = 01101_2$, and

$$\begin{aligned} 0 \oplus 1 &= 1 = k_3 \\ 1 \oplus 1 &= 0 = k_2 \\ 1 \oplus 0 &= 1 = k_1 \\ 0 \oplus 1 &= 1 = k_0 \end{aligned}$$

So,

$$n_p = (k_3 k_2 k_1 k_0)_2 = 1011_2 = 11$$

Figure 3.3 shows the result is correct.

$$WAL(13,t) = PAL(11,t)$$

The phasing of the functions as given in Figure 3.2 and 3.3 is known as Harmuth [25] phasing. This phasing emphasizes the phase similarities with sine-cosine functions.

Positive phasing [23: p.18] is where all of the functions begin at +1. This involves a sign change for many of the Figure 3.2 and 3.3 functions, and is the result of function derivation from Hadamard matrices (orthogonal matrices composed only of +1 and -1 elements; see Ref. 23, pages 24-25) or Rademacher functions (next section).

2. Derivation of the Walsh Functions

Products of selected Rademacher functions will yield a complete set of Walsh functions in natural order. Recall that the natural ordering of the Walsh functions was referred to as PAL(n,t).

In terms of Rademacher functions,

$$PAL(n,t) = \prod_{i=1}^{m+1} b_i R(i,t) \qquad (3.6)$$

where b_i is either a zero or a one, indicating the presence

or not of the i'th Rademacher function. To find the b_i's and [m], represent [n] as a binary number,

$$n = (b_{m+1}b_m b_{m-1}\cdots b_1)_2 \qquad (3.7)$$

with m = the highest power of two found in the binary number [n]. The b_i's present in the positions of base 2 [n] indicate the presence or not of the Rademacher function in Equation (3.6).

Consider PAL(9,t). Then

$$n = 9$$
$$n = 1001_2$$

with m = 3, $b_4 = 1$, $b_1 = 1$, and finally,

$$PAL(9,t) = R(4,t)R(1,t)$$

It should be noted that this product is positive phasing. Harmuth phasing can be obtained by defining the Rademacher functions over the interval $-\frac{1}{2} \le t \le \frac{1}{2}$. This definition inverts all of the functions shown in Figure 3.1. Products of the inverted functions will yield natural ordered and Harmuth phased Walsh functions. [23: p.22] The Walsh functions with sequency ordering can be derived with Rademacher functions by use of the Gray Code (Appendix C). Consider WAL(13,t) where n = 13.

In Gray Code, n = 13 is represented by 1011, and recognizing the ones of the Gray Code are in the fourth, second, and first positions, (similar to the derivation of the PAL(n,t) functions), [23: p.23]

$$WAL(13,t) = R(4,t)R(2,t)R(1,t)$$

Other derivations of the Walsh functions can be accomplished by difference equations, Hadamard matrices, and Boolean synthesis. See Reference 23, pages 20-26.

3. Walsh Series

It is well known that a time function f(t) can be expressed as a sum of a series of sine and cosine functions. Each function has a coefficient that determines the value of the function in that series.

The time function can be expressed in a similar way using the Walsh functions. [23: p.13]

$$f(t) = a_0 WAL(0,t) + \sum_{n=1}^{N-1} a_n WAL(n,t) \qquad (3.8)$$

where the coefficients would be calculated from

$$a_0/2 = 1/T \cdot \int_0^T f(t) WAL(0,t)\, dt \qquad (3.9)$$

$$a_n = 1/T \cdot \int_0^T f(t) WAL(n,t)\, dt \qquad (3.10)$$

with N = the desired number of Walsh terms, and T is a given length of the function.

Each Walsh function has a coefficient associated with it that gives the value of the function in the series the same way as does the Fourier Series coefficient. [23: p.13]

If the function is periodic, and T is normalized to be equal to 1, then $a_0/2$ is the mean of the function, since WAL(0,t) is equal to 1 over the interval $0 \le t \le 1$. The expressions for $a_0/2$ in both the Walsh and Fourier Series are equal with this normalization.

Consider that the function is absolutely integrable in the interval $0 \le t \le 1$. Then the function can be expanded in a Walsh series of the form [26: p.232 and 23: p.40]

$$f(t) = \sum_{n=0}^{\infty} a(n)\,WAL(n,t) \qquad (3.11)$$

where

$$a(n) = \int_0^1 f(t)\,WAL(n,t)\,dt \qquad (3.12)$$

A more general definition for a periodic function defined over an interval (0,T) is

$$f(t) = \sum_{n=0}^{\infty} a(n)\,WAL(n,t/T) \qquad (3.11a)$$

$$a(n) = 1/T \int_0^T f(t)\,WAL(n,t/T)\,dt \qquad (3.12a)$$

Now coefficient a_0 becomes the mean of the function, since $WAL(0,t/T) = 1$ over the normalized interval $0 \le t/T \le 1$.

The Walsh Series can be defined over the same interval (0,T) using the CAL and SAL notations, and an infinite number of terms: [26: p.232]

$$f(t) = a_0 WAL(0,t) + \sum_{i=1}^{\infty} \sum_{j=1}^{\infty} (a_i SAL(i,t) + b_j CAL(j,t)) \qquad (3.13)$$

with

$$a_s(n) = 1/T \cdot \int_0^T f(t)\,SAL(n,t/T)\,dt \qquad (3.14)$$

$$a_c(n) = 1/T \cdot \int_0^T f(t)\,CAL(n,t/T)\,dt \qquad (3.15)$$

A couple of simple examples follows to illustrate the Walsh Series expansion.

a. Expansion of Sin(t) in a Walsh Series

The sine function will be defined over one period, with a period of 2π, and the Walsh functions will be defined as t/T goes from 0 to 1.

Calculating the first coefficient, using Equation (3.12a),

$$a_0 = 1/2\pi \cdot \int_0^{2\pi} \sin(t)\,WAL(0,t/T)\,dt$$

$$a_0 = 1/2\pi \cdot \int_0^{2\pi} \sin(t)(1)\,dt$$

$$a_0 = 0$$

This is a confident calculation, as most students know that the average of a sinusoid is 0!

The second coefficient,

$$a_1 = 1/2\pi \cdot \int_0^{2\pi} \sin(t)\,WAL(t,t/T)\,dt$$

$$a_1 = 1/2\pi \cdot \left[\int_0^{\pi} \sin(t)(-1)\,dt + \int_{\pi}^{2\pi} \sin(t)(1)\,dt\right]$$

$$a_1 = -2/\pi = -.63611$$

A lot of menial integration will yield only these coefficients of any practical value:

$$a_5 = .26348$$
$$a_{13} = .12653$$

Coefficients numbered 2,6,9, and 10 are present but have values less than 0.06.

The function sin(t) is then approximated by

$$\sin(t) = a_1 WAL(1,t) + a_5 WAL(5,t) + a_{13} WAL(13,t)$$

where the coefficient values are given above.

Figure 3.4 [23: p. 15] shows the three Walsh functions used and their sum. The negative sign of the coefficient a_1 has been used to invert the Walsh(1,t) function.

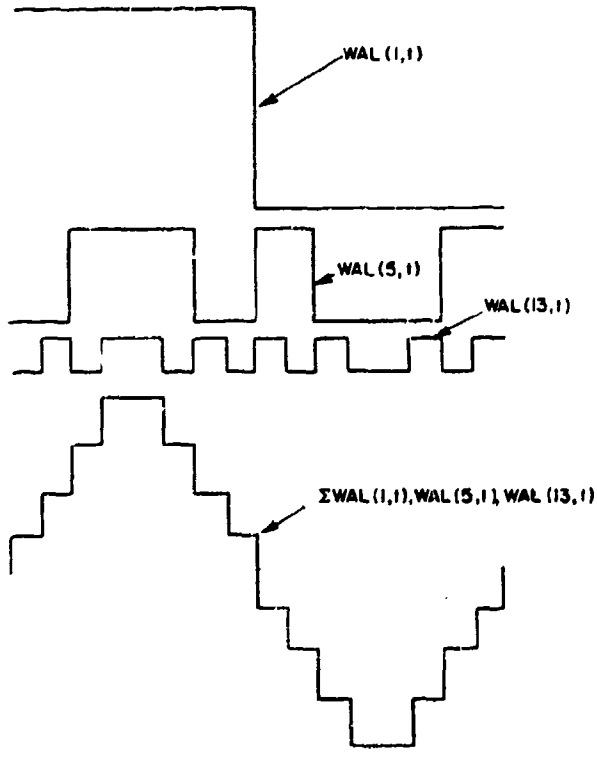

Figure 3.4. Sin(t) with a Limited Walsh Series

Of course, the addition of more of the terms of the Series would yield a better approximation. One can see that representing a smooth curve using rectangular shapes would require a large number of terms of the Walsh Series.

The Walsh Series will give better results representing a rectangular function.

b. Expansion of a Rectangular Function

A rectangular pulse function should lend itself nicely to representation by other rectangular functions.

Indeed, it is hoped that the representation might be exact or with small error in only a few terms.

Consider this function:

$$f(t) = \begin{array}{ll} 1 & 0 \le t \le .25 \\ 0 & .25 < t < .75 \\ 1 & .75 \le t \le 1.0 \end{array}$$

Proceeding with the coefficients,

$$a_0 = \int_0^1 f(t)\,WAL(0,t)\,dt$$

$$= \int_0^{.25} (1)(1)\,dt + \int_{.75}^{1.0} (1)(1)\,dt$$

$$= 0.5$$

and,

$$a_2 = \int_0^{.25} (1)(-1)\,dt + \int_{.75}^{1.0} (1)(-1)\,dt$$

$$= -.5$$

Coefficients a_1, a_3, and above will all calculate to be zero.

This rectangular time function, which could represent two radar pulses, can be represented exactly by two Walsh functions.

$$f(t) = 0.5WAL(0,t) - 0.5WAL(2,t)$$

Figure 3.5 shows the function, the Walsh functions, and the sum of the Walsh functions. This is quite a difference from the representation by Fourier Series, which would require a lot of terms to present an inexact representation.

c. Waveform Synthesis

These results obtained above indicate that a continuous waveform is more suited for Fourier transformation and a discontinuous waveform, certainly a rectangular one, is more suited for Walsh transformation. This conclusion should be easy to accept with examination of the structure of the orthogonal functions (sine-cosine and Walsh).

Figure 3.6 [23: p. 33] shows a reconstruction of two waveforms and the number of Fourier and Walsh terms used. The reconstruction supports the conclusion very well. In addition, Beauchamp [23: p.35] reports that the same conclusion can be drawn when the Fourier and Walsh Transform are used to reconstruct a continuous and a step waveform.

In coming to this conclusion, Beauchamp considered the effect of the number of allowed levels for quantizing the waveform and the sampling interval. [23: p.35] The sampling interval determines the number of coefficients

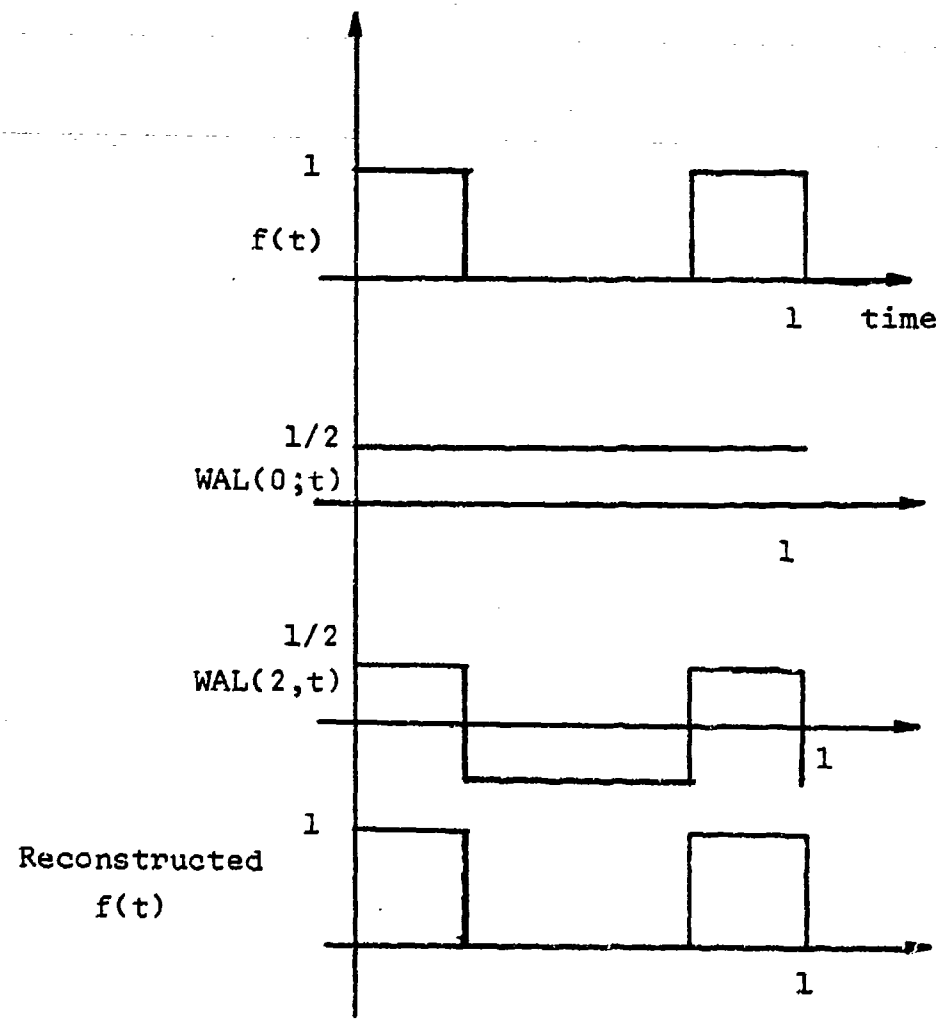

Figure 3.5. Expansion of a Rectangular Function.

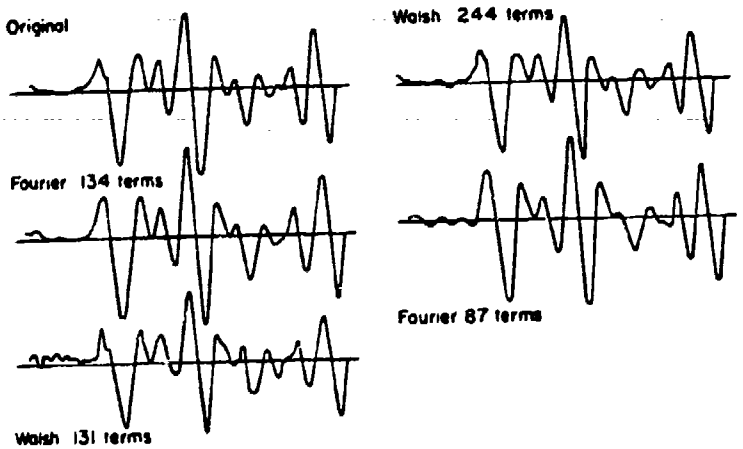

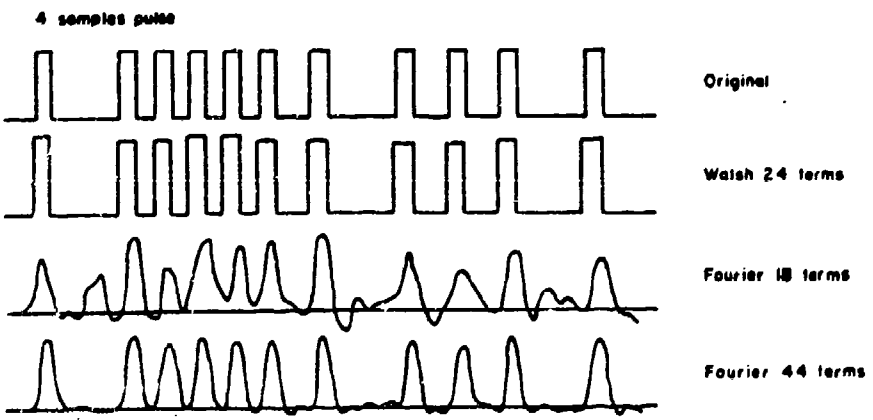

Figure 3.6. Waveform Synthesis Using Walsh Functions.

produced, and the highest Walsh coefficient found from the Transform determines the number of data points available for any quantized level. This is a built-in limitation on the accuracy of the Walsh Transform that the Fourier Transform doesn't have.

d. Digital Sampling

A theorem similar to the Sampling Theorem for sine-cosine functions is applicable to the Walsh functions.

The minimum sampling rate is [23: p.37]

$$f_s = 2^{k+1} \qquad (3.16)$$

with k being the power of 2 that represents the sequency bandwidth. The sequency bandwidth would be the sequency of the highest component desired to be represented.

Suppose a CAL(12,t) component had been determined and it was desired to include this component in the bandwidth. The sequency of this component is 12, and the closest power of 2 that is at least 12 is 4 ($2^4 = 16$). Thus k = 4 and

$$f_s = 2^{4+1} = 32$$

For comparison, a cosine of frequency 12 would require a sampling rate of 24 (2*frequency). Aliasing is equally applicable to the Walsh functions and should be considered. [23: p.37]

4. The Walsh Transform

Section 3 stated that a continuous function over the interval $0 \le t \le 1$ could be represented by a sum of Walsh functions, shown in Equation 3.11.

$$f(t) = \sum_{n=0}^{\infty} a_n WAL(n,t) \qquad (3.11)$$

where

$$a_n = \int_0^1 f(t) WAL(n,t)\, dt \qquad (3.12)$$

Thus, a transform pair can be defined: [23: p.40]

$$f(t) = \sum_{n=0}^{\infty} F(k) WAL(k,t) \qquad (3.17)$$

$$F(k) = \int_0^1 f(t) WAL(k,t)\, dt \qquad (3.18)$$

F(k) could be written, for an interval $0 \le t \le T$,

$$F(k) = 1/T \int_0^T f(t) WAL(k,t)\, dt \qquad (3.19)$$

Now suppose the interval T is divided into N parts, letting $t = i\Delta$, where Δ is a small time increment and i is an integer. The aim is to convert the integral into a summation for discrete computation.

Then,

$$F(k) = 1/T \int_0^T f(t) WAL(k,t)\, dt$$

$$\approx 1/N\Delta \cdot \sum_{i=0}^{N-1} f(i\Delta) WAL(k, i\Delta)$$

with

$$\Delta = dt$$

$$N\Delta = T$$

Remembering Δ to be a given small increment, but unchanging in value,

$$F(k) = 1/N \cdot \sum_{i=0}^{N-1} f(i)WAL(k,i) \qquad (3.22)$$

with

$f(i)$ = evaluation of $f(t)$ at intervals $i\Delta$

= a series of numbers

Change the notation from K to n, $f(i)$ to x_i, and $F(k) = X_n$, and write the finite discrete Walsh transform pair.

$$X_n = 1/N \cdot \sum_{n=0}^{N-1} x_i WAL(n,i) \qquad (3.23)$$

$$n = 0,1,2,\ldots N-1$$

and,

$$x_i = \sum_{n=0}^{N-1} X_n WAL(n,i) \qquad (3.24)$$

$$i = 0,1,2,\ldots N-1$$

The CAL and SAL transforms for a discrete series can also be found by using the equivalence of WAL with CAL and SAL notations:

$$X_c(k) = 1/N \cdot \sum_{i=0}^{N-1} x_i CAL(k,i) \qquad (3.25)$$

$$X_c(k) = 1/N \cdot \sum_{i=0}^{N-1} x_i SAL(n,i) \qquad (3.26)$$

An even or odd sequence when transformed will have similar properties as the discrete Fourier Coefficients from

even or odd functions. That is, an even sequence (symmetrical around its midpoint) will transform into only CAL function coefficients, and an odd sequence will transform into only SAL coefficients. [23: p.41]

The Discrete Walsh Transform (DWT) has some advantages over the Discrete Fourier Transform (DFT) because it involves only additions and subtractions, not multiplications as in the DFT. Also, the transform is not noisy because precise representations in the digital computer is possible. Precise representations of sine-cosine functions in the DFT is not. Finally, the Walsh transform kernel is ±1 and is considerably easier to calculate. [23: p.42]

An important point of the transform is that the DWT is its own inverse, and a separate inverse transform definition is not required. See Equations (3.23) and (3.24).

a. The Fast Walsh Transform

Computation of the DWT would involve N^2 mathematical operations of either addition or subtraction. This number of operations has been decreased by using the redundancy in the Walsh matrix representation of the Transform to $N\log_2 N$ operations, the same number as in the DFT. [23: p.54] Remember that the DWT involves additions/subtractions, not complex multiplications/additions as in the DFT.

The Fast Walsh Transform can be described in a signal flow diagram that results in a "butterfly" appearance just as in the FFT. See Figure 3.7 on the next page. Unique

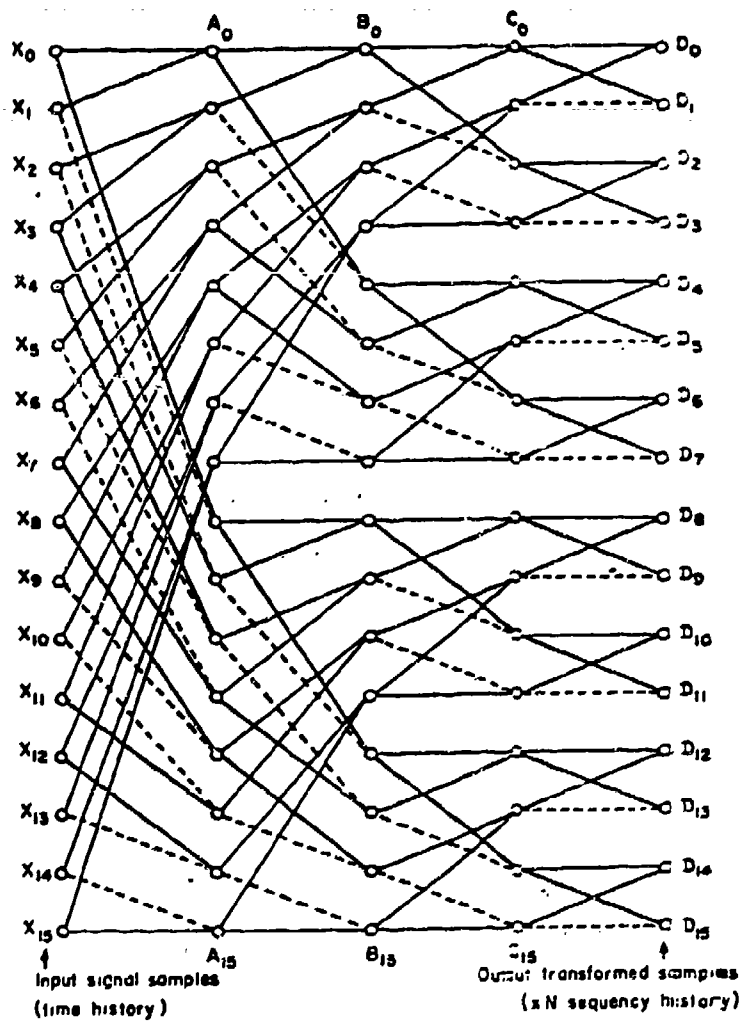

Figure 3.7. FWT "Butterfly": N = 16.

features of the butterfly in the final stages of calculations offer an opportunity to calculate the FWT "in-place", without using computer working space. [23: p.55] The result is not in sequency order, however, and a sorting routine must be included if sequency order is desired.

Appendix A gives listings of the FWT programs used in this thesis.

b. Walsh Coefficients and the Walsh Matrix

The computation of the coefficients from the FWT is very fast and takes advantage of the properties of a Hadamard matrix [23: p.52]

The Walsh matrix is related to the Hadamard matrix and can be used to determine the coefficients of the Walsh Series. [27: p.4] Consider this matrix equation,

$$[a_n] = 1/N \cdot [W] \cdot [x_i] \qquad (3.27)$$

where [W] is a N X N matrix of the Walsh functions, $[x_i]$ is a column vector of N sampled values of the function, and $[a_n]$, n = 0 to N-1, is a column vector of the Walsh coefficients.

The Walsh matrix can be thought of as the matrix of sampled Walsh functions, and thus, is composed of plus and minus ones. To compute the coefficients, simply perform addition and subtraction of the sampled values according to the row of the Walsh matrix being used. An example will show this computation.

Let the number of samples in the column vector = 8 = N. Writing the matrix equation, omitting the 1/N term,

$$[a_n] = [W] \cdot [x_i] \qquad (3.16)$$

$$\begin{bmatrix} a_0 \\ a_1 \\ a_2 \\ a_3 \\ a_4 \\ a_5 \\ a_6 \\ a_7 \end{bmatrix} = \begin{bmatrix} + & + & + & + & + & + & + & + \\ + & + & + & + & - & - & - & - \\ + & + & - & - & - & - & + & + \\ + & + & - & - & + & + & - & - \\ + & - & - & + & + & - & - & + \\ + & - & - & + & - & + & + & - \\ + & - & + & - & - & + & - & + \\ + & - & + & - & + & - & + & - \end{bmatrix} \begin{bmatrix} x_0 \\ x_1 \\ x_2 \\ x_3 \\ x_4 \\ x_5 \\ x_6 \\ x_7 \end{bmatrix}$$

For comparison, use N sampled values of the rectangular function on page 73. Thus,

$$[x_i]^T = [\ 1\ 1\ 0\ 0\ 0\ 0\ 1\ 1\ ]$$

$$i = 0,1,2,3,\ldots,7$$

Now evaluate the constants a_n using matrix multiplication. A plus sign in the Walsh matrix equals +1, and a minus sign means −1. Don't forget to divide each constant by N.

$a_0 = 0.5$ $\qquad$ $a_4 = 0$
$a_1 = 0$ $\qquad$ $a_5 = 0$
$a_2 = 0.5$ $\qquad$ $a_6 = 0$
$a_3 = 0$ $\qquad$ $a_7 = 0$

Comparing with the value of a_2 given in the Walsh Series expansion of this same function (page 73), we note a sign change. The reason lies in the use of positive phasing for the Walsh matrix and the use of Harmuth phasing in the Series expansion computation.

The same answer has been reached, although this is the discrete case.

Matrices can also be used to show the Inverse Discrete Walsh Transform. From Equation (3.24),

$$N \cdot [x_i] = [W] \cdot [a_n] \qquad (3.28)$$
$$= [W] \cdot [W] \cdot [x_i]$$

and

$$[x_i] = 1/N \cdot [W] \cdot [W] \cdot [x_i] \qquad (3.29)$$

Equation (3.29) says to get the sampled values of the original within a constant N, just multiply the coefficients by the Walsh matrix [W].

c. Input Time Shifts and Their Effect

The DFT magnitude is invariant to the phase of the input signal. Although Walsh Transform signals conform to Parseval's Theorem, the DWT is not invariant and the same spectral representation cannot be achieved independently of the phase or time shift of the signal. [23: p.42]

The DWT is time invariant when the time shift is obtained by dyadic translation [23: p.43]. Namely, if x_i, the input number series, is shifted to $z_i = x_{i \oplus p}$, where

$i \oplus p$ = modulo-2 addition

then,

$$Z_c^2(k) + Z_s^2(k) = X_c^2(k) + X_s^2(k)$$

if the coefficients are expressed in CAL notation (Z_c, X_c) and SAL notation (Z_s, X_s). See Appendix C for modulo-2 addition.

The importance of variations with time shift can be lessened by considering sums of squares of coefficients.

This is one definition of the Walsh Power Spectrum, and is considered in the next section.

5. The Walsh Power Spectrum

Spectral analysis using sequency has some advantages over analysis in the frequency (Fourier) domain. A defined power spectrum from the Walsh functions is easily applied to discontinuous or time limited functions, for example, and it is possible to have a sequency limited spectrum for a time limited function in contrast to the Fourier Spectrum. [23: p.87]

Although there are several derivations of the Walsh power spectrum [23: p.91], a more normal, i.e. analogous to Fourier, approach will be used to make a spectrum definition. As there are readily available methods (FWT) for calculating the Walsh coefficients, a combination, specifically the sum of the squares of related coefficients, would give an easy to use definition. Also, as stated earlier, by using the sum of the squares of certain coefficients, the time shift variance that plagues the Walsh Transform can be lessened.

Define, then, the Power Spectral Density (PSD) coefficients of the Walsh spectrum. [23: p.100]

$$P(0) = X_c^2(0,t) \qquad (3.31)$$

$$P(k) = X_c^2(k) + X_s^2(k)$$

$$P(N/2) = X_s^2(N/2)$$

$$k = 1,2,\ldots,(N/2 - 1)$$

Note that (N/2 + 1) spectral points are generated. This method is analogous to Fourier power spectral analysis, where the power coefficient is the sum of the squares of the real and imaginary parts of the complex Fourier Transform coefficients.

Beauchamp [23: p.100] states that taking the square root of P(k) does not give a sequency amplitude spectrum, but other references [26: p.233] use $\sqrt{P_k}$ as the definition of the sequency spectrum.

Another spectrum can be defined using the Walsh Coefficients. The name Group Spectrum is the author's term and will be used here. Beauchamp [23: p.106] refers to it as "the odd-harmonic sequency spectrum", and Campanella/Robinson [26: p.234] refer to this spectrum definition as a generalized Walsh-Fourier spectrum [28].

The power content of individual groups of frequency components has been shown to be equal to groups of components in the sequency domain. Any group of components, in either domain, is a collection of the orthogonal components that make up the original signal or function.

Call groups of sequency components G_n, with [n] an integer, and consider a discrete signal made up of a sequence (s_k) of length N.

The total energy of the signal is, by Parseval's Theorem, equal to the sum of the orthogonal components [2].

(These orthogonal sequency components have been grouped into G_n.) Then,

$$1/N \cdot \sum_{k=0}^{N-1} s_k^2 = \sum_{n=0}^{m} G_n \qquad (3.32)$$

and the number of groups [m] is given by

$$m = 1 + \log_2 N \qquad (3.33)$$

The groups G_0 and $G(\log_2 N)$ represent the power content of the d.c. component and the folding frequency component, respectively. The other Groups represent the power content of the component at n = 1, n = 2, n = 3, etc., plus all odd harmonics.

$$G_0 = P^2(0) \qquad (3.34)$$

$$G_1 = P^2(1) + P^2(3) + P^2(5) + \ldots$$

$$G_2 = P^2(2) + P^2(6) + P^2(10) + \ldots$$

$$G_3 = P^2(4) + P^2(12) + P^2(20) + \ldots$$

$$G_4 = P^2(8) + P^2(24) + P^2(40) + \ldots$$

and so on, until

$$G(\log_2 N) = P^2(N/2)$$

The plot of G_n versus n gives a discrete spectum that is unique for a certain time sequence [26: p.234], and invariant to a time shift of the input [23: p.106].

This spectrum is highly compressed (m points instead of N/2 + 1 points), and therefore doesn't present all characteristics of the data as well as the previously defined spectrum. [23: p.106]

6. The Application of the Fast Walsh Transform

The application of the Walsh Transform to continuous or discontinuous functions is easily accomplished using the FWT programs provided in Appendix A. The programs input a number series (which could represent a sampled waveform) and compute the FWT. With these coefficients, the Power Spectral Density and the Group spectrum can then be calculated. The FWT will be applied to the previous examples and the results will be compared and analyzed in terms of the elaborated theory in this chapter.

a. The FWT of a Sinusoid.

Figure 3.8 gives a normalized graph of the coefficients of the FWT of one cycle of a sinusoid in the Walsh interval 0 to 1. The actual magnitudes can be determined from the scale listed on the vertical axis. Running either program in Appendix A will give a listing of the coefficient magnitudes.

Note that the maximum coefficient (normalized to 1) is a WAL(n,t) = WAL(1,t). Equation (3.4) of the chapter reveals there is a SAL(1,t) with a sequency of 1 at this Walsh index. Thus, the one cycle sin wave in the Walsh interval 0 to 1 has a distinguishing feature at a sequency of 1. Perhaps not surprising since it is known that frequency is a special measure of sequency, and the one cycle in this interval can be thought of as having a frequency of 1.

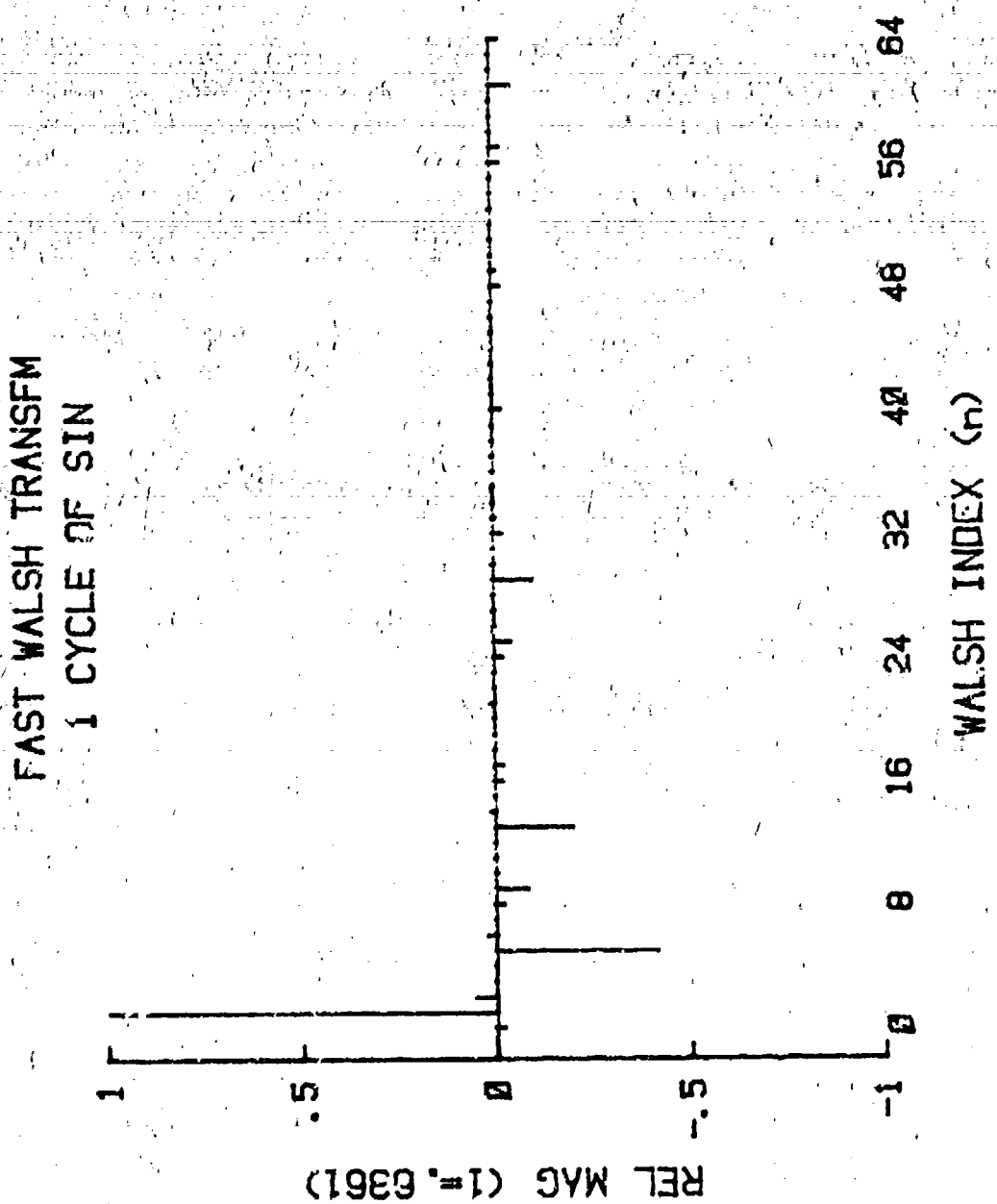

Figure 3.8. FWT of 1 Cycle of a Sine Function.

Also note the other prominent components at n = 5, 9, 13, and 29, with sequencies of 3, 5, 7, and 15, respectively. Our previous calculations with the Walsh series (page 71) predicted conspicuous coefficients at n = 5 and 13.

Applying equations (3.31) to these coefficients results in Figure 3.9, the Power Spectral Density (PSD). The maximum value of power is at a sequency of 1, and there is no DC power term (sequency of 0). Harmonic power is located at sequencies of 3, 7, and 15.

These odd number power components combine into a single component, G_1, in the Group spectrum, Figure 3.10. See Equation (3.34).

An increase of frequency gives similar results. Figures 3.11 to 3.13 show the FWT, PSD, and Group Spectrum of three cycles of a sinusoid in the Walsh interval 0 to 1. The maximum FWT coefficient lies at n = 5 [a SAL(3,t) component with a sequency of 3], with other major components at n = 1, 9, 13, 21, 25, 29, 53, and 57. All of these components are at odd sequencies, so the power will be located in the odd number sequencies of the PSD, and the odd numbered components will combine into one component of the Group Spectrum. Again, see Equations (3.34).

The FWT, PSD, and Group Spectrum of eight cycles of a sine wave in the Walsh interval is analyzed in Figures 3.14 to 3.16. The FWT is considerably simpler, with

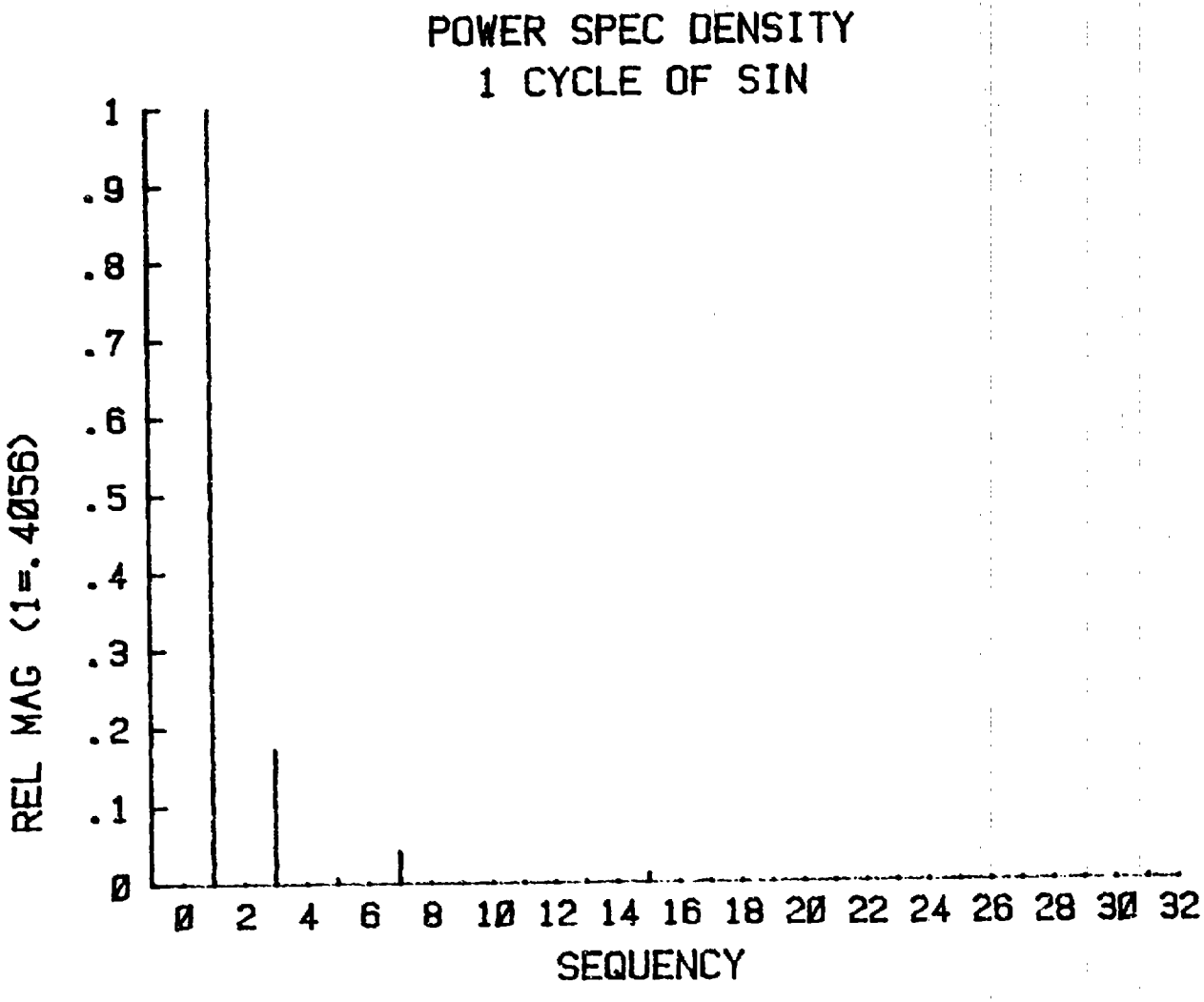

Figure 3.9. PSD of 1 Cycle of a Sine Function.

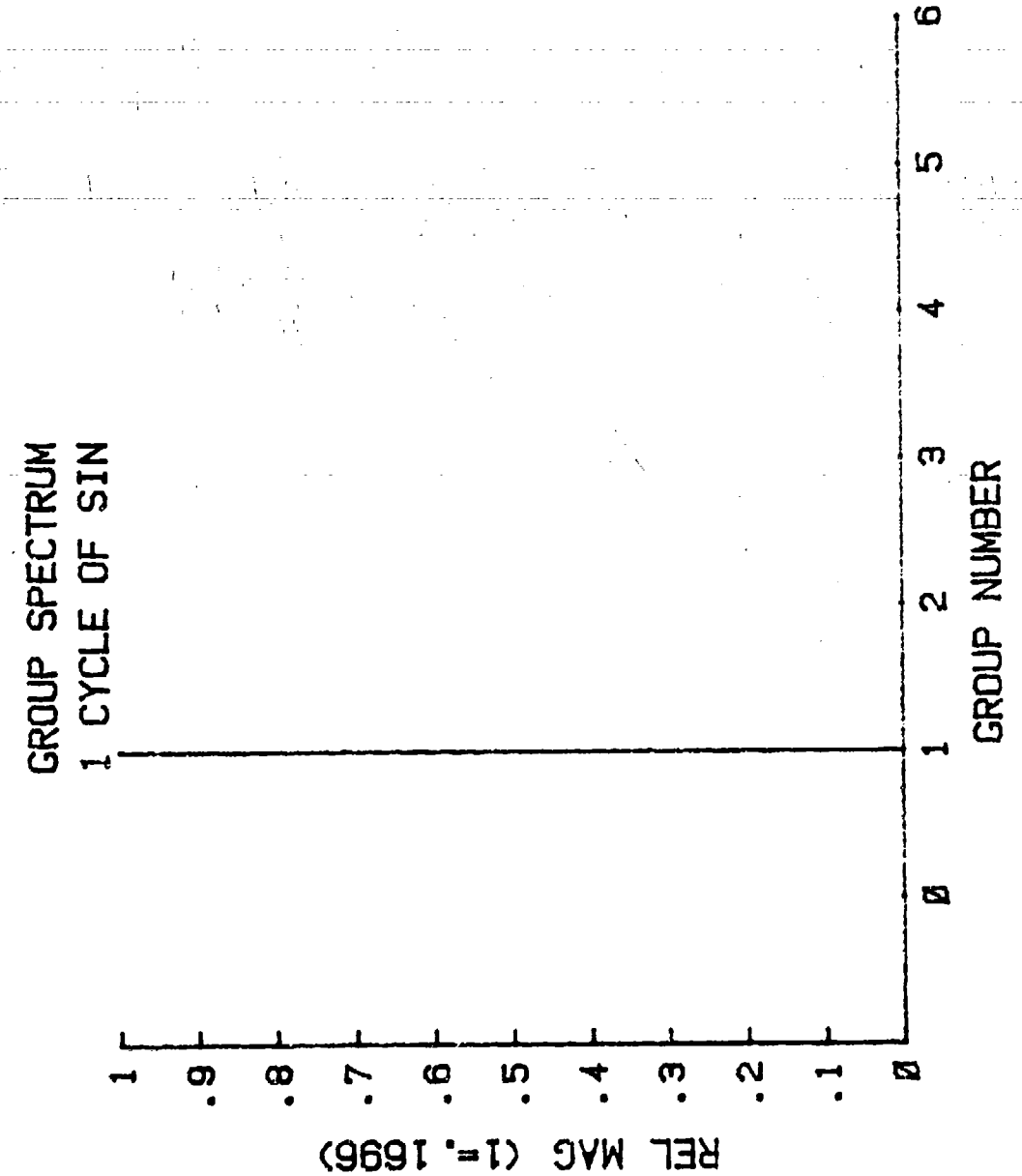

Figure 3.10. Group Spectrum of 1 Cycle of a Sine Function.

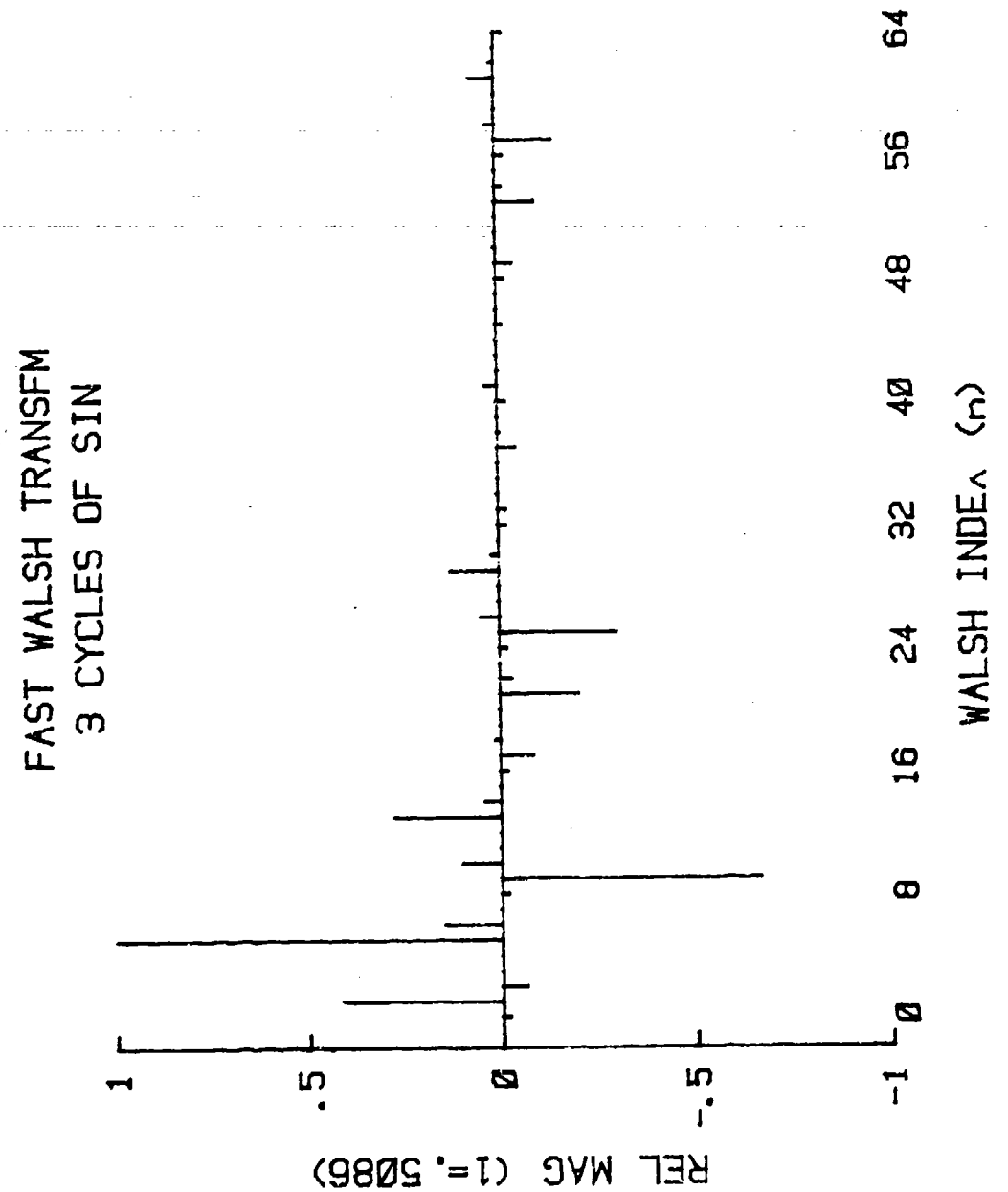

Figure 3.11. FWT of 3 Cycles of a Sine Function.

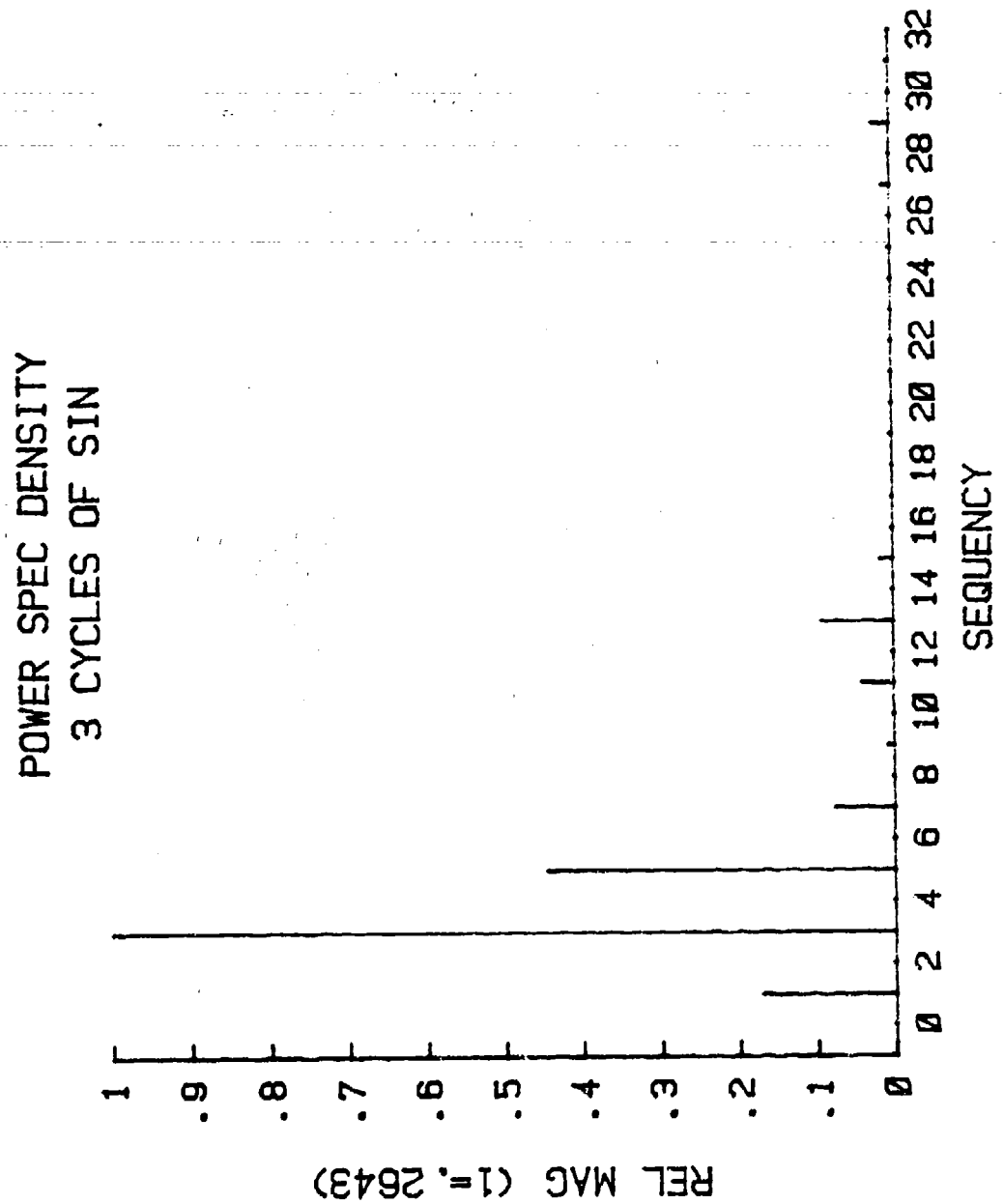

Figure 3.12. PSD of 3 Cycles of a Sine Function.

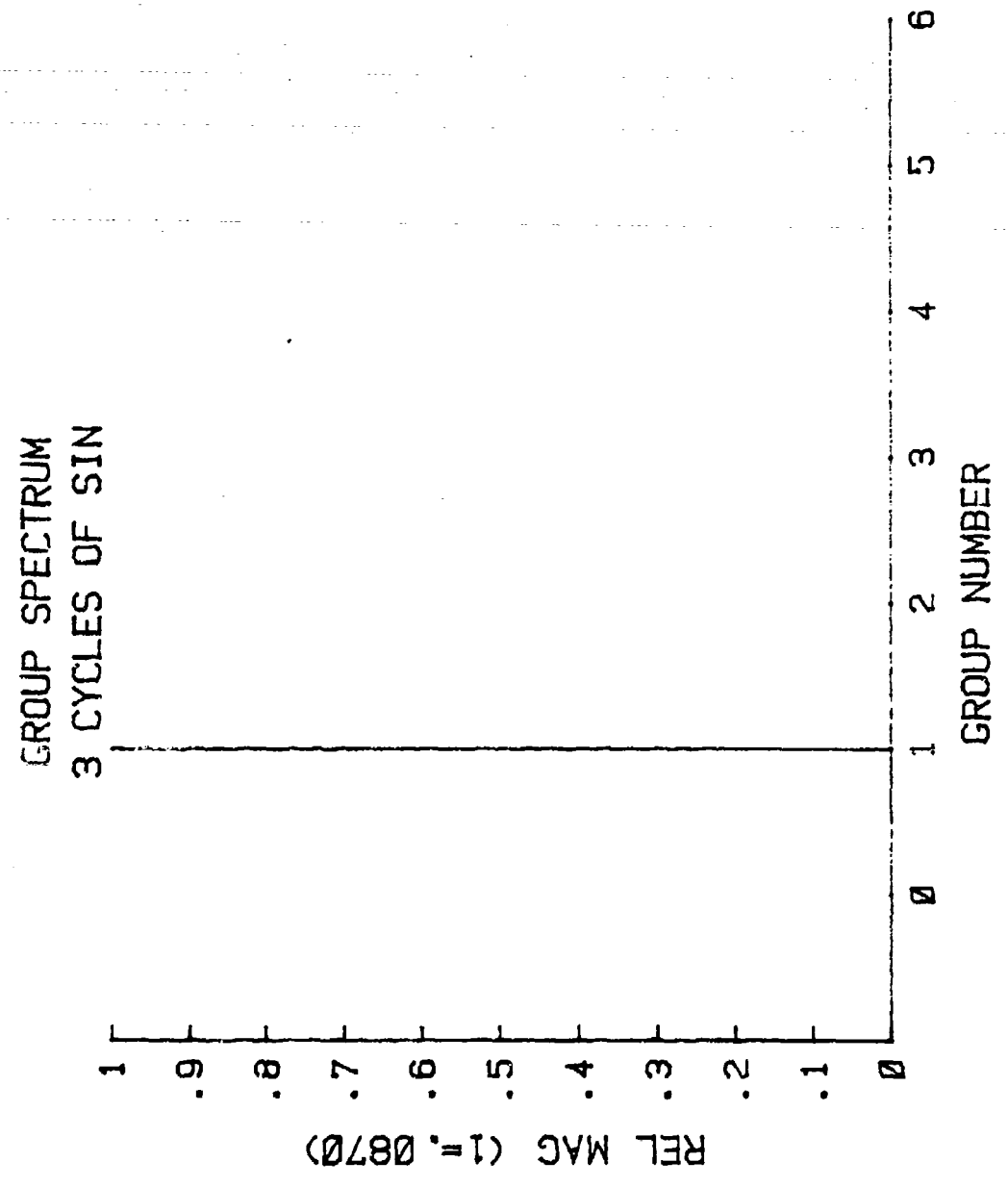

Figure 3.13. Group Spectrum of 3 Cycles of a Sine Function.

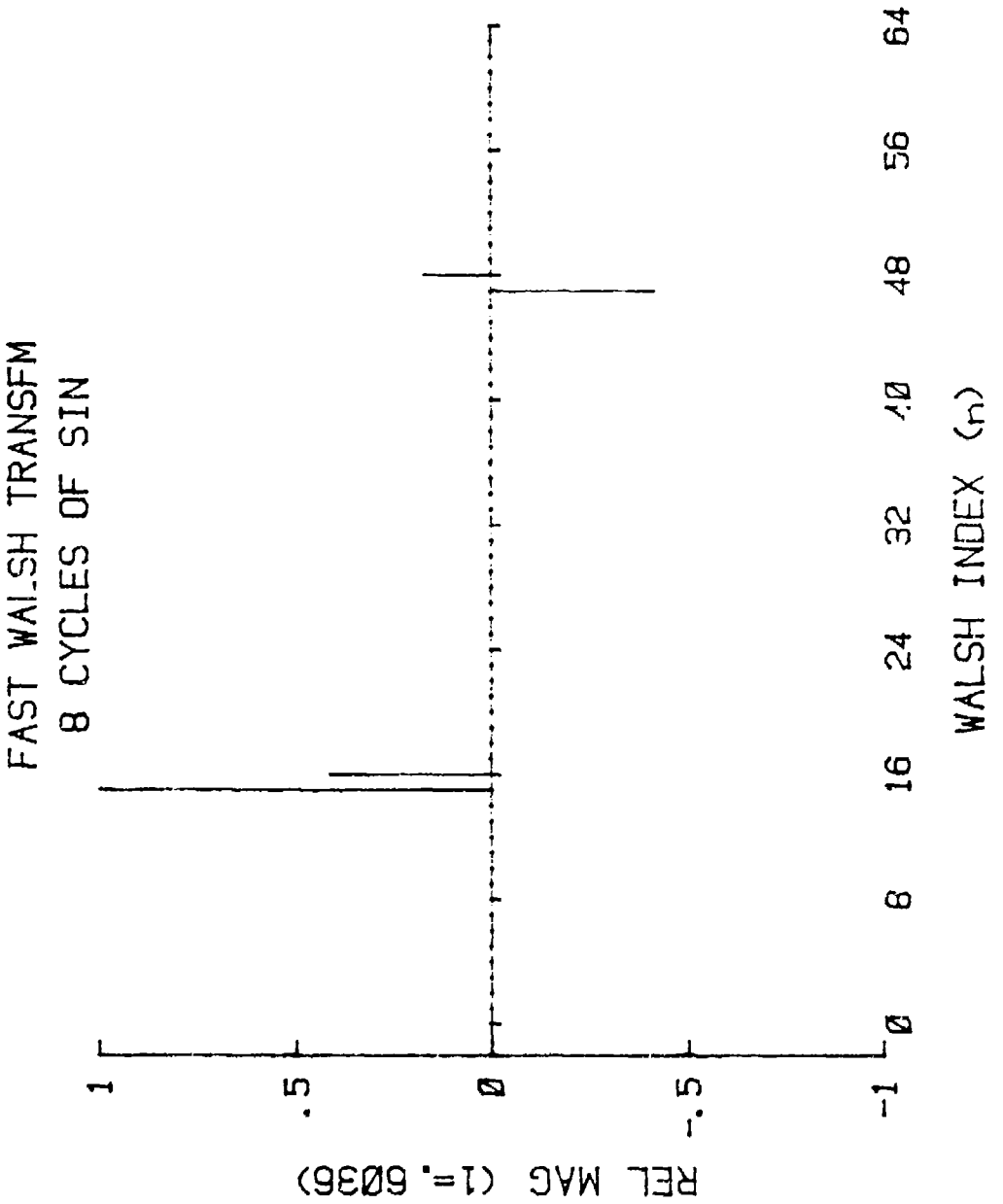

Figure 3.14. FWT of 8 Cycles of a Sine Function.

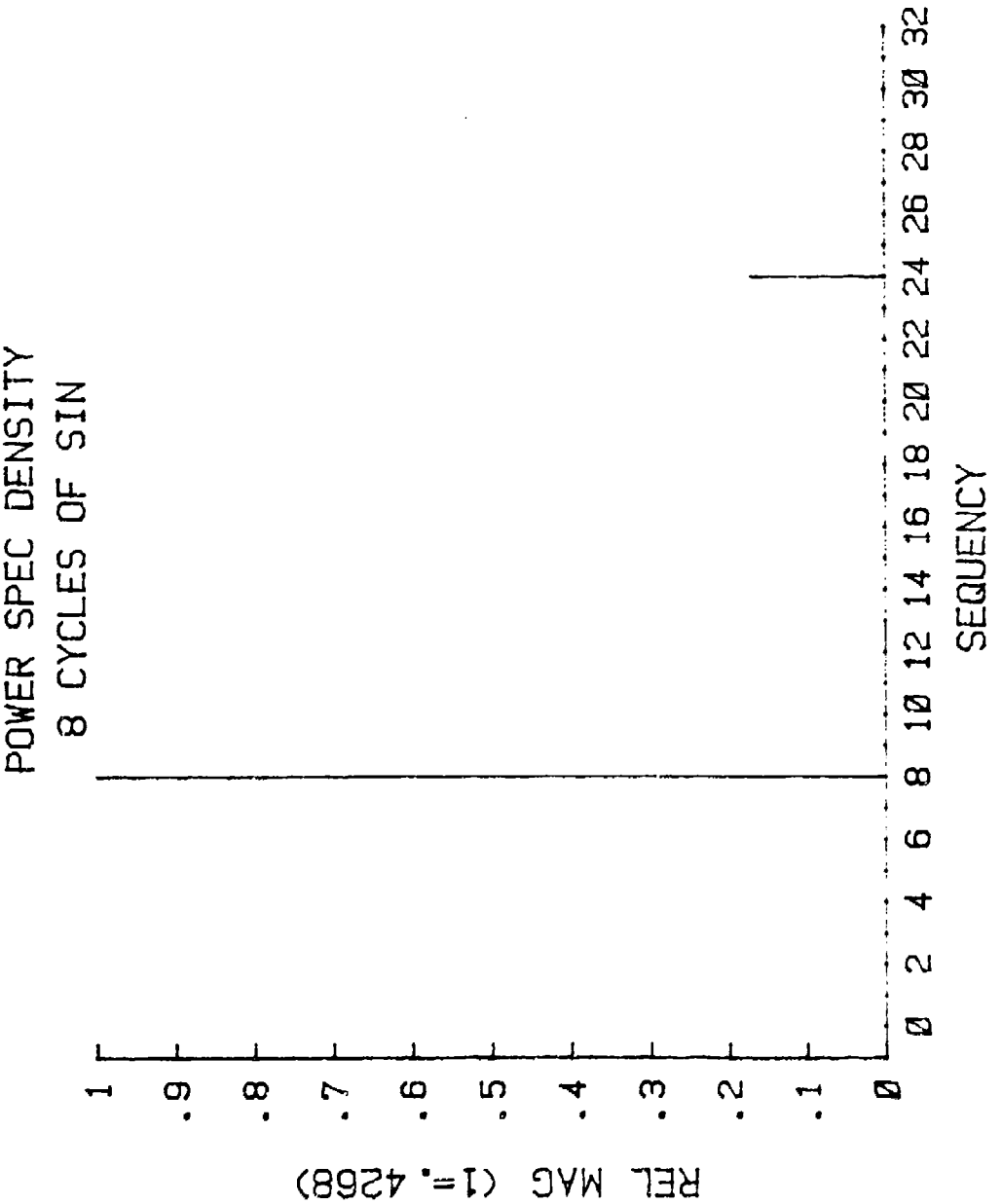

Figure 3.15. PSD of 8 Cycles of a Sine Function.

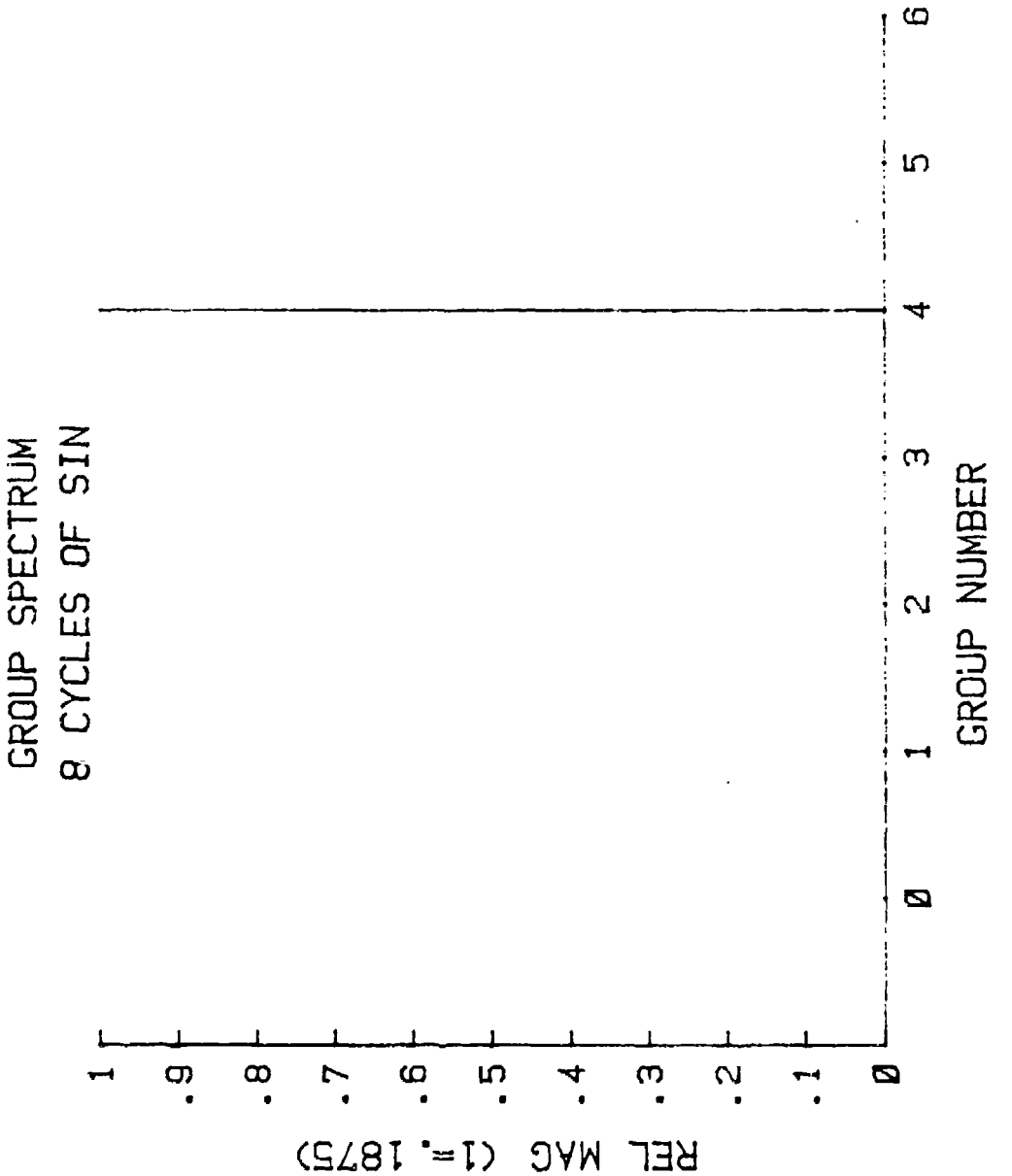

Figure 3.16. Group Spectrum of 8 Cycles of a Sine Function.

only 4 components at PSD sequencies of 8 and 24. The PSD shows the peak power at a sequency of 8 and a notable harmonic at 24. The Group Spectrum follows from Equations 3.34.

A few conclusions about the transform of a sinusoid could be drawn. The peak coefficient of the FWT falls at a Walsh index that translates to a sequency that is equal to the sinusoidal frequency. The PSD then has a component that is maximum at this sequency. In addition, this maximum power component is usually accompanied by notable components at harmonics of this sequency.

The Group Spectrum, although highly compressed and uncomplicated, requires a knowledge of the PSD for it to be useful. Note that the Group Spectrum of the 1 cycle sine wave is equal to the the Group Spectrum of the 3 cycle wave. An educated guess says that the Group Spectrum for all odd numbers of cycles would be the same, that of G_1, because only odd numbered components (Eq. 3.34) of sequency are present. Each component of the Group Spectrum could represent a series of sinusoidal frequencies, with no way to distinguish the actual frequency of the sinusoid without prior knowledge of the PSD.

b. The FWT of a Rectangular Function.

Consider the FWT, PSD, and Group Spectrum of a 4 hertz square wave. Knowing that the Walsh function lends itself readily to the reproduction of such a wave, simple

results for graphs of the transform and related computations would be expected.

Indeed this is the case. Figures 3.17 and 3.18 show the simplicity of representation for rectangular functions. The FWT component at n = 7, sequency = 4, is the only coefficient in Figure 3.17. (Note that a 4 hertz square wave is WAL(7,t)). All of the power lies at a sequency of 4 (Figure 3.18), and in a Group Number 3 (Eqn. 3.34). With a proper number of samples, any square wave of a particular frequency would be represented with similar characteristics.

A rectangular function, page 73, composed of square pulses was expanded in a Walsh Series in this chapter. Consider the FWT, PSD, and Group Spectrum of the function.

Figures 3.19, 3.20 and 3.21 show the results of the computation. These graphs are not normalized in order to show the similarities with the previously computed example on page 73. The FWT shows 2 coefficients of 0.5 magnitude, at n = 0 and n = 2, matching the results determined before. Since the FWT outputs coefficients based on positive phasing, this result is correct.

The power contained in the function is in the DC term and the first sequency component as shown in Figure 3.20. These sequency components result in 2 components in the Group Spectrum. See Equations 3.34.

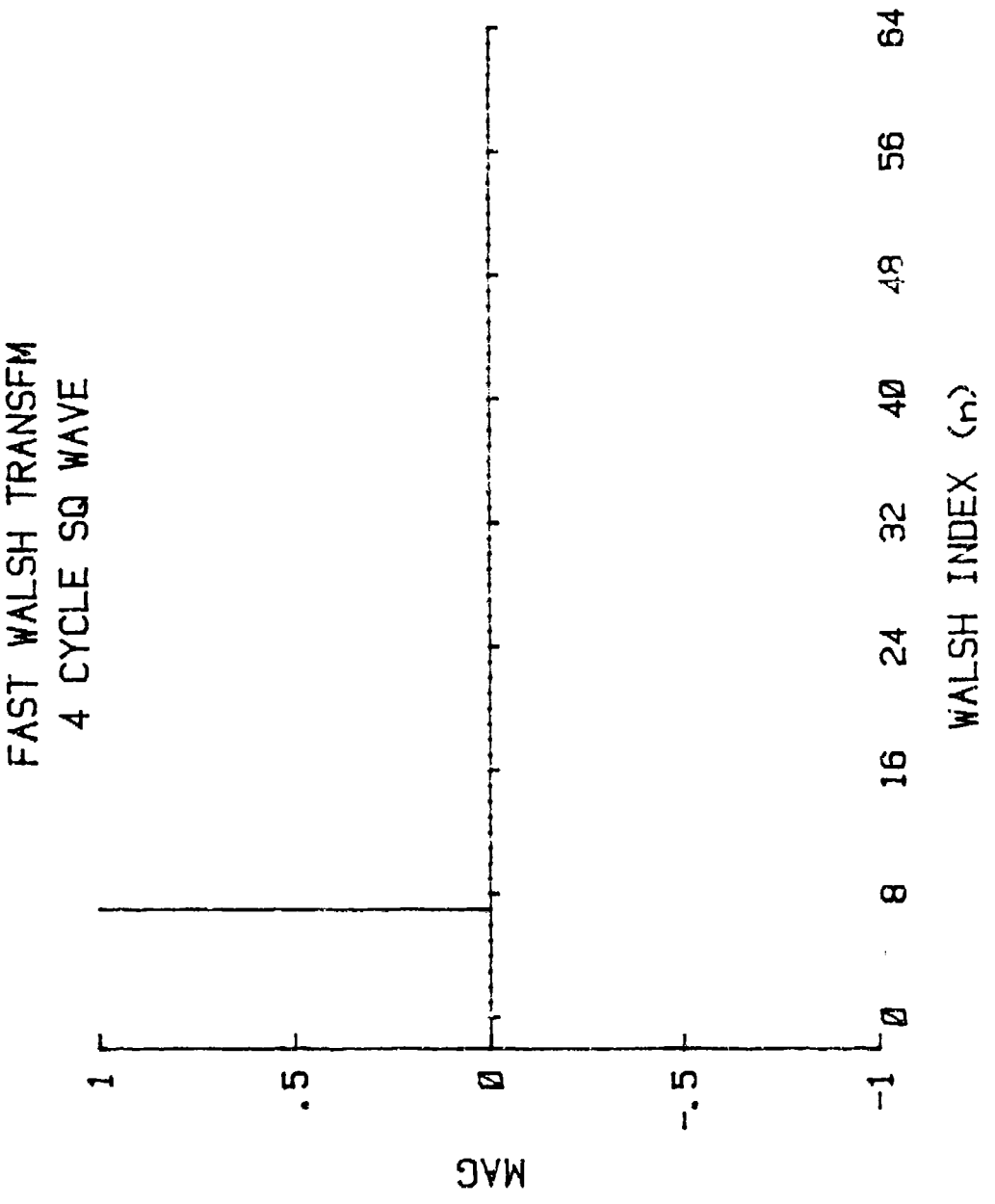

Figure 3.17. FWT of a 4 Cycle Square Wave.

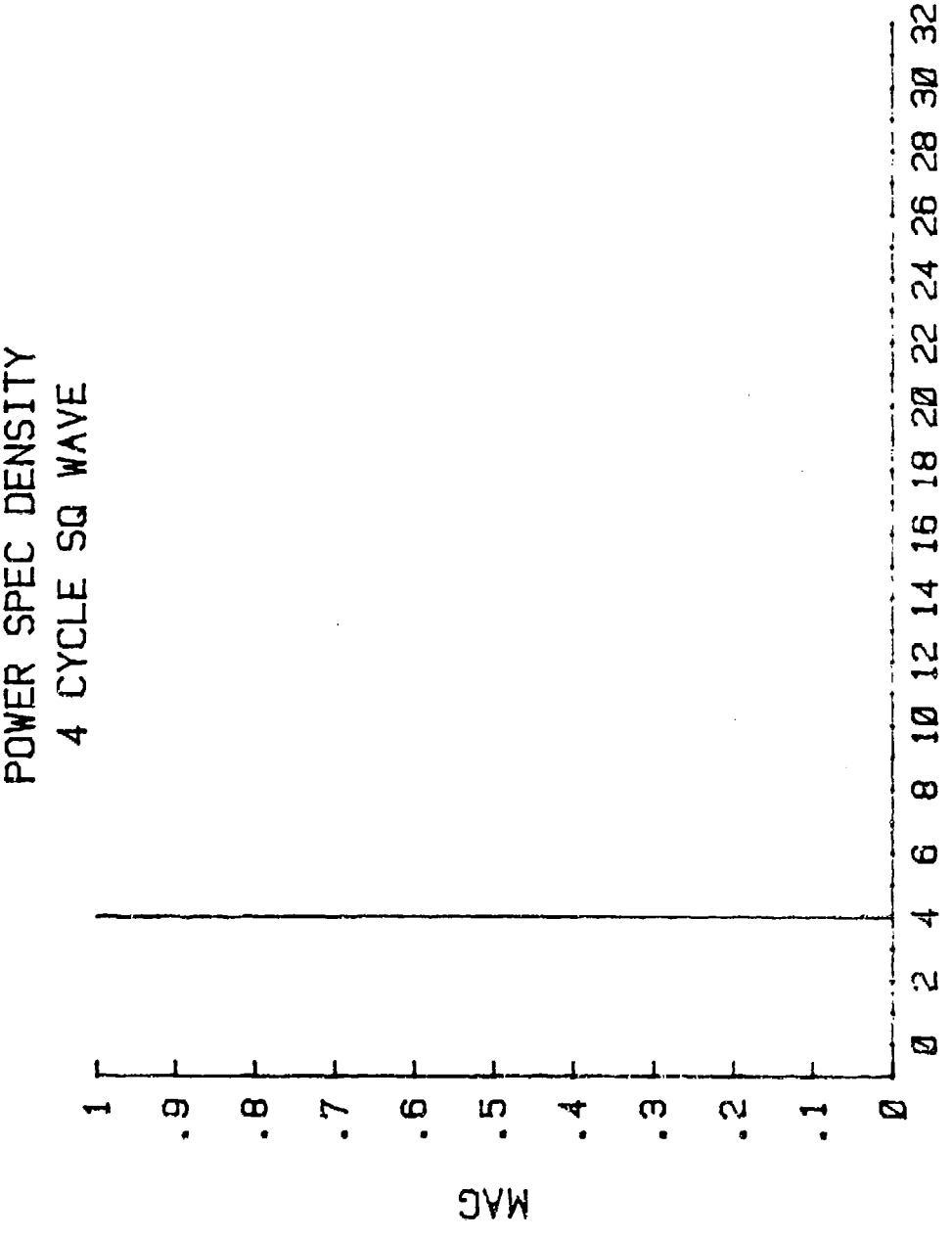

Figure 3.18. PSD of a 4 Cycle Square Wave.

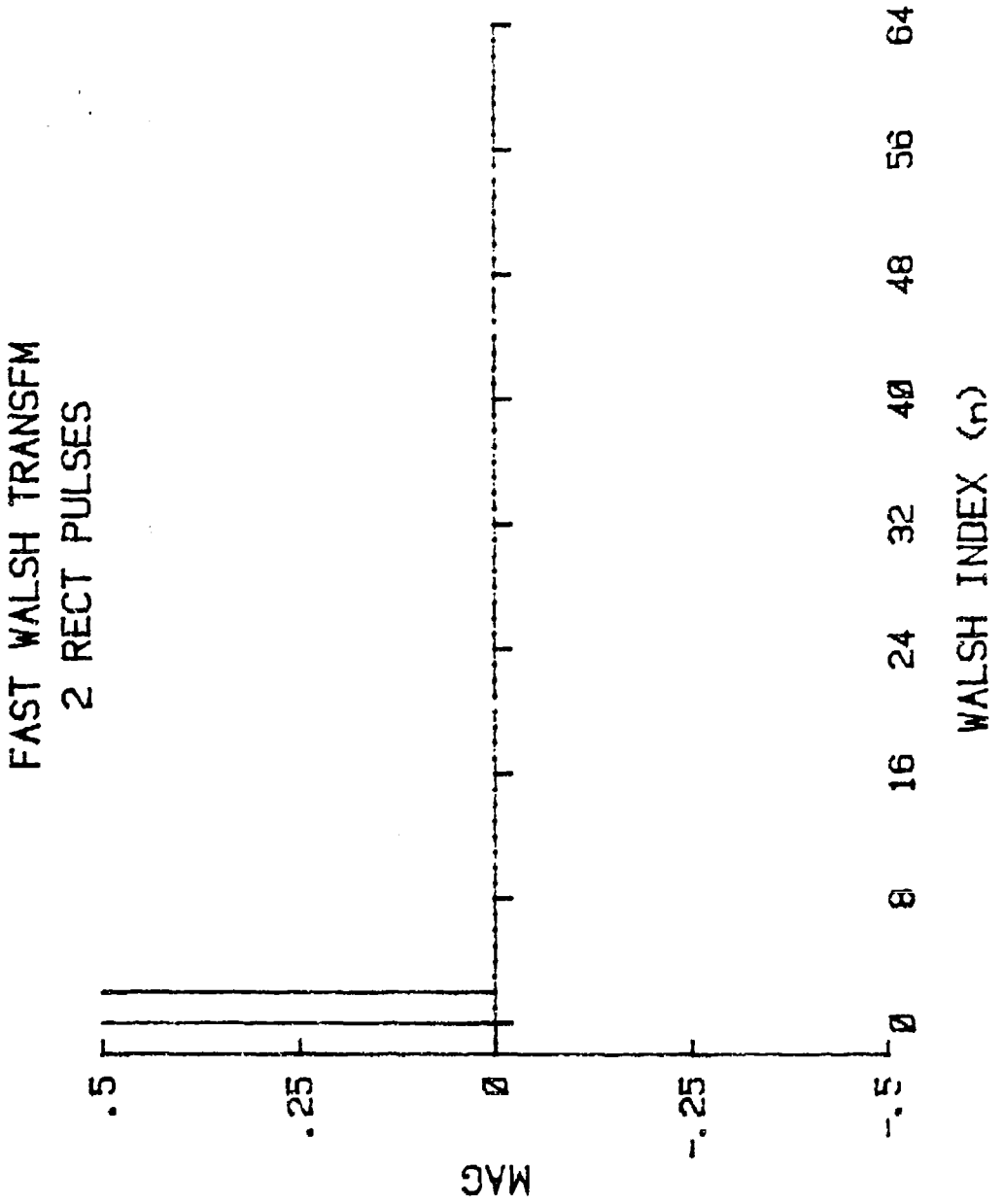

Figure 3.19. FWT of a 2 Rectangular Pulses.

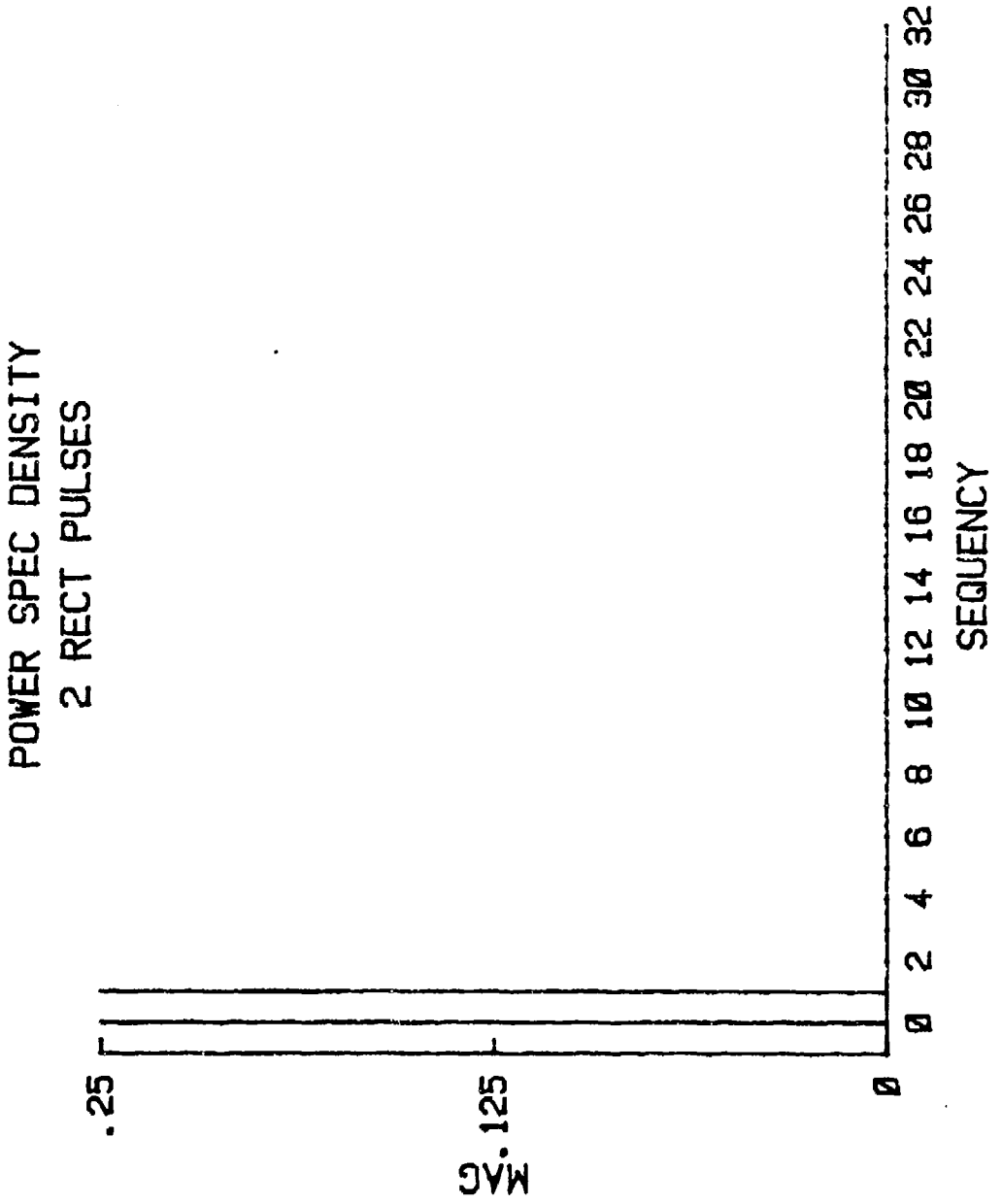

Figure 3.20. PSD of 2 Rectangular Pulses.

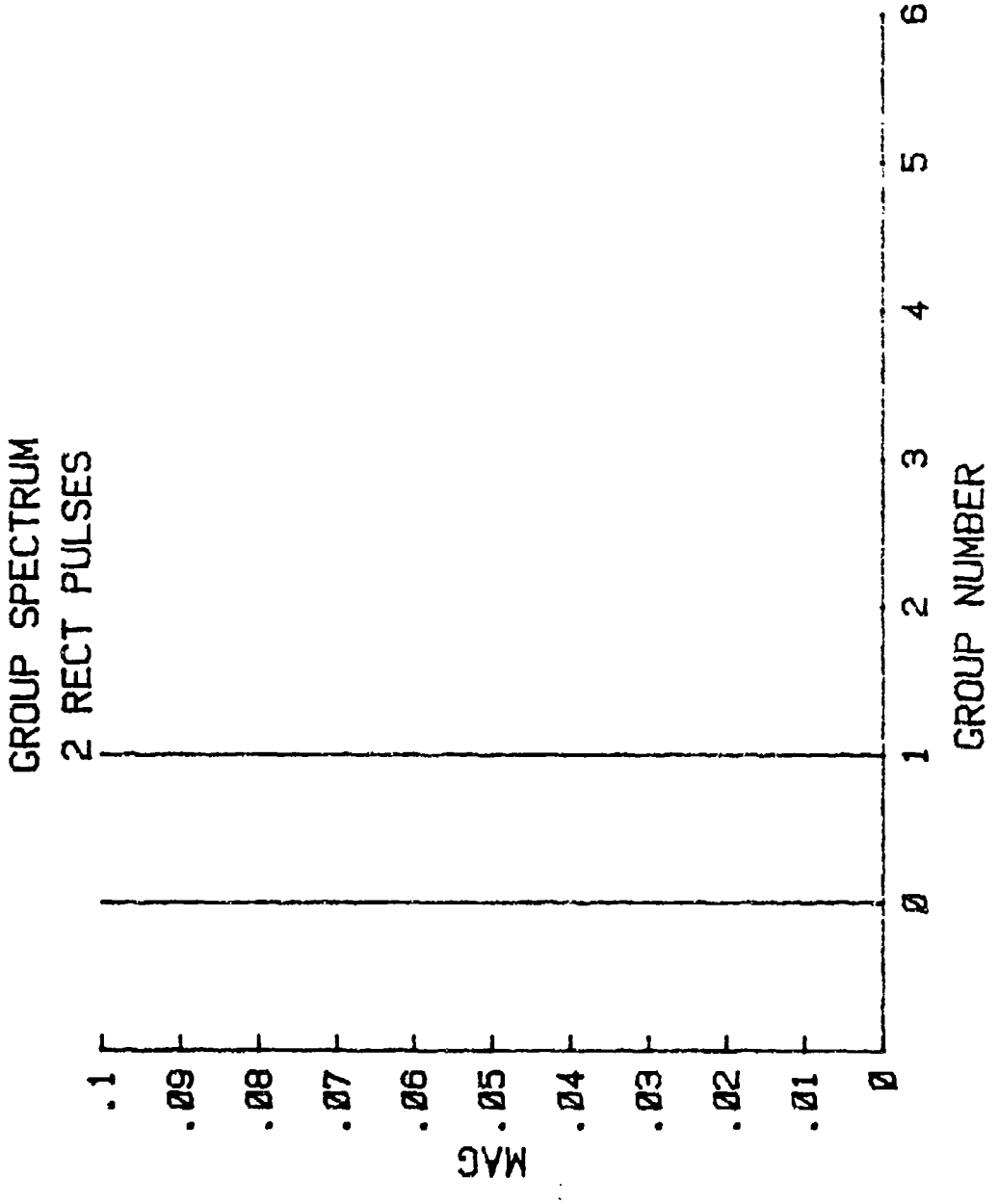

Figure 3.21. Group Spectrum of 2 Rectangular Pulses.

c. The FWT and a Input Time Shift.

Section 4-c stated that the Discrete Walsh Transform is not invariant to a time shift or phase shift of the input. Let sin(t) be circularly shifted $\pi/4$ to $\sin(t-\pi/4)$. Now examine Figures 3.22, 3.23, and 3.24 and compare with Figures 3.8, 3.9, and 3.10.

Note the shifted FWT coefficients pattern is more complex. A sizable component now lies at n = 2. This is a CAL(1,t) component with a sequency of 1. The unshifted FWT graph contained only a negligible CAL(1,t) component. Double components at n = 5 and 6, 13 and 14, and 29 and 30 represent sequencies of 3, 7, and 15, respectively, the same components that were contained in the unshifted sinusoid, but the magnitudes of the components at the same index [n] are not equal.

Although the FWT magnitudes are different at each index [n] of the shifted and unshifted sinusoids, remember that adjacent components combine to form a PSD coefficient of a particular sequency. The components vary in a reciprocal manner, so when they are squared and summed, the time variant effect is indeed lessened [23: p.89]. The result is a PSD that has sequency components that are very close to being time invariant.

One expectation that was revealed to be true was the time invariance of the Group Spectrum. Beauchamp [23: p.106] states this spectrum is time invariant to time shifts

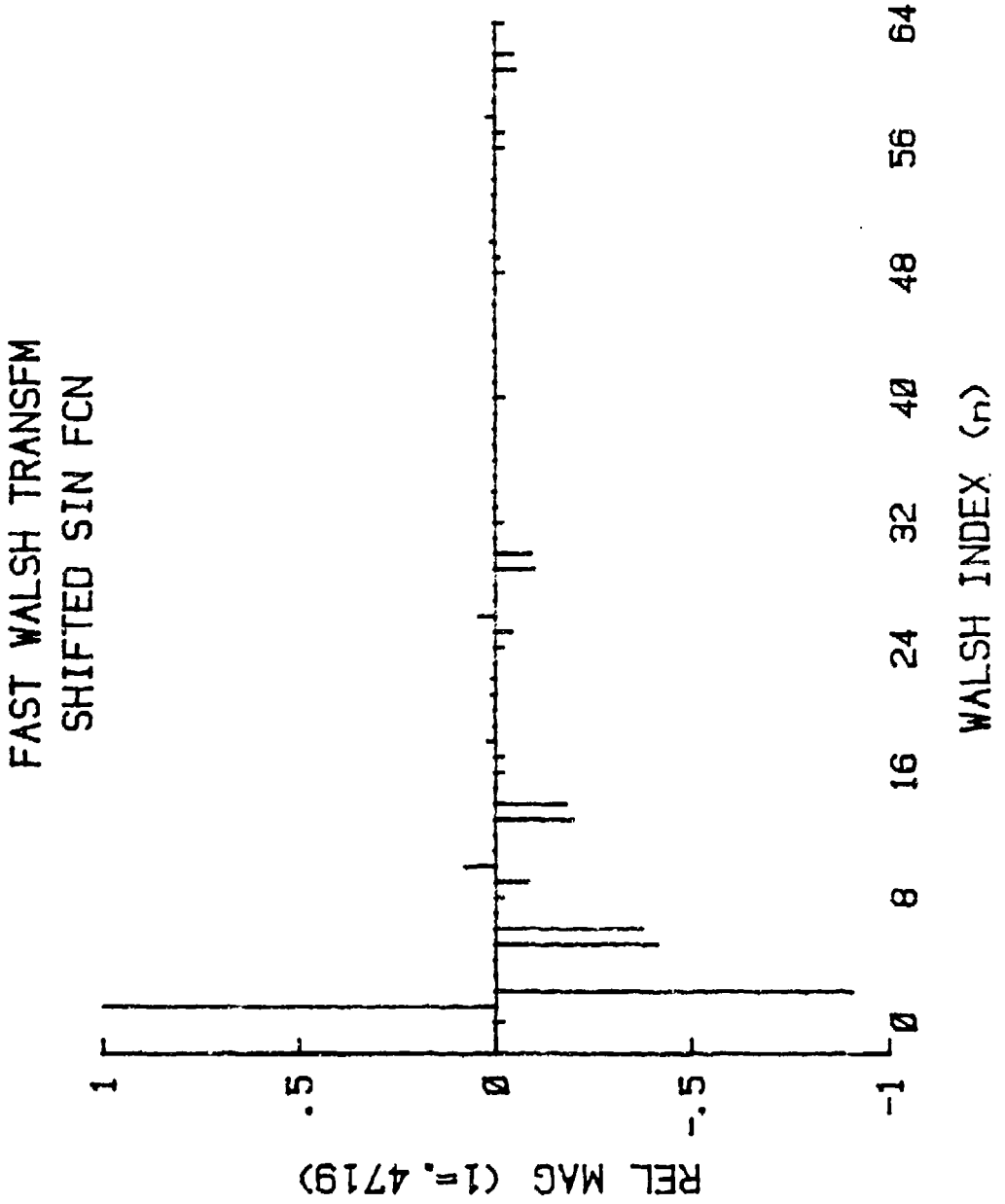

Figure 3.22. FWT of a Shifted Sinusoid.

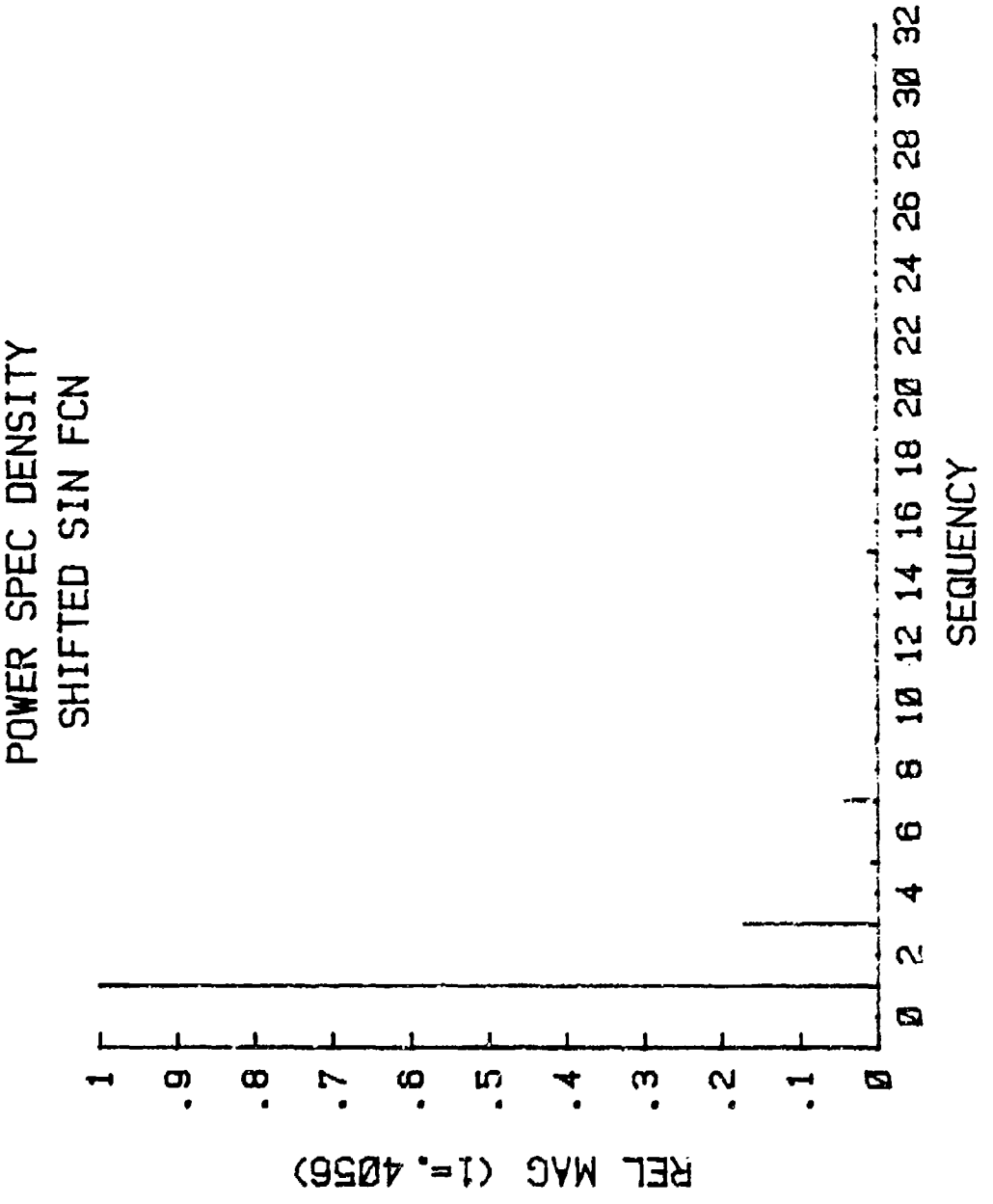

Figure 3.23. PSD of a Shifted Sinusoid.

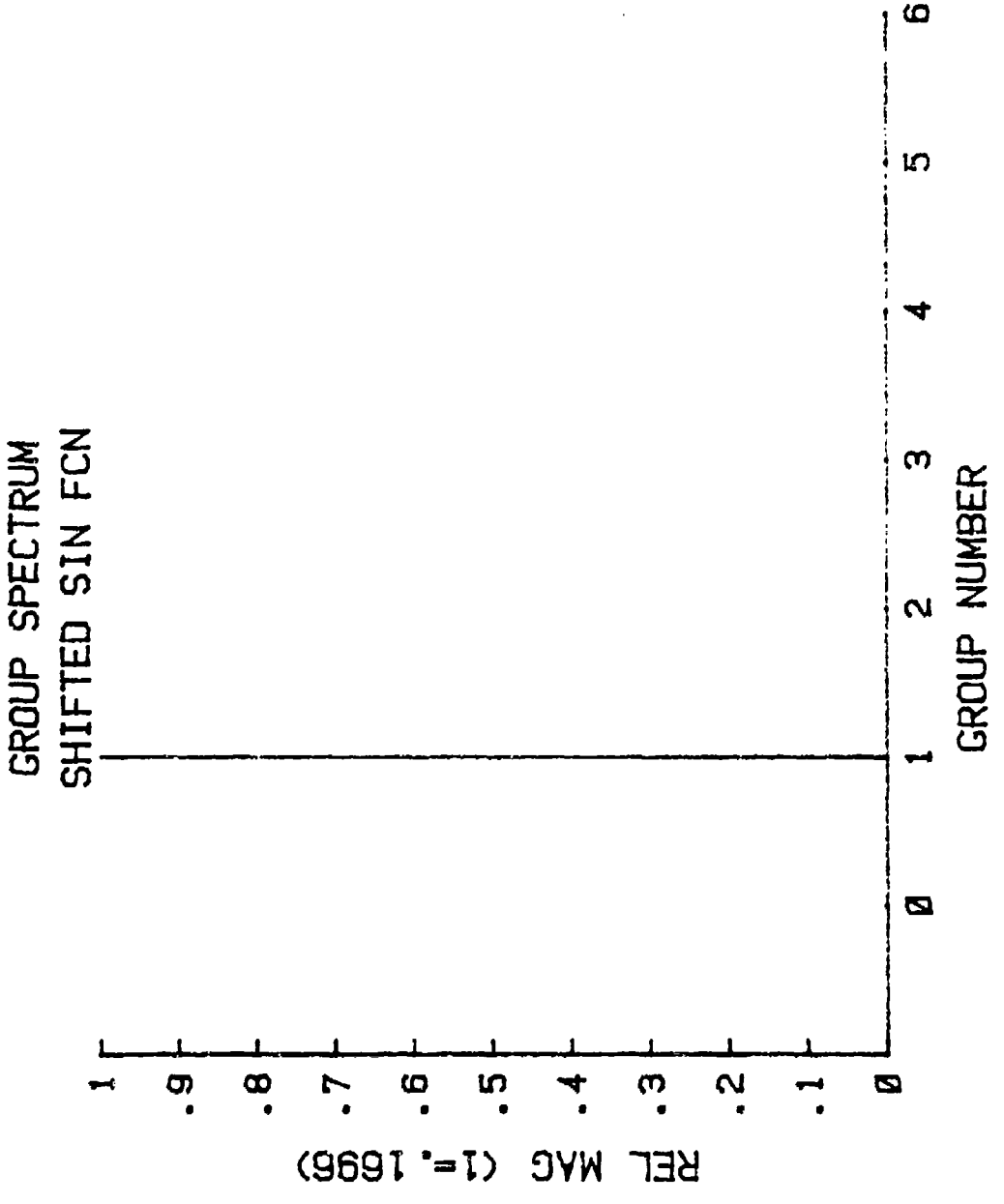

Figure 3.24. Group Spectrum of a Shifted Sinusoid.

of the input, and examination of Figure 3.23 and its magnitude gives an affirmative response to his assertion.

The rectangular pulse function will positively demonstrate the effects of time shift. The FWT, PSD, and Group Spectrum of Figure (3.25a) is shown in Figures 3.19, 3.20, and 3.21. The FWT and associated spectrums of Figure (3.25b) is shown in 3.26, 3.27, and 3.28.

Quite a difference in the FWT of the shifted function can be noticed. The coefficient pattern is much more "spread out", and the magnitudes of the prominent coefficients at n = 0 and 1 are less in the shifted rectangular function.

The PSD's are different also. With the power being spread among more sequencies in the shifted rectangular function, the magnitudes of the power coefficients at 0 and 1 are reduced.

The Group Spectrums are not alike in this case. The two input sequences to the FWT program are made up of samples of the original function and the shifted function. These sequences are not alike and generate different Group Spectrums.

Has Beauchamp's assertion [23: p.106] been violated? The answer is no. In the sinusoidal shift, it was assumed that the function was periodic outside the interval $0 \leq t \leq 1$ over which the Walsh functions are defined and over which the function was taken. When the sinusoid was shifted, the part shifted out of the interval "wrapped around" into the

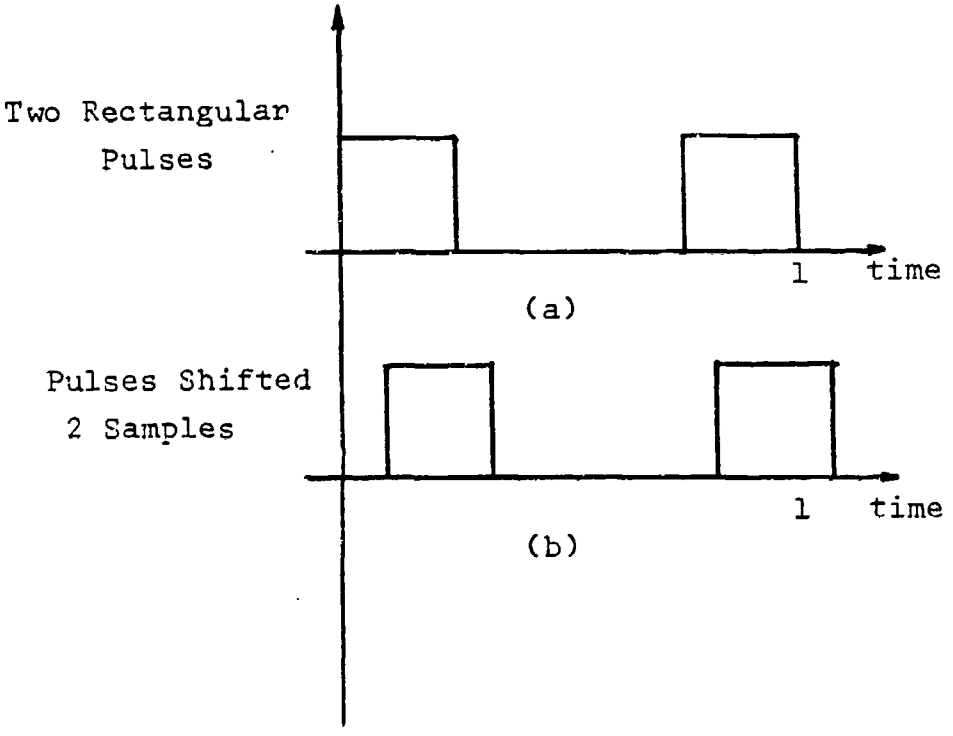

Figure 3.25. Two Rectangular Pulses, Shifted and Unshifted.

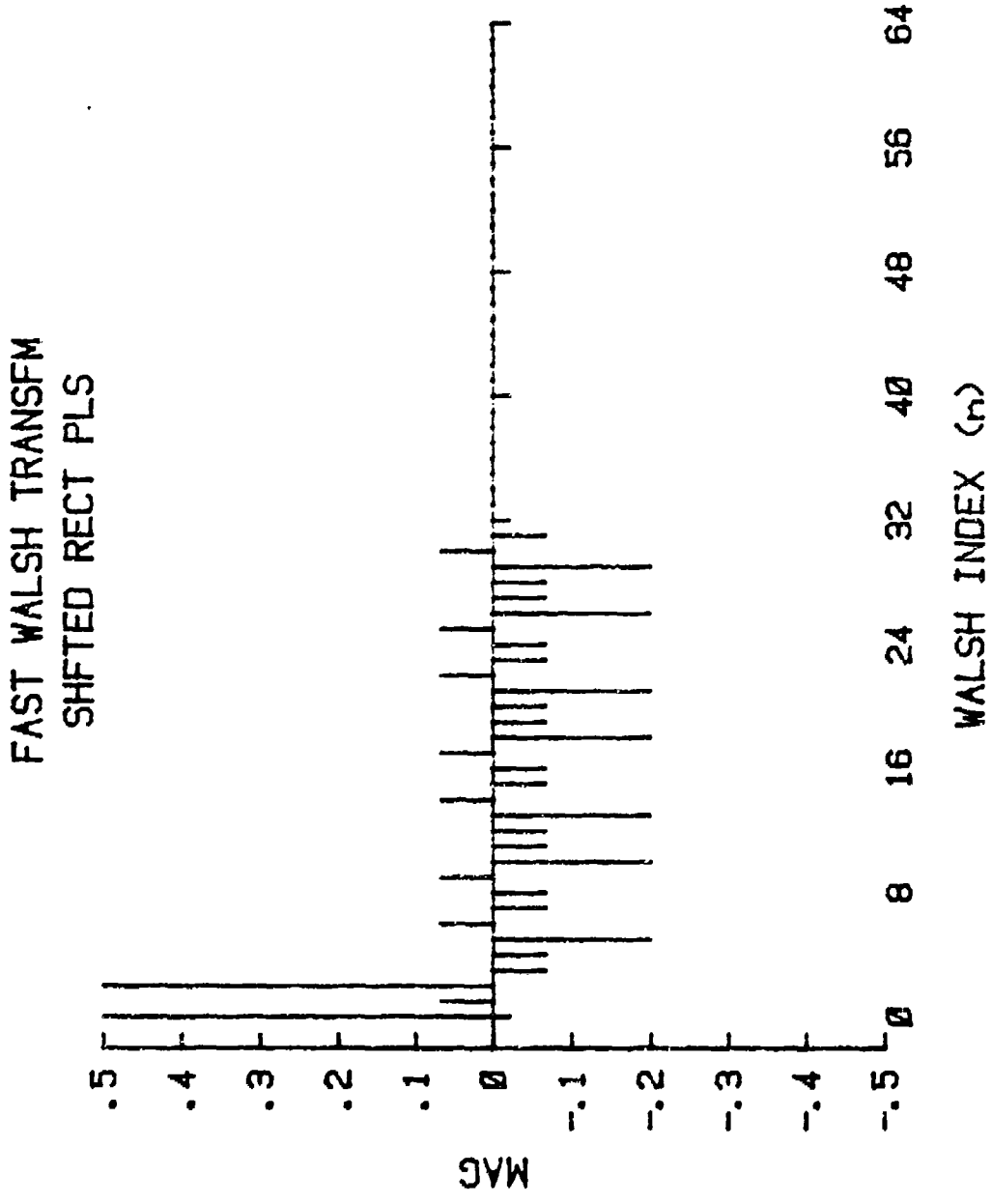

Figure 3.26. FWT of Shifted Rectangular Pulses.

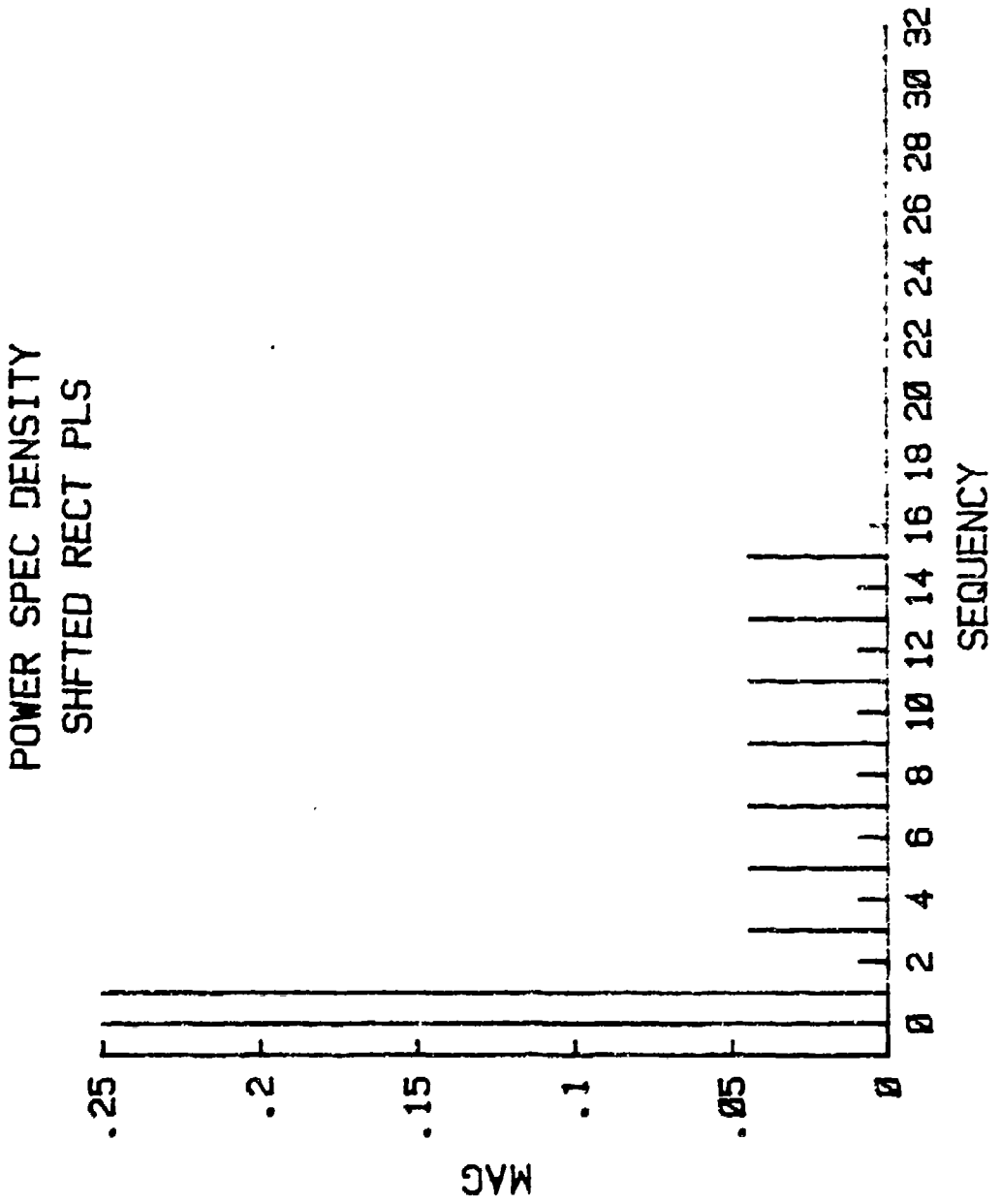

Figure 3.27. PSD of Shifted Rectangular Pulses.

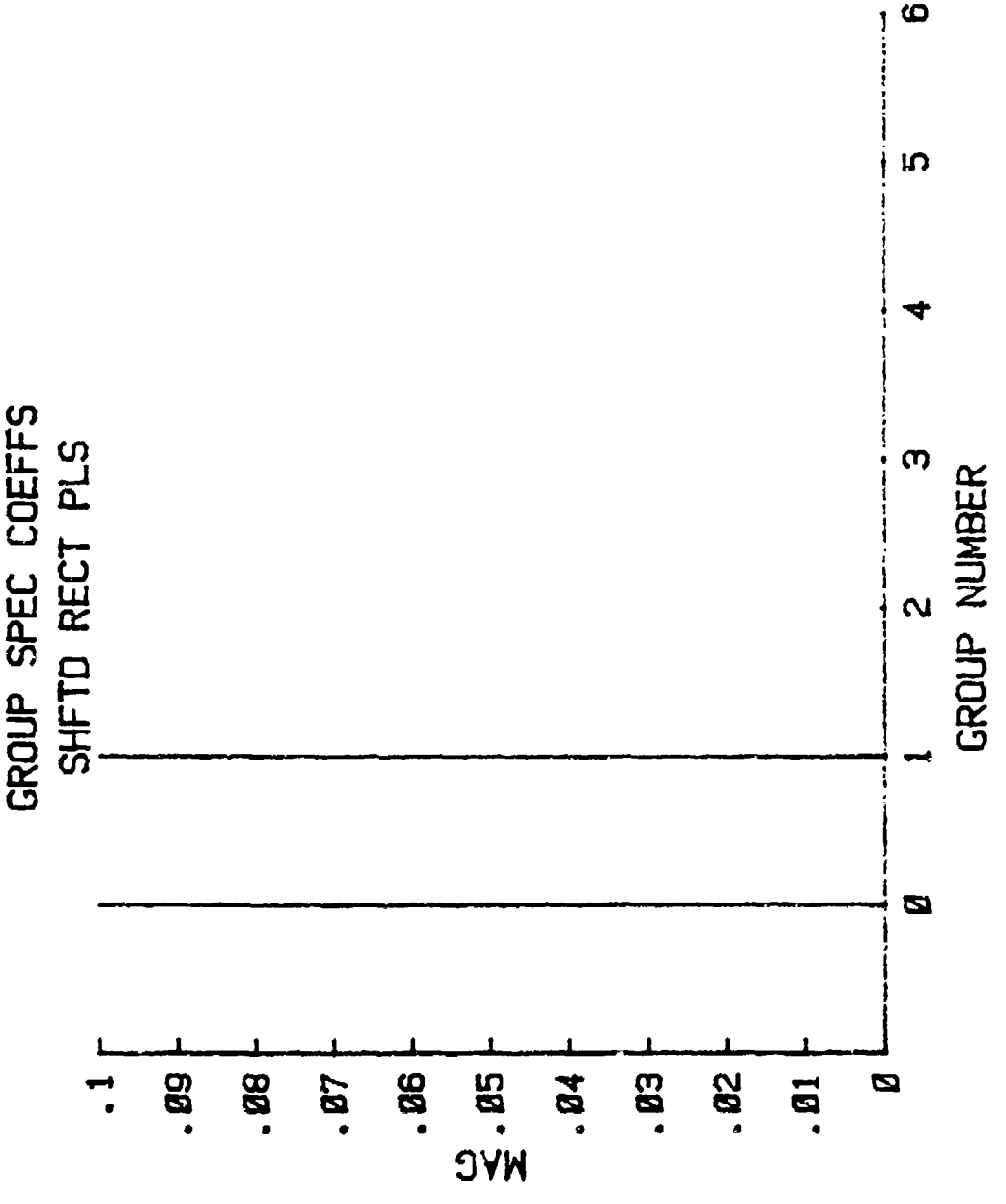

Figure 3.28. Group Spectrum of Shifted Rectangular Pulses.

first part of the interval (circular shift), resulting in the shifted function having the same power as the unshifted function.

However, the rectangular function wasn't defined as a periodic function, merely two pulses in an interval. When the rectangular function was shifted, the part that shifted outside the interval wasn't wrapped around to the front (not circularly shifted) and was lost, decreasing the total power found in the shifted function. The PSD or the Group Spectrum could not be the same as the unshifted function, since the amount of total power is different in each of the functions.

A conclusion is made that the Group Spectrum is time invariant to phase shifts in the input for periodic circular shifted functions only.

IV. THE WALSH TRANSFORM AND DEINTERLEAVING

The first two chapters presented some background for the appreciation of the role of ESM and the basic components of a typical ESM system. Understanding the tools and purpose of the trade, though, only gives a small insight into the nature of problem.

There's a lot of electromagnetic radiation out there! The combat environment presents an overwhelming amount of energy that has to be collected, analyzed, and sorted. The data stream pours into the system from all angles, with numerous frequencies and amplitudes. Corruptions, disturbances, reflections, and missing pulses make the deinterleaving process a most difficult problem. Today's techniques, described in Chapter Two, do a good job, but improvements are needed and sought after.

Unique in many respects, the Walsh Functions, which are described in Chapter Three, are examined for their usefulness in deinterleaving pulse trains into separate chains of pulses with different pulse repetition intervals. More specifically, this chapter attempts to determine if there is a PRI/PRF recognition feature in the Walsh Transform of the data presented by an ESM receiver.

A. REPRESENTATION OF ESM RECEIVER DATA

The operating element of the typical deinterleaving process is a computer data word (or words) of some format appropriate to the system.

The data word contains values of the initial parameters measured by the system, and basically these values are examined for matches in previously analyzed pulses. Software processing systems make these comparisons and places words of similar parameters into cells or histograms, patiently waiting until enough pulse information can be found to make an identification. Other algorithms process the data word and make calculations of PRI's, adding a new sorting parameter that is used in the deinterleaving process.

The investigation of deinterleaving with the FWT will need a different symbology for the receiver data, since the FWT operates on a series of N numbers, not a data word, to obtain the transform.

Imagine an absolute time line that consists of some point in the past, and ends at the present. Consider a received pulse as being represented by a vertical line stationed at the time of arrival (TOA) of that pulse. The height of the line could be made proportional to the amplitude of the received pulse. The point on the time line where the pulse "stands" is the time of arrival of the pulse.

Figure 4.1 looks like a messy situation, but there are really only four pulse trains of different PRI's on the line.

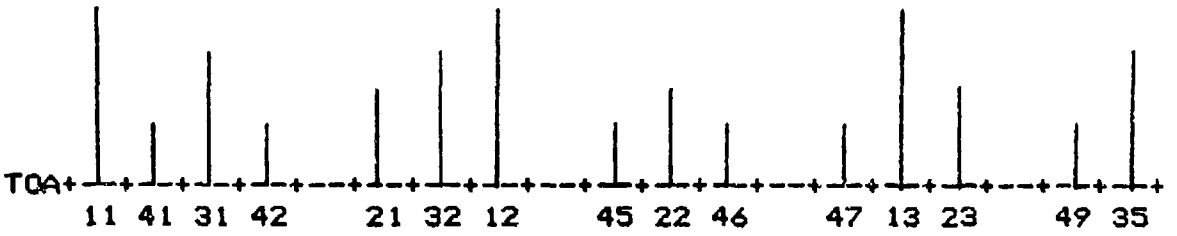

Figure 4.1. TOA representation of received pulses.

PRI's could be calculated by subtracting successive TOA's of pulses in the same pulse train.

$$PRI_1 = TOA_{12} - TOA_{11}$$
$$PRI_2 = TOA_{22} - TOA_{21}$$
$$PRI_3 = TOA_{32} - TOA_{31}$$
$$PRI_4 = TOA_{42} - TOA_{41}$$

This procedure is used when other parameters are present to identify the pulses.

Keep in mind that there is a steady stream of these pulses into the ESM system. In order to make things manageable, the number of pulses being examined has to be reduced.

Lemley [20 : p.12] calls this reduction mechanism the "presorting aperture." It is of variable width to accomodate high and low density environments and is similar to the time slice concept discussed under deinterleaving in Chapter Two. It reduces the number of pulses being processed at one time.

Another way of thinking of this reduction concept is to visualize a "window" on the stream of pulse lines. Only a certain number of pulse lines can be present in the window at anytime, and deinterleaving operations are carried out on

these pulse lnes. The window can be divided into small time intervals, which could be analogous to the TOA resolution specification of a receiver (usually 100-200 nanoseconds). If a pulse line is present in the time interval, a number proportional to the amplitude is generated for the pulse line representation. If not, a zero is used.

The author prefers to visualize that the receipt of a pulse triggers the collection of the next N time intervals for analysis and deinterleaving. Each interval could contain a pulse or not.

B. CONSTANT AMPLITUDE TOA STRINGS AND THE FWT

This chapter will work mostly with N = 64 intervals and pulse line representations. N must be a power of two to be used in the FWT.

The pulse line representation can be symbolized for computer work with the BASIC language DATA statement. Using the statement on the 64 pulse lines in the window gives a representation that accounts for the two variables that are present in the pulse line stream, the amplitude and TOA of the pulses.

Such a DATA line for Figure 4.1 would be

```
DATA  1,.3,.75,.3,0,.5,.75,1,0,.3,.5,.3,0,.3,1,.5,0,.3,.75
```
(4.1)

Each number represents the amplitude of a recognized pulse that occupies a TOA time interval.

Think of it in one of two ways:

1. The receiver outputs a measured value of a pulse amplitude each TOA resolution time interval. If no pulse was present, it outputs a zero. Or,

2. The receiver outputs a pulse amplitude only upon detection and analysis of a pulse. Time intervals of TOA resolution width in between pulse detections can be represented with zeroes.

Either way, the DATA line looks like (4.1).

Assume for simulation's sake that the period between DATA numbers is a known value of time, and the DATA line represents the output of an ESM receiver to the preprocessor. The numbers indicate amplitude of the received pulses, and their distance in intervals between similar pulses is a measure of their PRI's.

Things can be simplified a bit further by considering all pulse lines of the TOA string to be of the same amplitude. Only one variable would then be present in the string, the TOA.

A DATA line representation of a string of this type is

DATA 1,1,1,1,0,1,1,1,0,1,1,1,0,1,1,1,0,1,1, (4.2)

In short, this TOA string and its DATA representation is merely an indication of the receipt of a pulse or not during the resolution time interval.

A number of Fast Walsh Transforms were run on simulated DATA TOA strings, and plots of the coefficients were made. The Power Spectral Density and Group Spectrum coefficients were

also calculated and plotted. All of the Group Spectrum plots are not included, as the emphasis of this examination was placed on the FWT and PSD. Some of them are discussed in Section C of this chapter.

The plots are grouped by type (FWT or PSD) in Appendix D. Each plot is normalized by dividing all coefficients by the maximum coefficient. Actual values of the coefficients can be determined with the scale on the vertical axis. The maximum component's magnitude is shown in parenthesis.

These plots show the index number and sequency of the FWT and PSD components, respectively, but only their relative magnitude with respect to the maximum component. Keep that in mind when examining the plots. Where important, the FWT and PSD are replotted with the actual magnitudes on the vertical axis.

These DATA representations simulate single PRI pulse trains received by an ESM system. Note the number of intervals between successive pulses is indicated in the title of the plot. To calculate a simulated PRI of the train, simply multiply the number of intervals between sucessive pulses by the time interval resolution, a known value and a function of the receiver.

The plots are examined by type in the following sections, and conclusions are reached and reported. These single PRI representations are the building blocks for the interleaved pulses that are investigated later in the chapter.

1. Fast Walsh Transforms of the TOA Strings

An examination of the FWT's separated them into two groups of similar characteristics.

The first group is composed of FWT's with intervals between pulses that are even numbers. Examine each plot in Appendix D (page 176 to 197) and note that each even interval FWT is symmetrically even about a point midway between n = 31 and 32. Also, if the even number is a power of two (p.o.t.), the FWT is considerably less complex. Each successive p.o.t. interval is composed of the addition of a pair or pair of coefficients to the previous p.o.t. FWT, and its magnitude is one half the previous p.o.t. FWT.

For example, one pair of coefficients is added to TOA TAG 2 at n = 31 and 32 (sequency of 16) to form TOA TAG 4. Two pairs of coefficients, (n = 15 and 16, n = 47 and 48) are added to TOA TAG 4 to make TOA TAG 8, 4 pairs to make TOA TAG 16, etc. At N = 64, enough pairs of coefficients have been added to have one coefficient for each [n].

The odd numbered intervals do not have symmetrical characteristics. In addition, the highest relative magnitude Walsh index component or components seem to bear no relation to the interval number and thus the PRI of a pulse train. (An unfortunate conclusion for PRI recognition.)

Close scrutiny of both appearance groupings was made in an effort to notice a feature that is distinctive to the particular similated PRI. There doesn't seem to be any

present, either in magnitude or coefficient distribution, that is obvious without a detailed examination.

Of initial interest to the author was the magnitude of the WAL(0,t) component. This magnitude seemed to be related to the number of resolution intervals between the pulses. It holds for most but not all cases. Consider Table 4.1 which lists the TAG number and the WAL(0,t) component.

Table 4.1. Amplitude of WAL(0,t) and TAG No. Inverse

TOA TAG no.	WAL(0,t) amplitude	TAG no. inverse
1	1.0	1.0
2	0.5	0.5
3	0.34375	0.3333
4	0.25	0.25
5	0.203125	0.20
6	0.171875	0.1667
7	0.15625	0.1429
8	0.125	0.125
9	0.125	0.1111
10	0.109375	0.1
11	0.09375	0.0909
12	0.09375	0.0833
13	0.078125	0.076923
14	0.078125	0.071429
15	0.078125	0.0667
16	0.0625	0.0625
19	0.0625	0.0526
22	0.046875	0.045455
25	0.046875	0.04
32	0.03125	0.03125
40	0.03125	0.025
51	0.03125	0.019608
64	0.015625	0.015625

For instance, TOA TAG 2 has two intervals between pulses, and the magnitudeof WAL(0,t) is 0.5, or the inverse of 2. TOA TAG 3 has a magnitude of .34375, which is close to the

inverse of 3. TOA TAG 4 has a WAL(8,t) amplitude of .25, which is one divided by four, the number of intervals between pulses in the representation.

If there was a relationship between the number of intervals between the pulses in the DATA line and the amplitude, then perhaps this would carry over into the interleaved pulse trains composed of these single PRI representations. Exceptions are evident, though, such as TOA TAG 9, which has the same magnitude as TOA TAG 8, although the coefficient distribution is not the same. This implies that any recognition feature will probably depend upon two variables, perhaps the amplitude and the sequency of the coefficients.

2. Power Spectral Densities of the TOA Strings

An examination of the PSD's in Appendix D, page 198 through page 219, will yield similar conclusions.

PSD's of even intervaled TOA strings are symmetrically even about a sequency of 16. PSD's of even numbers that are also a p.o.t. are considerable less complex, and are one fourth the magnitude of the previous p.o.t. PSD (except for TOA TAG 2 to TOA TAG 4).

The odd numbered PSD's have no symmetry, and sequency components that stand out in relative magnitude do not bear a relationship to the simulated PRI of the string. (Remember the number of intervals between the TAG's is a measure of the PRI of the simulated pulse train, when the time interval between numbers is known.)

3. General Comments

The entire purpose of this examination has been to recognize similarities or relationships between succcessive TOA TAG representations in order to recognize the same features (if they exist) in an interleaved pulse train DATA line representation.

At this point, the results are very general and an optimistic mood regarding any usable features might belong only to the optimist. It seems that the even numbered graphs (FWT and PSD) are the only graphs that show any usable features that could be used for recogniton. One shouldn't give up all hope, though.

The author believes it to be possible to develop a computer algorithm that would recognize and determine the TOA TAG number (and thus a PRI of a simulated pulse train) for a given single pulse train DATA line representation. Enough features exist in the FWT and PSD that could be used to process a particular single PRI representation with a known resolution time interval and output the correct PRI. The program would have to determine the PRI by matching characteristics (sequency components and magnitudes) of the FWT and/or PSD to a data bank composed of characteristics of the FWT's and PSD's of single pulse train representations. For example, it could first take into account the symmetry of the FWT/PSD. If it is symmetrically even, then it isn't an odd interval TOA TAG.

The algorithm would be reasonably complex for just this simple TOA TAG representation of a single pulse train of a particular PRI. But it could be done.

Since it addresses only single PRI TAG representations, the algorithm would only be effective if you could convince an opponent to use only one radar at a time against the ESM platform. Obviously, this isn't practical.

More realistically, an examination of interleaved pulse trains and a determination of a PRI recognition feature, if one exists, would be in order. This will be done in Section D. after discussion of the effects of a time shift in the TOA TAG string.

Some limitations of the DATA line symbology should be stated. Using N = 64 and a resolution between numbers of 200 nanoseconds means the window length is less than 2 microseconds long. This is not a realistic figure, since a high density of 10^6 pulses per second gives an average of 1 pulse every microsecond. The use of N = 1024 for an interleaved DATA line representation might be far better in the numbers of coefficients (and more realistic in length of the window), but unless an identifiable PRI feature is present, the extra data is exactly that, extra data.

An additional limitation of this representation concerns coincident pulses. Pulses arriving at the receiver at the same time (falling in the same resolution time interval) are not individually represented in the DATA line

symbology. For this reason, one cannot represent a TOA TAG 2 and any other even numbered TAG. This limitation is a problem that will affect the FWT and PSD of the interleaved pulse train representation.

C. TIME SHIFTED TOA STRINGS

Chapter Three has stated that the FWT and PSD are not time invariant to circular shifts of the input number series. Figures 4.2 through 4.5 are FWT's of shifted TOA TAGS . Compare them with Figures D.4, D.11, D.13, and D.16.

The magnitudes of the FWT coefficients at each [n] are not the same in the shifted TAGS. Compare TOA TAG 5 and TOA TAG 5 SHF 1. However, notice that shifted TOA TAG 12 (TOA TAG 12 SHF 1) has the same magnitude at each WALSH index [n] as does the unshifted TOA TAG, but the components from n = 32 to n = 63 are opposite in sign. The even symmetry of the even numbered FWT about the midpoint has been changed to odd symmetry about midpoint.

This is a very neat and clean distinction, and further emphasizes the distinction between even and odd numbered TOA TAGS. It is further evidence that at least some general features exist which could be made to work in a computer algorithm to identify individual PRI's.

FWT's of odd numbered intervals have no general distinctive change between shifted plots and standard plots. In a few shifted odd numbered plots, there are some particular

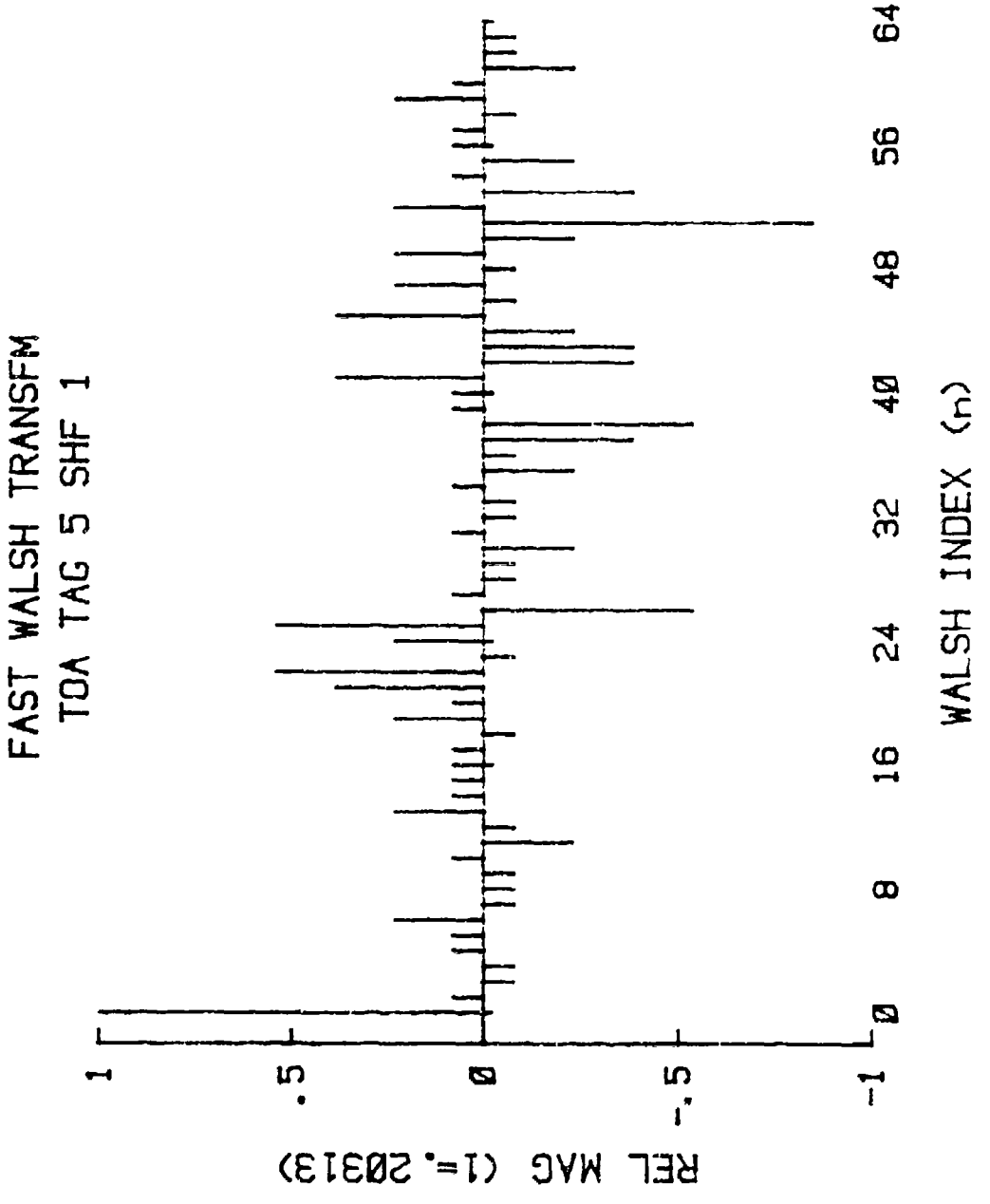

Figure 4.2. FWT : TOA TAG 5 SHIFT 1

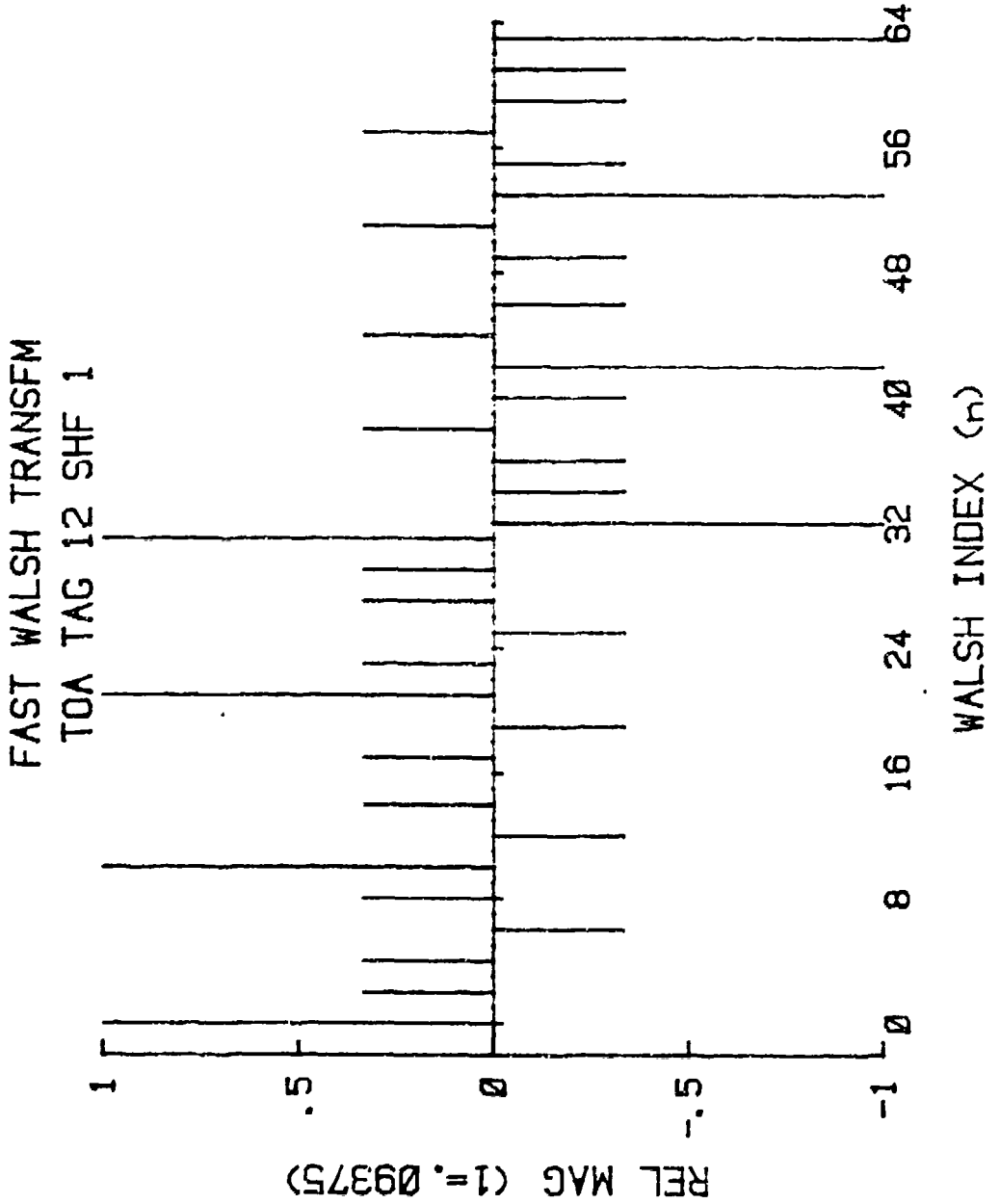

Figure 4.3. FWT : TOA TAG 12 SHIFT 1

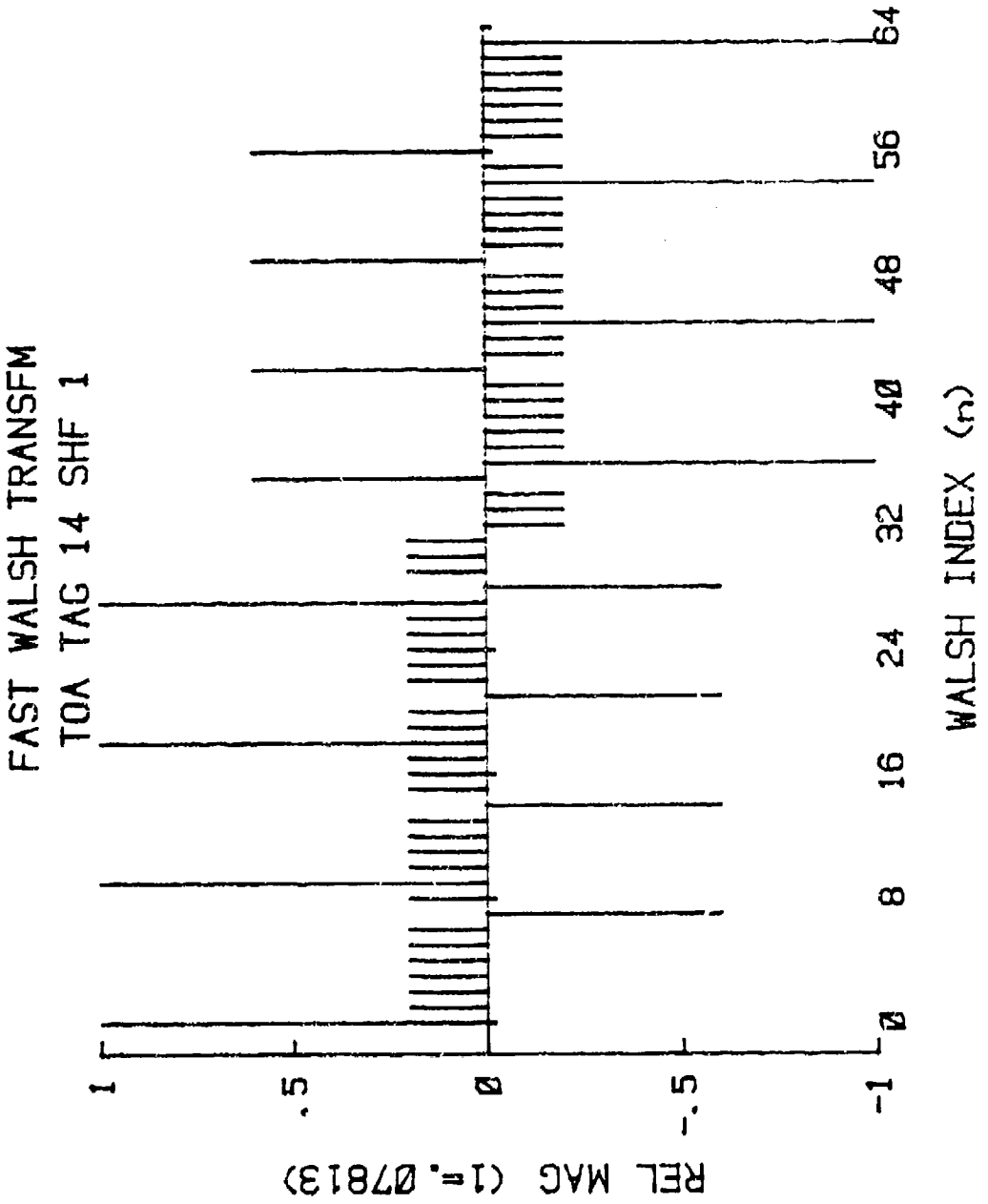

Figure 4.4. FWT : TOA TAG 14 SHIFT 1

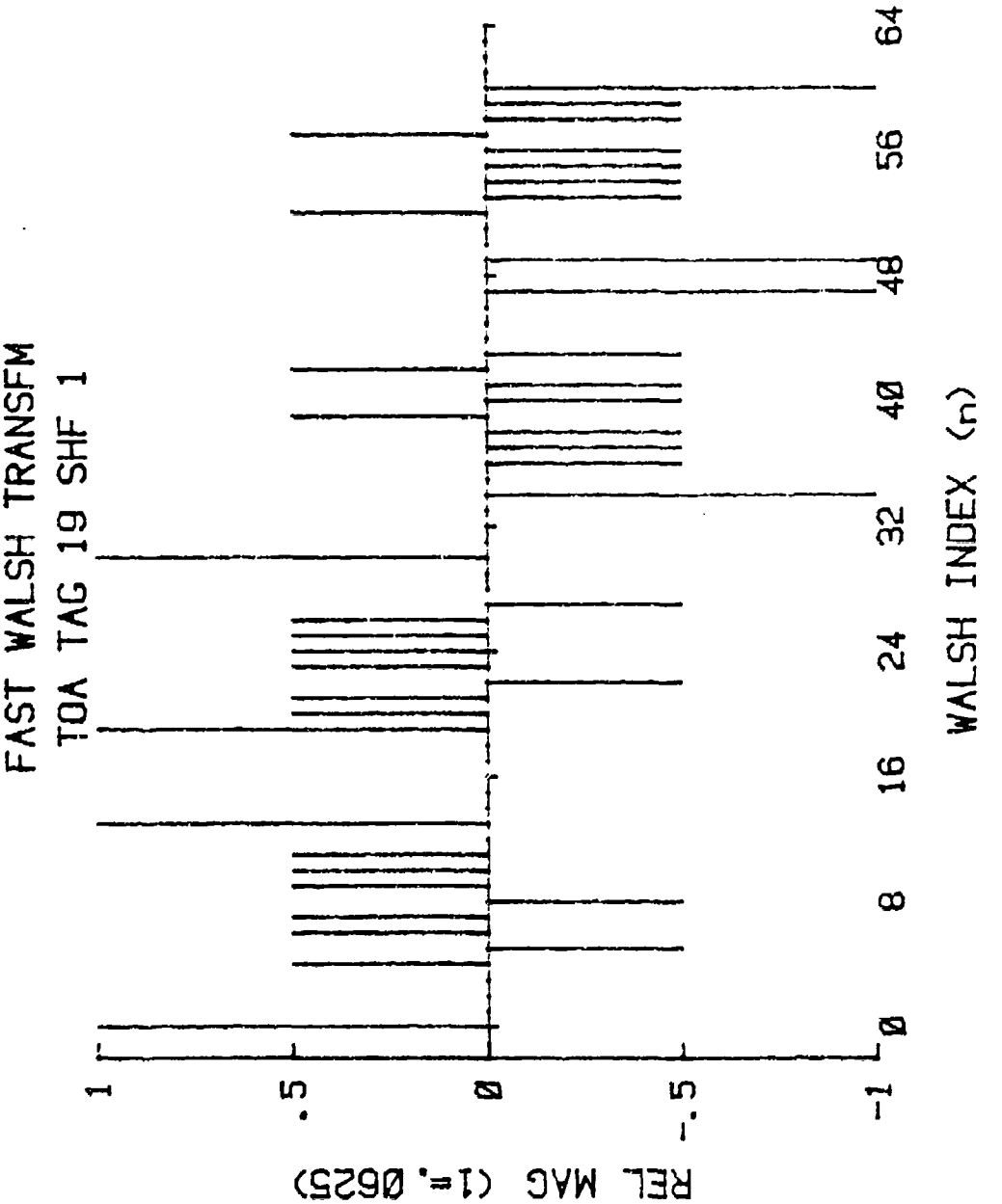

Figure 4.5. FWT : TOA TAG 19 SHIFT 1

magnitudes of index [n] that remain the same or increase proportionately, but others do not. If any real relationship between the shifted and unshifted odd numbered FWT plots exist, then it will have to be revealed with a much more detailed study.

Quite simply, odd numbered shifted FWT plots show no major distinctive features that are readily apparent. Even numbered shifted FWT plots follow the sign change rule for components at n = 32 to 63, but the magnitudes of the components of both plots are the same.

Although the odd numbered PSD plots change in the amplitude of the sequency components from unshifted to shifted, the even numbered PSD's are the same in both shifted and unshifted plots. Indeed, they are the same in both magnitude and location of sequency components. Compare Figures 4.6 to 4.9 on the following pages with Figures D.26, D.33, D.35, and D.38 in Appendix D.

Thus, the even numbered PSD's of this DATA line representation join the time invariant Group Spectrums in being immune to the effects of a circular time shift. Compare the shifted Group Spectrums Figures 4.10 to 4.13, with the unshifted Group Spectrums in Appendix E, Figures E.1 through E.4.

Again the point is made that these general features could be recognized in a PRI recognition algorithm. At the very

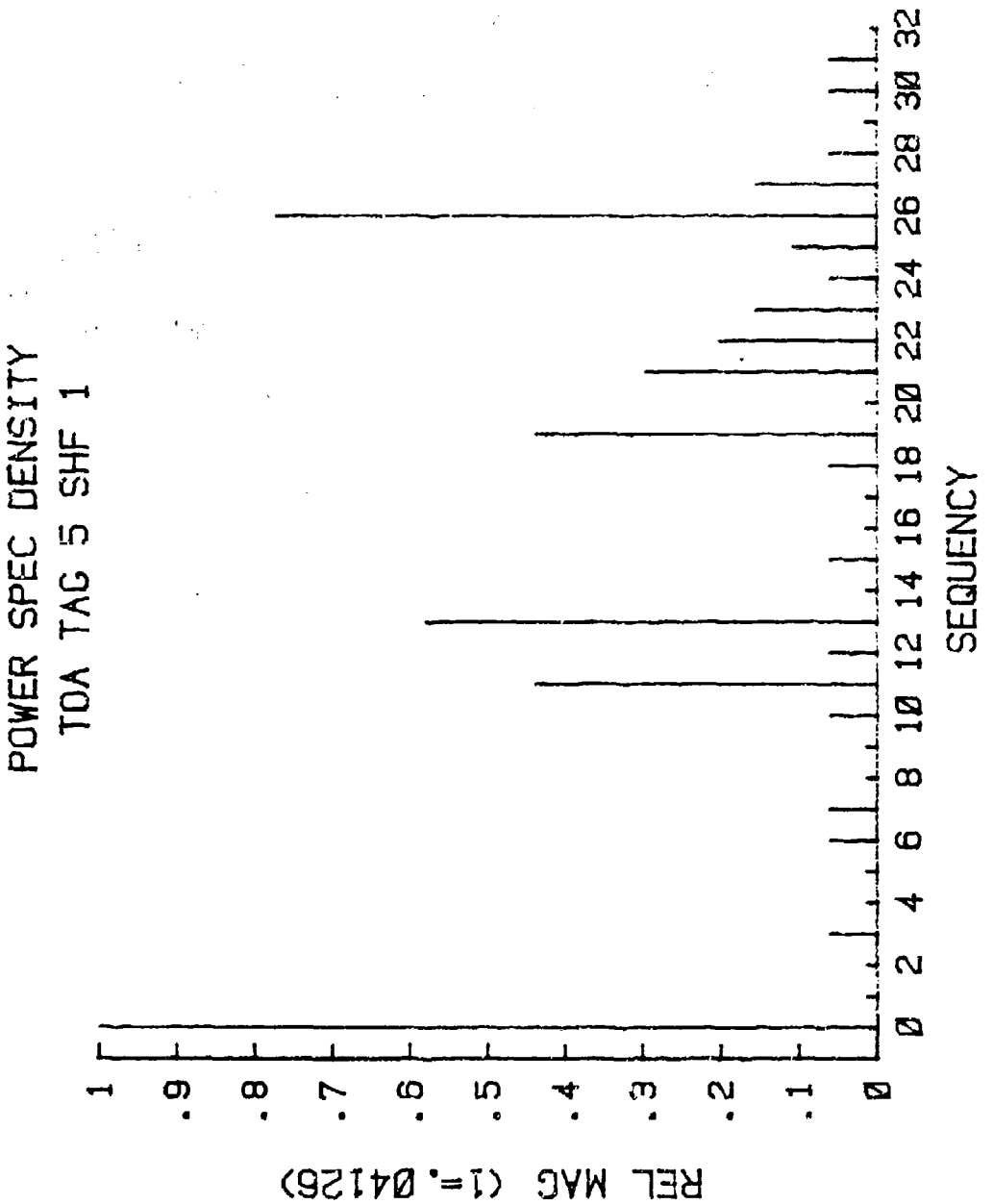

Figure 4.6. PSD : TOA TAG 5 SHIFT 1

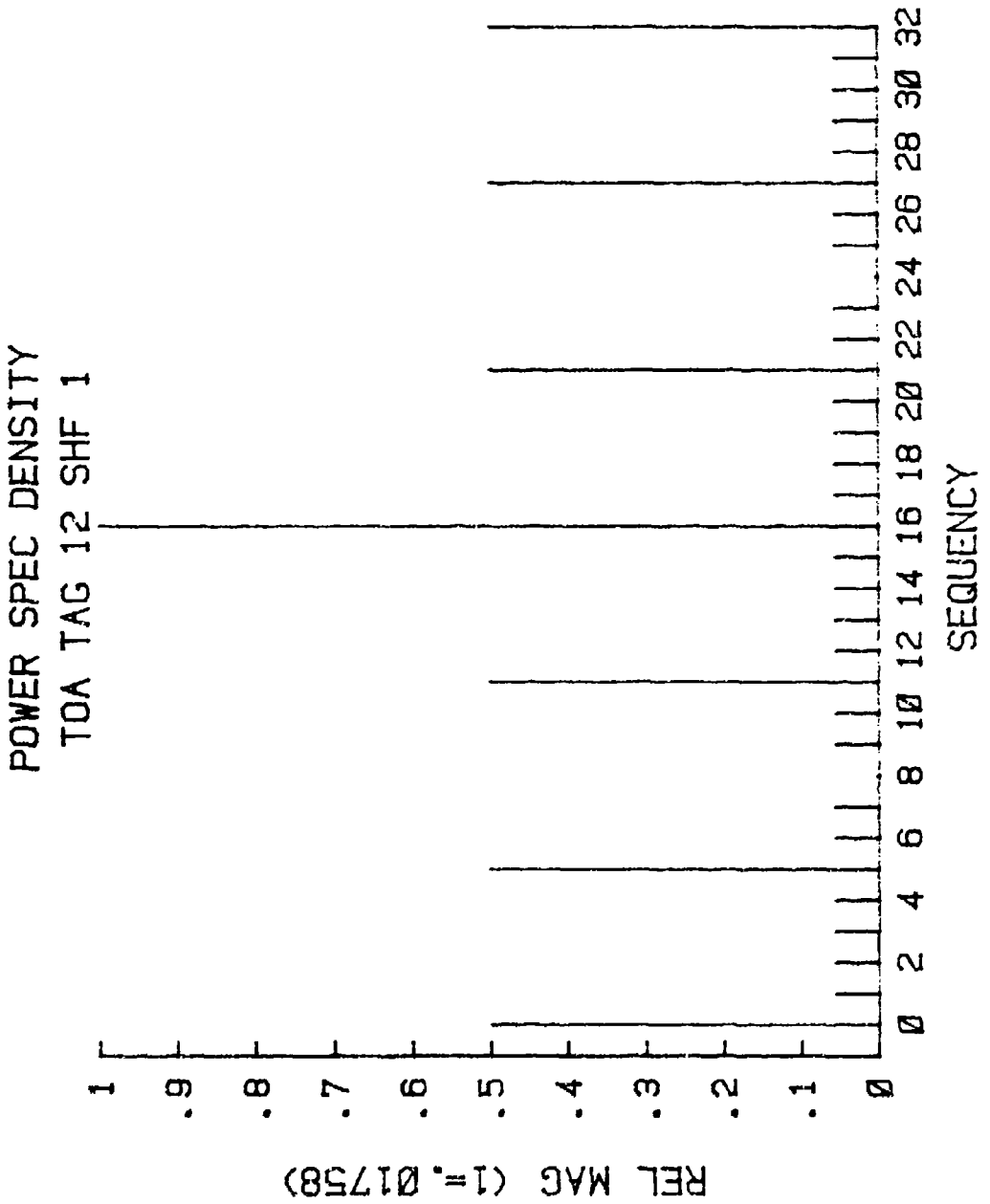

Figure 4.7. PSD : TOA TAG 12 SHIFT 1

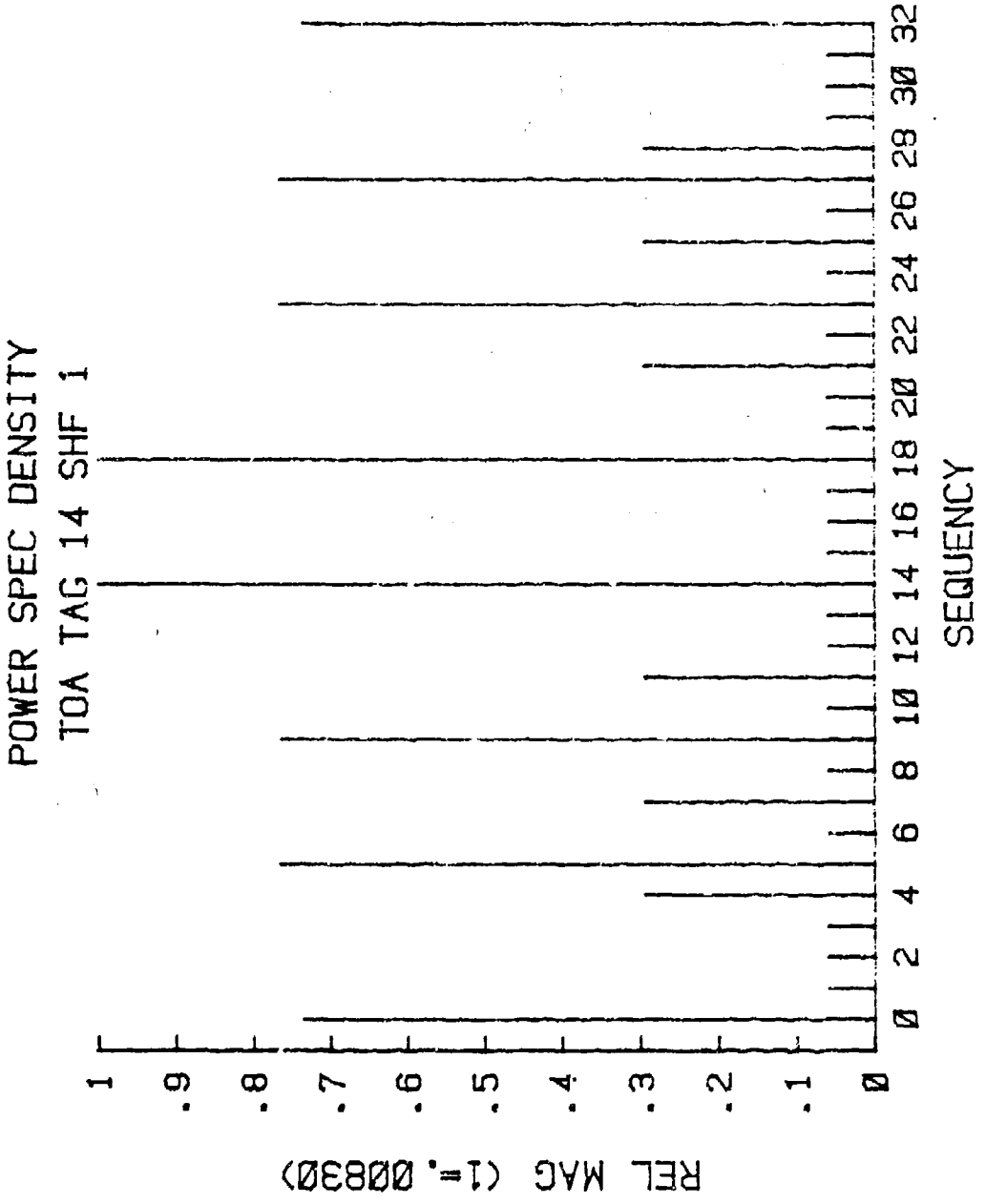

Figure 4.8. PSD : TOA TAG 14 SHIFT 1

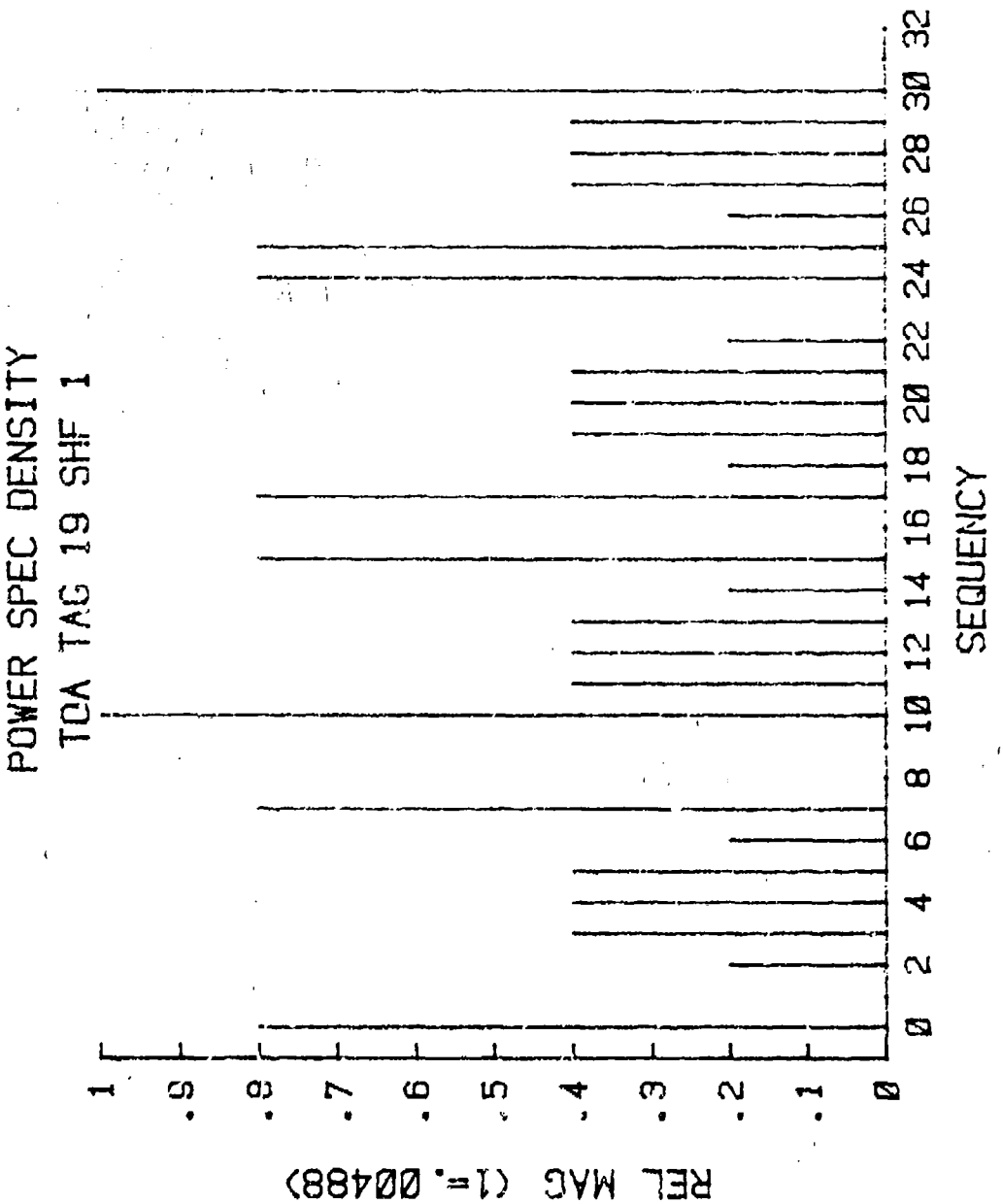

Figure 4.9. PSD : TOA TAG 19 SHIFT 1

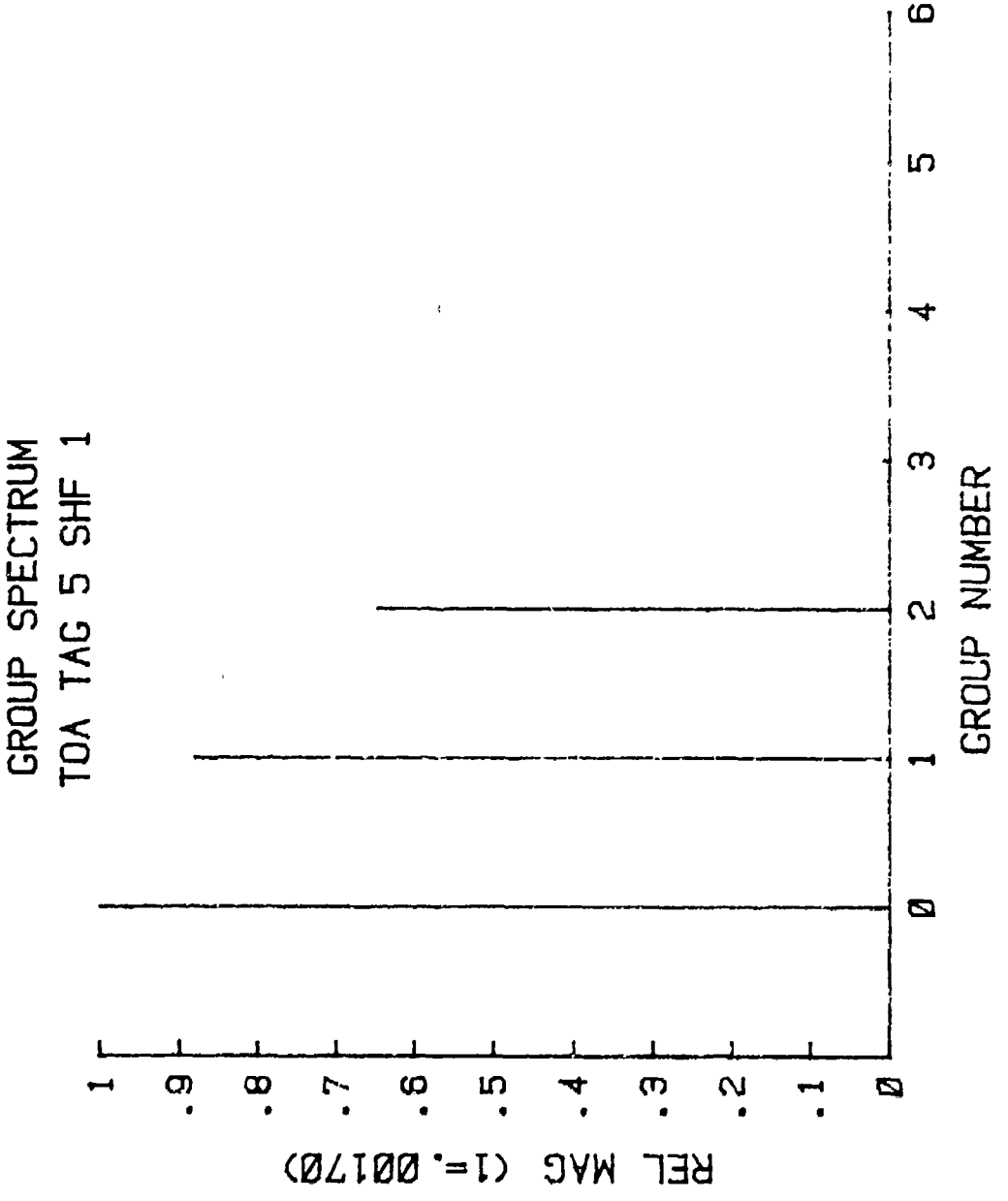

Figure 4.10. GROUP SPECTRUM : TOA TAG 5 SHIFT 1

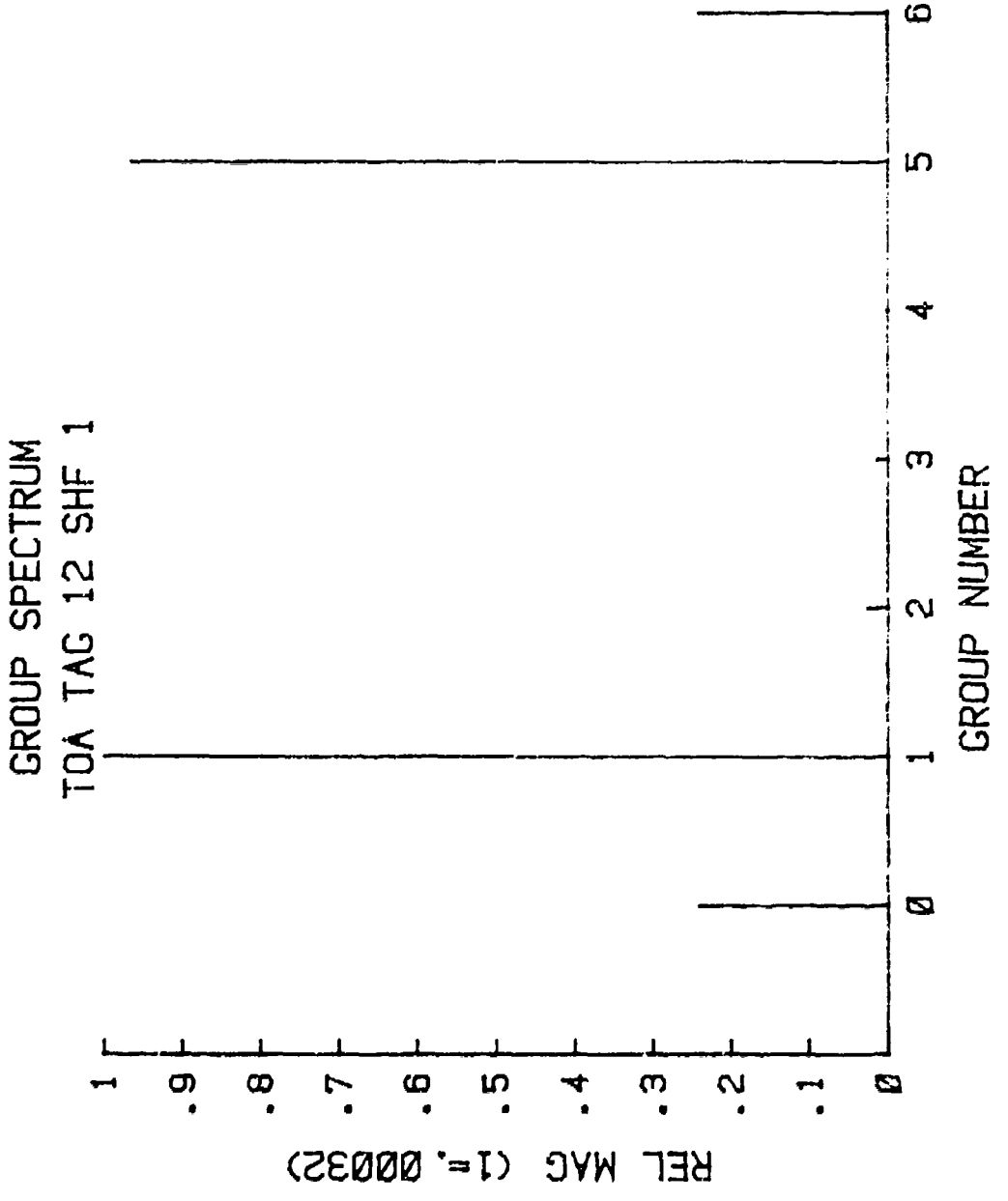

Figure 4.11. GROUP SPECTRUM : TOA TAG 12 SHIFT 1

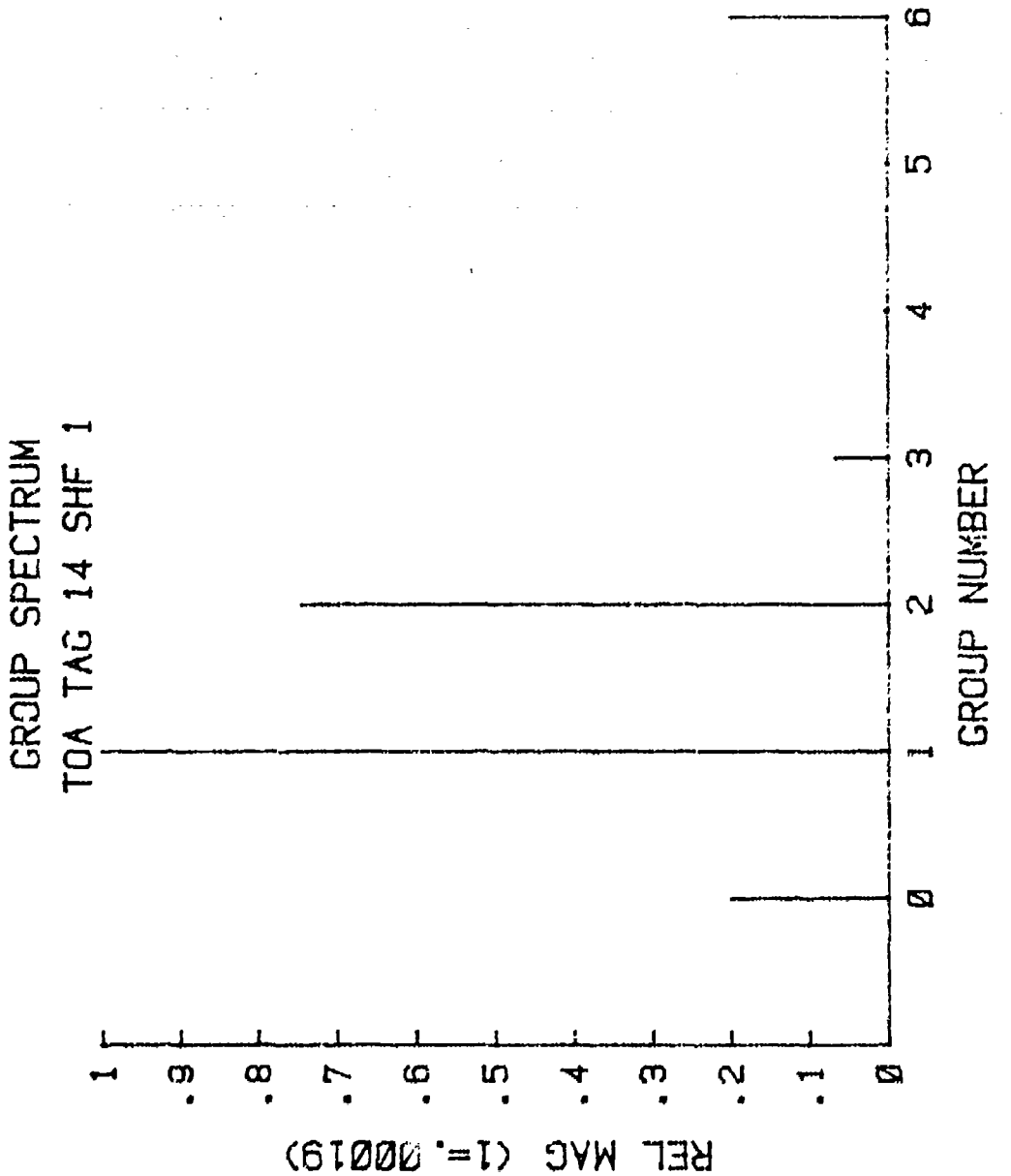

Figure 4.12. GROUP SPECTRUM : TOA TAG 14 SHIFT 1

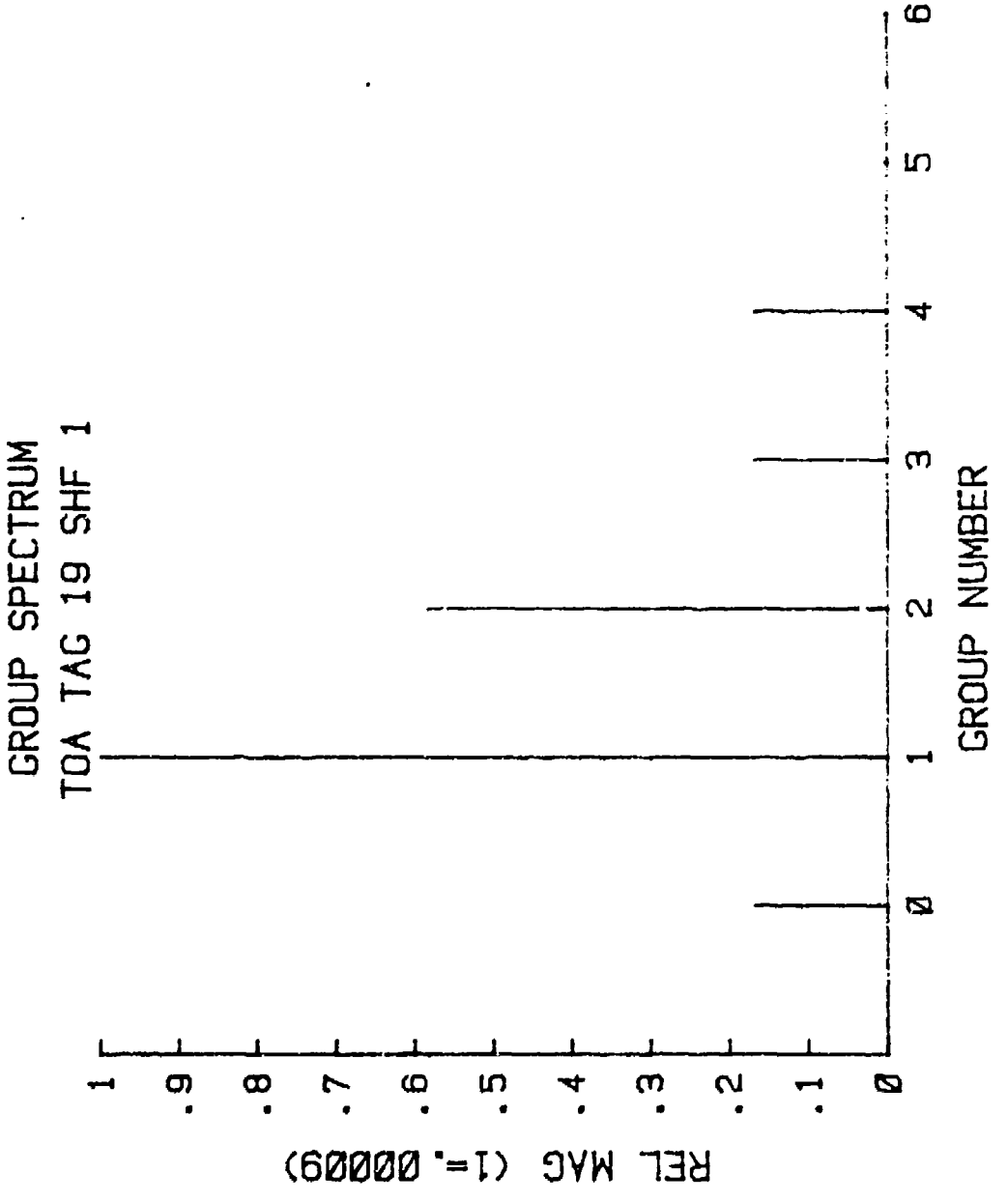

Figure 4.13. GROUP SPECTRUM : TOA TAG 19 SHIFT 1

least, it would eliminate the odd or even choices of time intervals between numbers of the single PRI representation.

D. INTERLEAVED TOA STRINGS AND THE FWT

The receipt of radar pulses from several different emitters results in individual pulse trains that are interleaved into a data stream from the receiver. Separation or deinterleaving of these pulse trains from the data stream must be done to identify the individual emitters. This section examines the plots of the FWT and PSD coefficients of a DATA line representation of interleaved pulse trains composed of the TOA TAG representation in Section B. of this chapter.

It is desired to answer the following questions:

1. Are the components of the FWT and PSD of an interleaved representation identifiable as belonging to a particular PRI?

2. Is there a relationship between the magnitude or sequency of the components of an interleaved plot with that of plots of single PRI trains?

3. Are interleaved plots made by simply adding single PRI plots?

Begin by considering interleaved TOA TAGS of Table 4.2. The DATA line representation for TOA TAG 5 with N = 64 is

```
DATA  1,0,0,0,0,1,0,0,0,0,1,0,0,0,0,1,0,0,0,0,1,0,0,0,0,1,0,
      0,0,0,1,0,0,0,0,1,0,0,0,0,1,0,0,0,0,1,0,0,0,0,1,0,0,0,
      0,1,0,0,0,0,1,0,0,0                                    (4.3)
```

and for TOA TAG 8,

```
DATA  1,0,0,0,0,0,0,0,1,0,0,0,0,0,0,0,1,0,0,0,0,0,0,0,1,0,0,
      0,0,0,0,0,0,1,0,0,0,0,0,0,0,0,1,0,0,0,0,0,0,0,1,0,0,0,0,0,
      0,0,1,0,0,0,0,0,0,0                                    (4.4)
```

Now, interleave the two,

```
DATA  1,0,0,0,0,1,0,0,1,0,1,0,0,0,0,1,1,0,0,0,1,0,0,0,1,1,0,
      0,0,0,1,0,1,0,0,1,0,0,0,0,1,0,0,0,1,0,0,1,0,1,0,0,0,
      0,1,1,0,0,0,1,0,0,0                                    (4.5)
```

Notice that the first pulse of each TAG is coincident and both are represented by the first pulse of the interleaved DATA line.

The FWT of TAGS 5 and 8 are shown in Figures 4.14 and D.7. TOA TAG 5 components are emphasized by setting the WAL(0,t) components equal to 0 before plotting. The plotting routine then normalizes to a smaller magnitude component and increases the relative magnitude of the other components.

Examine the interleaved FWT, Figure 4.15. Note sizable components at 9, 22, 25, 31, 32, 37, 45, 48, 50, 60, and 63. Now examine TOA TAG 5 with WAL(0,t) equal to 0. Note emphasized components at 25, 37, 44, 45, 50, 51, and 52.

There's some commonality between the plots. Components at 25, 37, 45, 50, and 52 are obviously associated with TOA TAG 5. So where is TOA TAG 8? A closer look reveals its influence on the interleaved FWT. Note identical relative magnitude pairs at n = 15 and 16 and n = 31 and 32. These are generated by the coefficient pairs of these [n] from TOA TAG 8. Note also that n = 48 of the interleaved FWT is higher in relative magnitude because there is a small n = 48 component of TOA TAG 5.

How would one use this interleaved FWT to deinterleave pulse trains? A direct computation method using a correlation

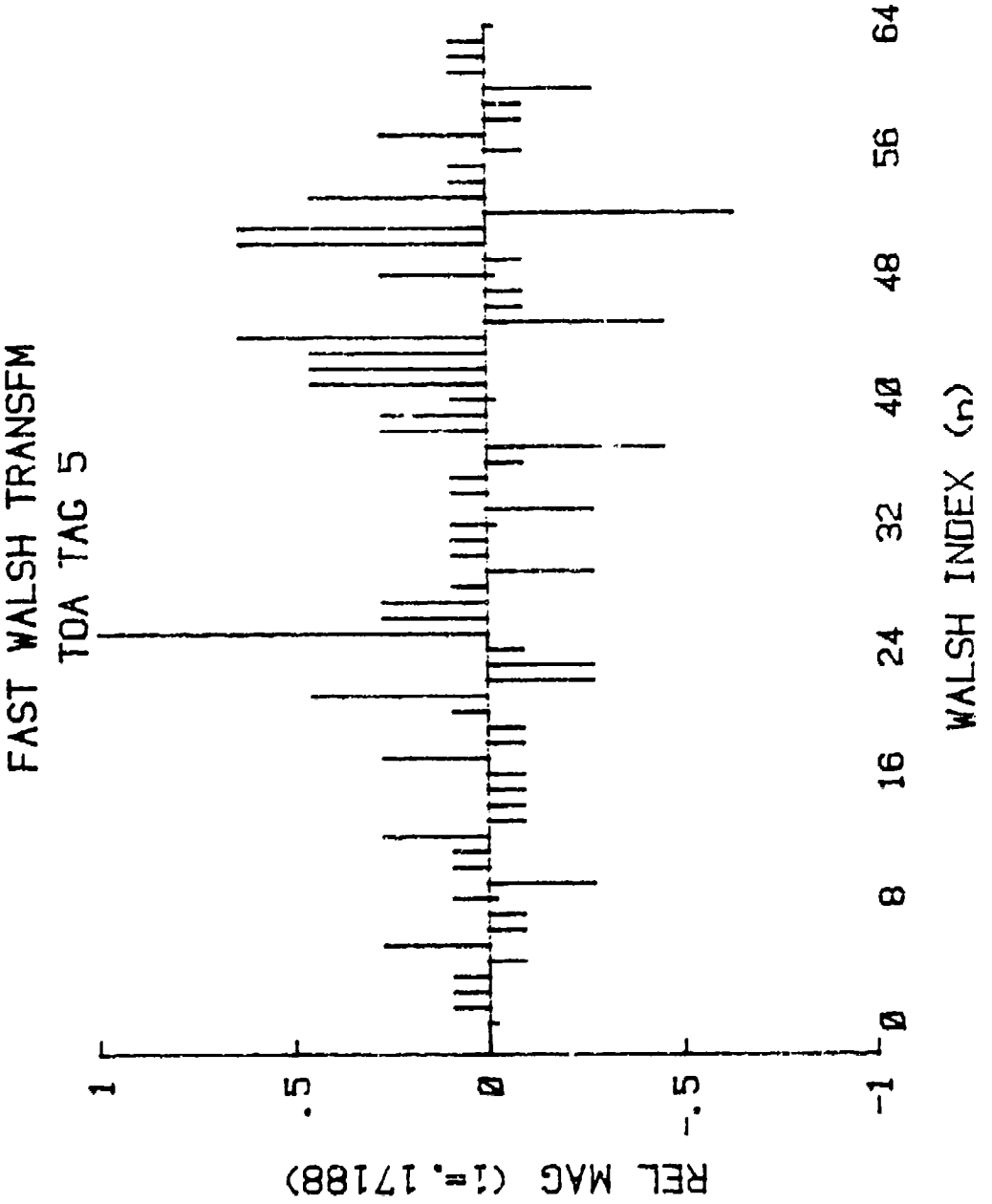

Figure. 4.14. FWT : TOA TAG 5

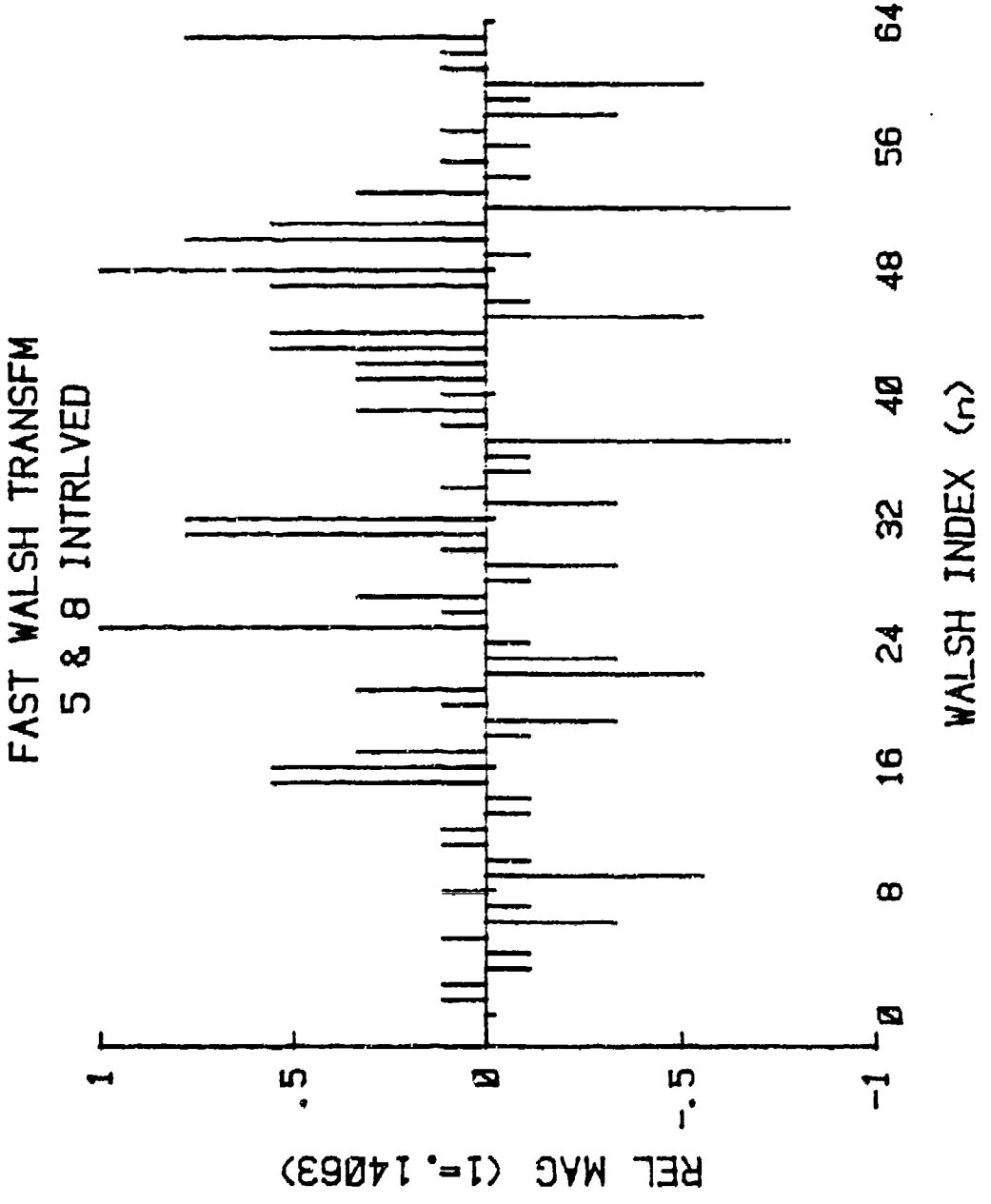

Figure. 4.15. FWT : TOA TAG 5 AND 8 INTERLEAVED.

algorithm is considered in the next section. The author suggests a "matching" algorithm could be written that would scan the interleaved FWT, and note relatively high magnitudes at certain [n] above some threshold. These [n] could be matched to a data bank of important [n] components of single PRI FWT plots, along with any special characteristics of the interleaved FWT (identical components at successive [n], for example). Promising matches between the interleaved parameters and single PRI parameters would result in a decision or choice of which single PRI trains make up the interleaved pulse train.

Scrutiny of the PSD plots generates similar conclusions. Figure 4.16 shows the interleaved PSD plot. Components of relative magnitude of 0.3 or greater are 8, 13, 16, 19, 22, 24, 25, 26, and 32.

Now note the PSD's of TOA TAG 5 and 8 (Figures 4.17 and D.29. TOA TAG 5 contributes components at sequencies of 13, 22, 25, and 26. TOA TAG 8 contributes components at 8, 16, 24, and 32.

Before moving on to another interleaved case, a discussion of the magnitudes of the interleaved components (both FWT and PSD) is in order. A definite relationship is not apparent between components of individual plots and interleaved plots.

The author can say that one's intuition about components of interleaved plots generally holds true. For instance, a large positive FWT component of one TAG and a negative FWT

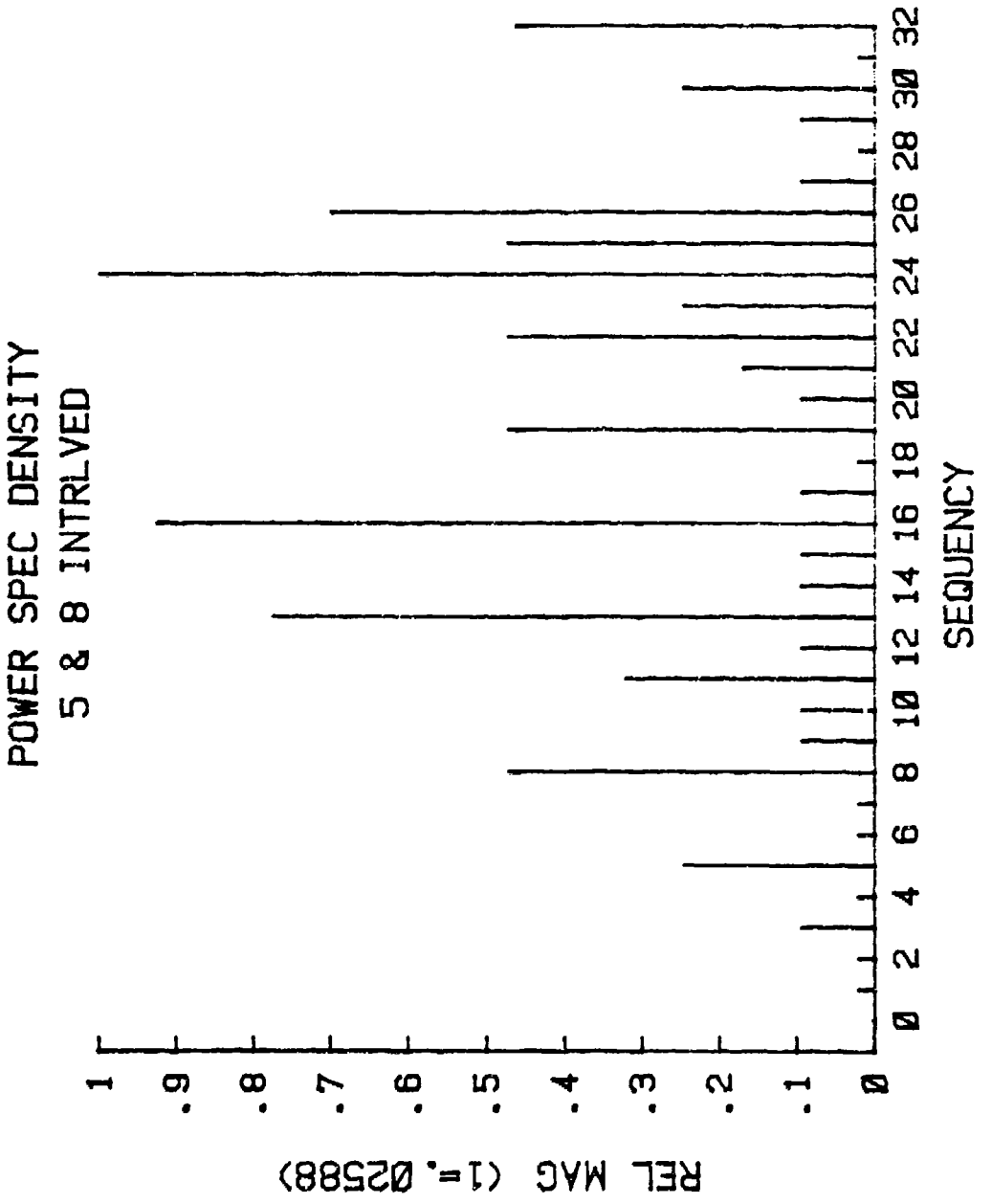

Figure. 4.16. PSD : TOA TAG 5 AND 8 INTERLEAVED.

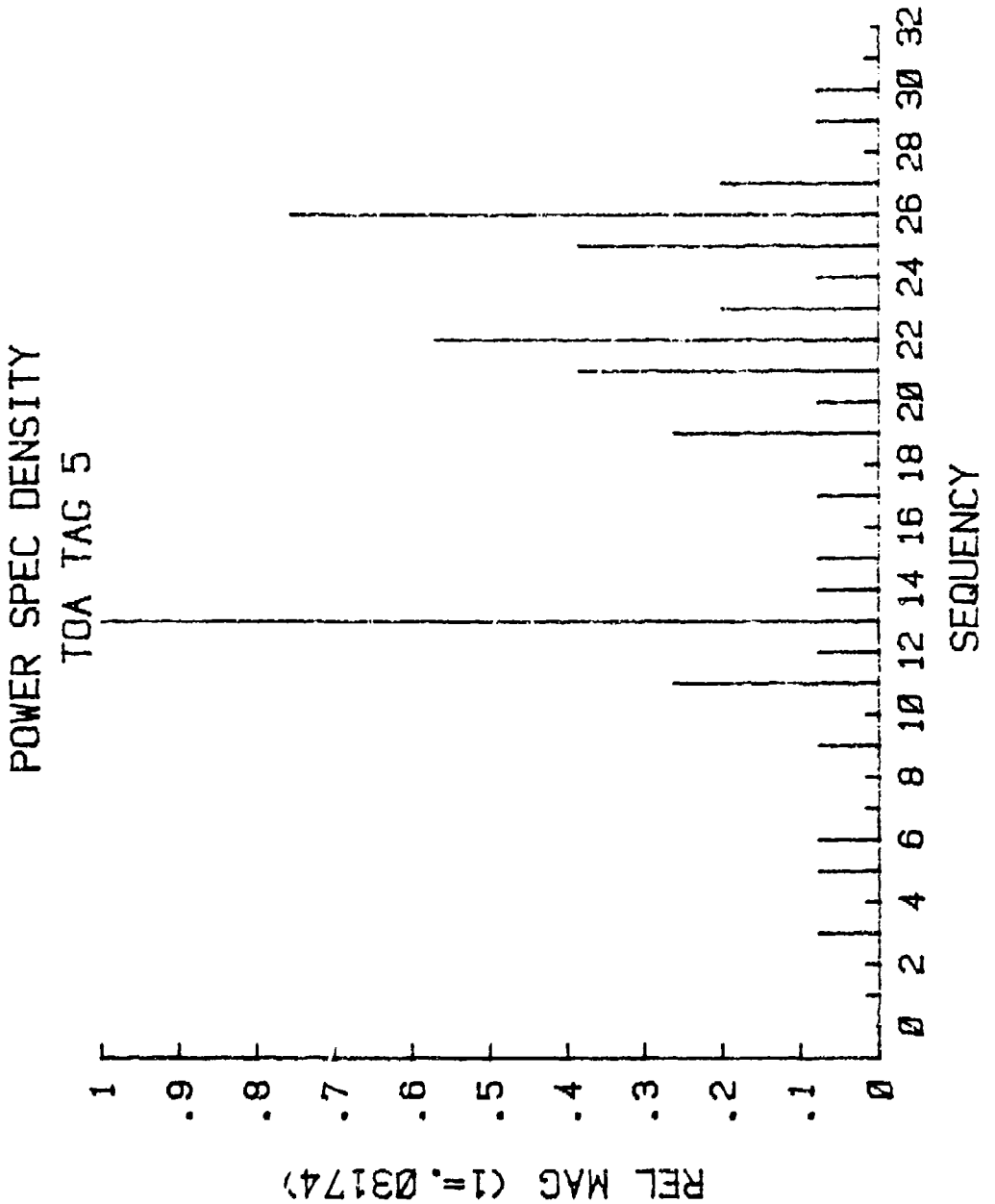

Figure. 4.17. PSD : TOA TAG 5.

component of another TAG at the same [n] will usually generate a smaller component in a FWT component of the interleaved TAG's. The result is not a simple addition, but the actual magnitude of the interleaved component is usually smaller than the added values of the single components. No fast and easy rule applies.

In a matching algorithm, the magnitude would have only a comparative benefit. The actual promise of the algorithm lies in matching component locations (either [n] or sequency) to a data bank of single PRI component locations, with magnitude and other special characteristics as a decision making aid.

One more interleaved case is examined. This one is different because there are no coincident pulses. The shift in TOA TAG 5 causes it to interleave perfectly with TOA TAG 19.

TOA TAG 5 SHF 1 (Figure 4.2 and 4.6) DATA line:

```
DATA  0,1,0,0,0,0,1,0,0,0,0,1,0,0,0,0,1,0,0,0,0,1,0,0,0,1,0,
      0,0,0,1,0,0,0,0,1,0,0,0,0,1,0,0,0,0,1,0,0,0,0,1,0,0,0,
      0,1,0,0,0,0,1,0,0                                    (4.5)
```

TOA TAG 19 (Figure 4.18 and 4.19) DATA line:

```
DATA  1,0,0,0,0,0,0,0,0,0,0,0,0,0,0,0,0,0,1,0,0,0,0,0,0,0,0,
      0,0,0,0,0,0,0,0,0,0,1,0,0,0,0,0,0,0,0,0,0,0,0,0,0,0,0,
      0,0,1,0,0,0,0,0,0                                    (4.6)
```

And the interleaved DATA line:

```
DATA  1,1,0,0,0,0,1,0,0,0,0,1,0,0,0,0,1,0,0,1,0,1,0,0,0,0,1,0,
      0,0,0,1,0,0,0,0,1,0,1,0,0,1,0,0,0,0,1,0,0,0,0,1,0,0,0,
      0,1,1,0,0,0,1,0,0                                    (4.5)
```

Figure 4.20 and 4.21 show the FWT and PSD of the interleaved TAG's. Interleaved components of both single PRI

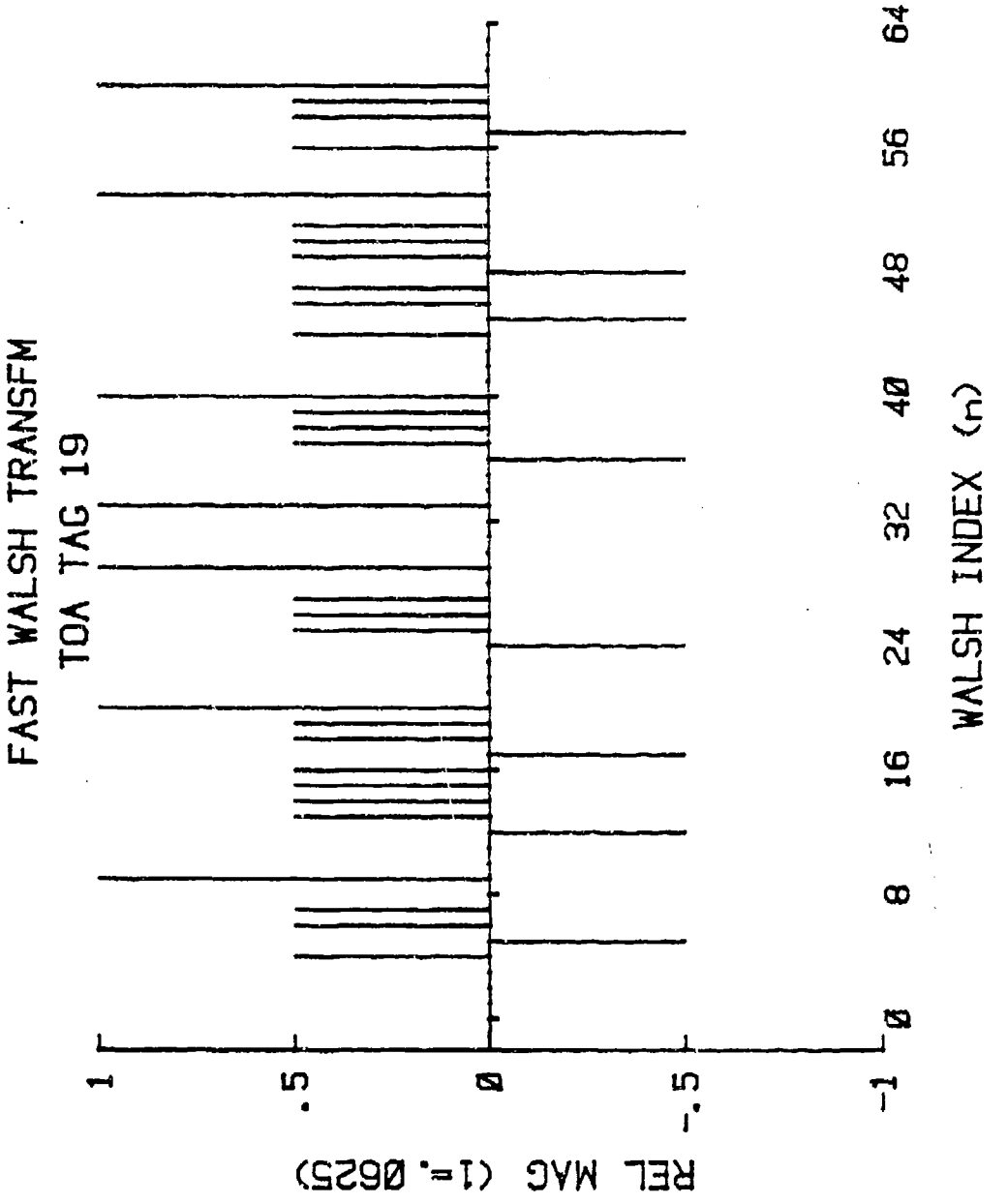

Figure. 4.18. FWT : TOA TAG 19.

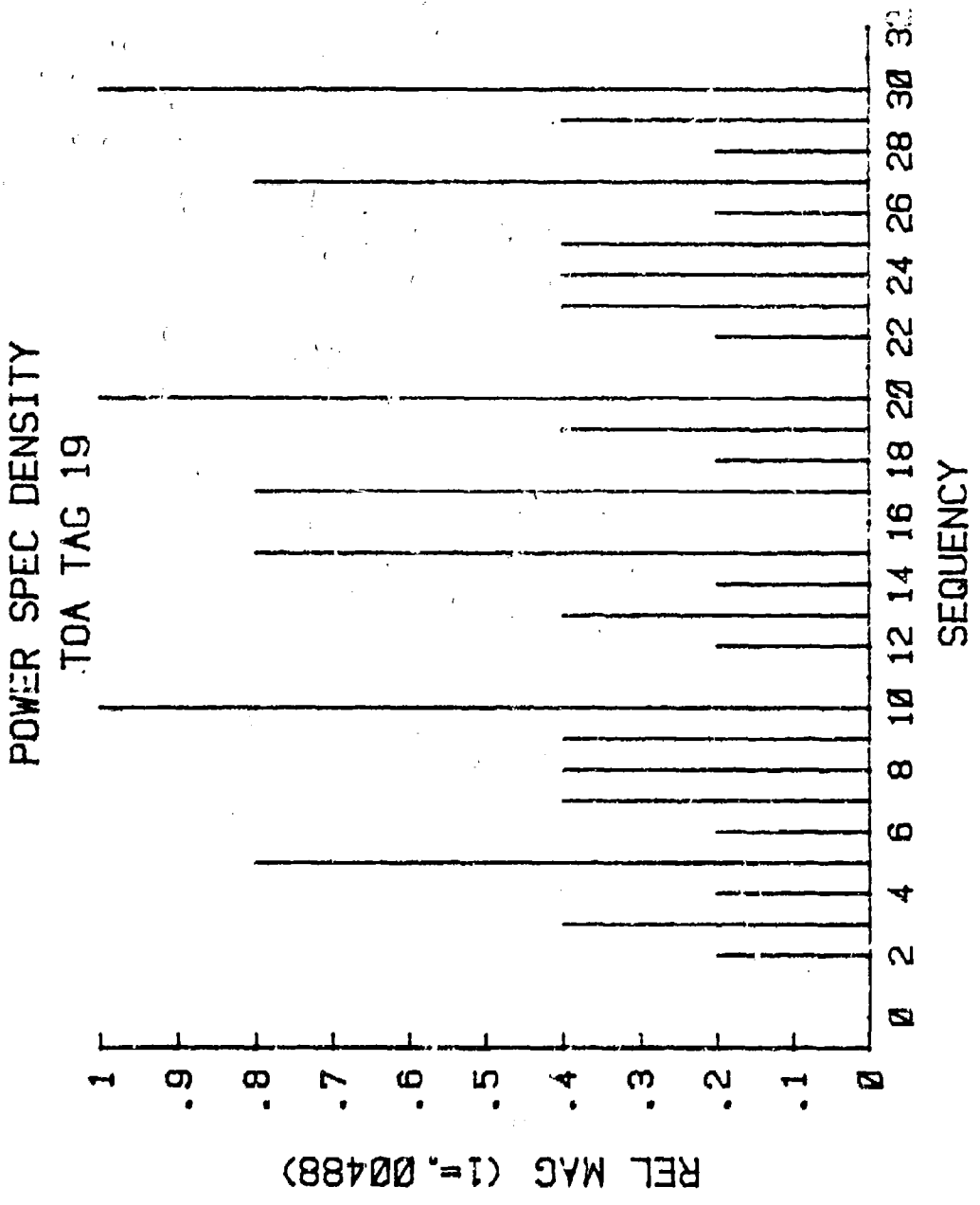

Figure. 4.19. PSD : TOA TAG 19.

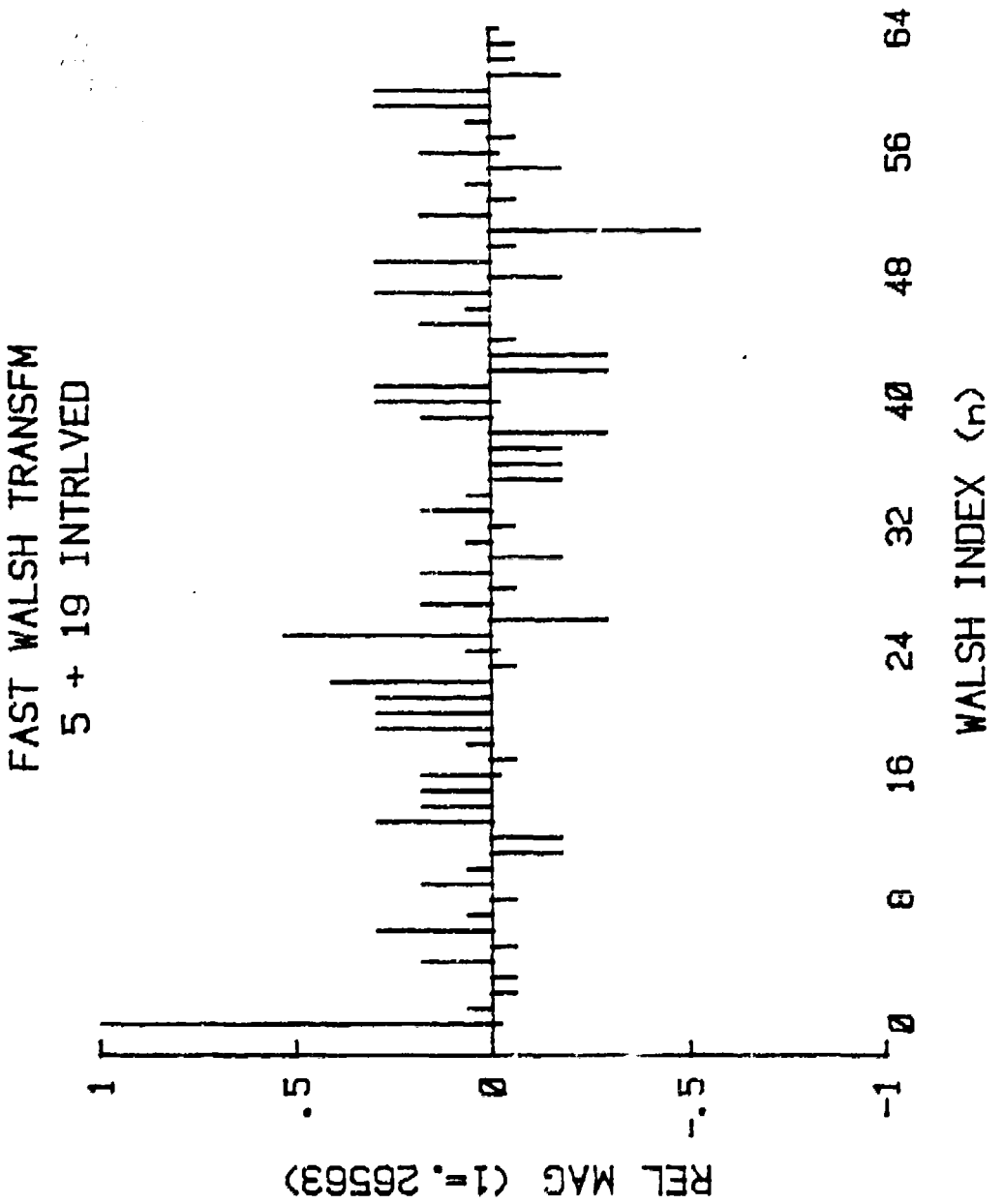

Figure. 4.20. FWT : TOA TAG 5 AND 19 INTERLEAVED.

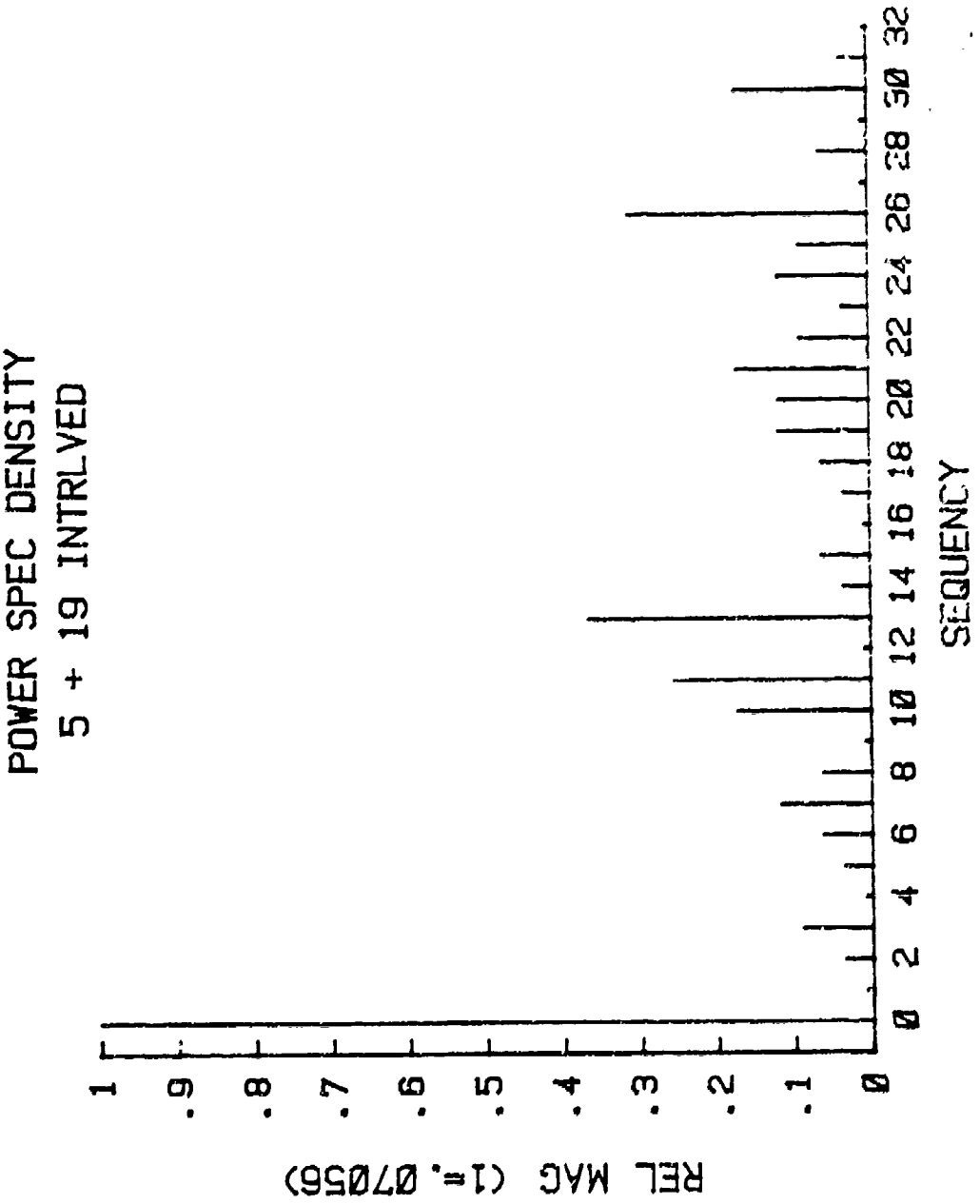

Figure. 4.21. PSD : TOA TAG 5 AND 19 INTERLEAVED.

TAGS are present, and the same process as before is used to identify them. A new discovery of this examination reveals that some feature PSD components of TOA TAG 5 SHF 1 are passed directly to the interleaved PSD. Note the magnitude of sequencies 11, 16, and 21 of the interleaved PSD is the same as the PSD of TOA TAG 5 SHF 1, and that the magnitudes of TOA TAG 17 PSD at these sequencies is zero. This is the first evidence of two single train representations generating an interleaved components magnitude by merely adding the simple PRI components. A more closer study could be done to see if it is merely coincidence. The real question is," Did the fact that there are no coincident pulses in the interleaved representation allow me to add certain single PRI components to form an interleaved component?"

A partial answer to the question probably is evident since only certain components of the two single PRI PSD plots have this feature of simple addition.

E. CORRELATION AND THE PSD COEFFICIENTS

Throughout this chapter the emphasis has been placed on the location and relative magnitudes of components located in the Walsh index domain or the sequency domain. Most of the plots show the magnitude of the components relative to the maximum component magnitude of that particular plot. It was stated several times that the actual magnitudes of the individual PRI (TOA TAG) components didn't seem to have a

recognizable relationship with the magnitudes of the components of the interleaved plots.

It was thought that the magnitudes might be related, and a correlation of the interleaved component magnitudes with those of the individual PRI magnitudes might show their presence. The PSD coefficients were chosen because they are defined from the FWT coefficients, and exhibit the same characteristics and information about the transform in terms of symmetry and relative magnitude components.

Without any mathematical fanfare, the correlation coefficient ρ is presented.

$$\rho = E\ (\ (X-X')/\sigma_X \cdot (Y-Y')/\sigma_Y\ ) \qquad (4.6)$$

where

X,Y are random variables
X', Y' are the mean of the variables
$\sigma_{X,Y}$ are the variances of the variables

The correlation coefficient expresses the degree to which two random variables are correlated without regard to the magnitude of either one. [30: p.83] It is a normalized quantity and will be a value between -1 and +1.

In this application, X are the PSD coefficients of the interleaved situation and Y are the PSD coefficients of the individual TAG situation.

A correlation BASIC language routine was written specifically for the 32 PSD components of the interleaved and individual TOA TAGS. This program was adapted from a

correlation routine in the IMSL library contained in the Naval Postgraduate School IBM 3033 computer. It was not adapted for general application but specifically for this situation. For this reason it is not provided in Appendix A.

The correlation routine merely reads in the component values of the individual PRI TAG representations and the interleaved representation generated by the FWT/PSD/Group Spectrum program provided in Appendix A. It correlated the two, based upon Equation (4.6), and outputed a single number, the correlation coefficient.

The PSD coefficients of the interleaved situation of TOA TAG 5 and TOA TAG 19 were used (Figure E.5 in Appendix E). This interleaved situation is different from that of page 148 because TOA TAG 5 wasn't shifted before interleaving, causing the first pulse of TOA TAG 5 and 19 to be coincident. With these coefficients, the values of the individual TOA TAG components from 3 to 64 were then correlated with the interleaved values using the correlation routine.

Table 4.2 gives the TOA TAG number, and the correlation coefficient generated.

Examination of the correlation coefficients shows strong correlation with TOA TAG 5. Great! It is desired to have a high correlation value with TOA TAG's 5 and 19, since the interleaved representation was composed of these two TAG representations. The TOA TAG 5 correlation coefficients fits the need nicely.

Table 4.2. Correlation of Interleaved PSD coefficients with individual TOA TAGS

TOA TAG number	Correlation Coefficient
3	0.665
4	0.234
5	0.963
6	0.582
7	0.305
8	0.030
9	0.166
10	0.709
11	0.259
12	0.183
13	0.274
14	0.191
15	0.365
16	-0.065
19	0.140
22	0.330
25	-0.028
32	-0.055
40	0.106
51	0.059
64	-0.722

On the down side, the interleaved PSD coefficients do not show a high value of correlation with TOA TAG 19. The initial success of TOA TAG 5 certainly indicates that this is an area for further investigation, however.

The author suggests that the correlation procedure could be used in an effective deinterleaving algorithm if it was applied to the sequential method of extracting PRI's. Once the initial correlation routine is carried out and a high value of correlation coefficient is identified and associated with an individual TOA TAG string, then the algorithm could return to

the interleaved DATA stream representation and subtract (set equal to zero) those TOA TAG's associated with the determined PRI.

Now repeat the entire process. Take the FWT and PSD of the remaining TOA TAG representation, correlate the PSD coefficients with the data bank of individual TOA TAG PSD coefficients, and see if a new TOA TAG has been identified with another high value of correlation coefficient. If it has, then strip these TOA TAG's from the original string.

The process could be repeated until calculation of the PSD yields no further useful coefficients, or until no correlation IS found. The stripped TAG's represent the individual pulse trains that make up the interleaved pulse string.

This suggested process is similar to the way a preprocessor sorts the incoming data stream. After identifying particular pulses in the stream, the preprocessor strips these pulses from the stream, simplifying the follow-on process, which continues to identify (deinterleave) individual pulse trains of the remaining stream. Each identified train is then removed from the incoming data from the receiver.

A problem that plagues current deinterleaving techniques, that of coincident or missing pulses, would probably plague this correlation deinterleaving procedure.

The TOA TAG representation does not indicate coincident pulses separately. Coincident pulses are represented by a single TOA TAG. Only the receiver knows which one it detected

and represented as a received pulse. Therefore, the stripping of this TAG generated when two pulses had arrived at the receiver at the same time inadvertently strips a TOA TAG from the remaining pulse representation.

If the PSD coefficients of the remaining string with the inadvertently stripped TAG were now calculated, one would find they are different than those calculated from the remaining string that included the inadvertently stripped TAG.

These PSD coefficients, those calculated from the missing TAG string, cannot correlate higher with the individual TOA TAG strings (used by the correlation routine) than the coefficients of the complete remaining string.

The individual TAG PSD coefficients were calculated from TOA TAG strings with no missing pulses. So, coefficients from strings with missing pulses will not correlate as well as coefficients calculated from complete strings.

A possible solution could be the use of a large number of TOA TAG's in the interleaved representation, say 1024 or 2048. In other words, expand the "window" or aperture on the data stream. This would allow the interleaved representation to be more realistic and comparable to the receiver's own TOA resolution. More coefficients might help the correlation procedure and lessen the effect of missing and coincident pulses.

V. CONCLUSIONS AND RECOMMENDATIONS

Before discussing the conclusions of the research effort and making recommendations for follow-on work, a review of the investigation steps that were taken by the author and translated into the substance of this thesis will be beneficial.

For background, the importance of the ESM effort and its place in Electronic Warfare was studied. A typical ESM system was examined, and the problem of deinterleaving the pulse stream output from an ESM receiver was considered, along with current techniques for deinterleaving already in use.

Having no previous idea of even the existence of the Walsh functions set the stage for the study of these unique and interesting functions. As the study proceeded through the definition of the Walsh Transform, the constant comparisons of the Walsh Transform properties with the familiar properties of the Fourier Transform brought review of this area.

Reference 23 provided the FWT program that became the tool of the investigation. Adaptation of the program to the BASIC language and a gathering of evidence that supported belief in its output took a considerable time. Searches of the literature for examples of FWT's of familiar waveshapes finally provided the proof of the program.

With the guidance of the thesis advisor, the representation of the receiver data stream with time of

arrival tags was accepted, and the FWT program was applied to many individual tag strings. The purpose was to determine if a TOA TAG string representing a particular PRI pulse train could be recognized by certain features of the Walsh Transform or the Power Spectral Density. The FWT, PSD, and Group Spectrum of interleaved TOA TAGS were then closely examined for PRI recognition features. Finally, a correlation algorithm was used to determine the degree of correlation between interleaved PSD coeffcients and single pulse train PSD coefficients. An examination of the correlation coefficients was done to see if a PRI could be determined by noting the magnitude of the coefficient.

A. CONCLUSIONS

One result of the effort was the demonstration of the ease of computation of the Walsh Transform and Power Spectral Density of a number series. The algorithm is fast and efficient, and easily adapted to a BASIC language implementation. This allows the computation of the transform and calculation of the PSD coeffcients on a microcomputer, easily used and readily available in the work space.

When applied to a TOA TAG representation of a single PRI pulse train, the transform snows features that can be used to recognize this pulse train when compared to the transforms of other PRI pulse trains. Symmetry of the coefficient distribution, and the relative magnitude of certain Walsh index or sequency components are the features that allow this identification.

It was shown in Chapter 4 that each single PRI pulse train's Walsh transform has unique and distinctive components that distinguish it from other transforms of single PRI representations. No single feature, however, such as a relative maximum sequency component, can be connected with the PRI of the pulse train. Each particular PRI transform simply has individual features that identify it, and only certain characteristics, such as symmetry, are common between groups of individual pulse train transforms.

The Walsh transform and PSD's of interleaved TOA TAG representations have features that can be identified as belonging to the transforms or PSD's of component individual pulse trains. However, these features are not readily apparent and one could not identify or associate them with a particular single PRI transform without prior knowledge of single PRI transform features. Like the transforms of single PRI pulse trains, the interleaved transform or PSD does not have any features that can identify component PRI's from the transform or PSD alone.

This lack of component PRI features in the transform or PSD effectively prevents its use in a practical deinterleaving algorithm. At the outset of the research effort, it was hoped that the transform of a representation of the pulse stream from a ESM receiver would identify the individual PRI's of the component pulse trains. Neither the transform or the PSD does this, although there are common features between the interleaved transform/PSD and component transform/PSD.

The application of a correlation routine between the the interleaved PSD coefficients and the individual TOA TAG PSD coefficients was seen to be effective in identifying one of the component PRI's. It did not identify all component PRI's, and any algorithm that uses this approach will have to go through additional steps to do so. These required additional steps quickly negate the speed of computation advantage that the Walsh transform exhibits, and the approach becomes quite similar to current sequential PRI extraction techniques.

In summary, the transform of the interleaved TOA TAG representation failed to produce a simple PRI recognition feature. Recognition features are present, however, in the interleaved transform and PSD that would allow the identification of component pulse trains in an interleaved representation if a data bank of individual PRI transform/PSD features was available.

B. RECOMMENDATIONS

It is recommended that an effort at writing a "matching feature" deinterleaving program be made. The program would use a data bank of parameters that describe the interesting properties and features of the Walsh transform and/or PSD of a TOA TAG representation of a single PRI pulse train.

The data bank would be the measure of attaining a successful deinterleaving program. Properties such as even symmetry, double components of power of two interval

representations, and distinctive index or sequency components of the odd numbered TOA TAG representations would be included.

The algorithm would scan the FWT/PSD of the interleaved TOA TAG representation for recognizable features, then match these features to the data bank. Appropriate tolerances could be included to be used in decisions about whether a single PRI is a component of the interleaved train.

Additional study could possibly yield the optimal features to include in the bank. For certain, a closer look at single PRI representations must be done to determine which components are shared among them. The author firmly believes that there will always be a FWT/PSD feature of a single PRI representation, whether a particular index or sequency component, or a symmetrical characteristic, that can be used to distinguish it from other single PRI representations.

Closer study of whether there is a relationship between interleaved and individual index or sequency magnitudes should be completed. It is a feature that could possibly be used in a matching algorithm, and it certainly can be used in direct compuation methods, such as a least mean squares or correlation routine that might generate an individual PRI indication.

The quite tentative but interesting result found in the last section of Chapter 4 should be explored completely. All coefficients should be involved, including the Group Spectrum

coefficients. In this thesis, the Group Spectrum coefficients have mainly been used to show the time invariance nature of their character, but they might offer some interesting direct computation features.

APPENDIX A

FAST WALSH TRANSFORM PROGRAMS

The following pages contains listings of the Walsh Transform programs used in this thesis. The first program is written for an IBM Personal Computer, and the second was written for the HP-85.

The FWT subroutine was adapted from a FORTRAN program in "Walsh Functions and their Applications," by K.G. Beauchamp.

The PSD and Group Spectrum subroutines were written by the author.

Both programs were run on the respective computer BASIC interpreter (uncompiled). A compiled version would probably run faster, although a 128 number FWT ran on the IBM PC in about 4 seconds using only the interpreter.

```
10 '  This program computes the Fast Walsh Tranform , the
      Power Spectral Density, and the Group Spectrum
20 '  Coefficients of a number series.
30 '  The FWT subroutine is a BASIC adaptation of a FORTRAN
      program listed 40 ' in " Walsh Functions and Their
      Applications," by K.G. Beauchamp.
45 '  The PSD and Group Spectrum subroutines were written by
      the author.
50 '  This program runs on a IBM Personal Computer.  The
      printer used was a NEC 8023.
60 DIM X(100),Y(64),P(64),G(11),F(64)     'dimension arrays
65 LPRINT CHR$(27);"L";"008"      'set left margin
70 N = 64           ' number of input numbers
80 FOR I = 1 TO N       ' read in data .........
90 'READ X(I)          'from the DATA line, or.....
100 X(I) = SIN(1*I/N*2*3.1416)    'calculate your own
110 NEXT 'I
120 GOSUB 310       'calculate FWT of input series
130 FOR B = 1 TO N     'divide all coeffs by N and downshft 1
140 F(B-1) = X(B)/N   ' this array contains the FWT coeffs
150 NEXT 'B
160 GOSUB 600     'calculate power spectrum coefficients
170 GOSUB 720     ' calculate group spectrum
180 GOSUB 840   'output the FWT coeffs
190 GOSUB 950   'output the PSD coeffs
200 GOSUB 1047   'output the group coeffs
230 END
235 '
240 '              SUBROUTINE FHT(N,X,Y)
250 '
260 '  This routine performs a FWT of an input series in array
      X.  The array Y is used for working space.
270 ' The dimensions of X and Y must be a power of 2.
280 ' The results of the FWT are in sequency order, positive
290 ' phasing, and in array X. The subroutine uses a Hadamard
      transform.
300 '
310 N2 = N/2
320 M = 6           ' M equals the base 2 logarithm of N
330 FOR L = 1 TO M
340   NY = 0
350   NZ = 2^(L-1)
360   NZI = 2 * NZ
370   NZN = N/NZI
380   FOR I = 1 TO NZN
390     NX = NY + 1
400     NY = NY + NZ
410     JS = (I-1) * NZI
420     JD = JS + NZI + 1
430     FOR J = NX TO NY
440       JS = JS + 1
```

```
450         J2 = J + N2
460         Y(JS) = X(J) + X(J2)
470         JD = JD - 1
480         Y(JD) = X(J)- X(J2)
490       NEXT 'J
500     NEXT 'I
510    FOR B = 1 TO N
520    X(B) = Y(B)
530    NEXT 'B
540 NEXT 'L
550 RETURN
555 '                          SUBROUTINE PSD(N)
560 '
570 '
580 '  This routine calculates the Walsh Power Spectral
      Density Coefficients.
590 '
600 P(0) = (F(0))^2              'first PSD coefficient
610 K=1
620 FOR I = 1 TO (N/2)-1     'coefficients 1 to N/2-1
630       P(I)= (F(K))^2 + (F(K+1))^2
640       K = K + 2
650 NEXT 'I
660 P(N/2)=(F(N-1))^2        'last PSD coefficient
670 RETURN
680 '
690 '                    SUBROUTINE GROUP SPECTRUM(M)
700 '
710 ' This subroutine calculates the group spectrum
      coefficients.
720 D=1
730 G(0) = P(0)^2
740 FOR B = 0 TO M-1
750 FOR C =(2^B) TO N/2-1  STEP (2*2^B)
760 G(D) = G(D) + P(C)^2
770 NEXT 'C
780 D = D+1
790 NEXT 'B
800 G(M) = P(N/2)^2
810 RETURN
820 '
830 '  This subroutine outputs the Walsh Transform
      Coefficients.
840 '
841 FOR C = 1 TO 5: LPRINT: NEXT        ' 1 inch top margin
842 LPRINT"            FWT COEFFICIENTS FOR 1 CYCLE SINE
FUNCTION"
843 LPRINT:  LPRINT    'skip two lines
850 LPRINT "Walsh Function" TAB(20) "Coeff." TAB(35)"Walsh
      Function" TAB(55) "Coeff."
```

```
860 LPRINT STRING$(15,45) TAB(20) STRING$(6,45) TAB(35)
      STRING$(15,45) TAB(55) STRING$(6,45)
870 FOR B = 1 TO 32      'output the coeffs
880 LPRINT "WAL(";B-1;",t)" TAB(16):  LPRINT USING
      "##.#######";F(B-1);: LPRINT" "     TAB(35)
890 LPRINT "WAL(";B+31;",t)" TAB(52) :  LPRINT USING
      "##.#######";F(B+31)
900 NEXT 'B
910 FOR C = 1 TO 16 : LPRINT: NEXT     'skip 16 lines
911 LPRINT"                                    xx"    'print pg. no
912 LPRINT CHR$(12)   'form feed
920 RETURN
930 '
940 '        Output the PSD coefficients.
950 '
951 FOR C = 1 TO 5: LPRINT: NEXT
970 LPRINT "           PSD COEFFICIENTS FOR A 1 CYCLE SINE
      FUNCTION"
980 LPRINT : LPRINT
990 FOR B = 0 TO N/2
1000 LPRINT "P("; B ;")=" ;: LPRINT USING "##.########";P(B)
1020 NEXT 'B
1025 LPRINT: LPRINT
1040 RETURN
1044 '
1045 '  Output the group coefficients
1046 '
1047 LPRINT"    GROUP SPECTRUM COEFFICIENTS OF A 1 CYCLE SINE
      FUNCTION"
1048 LPRINT: LPRINT
1050 FOR B = 0 TO M
1060 LPRINT "G(";B;")= ";:LPRINT USING "##.########";G(B)
1070 NEXT 'B
1071 FOR C = 1 TO 7: LPRINT: NEXT
1072 LPRINT "                                  xx"
1073 LPRINT CHR$(12)     'form feed
1080 RETURN
```

```
10 !  This program computes the Fast Walsh Tranform , the
      Power Spectral Density, and the Group Spectrum
20 !  Coefficients of a number series.
30 !  The FWT subroutine is a BASIC adaptation of a FORTRAN
      program listed 40 ! in " Walsh Functions and Their
      Applications," by K.G. Beauchamp.
45 !  The PSD and Group Spectrum subroutines were written by
      the author.
50 !  This program runs on HP 85 Computer, and writes the
      coefficients to data files named "FWT","PSD",and "GRP".
60 DIM X(100),Y(64),P(64),G(11),F(64)    !dimension arrays
65 PRINTER IS 2    ! select printer for output of print
70 N = 64          ! number of input numbers
80 FOR I = 1 TO N      ! read in data .........
90 !READ X(I)         !from the DATA line, or...........
100 X(I) = SIN(1%I/N%2%3.1416)   !calculate your own
110 NEXT I
120 GOSUB 310       !calculate FWT of input series
130 FOR B = 1 TO N    !divide all coeffs by N
140 X(B) = X(B)/N  ! this array contains the FWT coeffs
150 NEXT B
155 BEEP @ CLEAR
156 DISP "FWT CAL OVER"
160 GOSUB 600     !calculate power spectrum coefficients
165 DISP "PSD CAL OVER"
170 GOSUB 720     ! calculate group spectrum
175 DISP "GRP COEFF CAL OVER"
180 GOSUB 840  !output the FWT coeffs
190 GOSUB 950  !output the PSD coeffs
200 GOSUB 1047  !output the group coeffs
205 CREATE "FWT",30          ! creates file
206 ASSIGN #1 TO "FWT"    ! opens file
207 FOR B = 1 TO 64
208 PRINT# 1; X(B)
209 NEXT B
210 ASSIGN# 1 TO %       !closes file
211 CREATE "PSD", 20
212 ASSIGN #1 TO "PSD"
213 FOR B = 0 TO N/2
214 PRINT# 1; P(B)
215 NEXT B
216 ASSIGN# 1 TO %
217 CREATE "GRP", 20
218 ASSIGN #1 TO "GRP"
219 FOR B = 0 TO M
220 PRINT# 1; G(B)
221 NEXT B
222 ASSIGN# 1 TO %
225 BEEP @ DISP "PROGRAM OVER"
230 END
231 !
```

```
235 !
240 !              SUBROUTINE FHT(N,X,Y)
250 !
260 !  This routine performs a FWT of an input series in array
      X.  The array Y is used for working space.
270 ! The dimensions of X and Y must be a power of 2.
280 ! The results of the FWT are in sequency order, positive
290 ! phasing, and in array X. The subroutine uses a Hadamard
      transform.
300 !
310 N2 = N/2
320 M = 6            ! M equals the base 2 logarithm of N
330 FOR L = 1 TO M
340   N1 = 0
350   N3 = 2^(L-1)
360   N4 = 2 * N3
370   N5 = N/N4
380   FOR I = 1 TO N5
390     N6 = N1 + 1
400     N1 = N1 + N3
410     J1 = (I-1) * N4
420     J3 = J1 + N4 + 1
430     FOR J = N6 TO N1
440       J1 = J1 + 1
450       J2 = J + N2
460       Y(J1) = X(J) + X(J2)
470       J3 = J3 - 1
480       Y(J3) = X(J)- X(J2)
490     NEXT J
500   NEXT I
510  FOR B = 1 TO N
520  X(B) = Y(B)
530  NEXT B
540 NEXT L
550 RETURN
555 !                        SUBROUTINE PSD(N)
560 !
570 !
580 !  This routine calculates the Walsh Power Spectral
      Density Coefficients.
590 !
600 P(0) = (F(0))^2             !first PSD coefficient
610 K=1
620 FOR I = 1 TO (N/2)-1     !coefficients 1 to N/2-1
630     P(I)= (F(K))^2 + (F(K+1))^2
640     K = K + 2
650 NEXT !I
663 P(N/2)=(F(N-1))^2      !last PSD coefficient
670 RETURN
671 !
672 !
```

```
680 !
690 !                    SUBROUTINE GROUP SPECTRUM(M)
700 !
710 ! This subroutine calculates the group spectrum
      coefficients.
720 D=1
730 G(0) = P(0)^2
740 FOR B = 0 TO M-1
750 FOR C =(2^B) TO N/2-1  STEP (2*2^B)
760 G(D) = G(D) + P(C)^2
770 NEXT !C
780 D = D+1
790 NEXT B
800 G(M) = P(N/2)^2
810 RETURN
820 !
830 !  This subroutine outputs the Walsh Transform
      Coefficients.
840 !
850 PRINT "Walsh Function";TAB(20);"Coefficient" @ PRINT
870 FOR B = 1 TO 64      !output the coeffs
880 PRINT "WAL(";B-1;",t)";TAB(20); F(B)
900 NEXT B
929 RETURN
930 !
940 !        Output the PSD coefficients.
950 !
960 PRINT
970 PRINT "POWER SPECTRUM COEFFS" @ PRINT
990 FOR B = 0 TO N/2
1000 PRINT "P("; B ;")=" ; P(B)
1020 NEXT B
1040 RETURN
1044 !
1045 !  Output the group coefficients
1046 !
1048 PRINT@ PRINT
1049 PRINT "GROUP SPECTRUM COEFFICIENTS" @ PRINT
1050 FOR B = 0 TO M
1060 PRINT "G(";B;")= ";@PRINT USING "##.########";G(B)
1070 NEXT B
1080 RETURN
1085 !  This is a typical DATA line of numbers representing
       TOA TAGS
1090 !DATA 1,0,0,0,0,0,0,0,1,0,0,0,0,0,0,0,1,0,0,0,0,0,0,0,1,
          0,0,0,0,0,0,0,1   'etc. for N = 64
```

APPENDIX B

ORTHOGONALITY

The concept of orthogonality in a set of functions is important because only orthogonal sets of functions can be made to represent another function with a required degree of accuracy. The term itself often brings into mind the word "perpendicular", and this thought can be a visualization of the structure of the members of an orthogonal set.

Consider that we have a function set, $S_n(t)$, where $n = 0,1,2,3,...$ The set is said to be orthogonal with weight K over the interval $0 \geq t \geq T$ if

$$\int_0^T K \cdot S_n(t) S_m(t)\,dt = \begin{cases} K & \text{if } n=m \\ 0 & n \neq m \end{cases} \qquad (B.1)$$

with n and m being integer values. If the constant K is equal to 1 then the set is normalized and the set is referred to as an orthonormal set.

With this orthogonal set, we may now represent another function, f(t), defined over the interval (0,T), as

$$f(t) = \sum_0^T C_n S_n(t) \qquad (B.2)$$

and C_n is a number that indicates the value of the function $S_n(t)$. C_n can be chosen so as to mimimize the mean-square error in representing f(t).

$$C_n = 1/T \cdot \int_0^T f(t) S_n(t)\, dt \qquad (B.3)$$

This orthogonal function series representation reduces the number of coefficients needed to completely represent the signal. [23: pp.1-3]

APPENDIX C

MODULO-2 ADDITION AND THE GRAY CODE

Modulo-2 addition is an important mathematical operation in Walsh Theory. Its operation is used in the definition of the Paley ordered Walsh functions with Rademacher functions, and also in the product of two Walsh functions, namely,

$$WAL(n,t)WAL(m,t) = WAL(n \oplus m,t) \qquad (C.1)$$

where $n \oplus m$ indicates modulo-2 addition.

Modulo-2 addition is really binary sums without the carry, and obey the rules

$$0+0=0, \quad 0+1=1, \quad 1+0=1, \text{ and } 1+1=0$$

The Gray Code is a binary code that is often used in communications because the codes for successive decimal digits differs by only 1 bit. It is not a weighted code, meaning that the decimal value of a coded digit cannot be computed by a simple formula.

Table C.1. Gray Code for 16 Digits.

Decimal	Code	Decimal	Code
0	0000	8	1100
1	0001	9	1101
2	0011	10	1111
3	0010	11	1110
4	0110	12	1010
5	0111	13	1011
6	0101	14	1001
7	0100	15	1000

APPENDIX D

FAST WALSH TRANSFORM AND POWER SPECTRAL DENSITY PLOTS

The following pages are the plots of the FWT and PSD coefficient of the simulated TOA TAG strings used in the thesis.

The plots are normalized to the maximum component and thus show the relative value of each component to this maximum.

The value of the maximum component is indicated on the vertical axis.

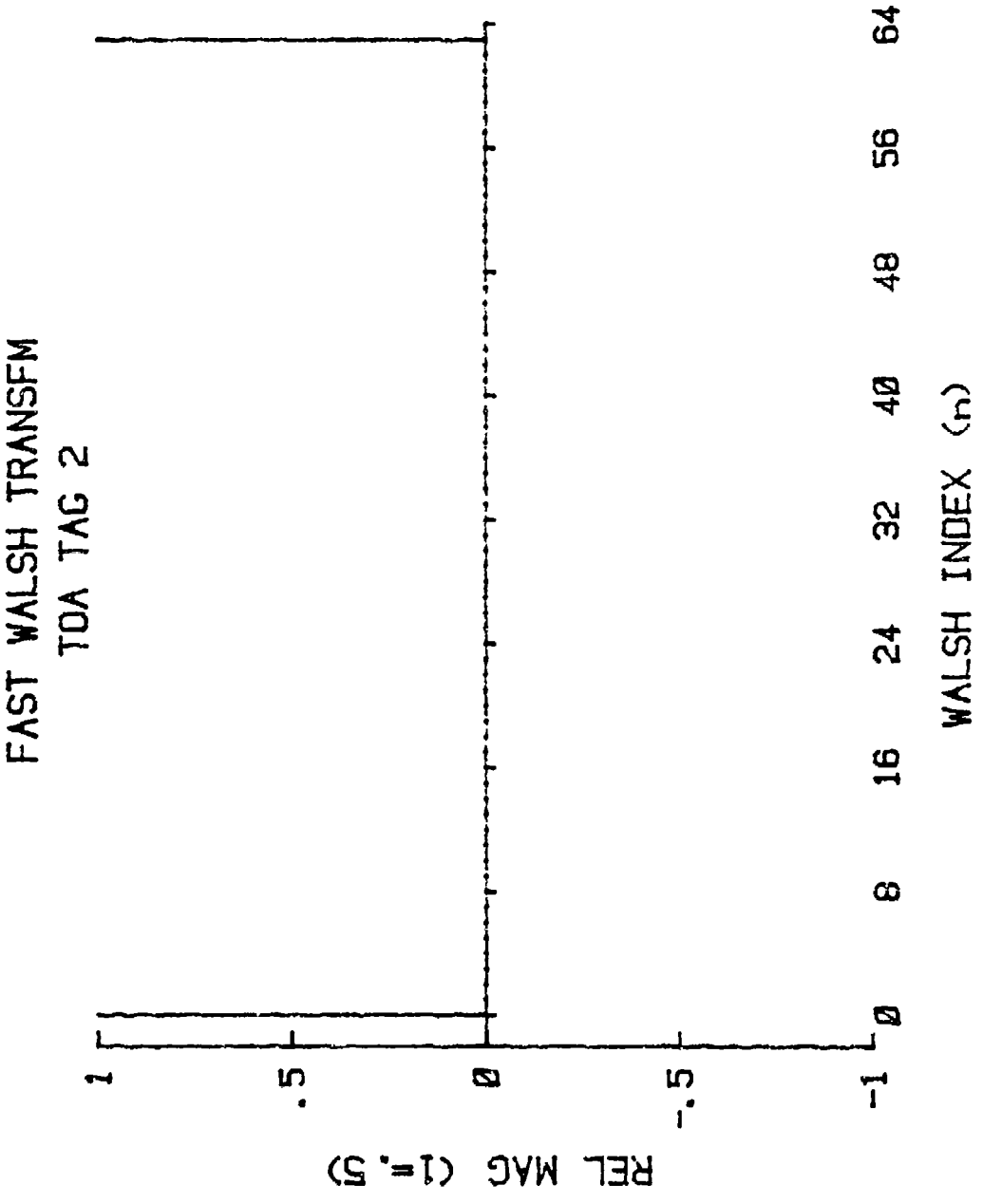

Figure D.1. FWT : TOA TAG 2.

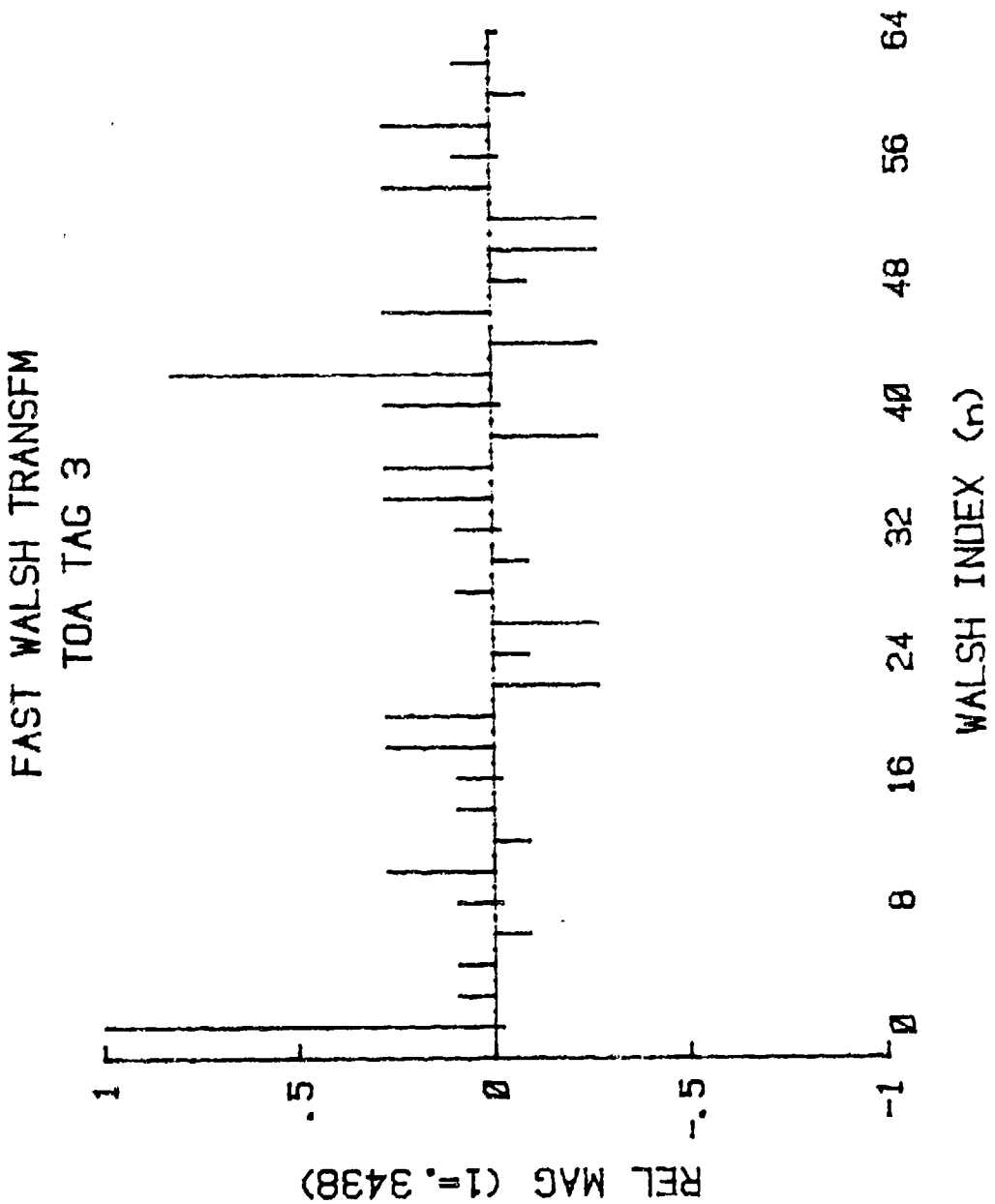

Figure D.2. FWT : TOA TAG 3.

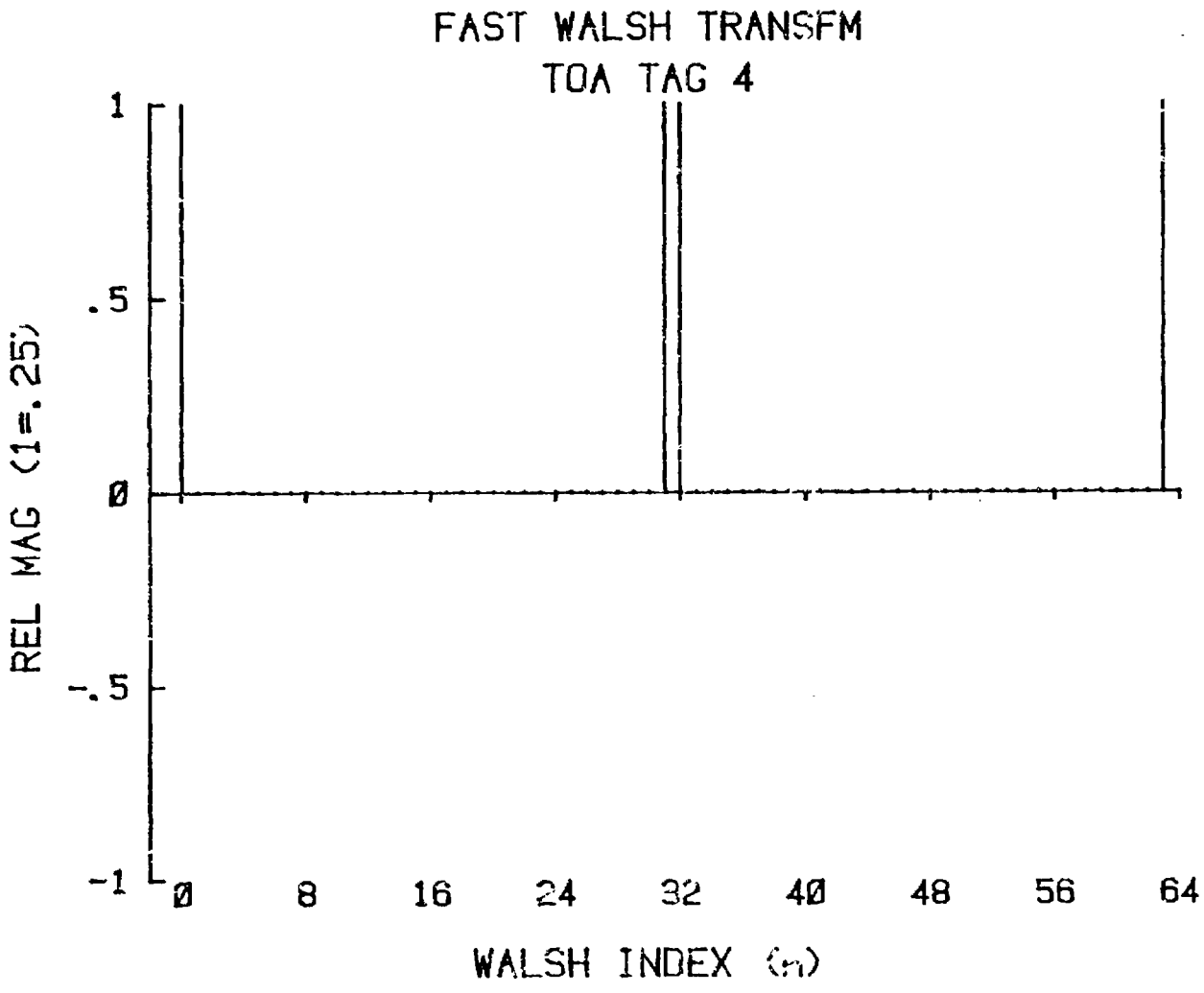

Figure 0.3. FWT : TOA TAG 4.

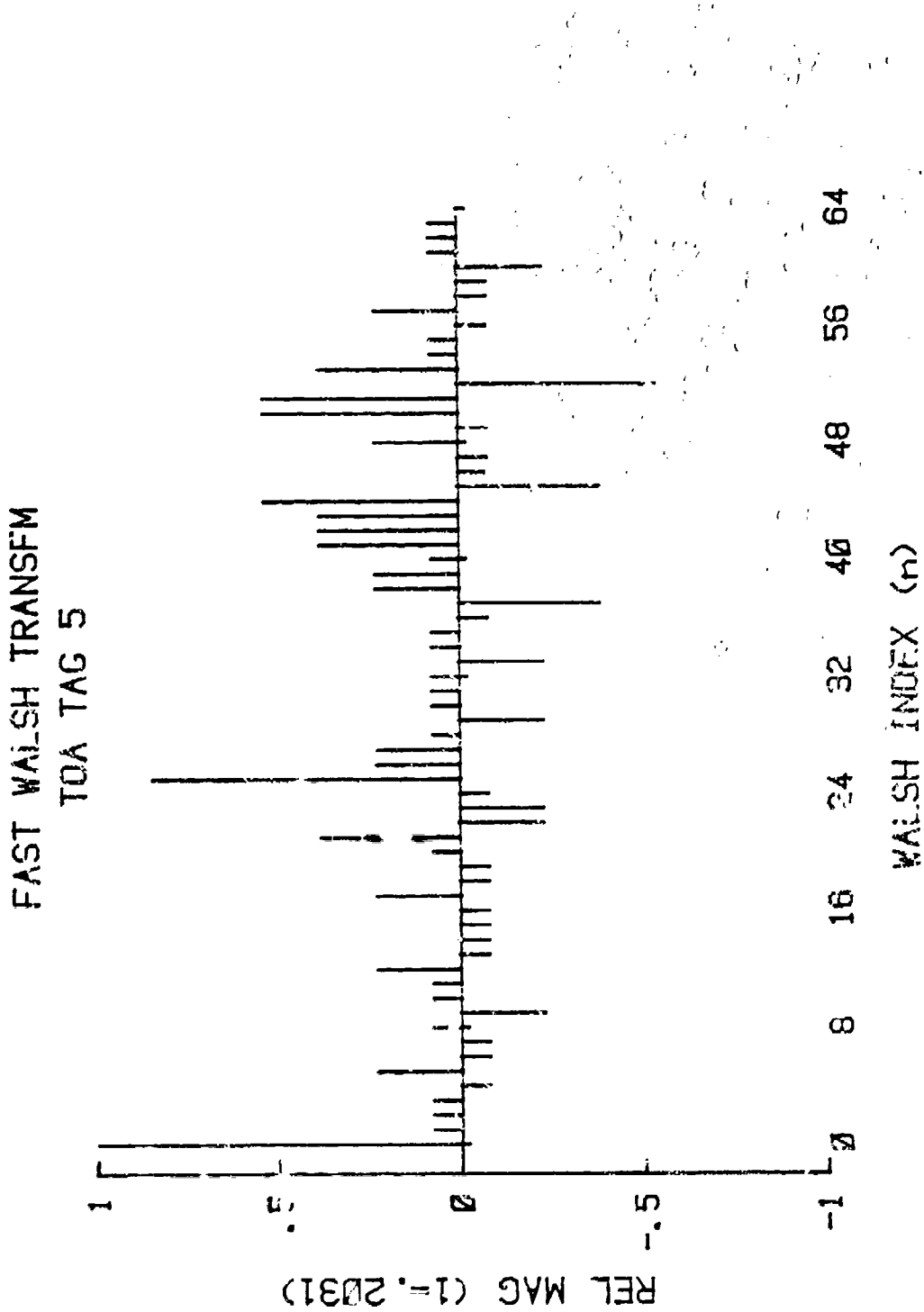

Figure D.4. FWT : TOA TAG 5.

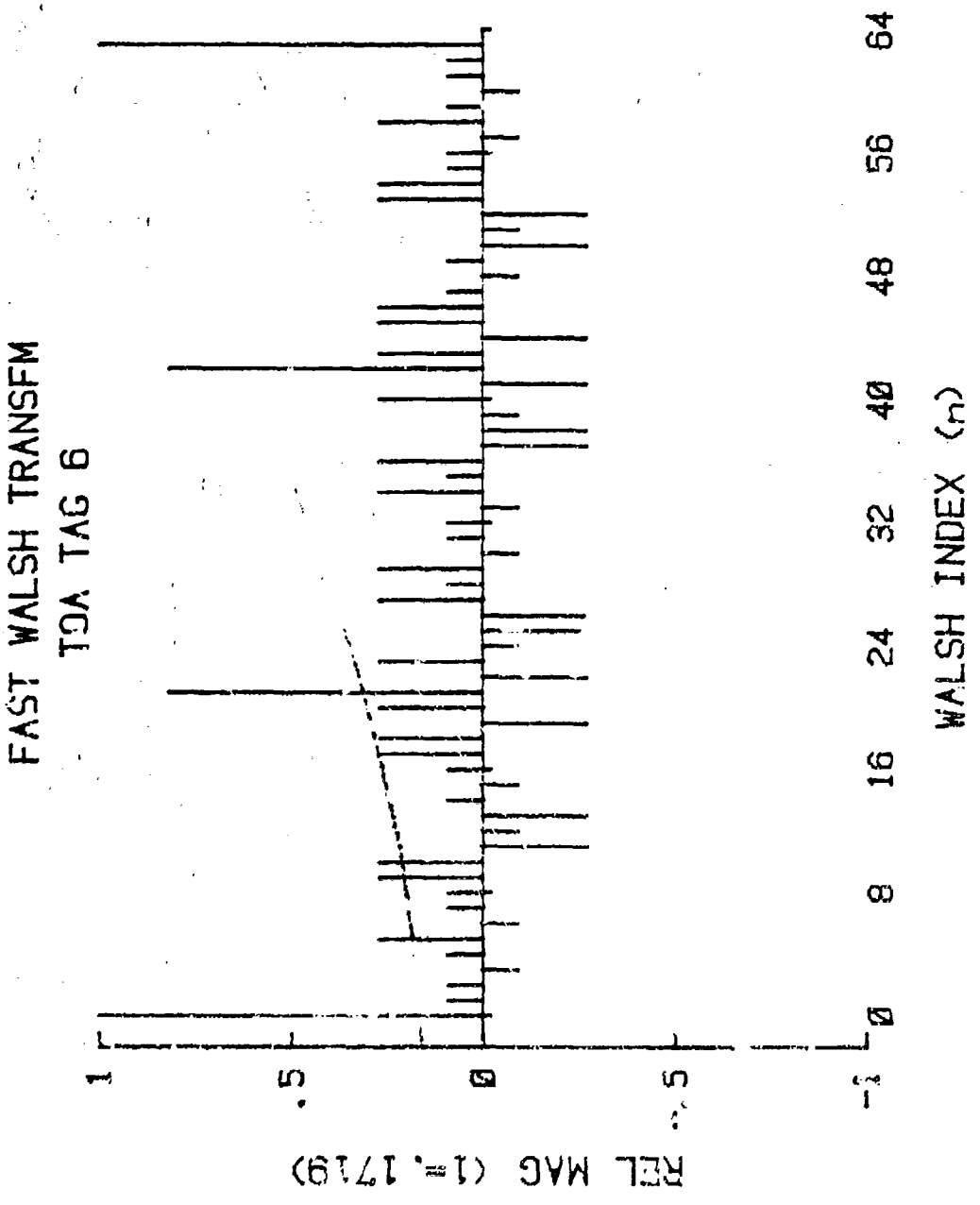

Figure D.5. FWT : TOA TAG 6

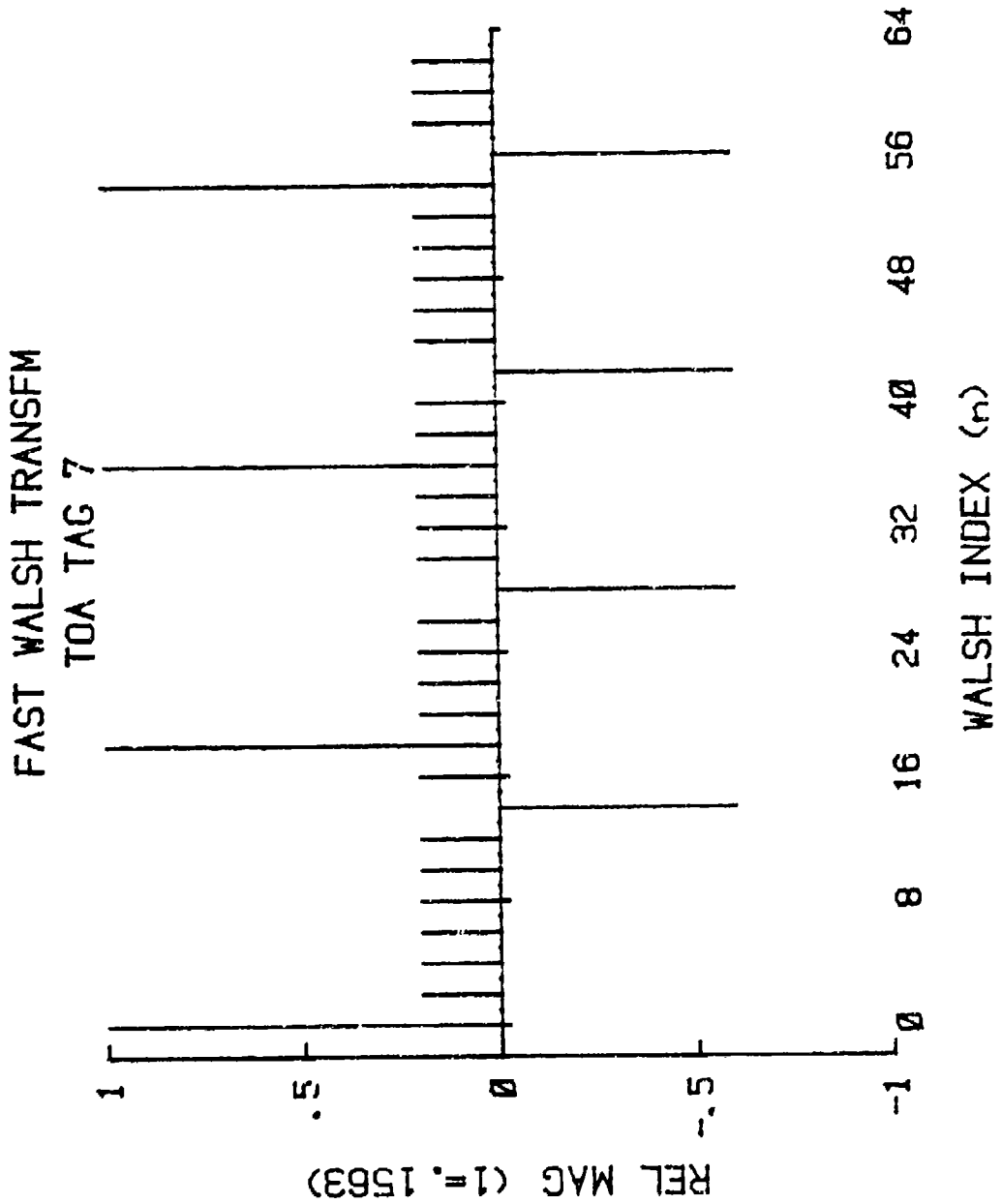

Figure D.6. FWT : TOA TAG 7.

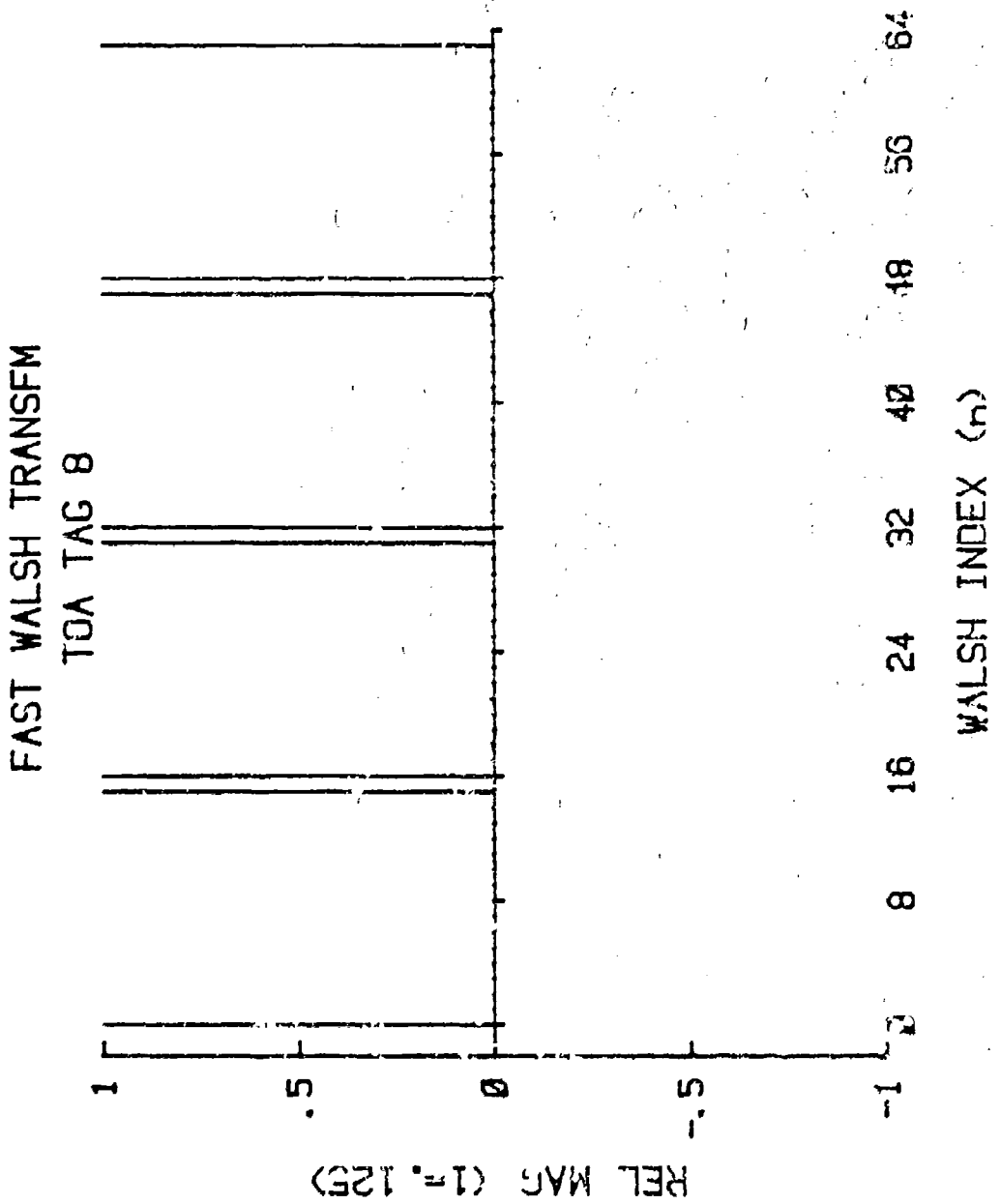

Figure D.7. FWT : TOA TAG 8.

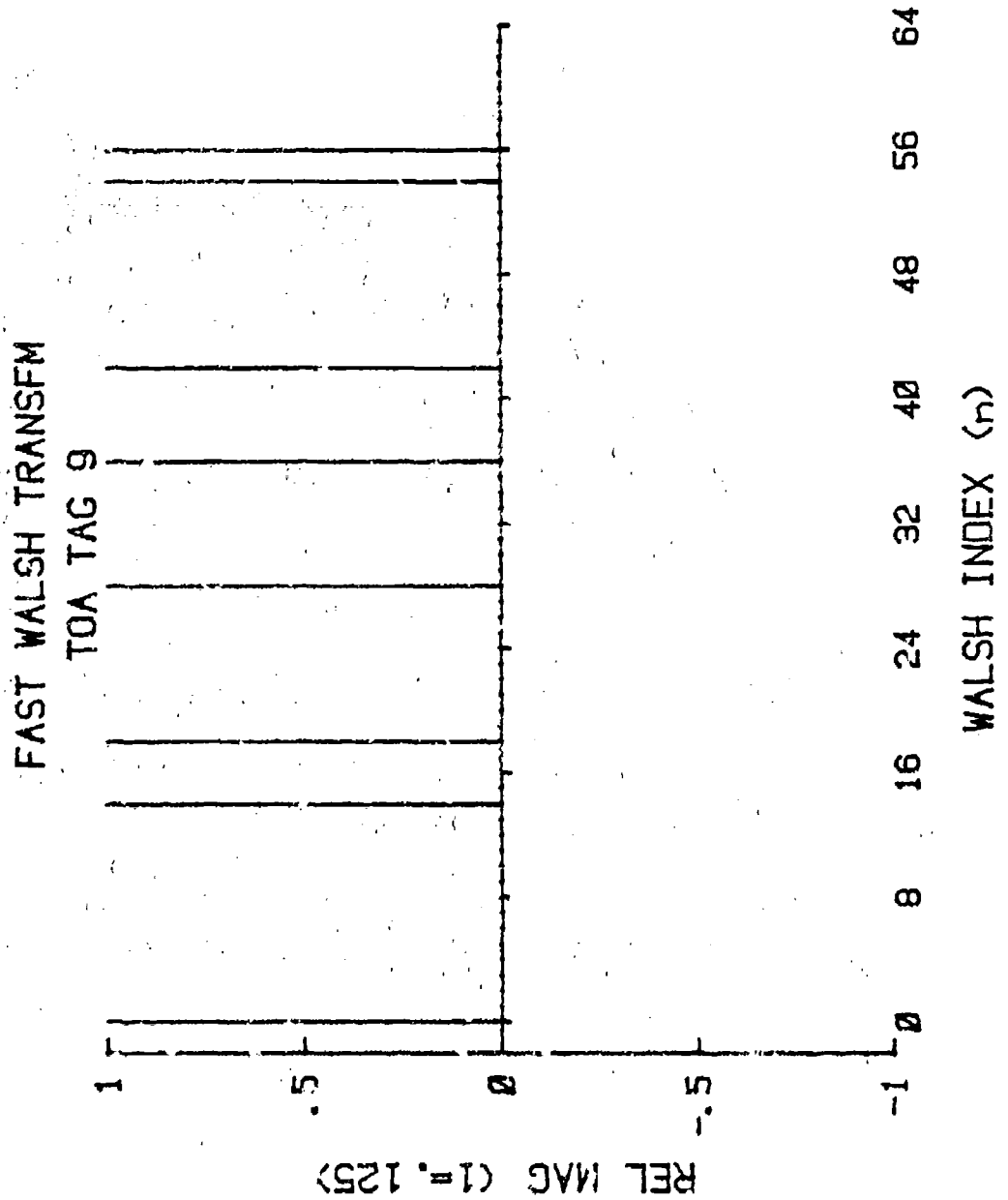

Figure D.8. FWT : TOA TAG 9.

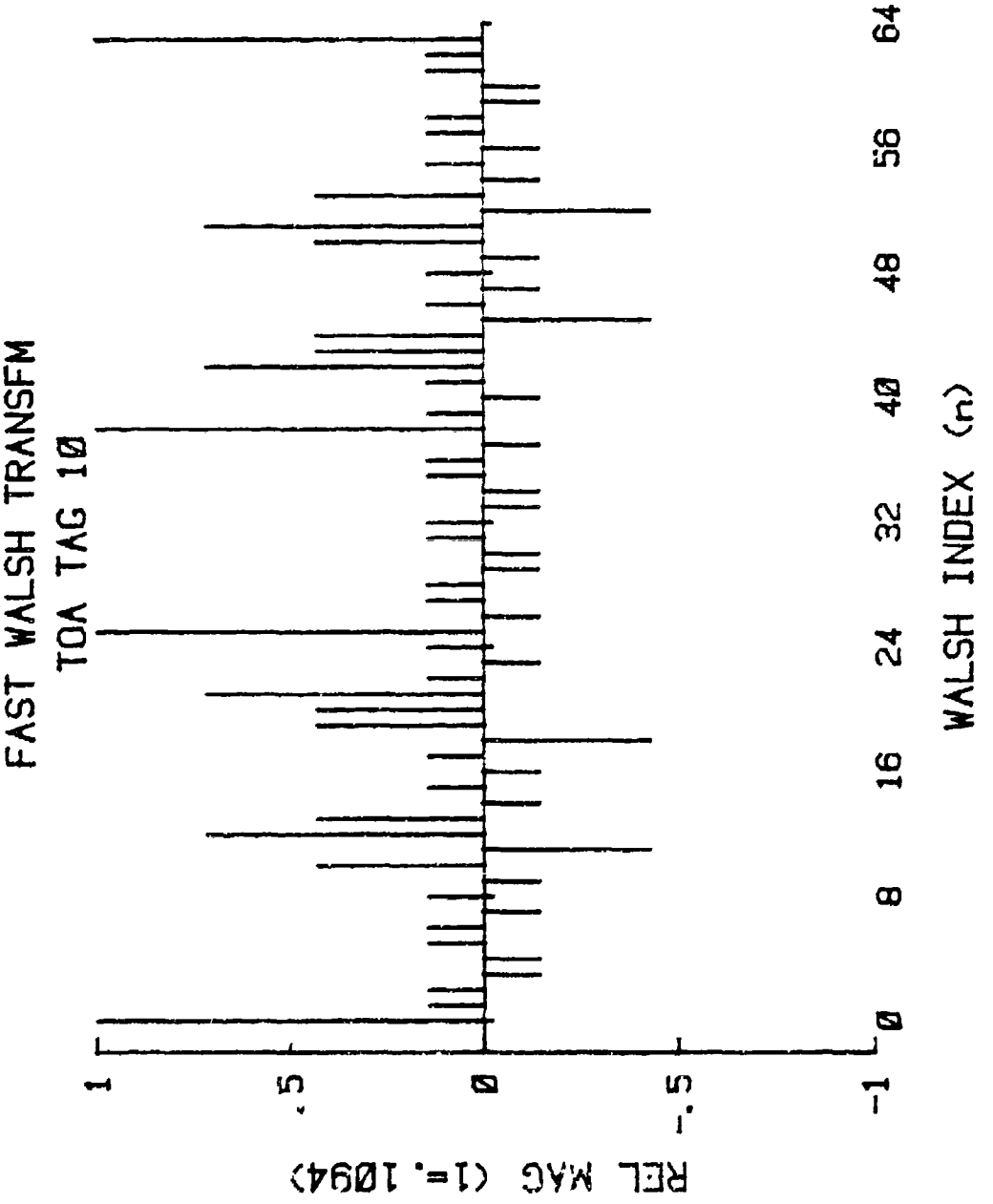

Figure D.9. FWT : TOA TAG 16.

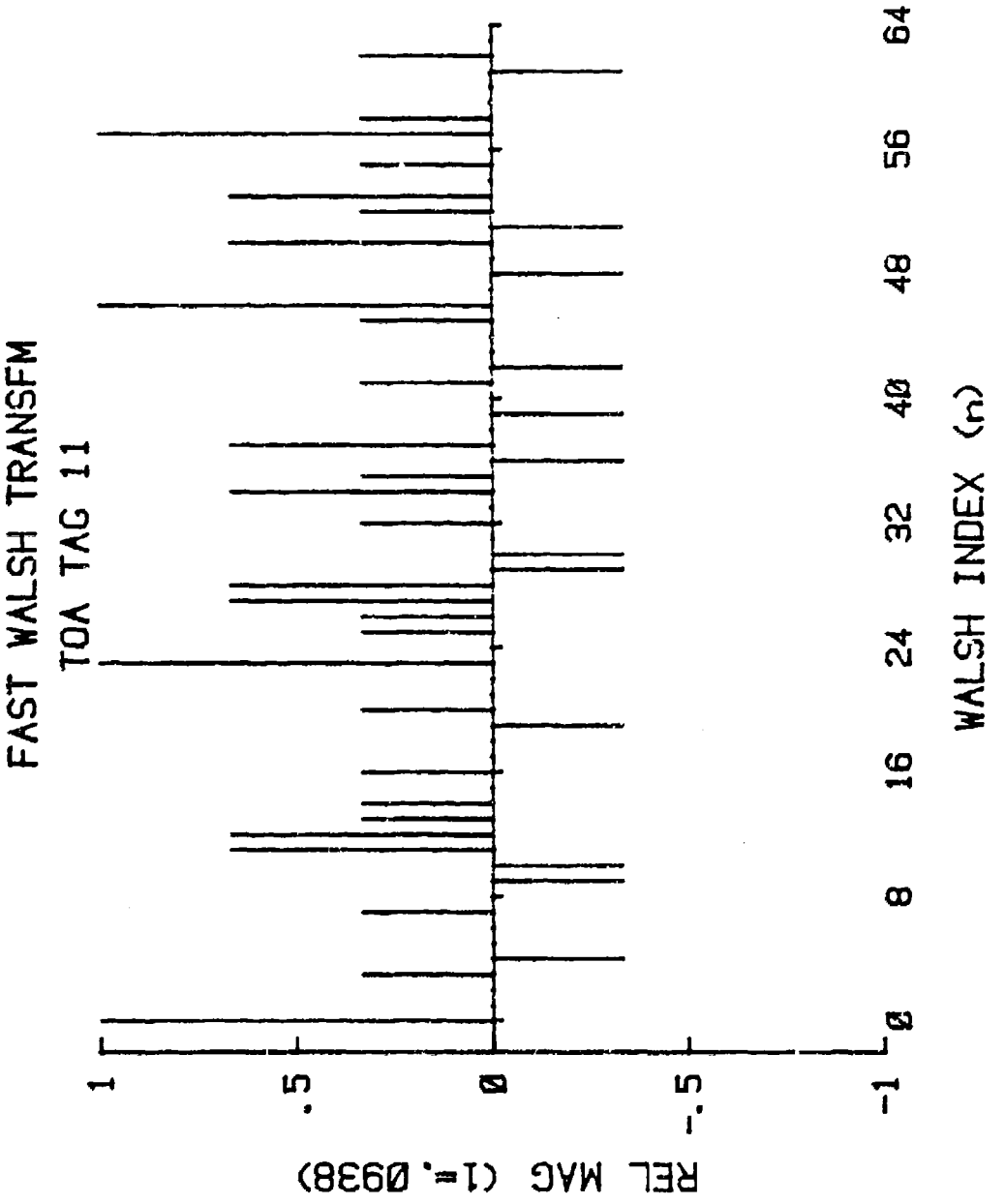

Figure D.10. FWT : TOA TAG 11.

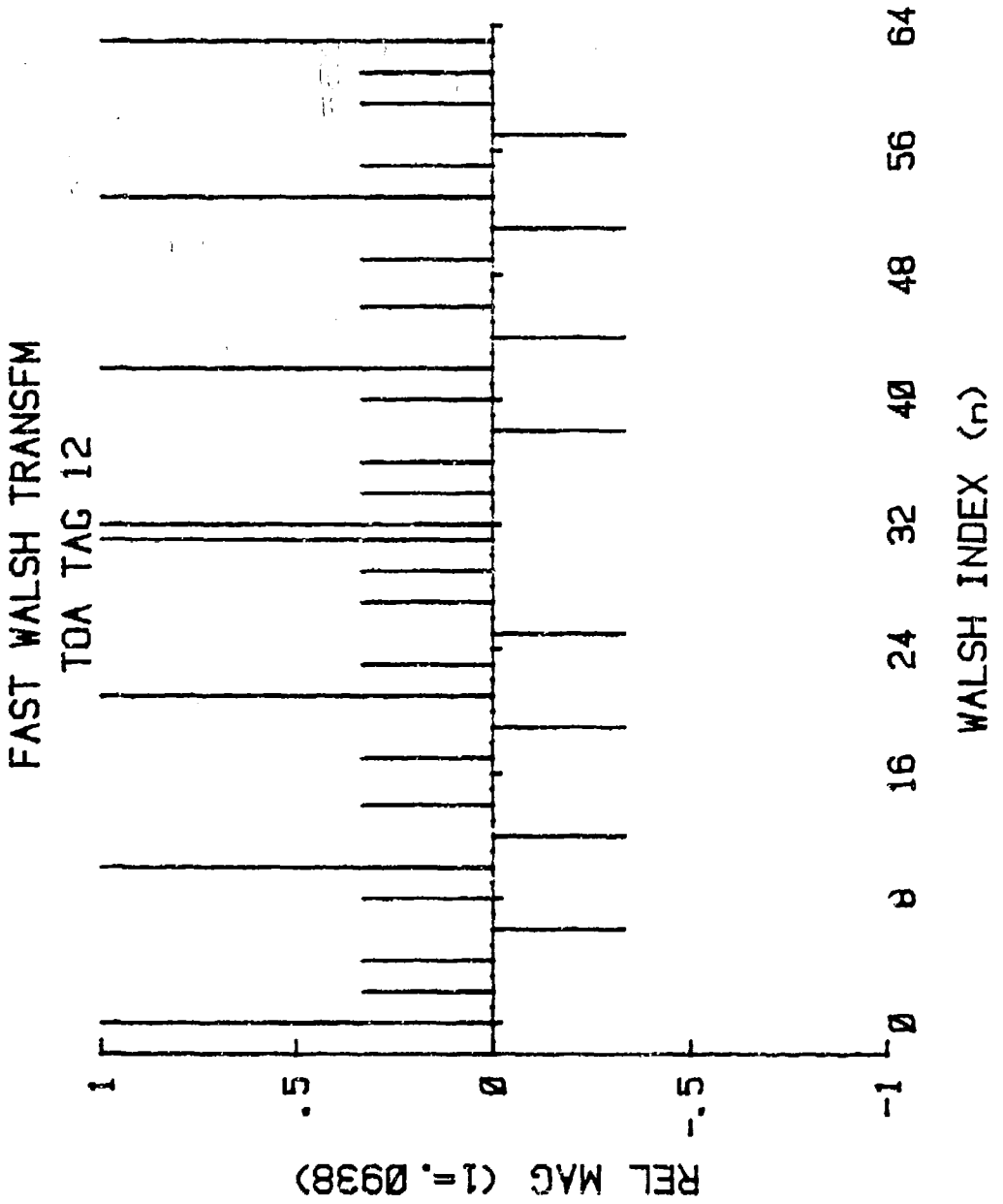

Figure D.11. FWT : TOA TAG 12.

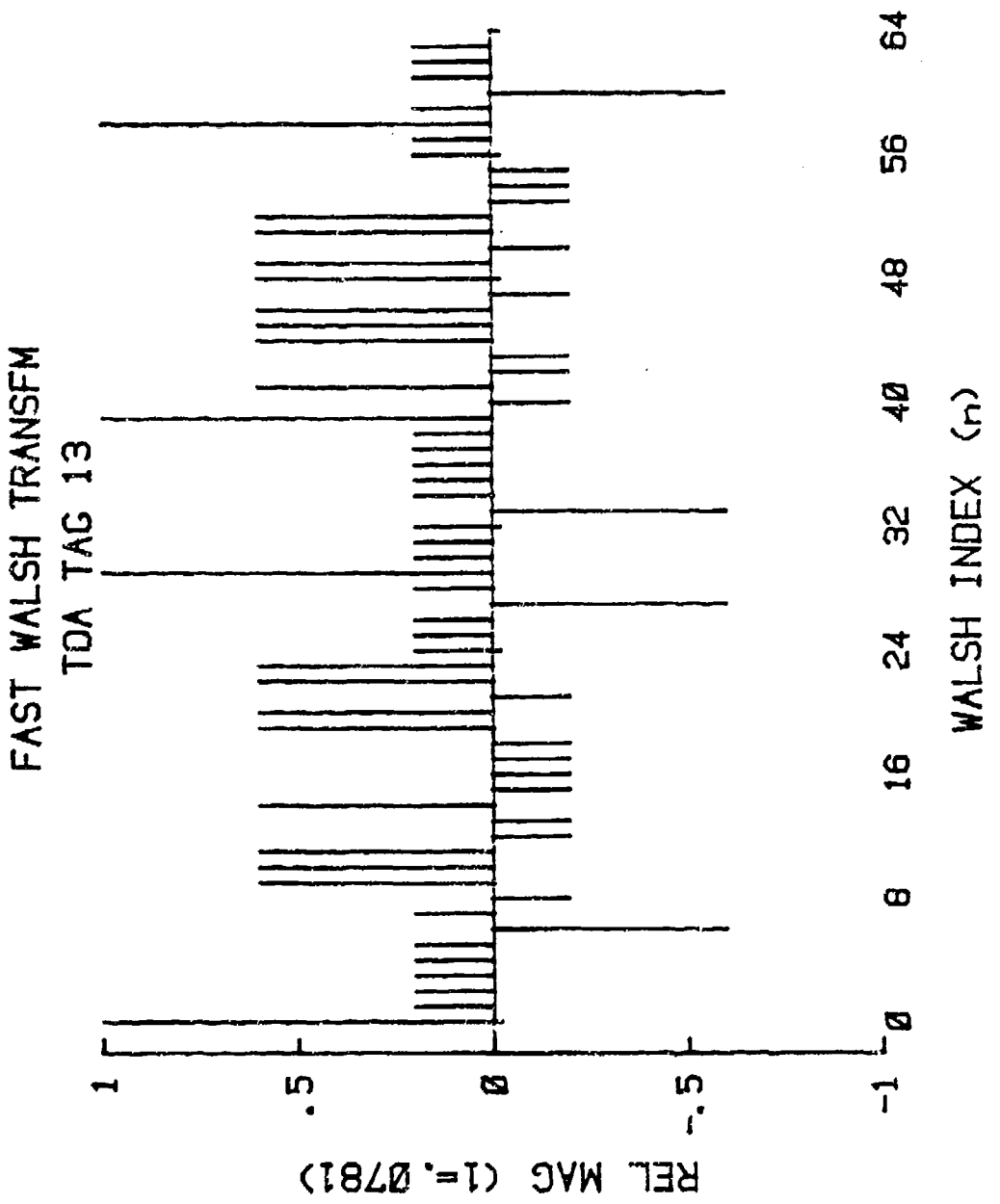

Figure D.12. FWT : TOA TAG 13.

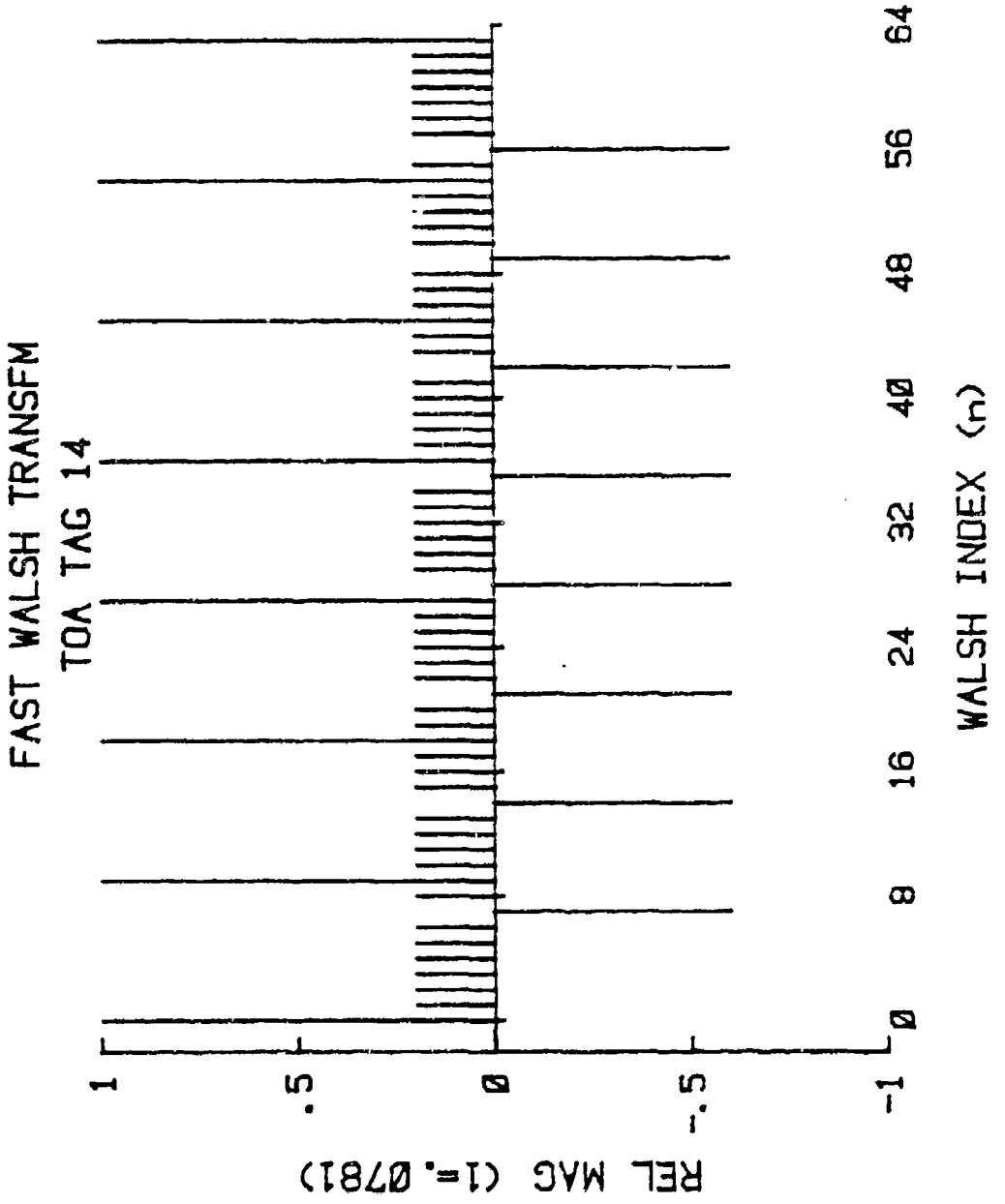

Figure D.13. FWT : TOA TAG 14.

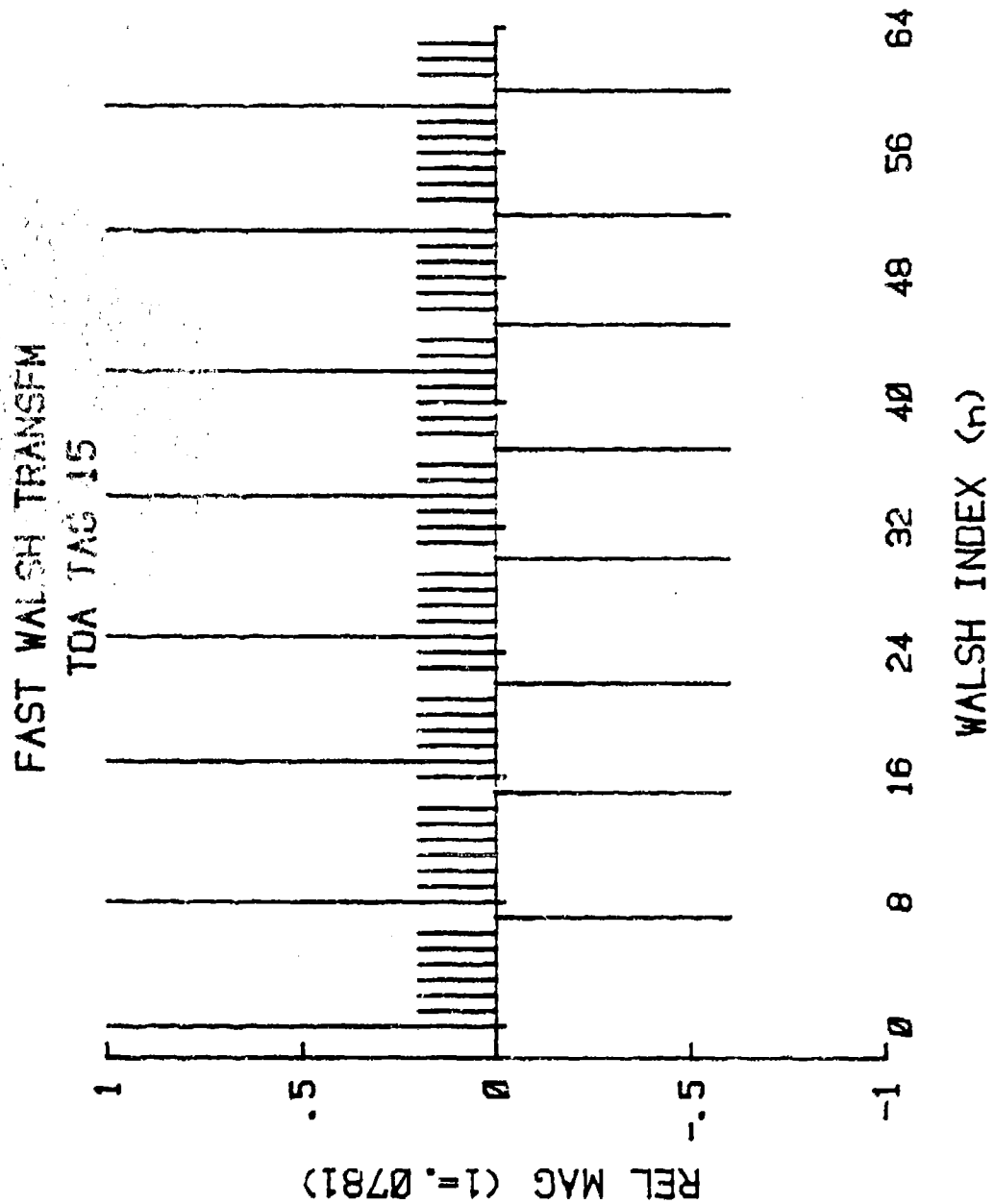

Figure D.14. FWT : TOA TAG 15.

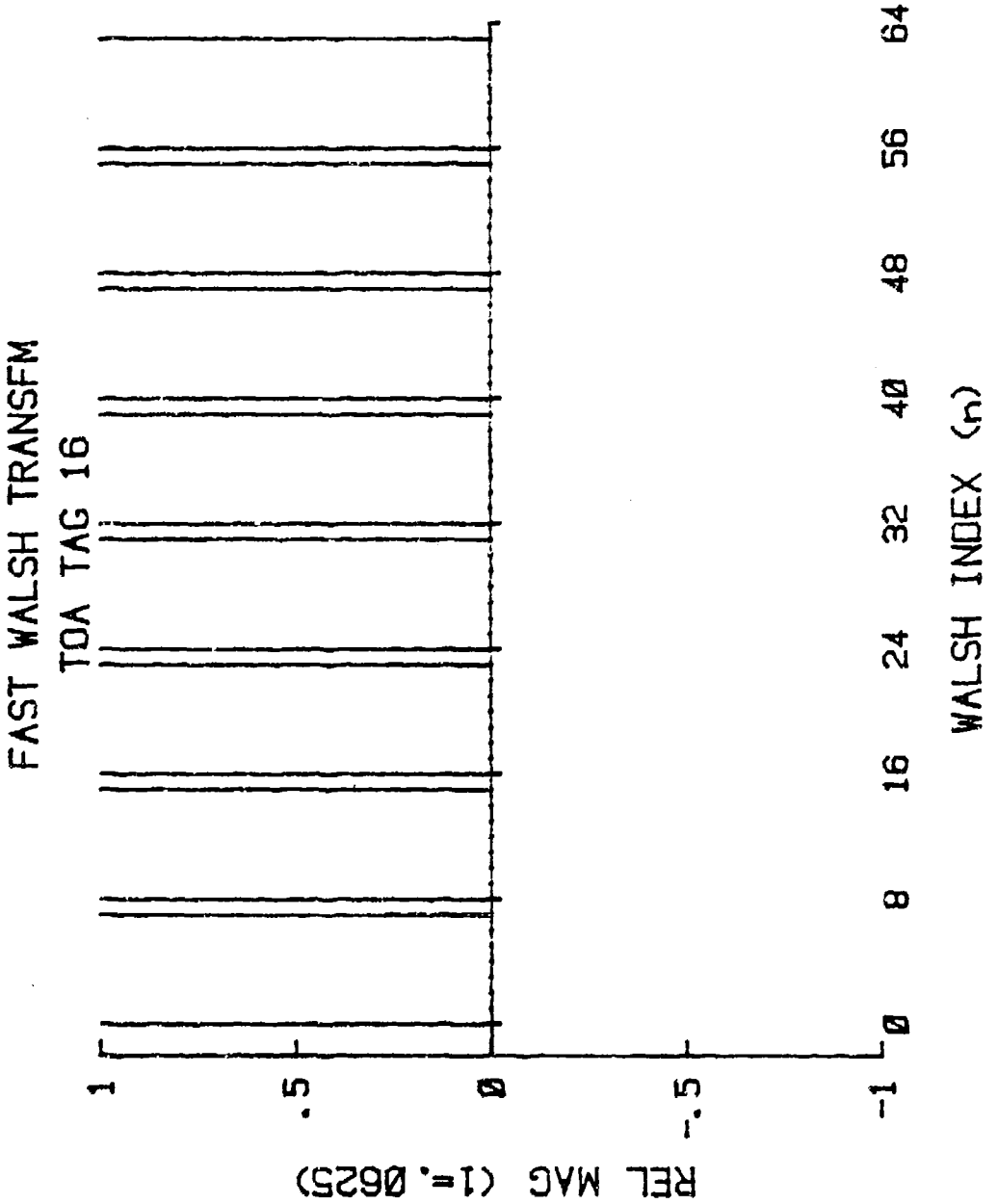

Figure D.15. FWT : TOA TAG 16.

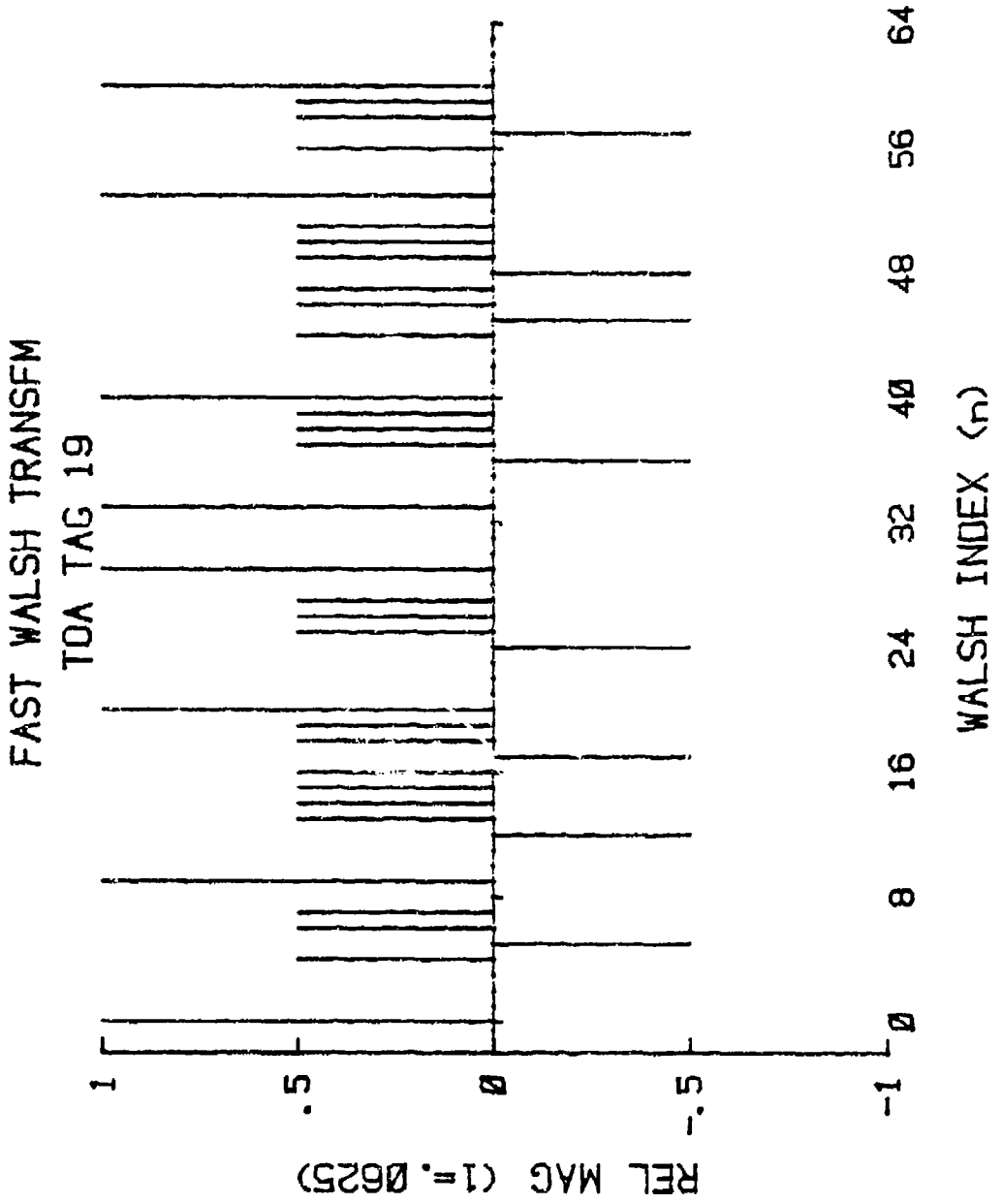

Figure D.16. FWT : TOA TAG 19.

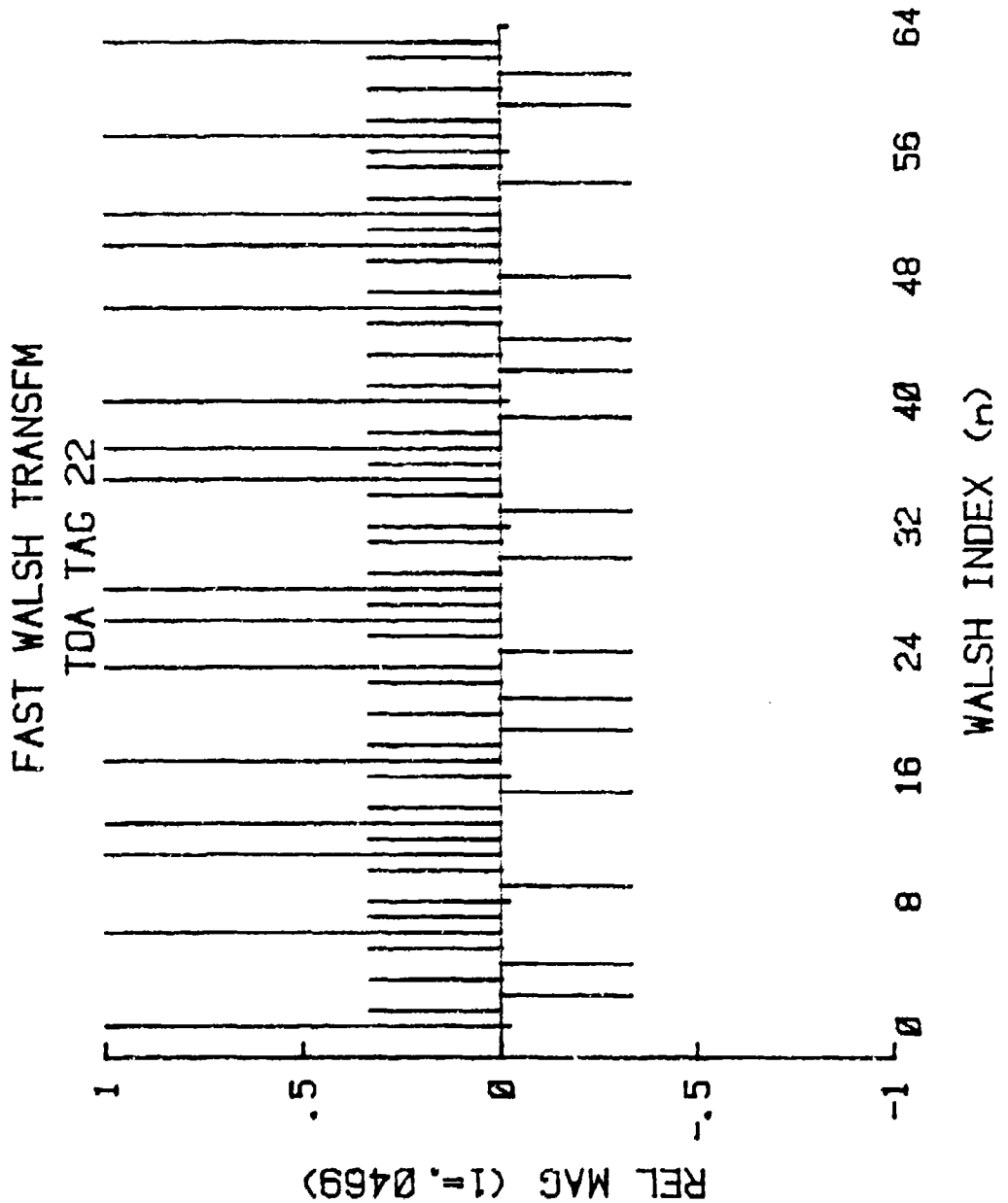

Figure D.17. FWT : TOA TAG 22.

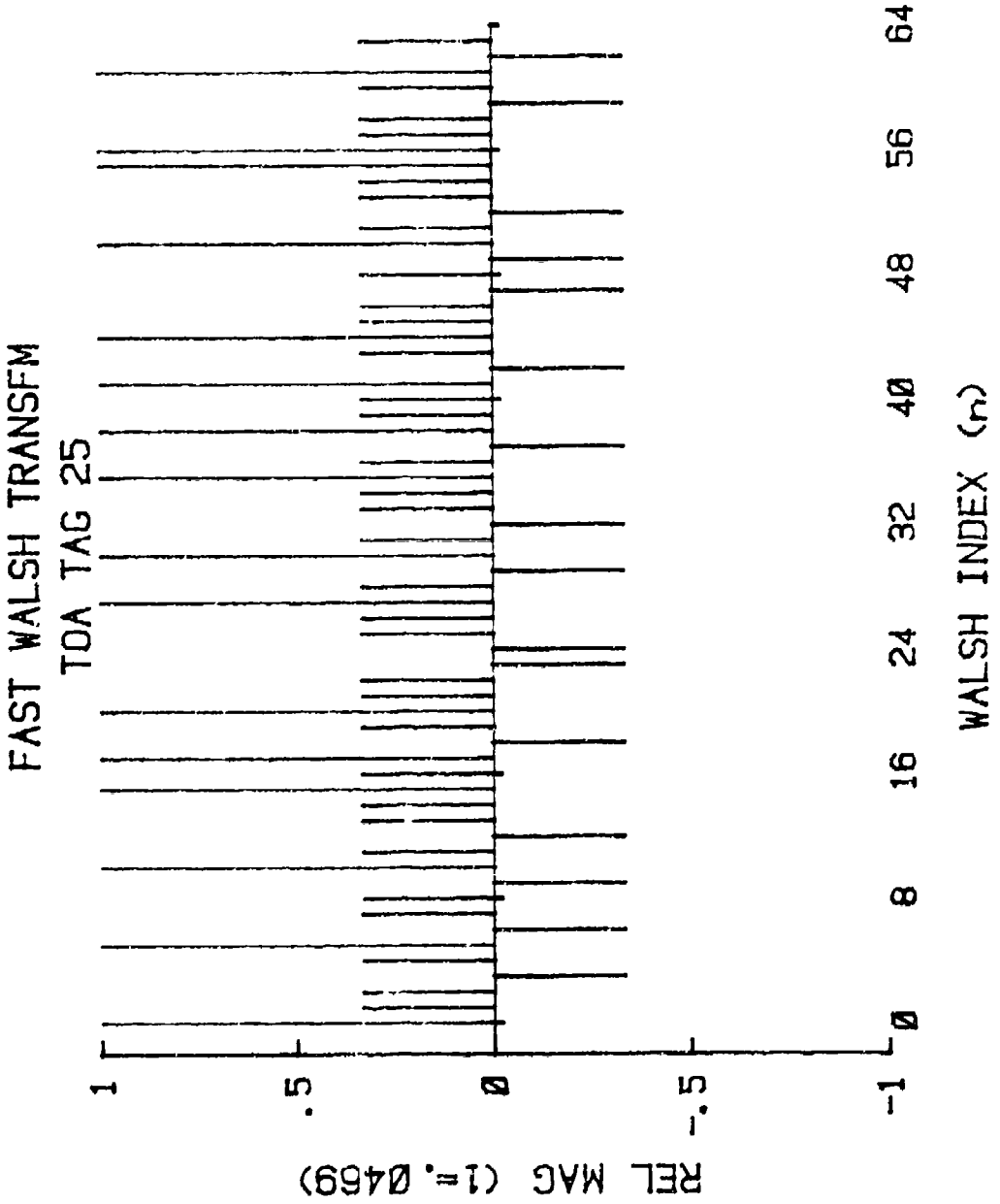

Figure D.18. FWT : TOA TAG 25.

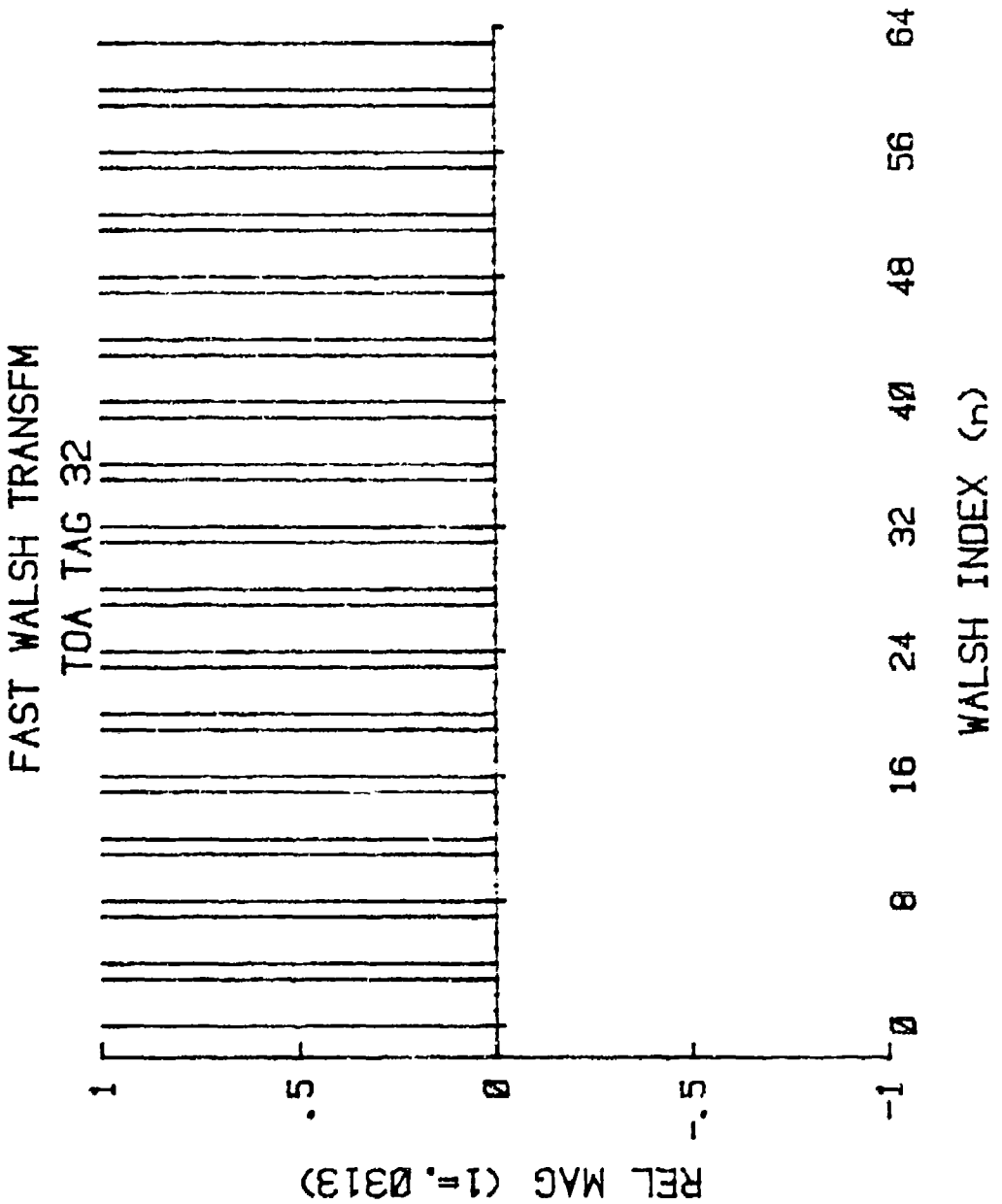

Figure D.19. FWT : TOA TAG 32.

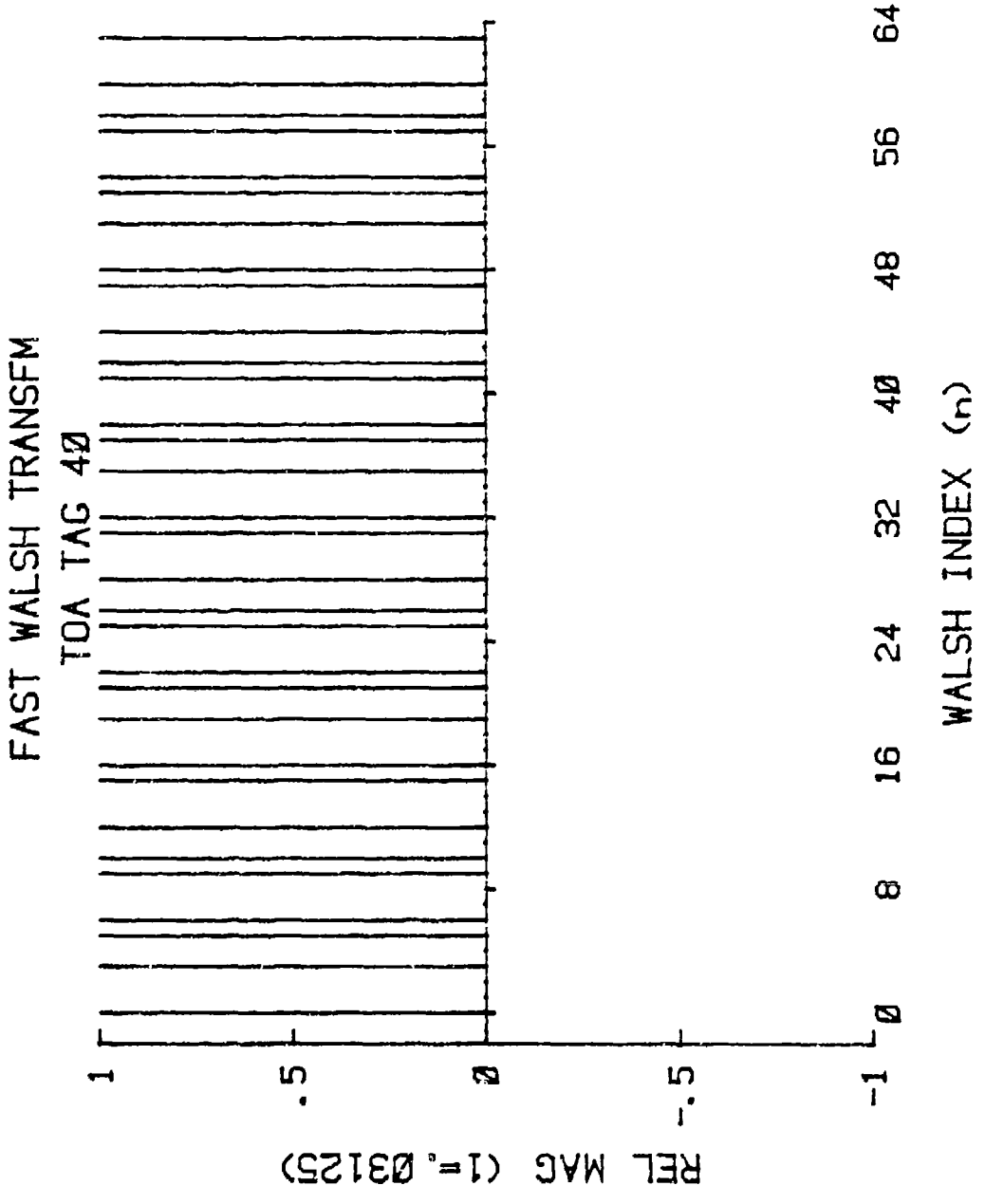

Figure D.20. FWT : TOA TAG 40.

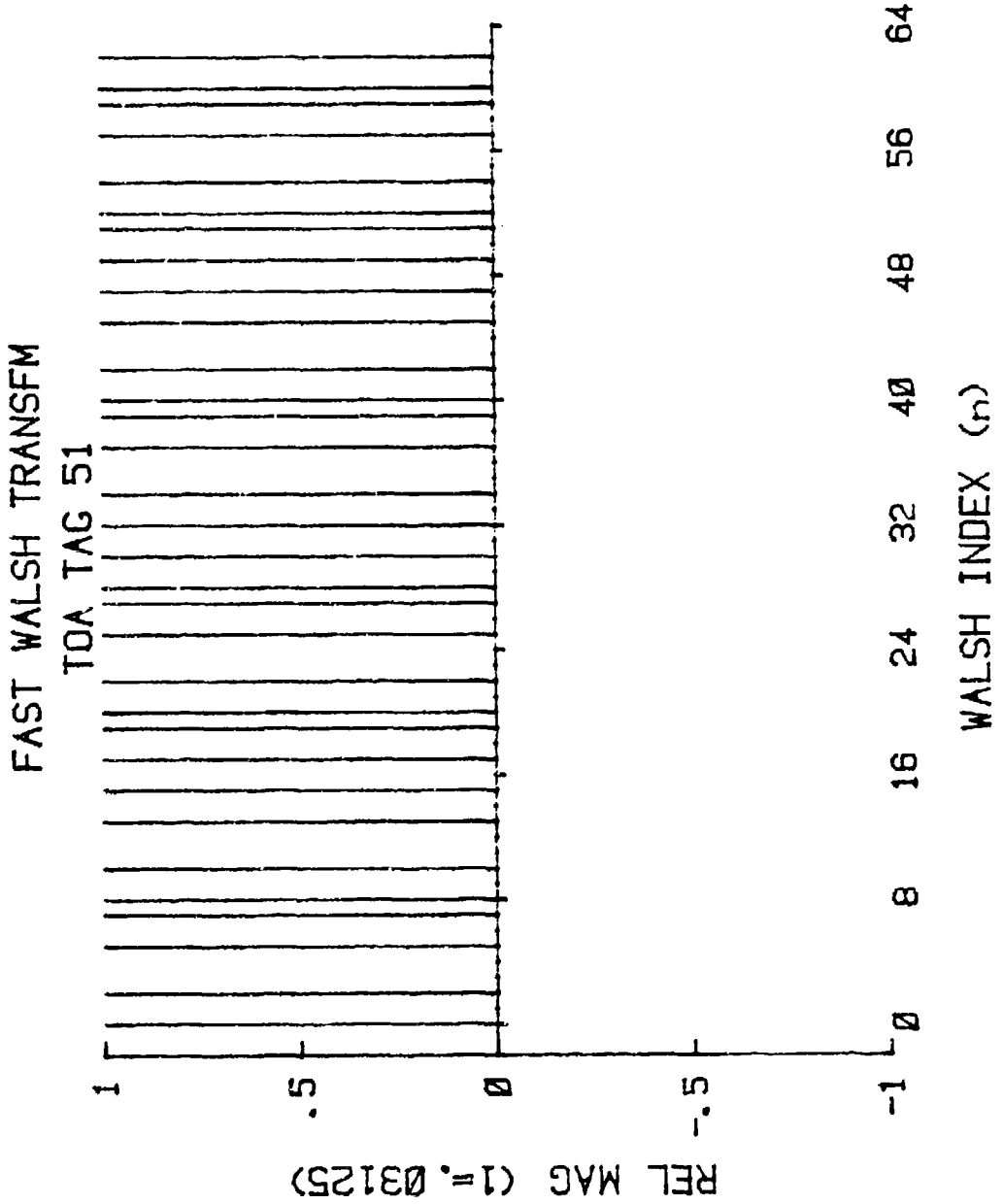

Figure D.21. FWT : TOA TAG 51.

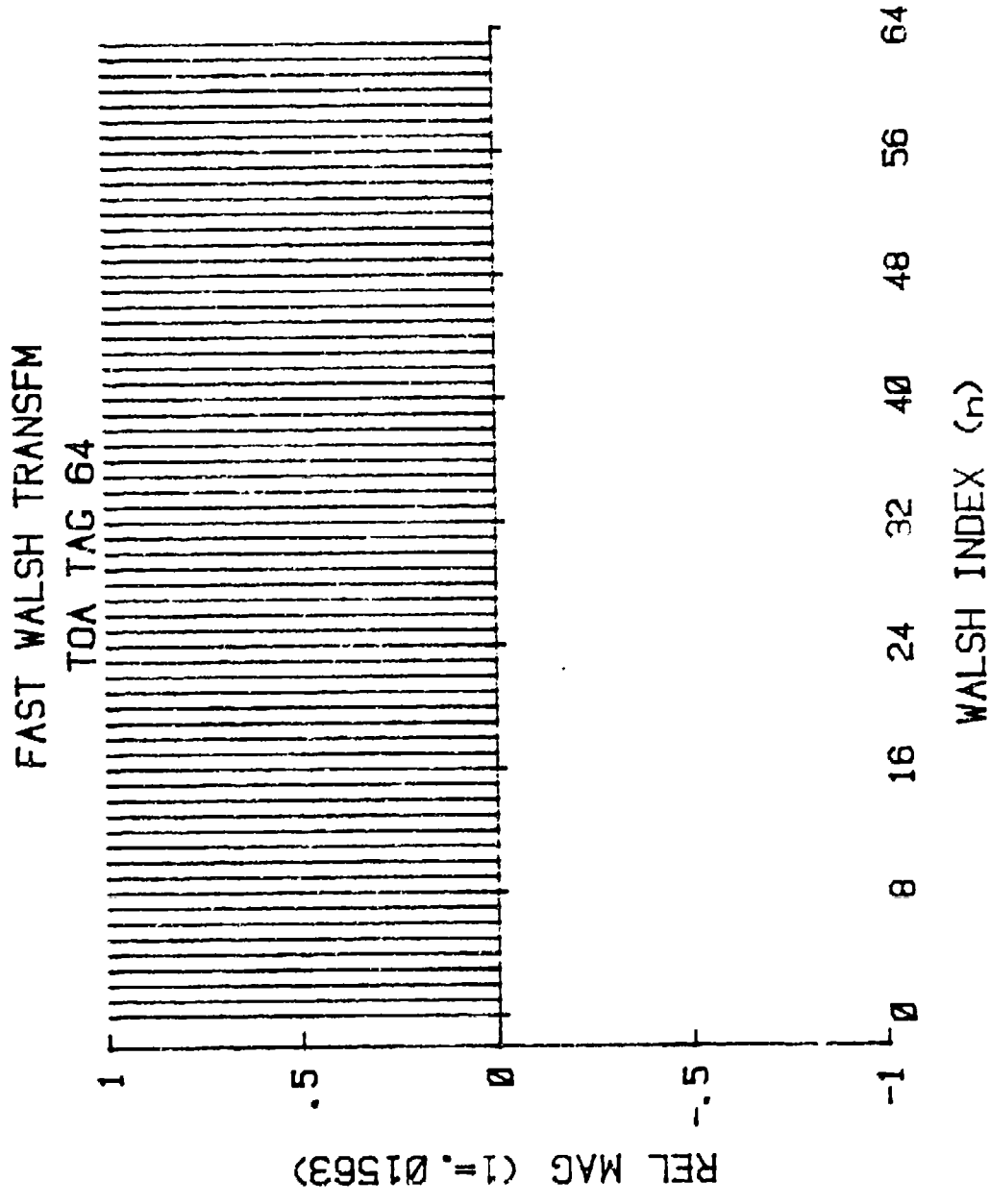

Figure D.22. FWT : TOA TAG 64.

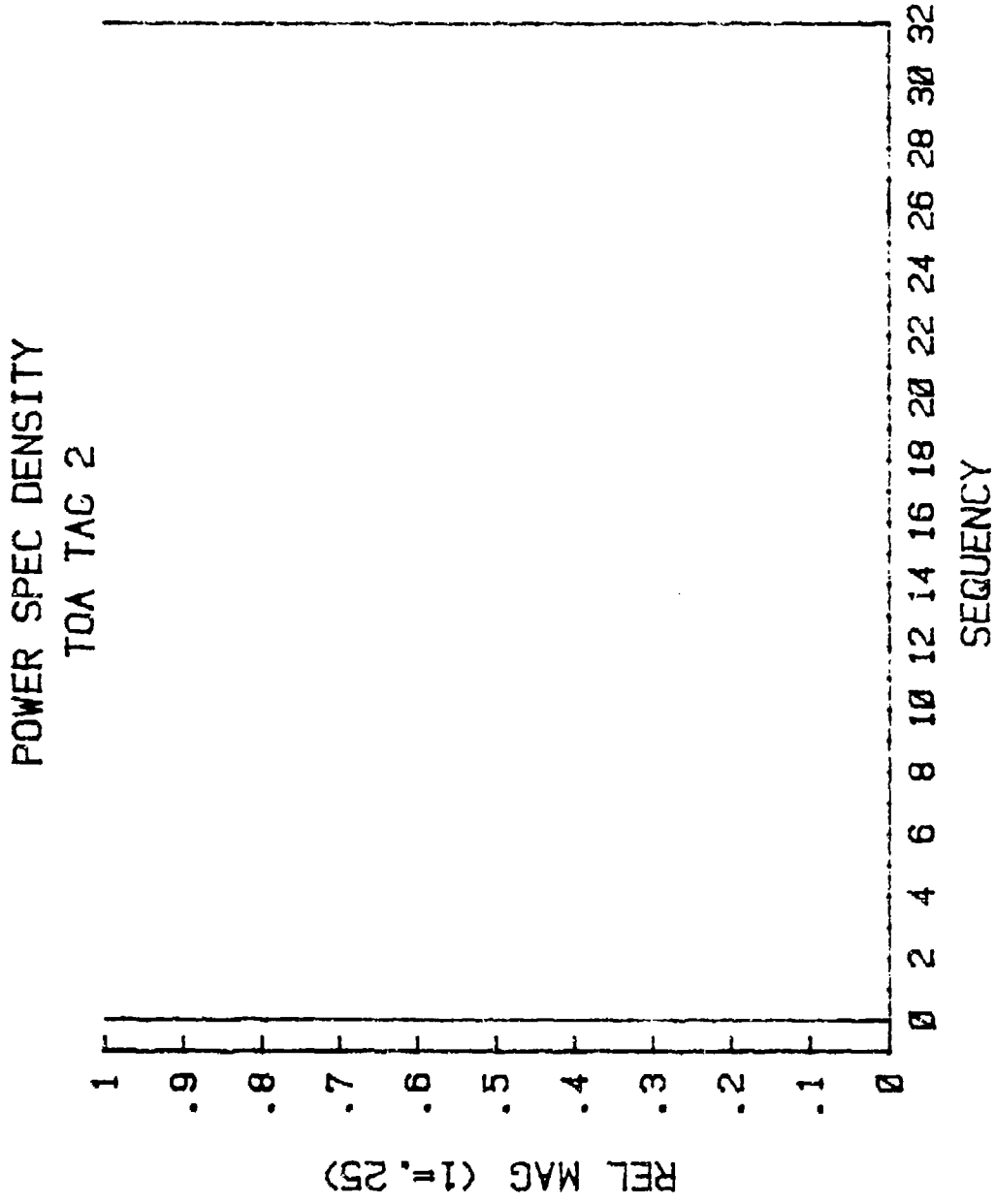

Figure D.23. PSD : TOA TAG 2.

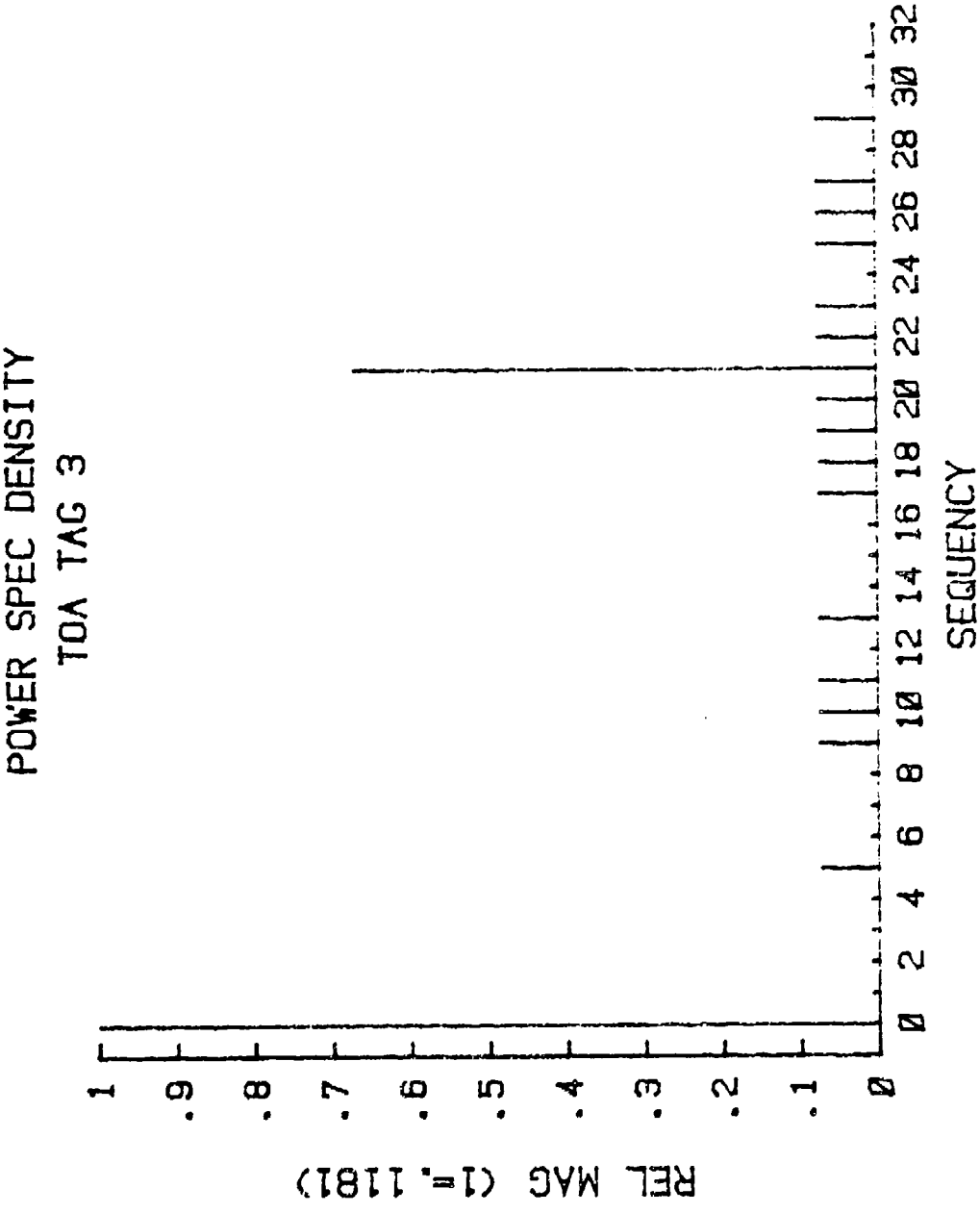

Figure D.24. PSD : TOA TAG 3.

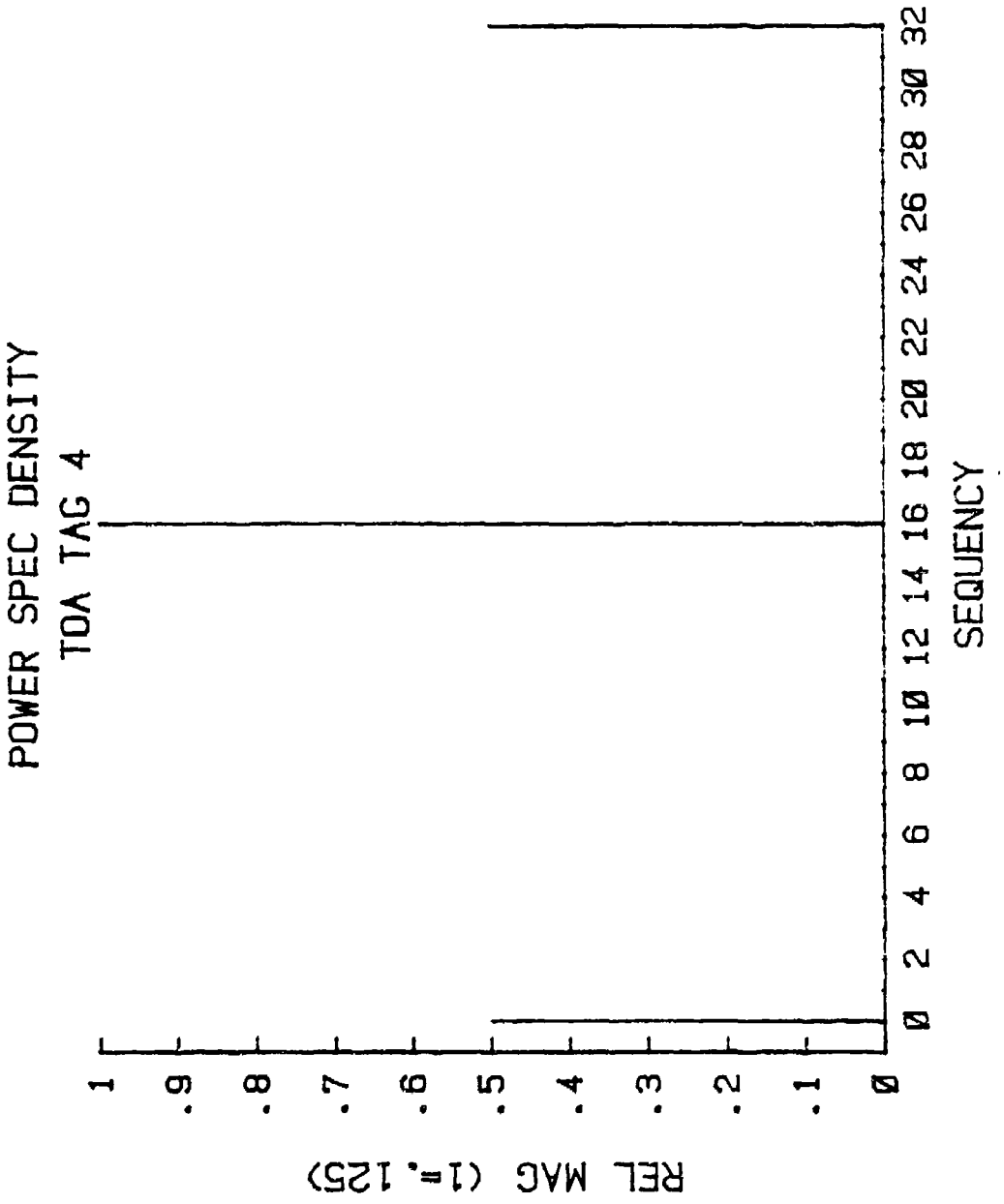

Figure D.25. PSD : TOA TAG 4.

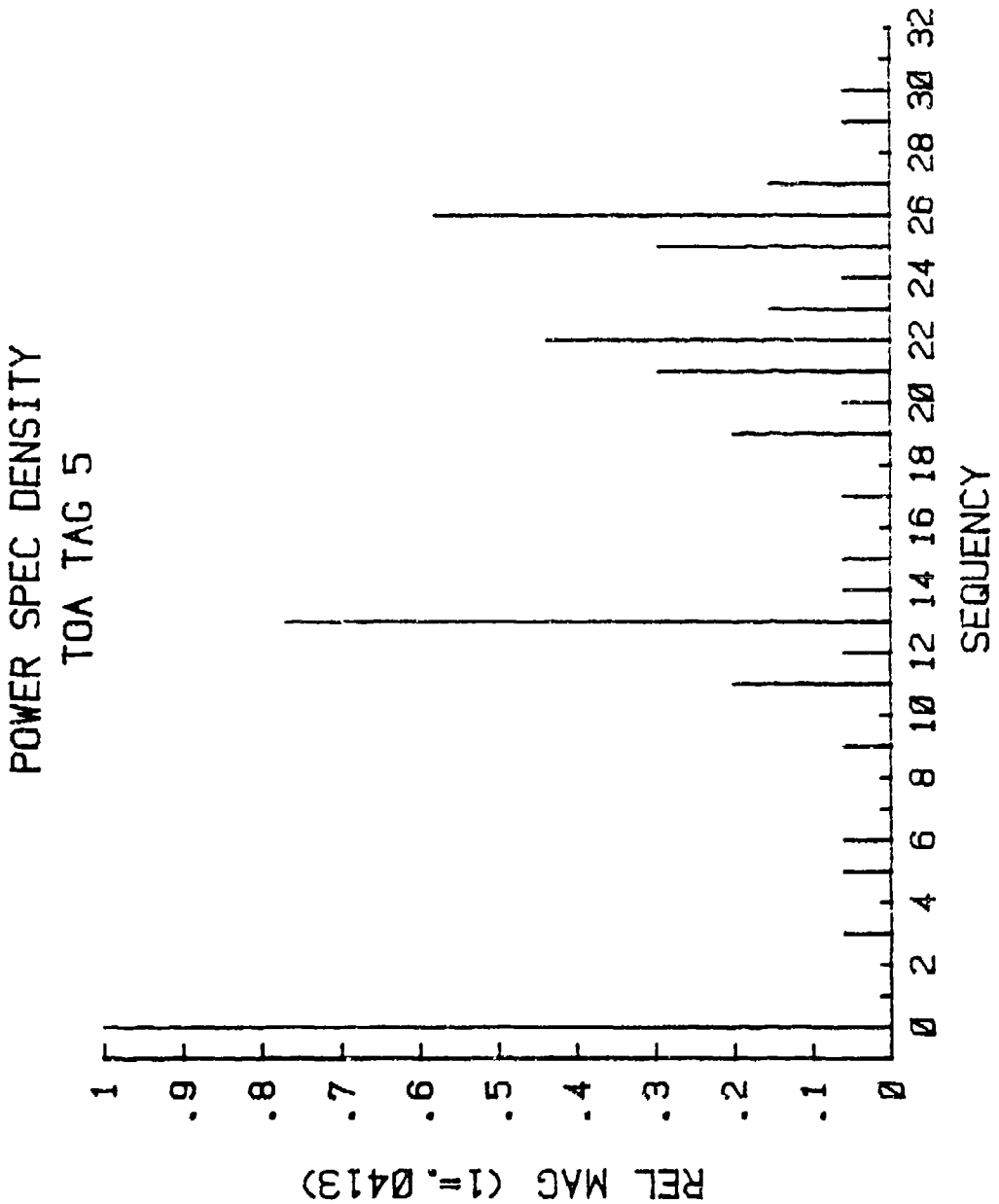

Figure D.26. PSD : TOA TAG 5.

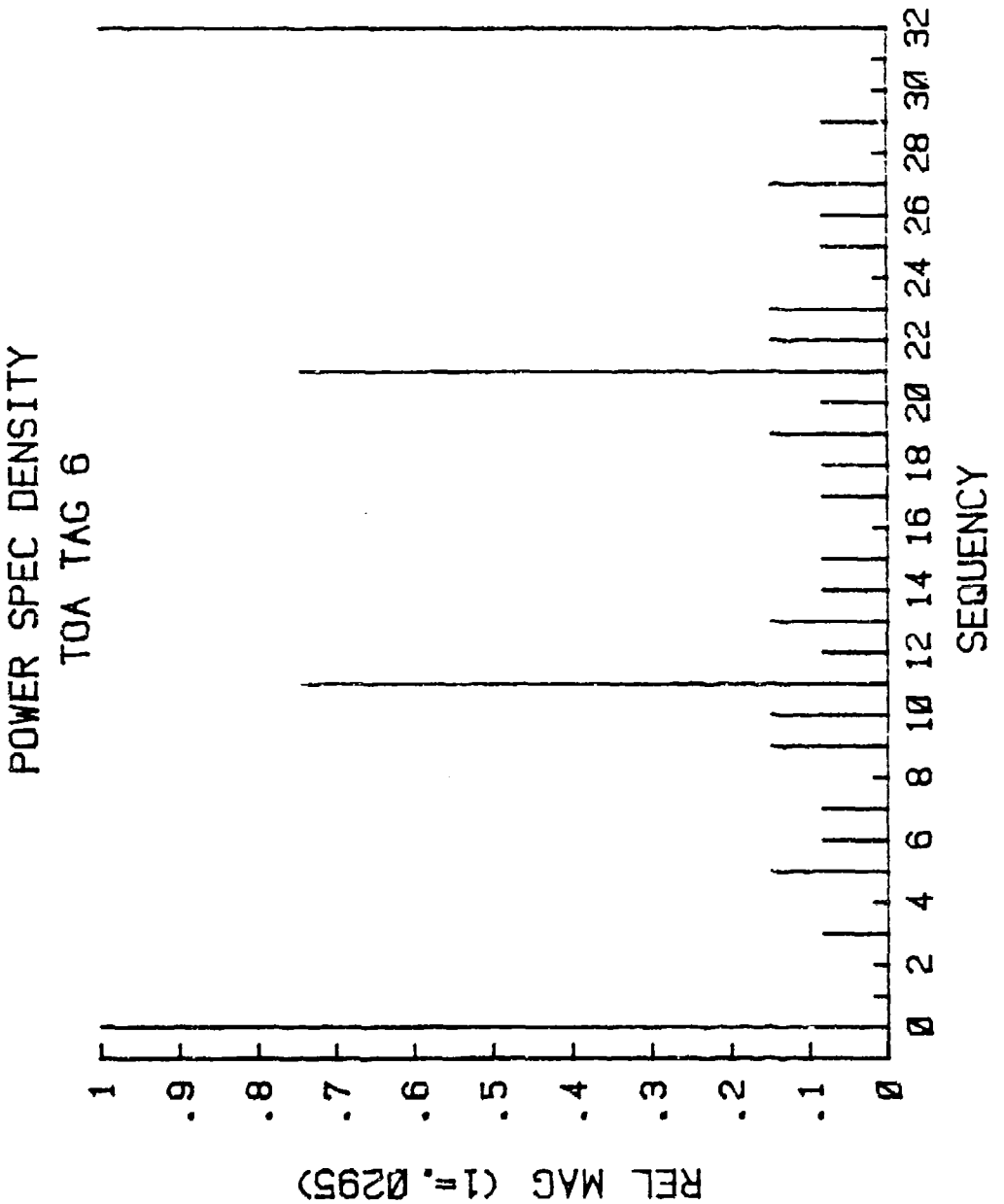

Figure D.27. PSD : TOA TAG 6.

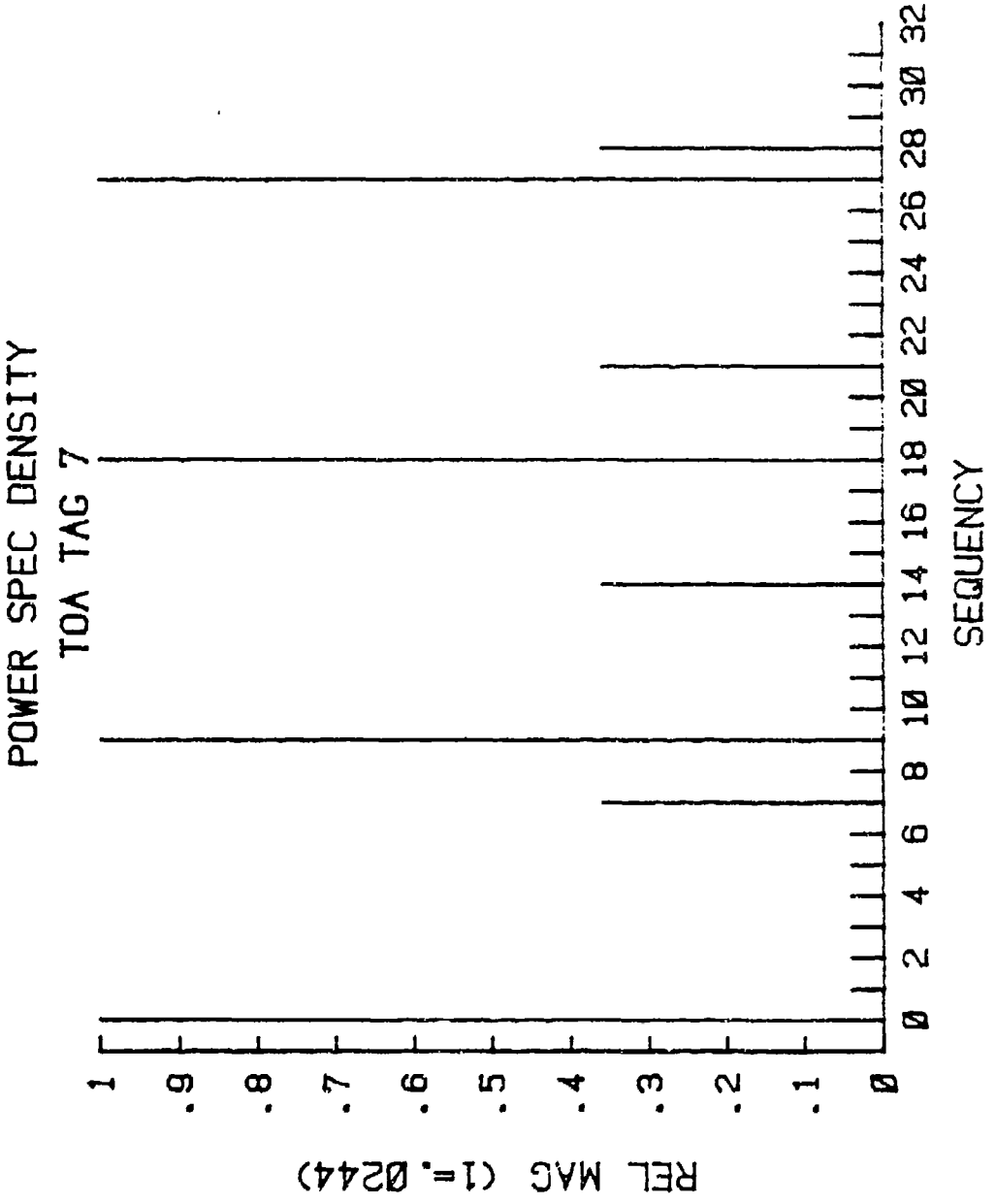

Figure D.28. PSD : TOA TAG 7.

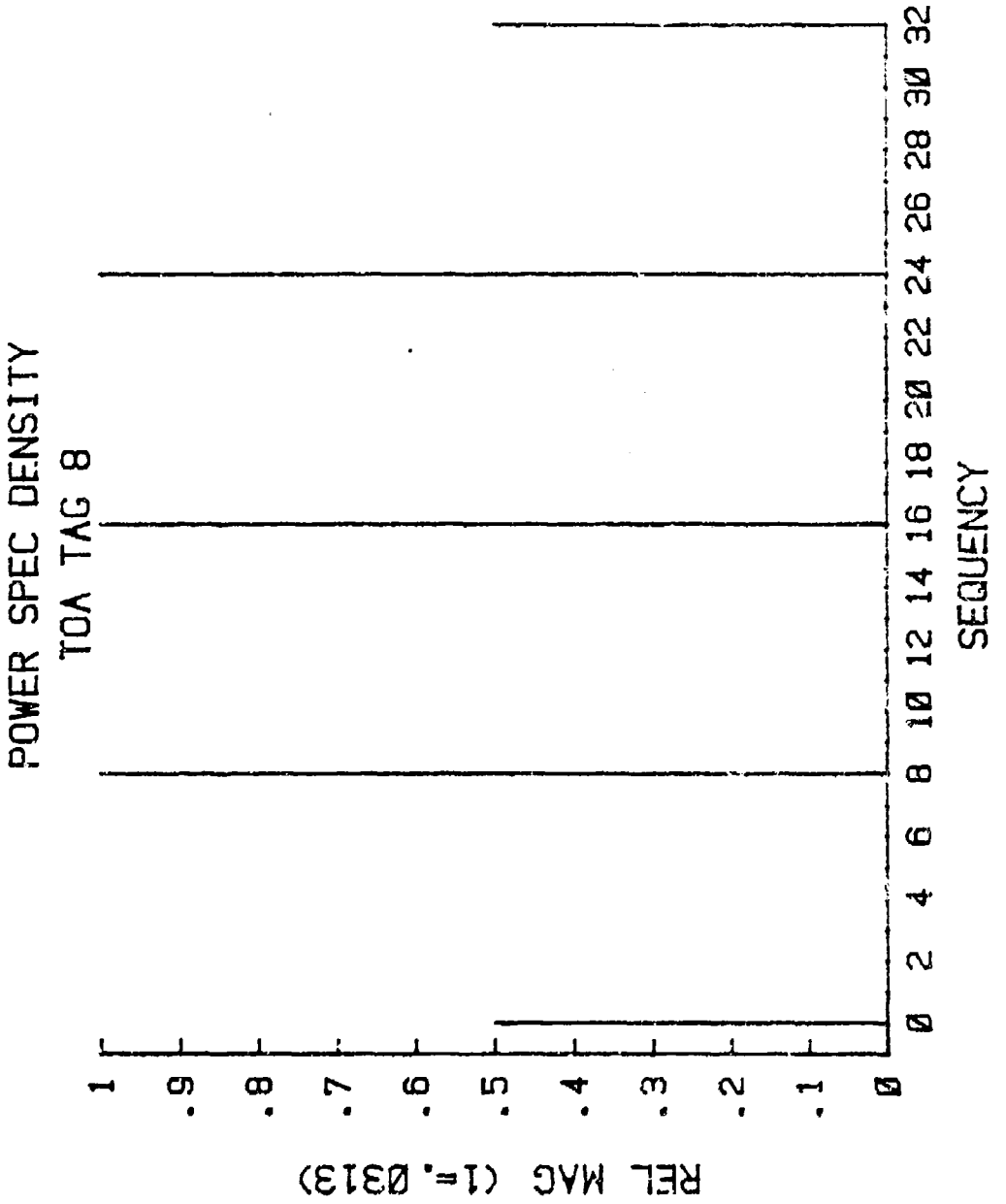

Figure D.29. PSD : TOA TAG 8.

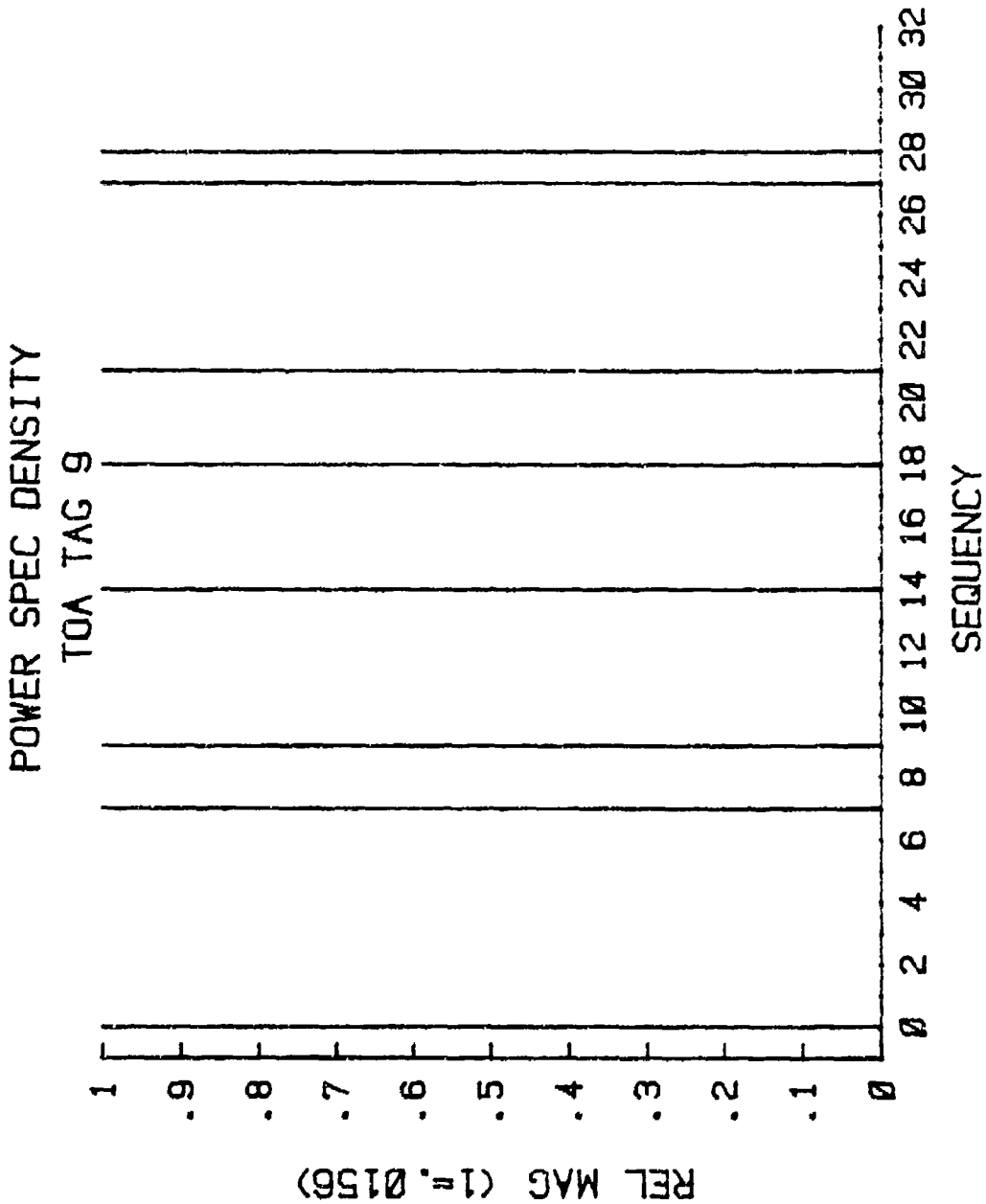

Figure D.30. PSD : TOA TAG 9.

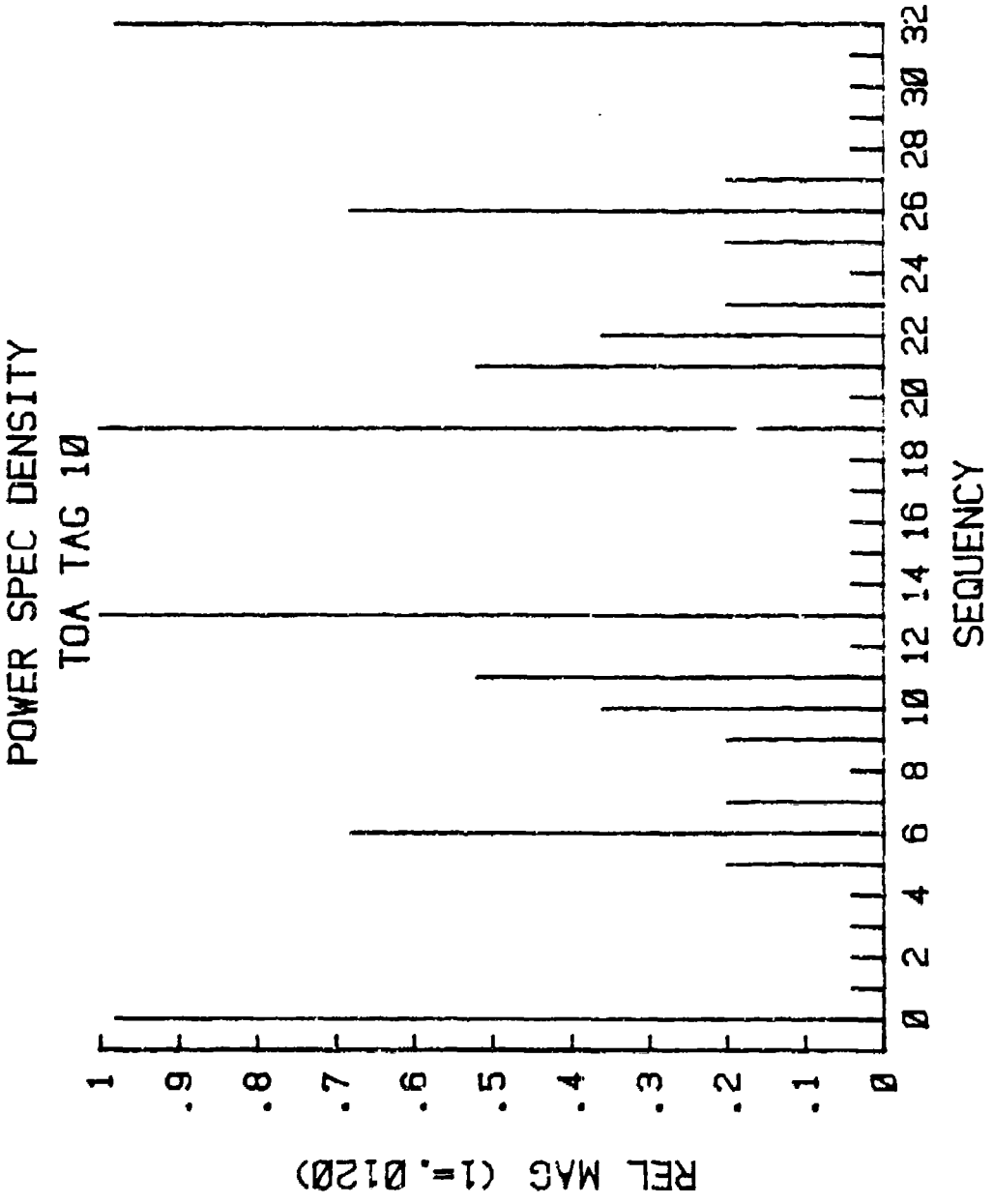

Figure D.31. PSD : TOA TAG 10.

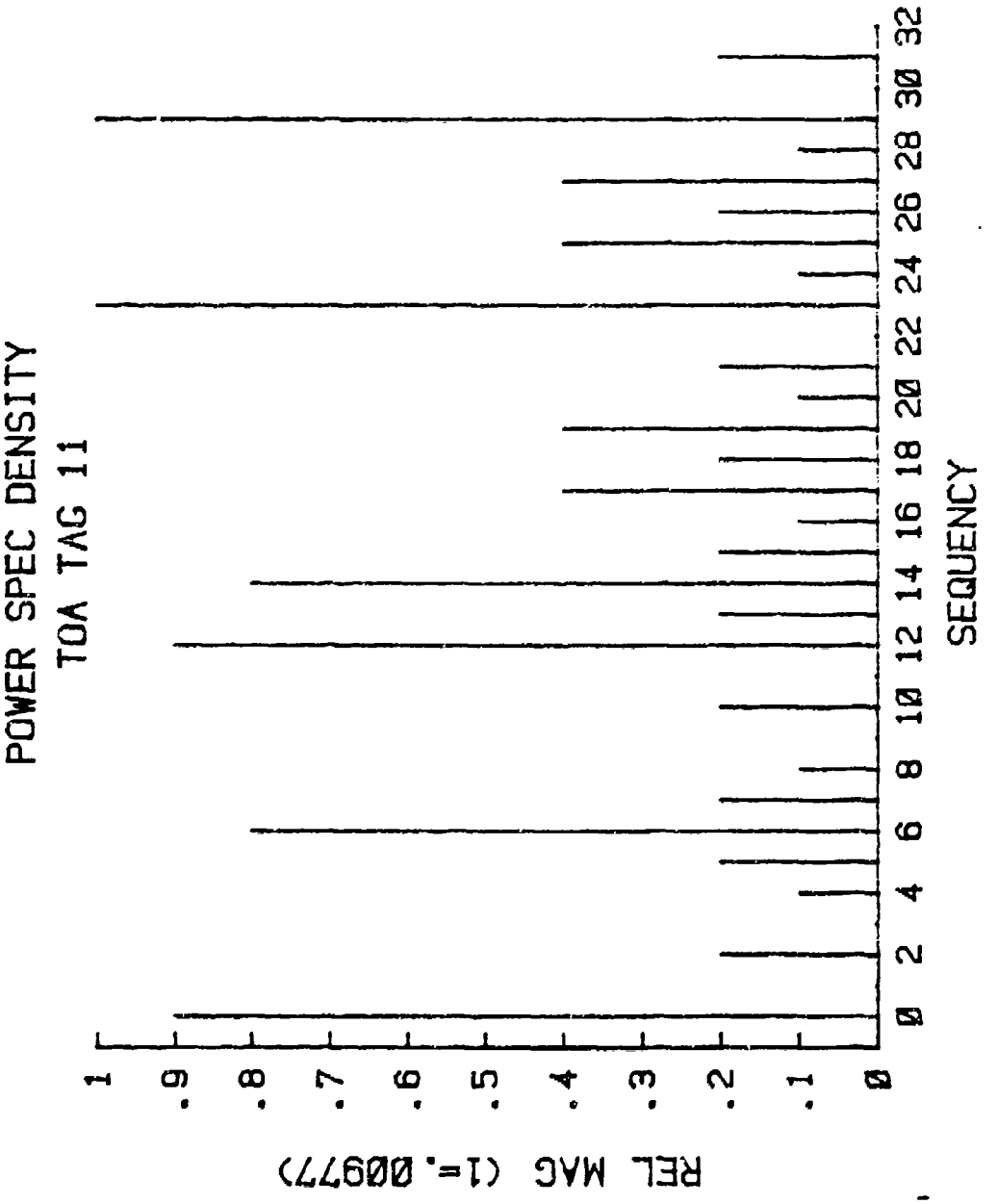

Figure D.32. PSD : TOA TAG 11.

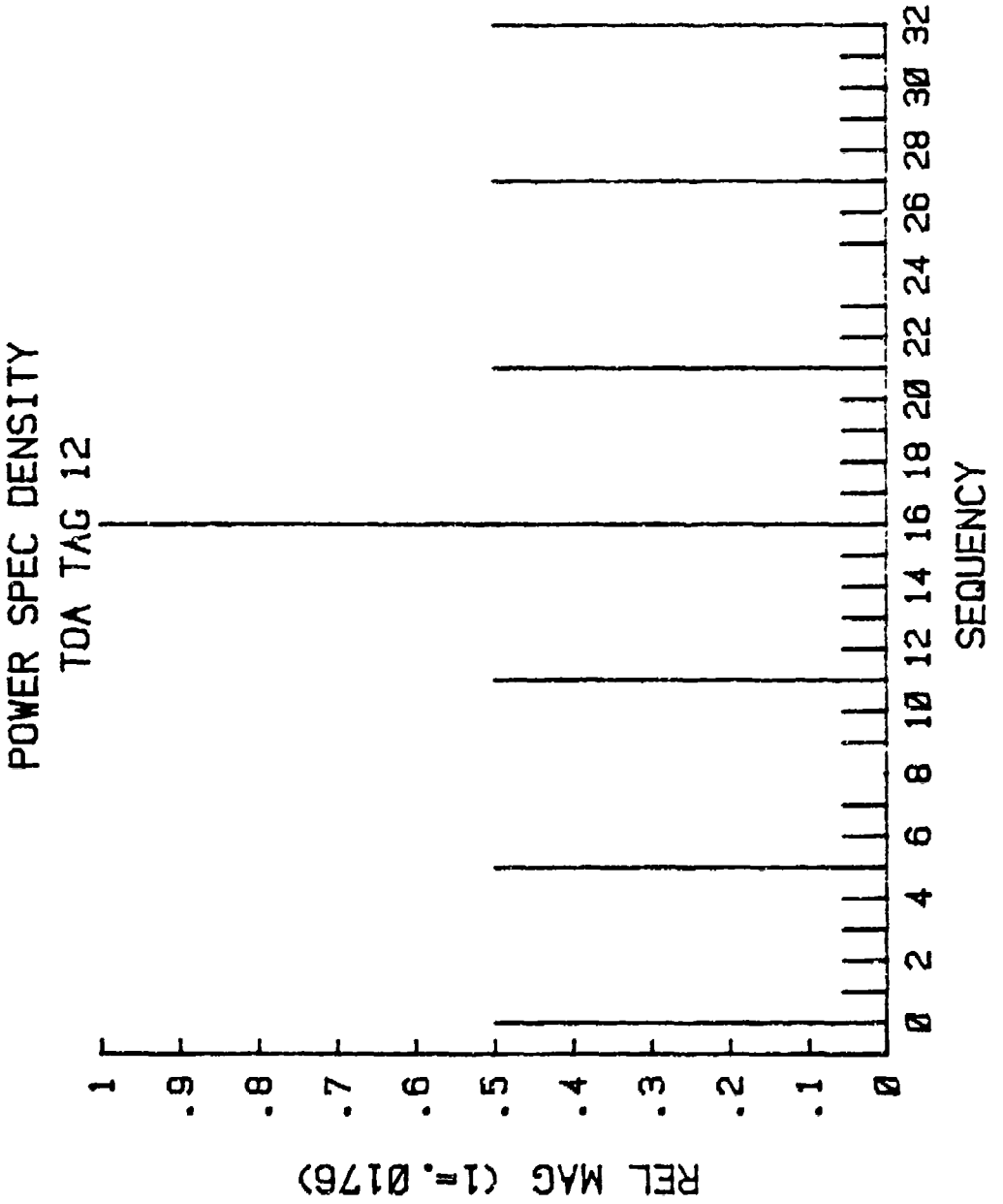

Figure D.33. PSD : TOA TAG 12.

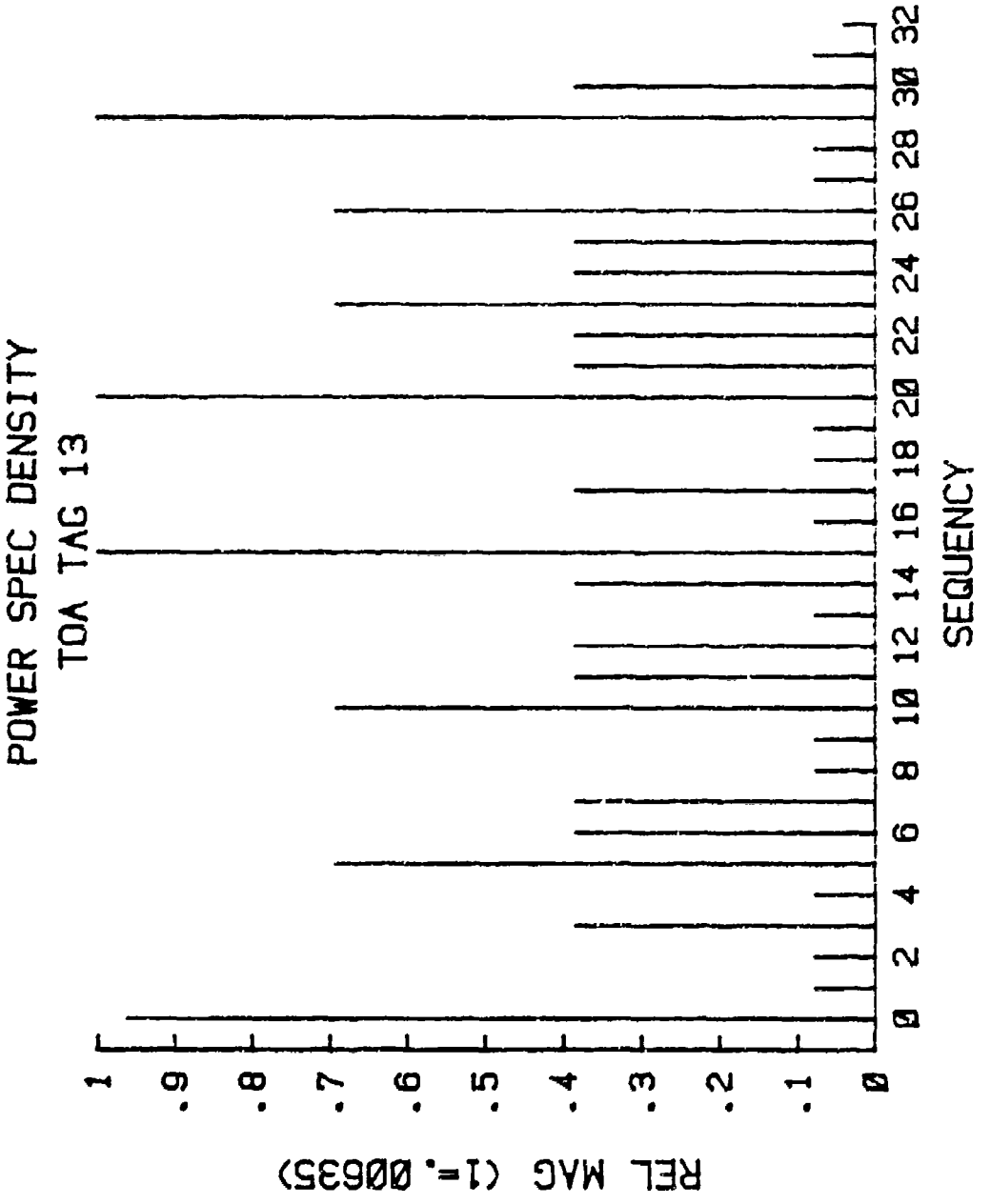

Figure D.34. PSD : TOA TAG 13.

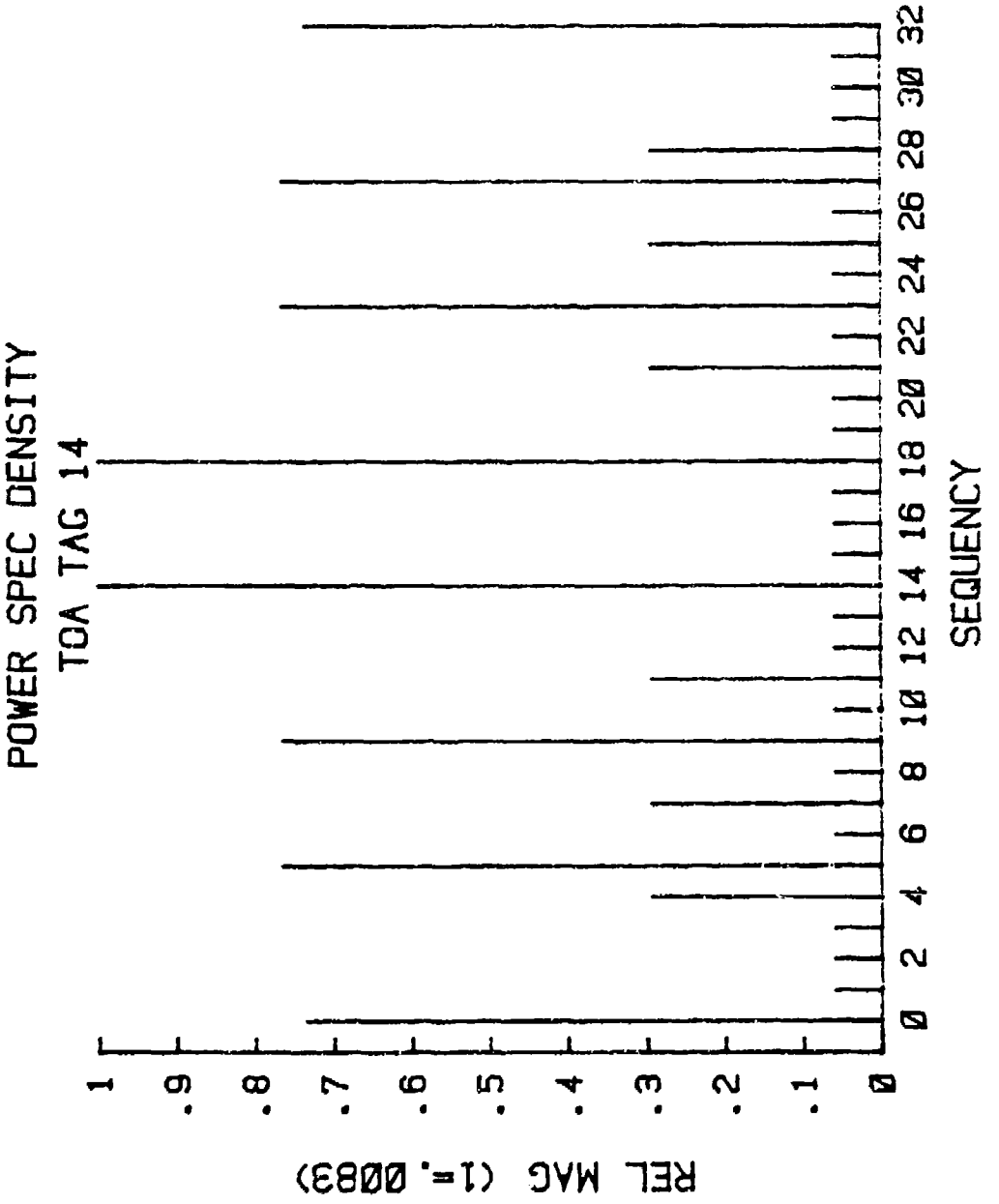

Figure D.35. PSD : TOA TAG 14.

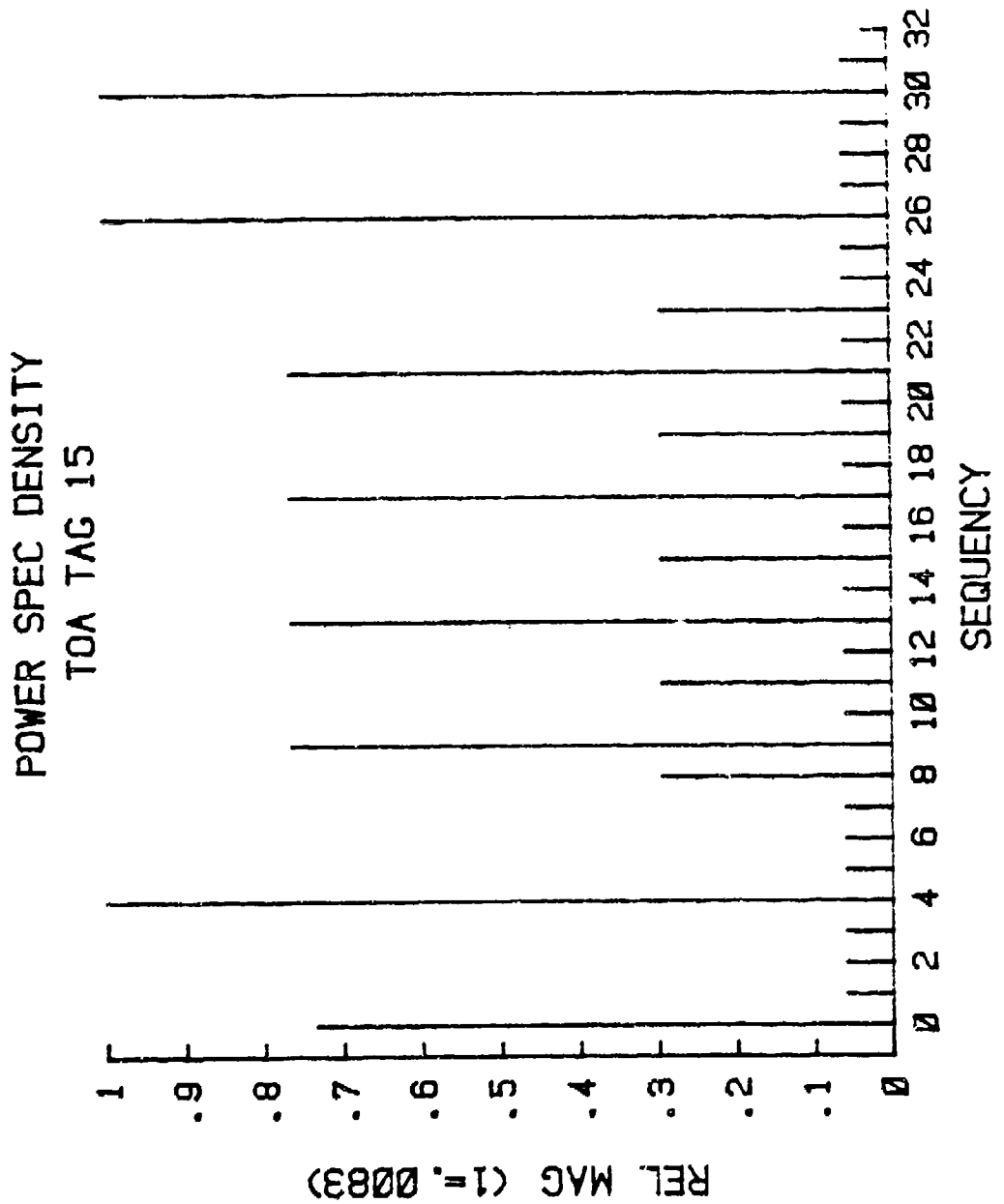

Figure D.36. PSD : TOA TAG 15.

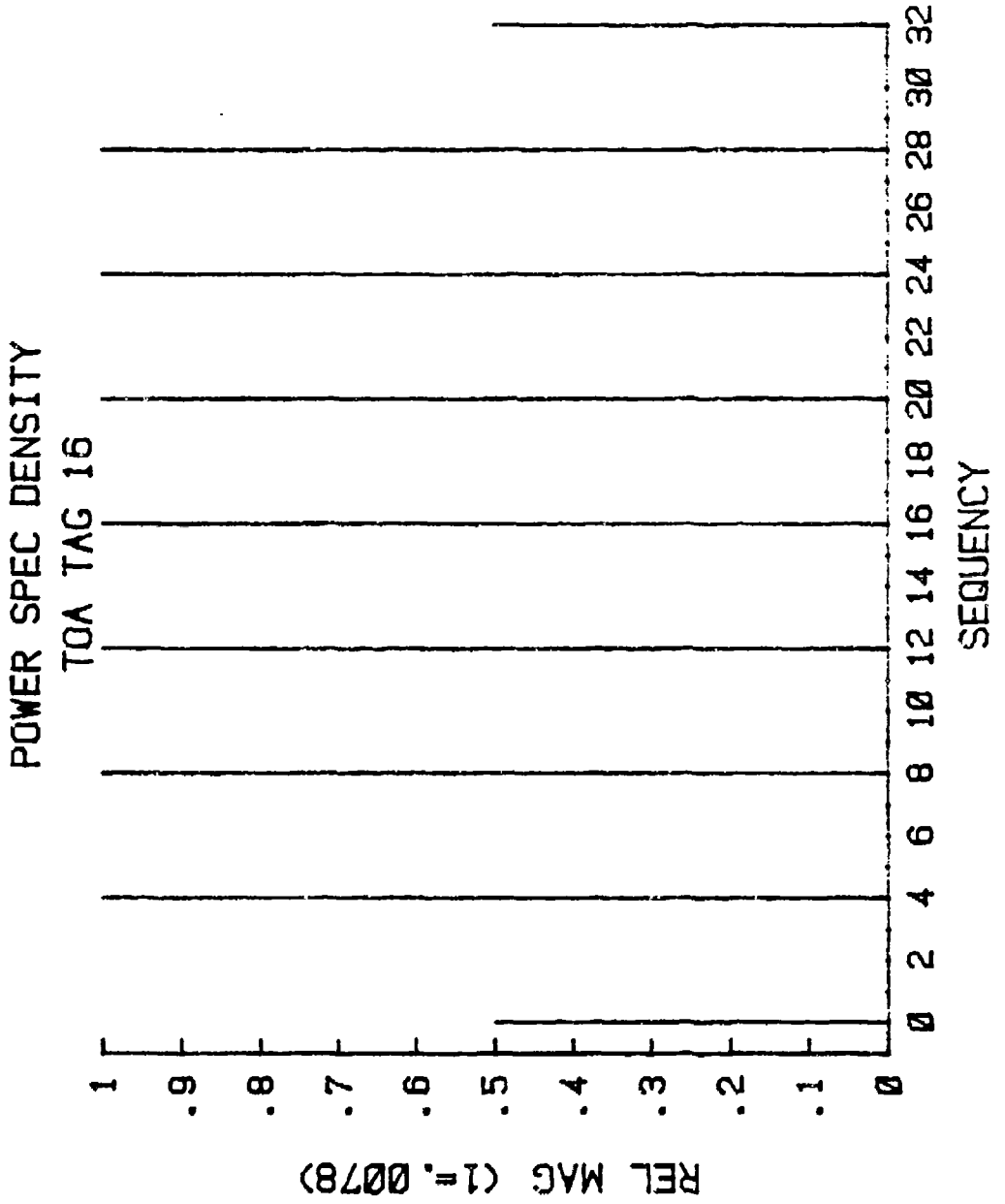

Figure D.37. PSD : TOA TAG 16.

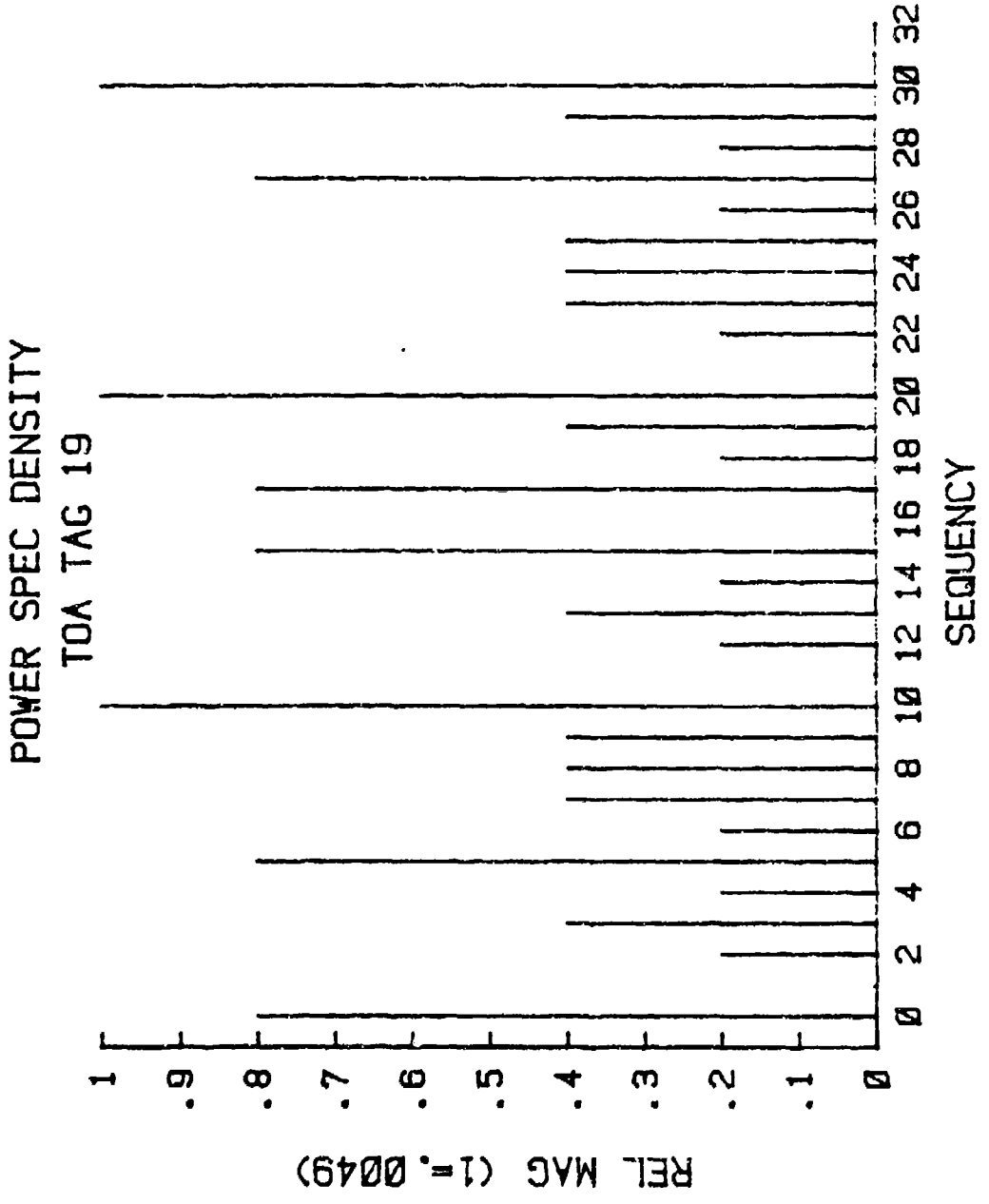

Figure D.38. PSD : TOA TAG 19.

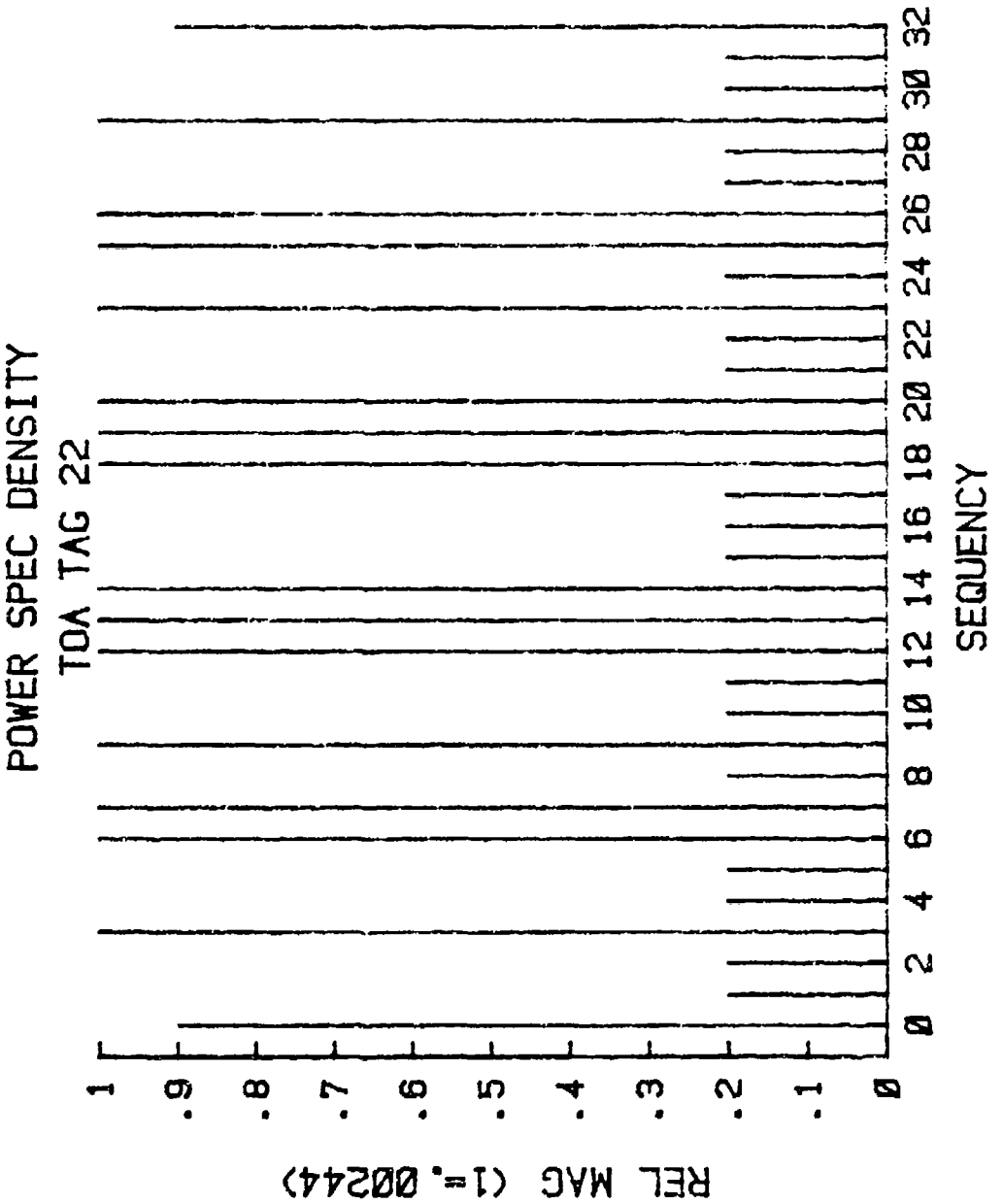

Figure D.39. PSD : TOA TAG 22.

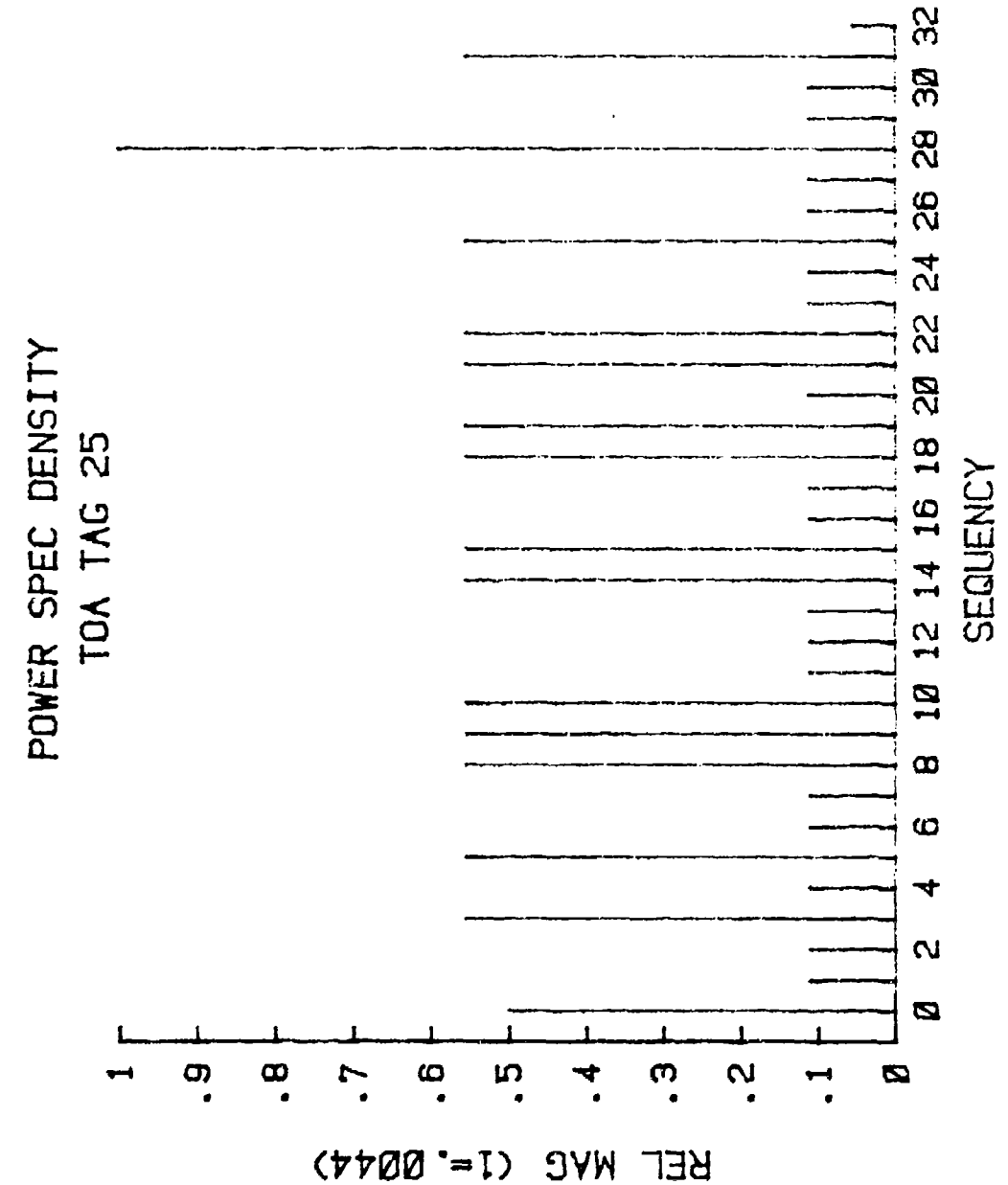

Figure D.40. PSD : TOA TAG 25.

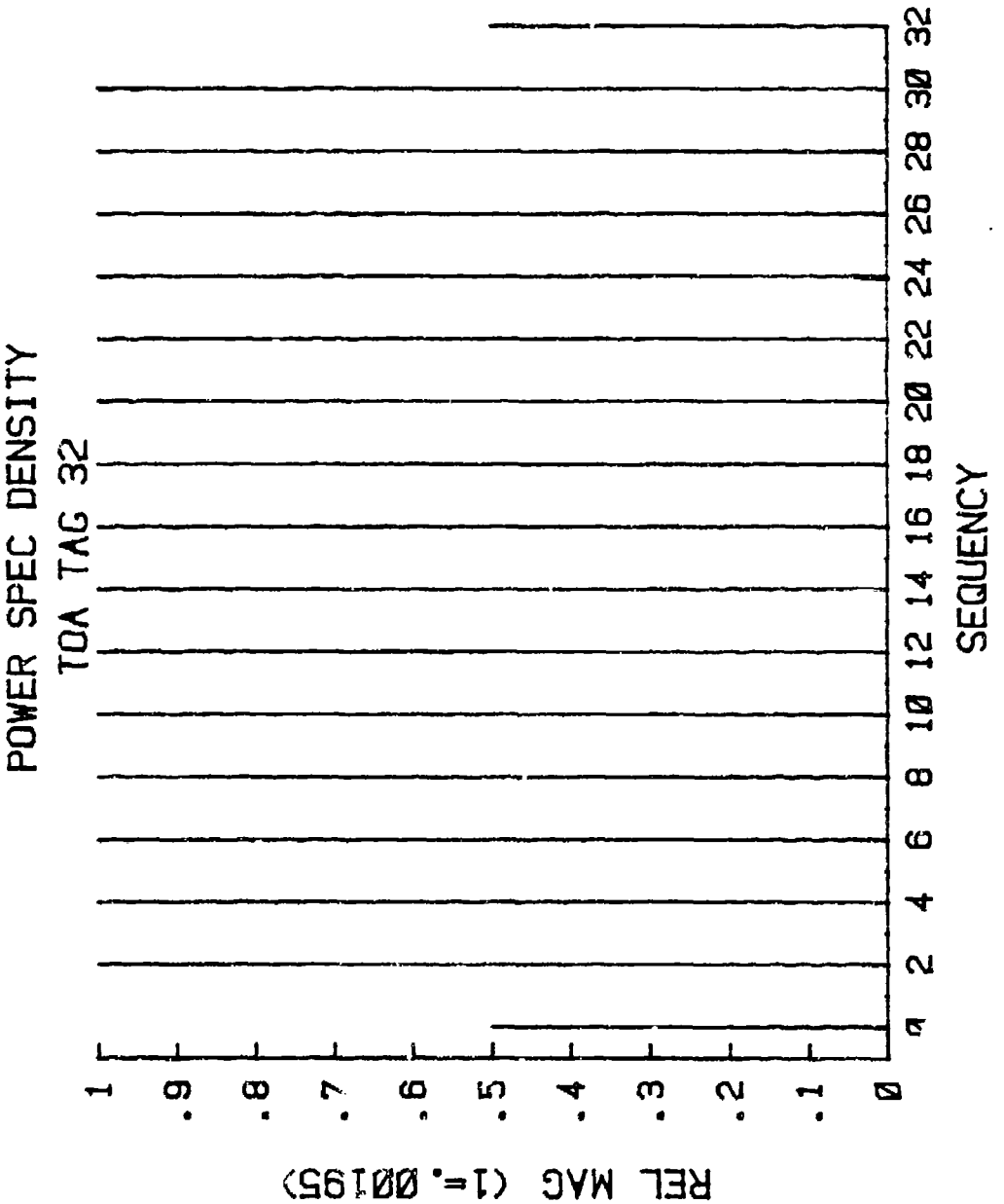

Figure D.41. PSD : TOA TAG 32.

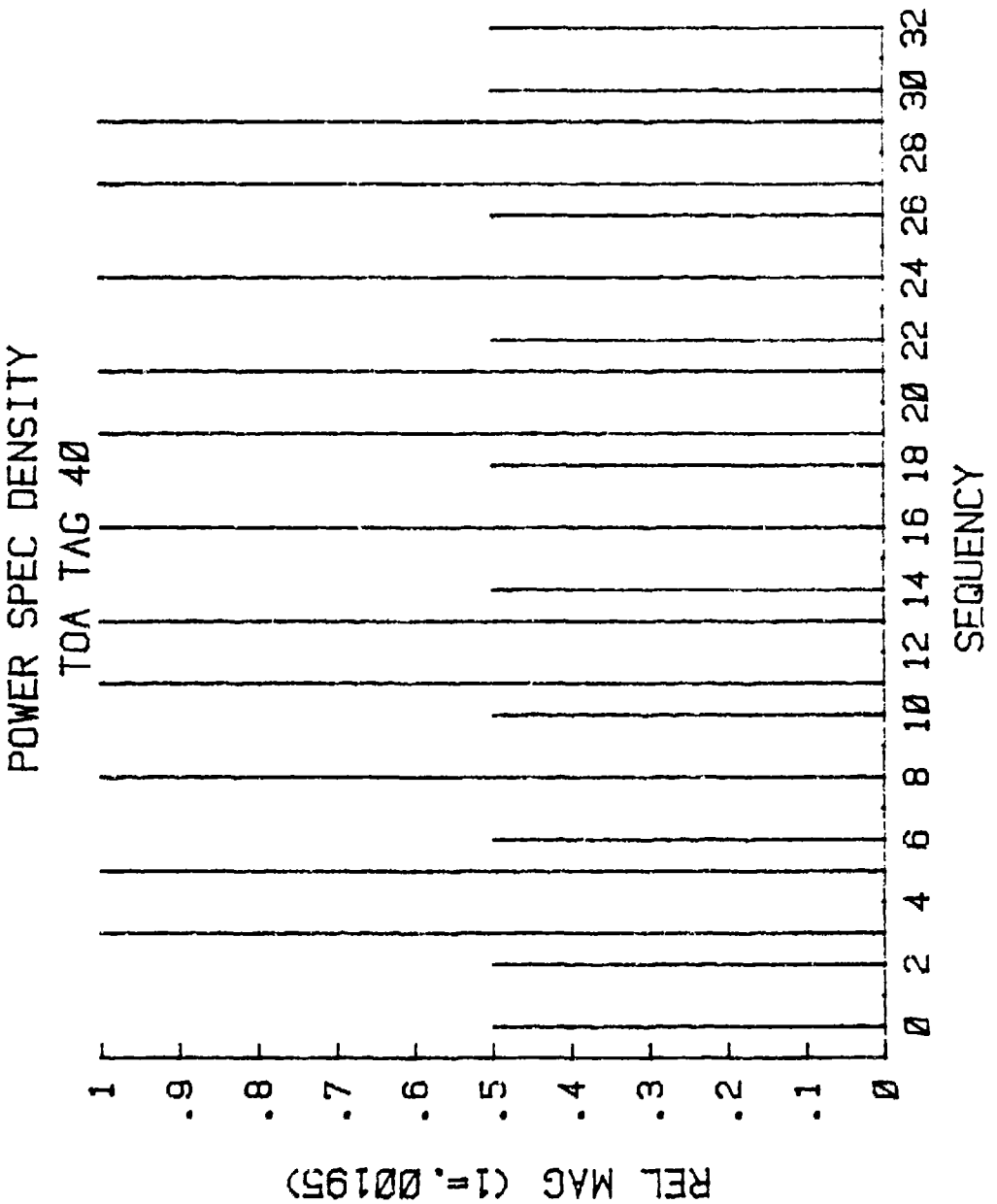

Figure D.42. PSD : TOA TAG 40.

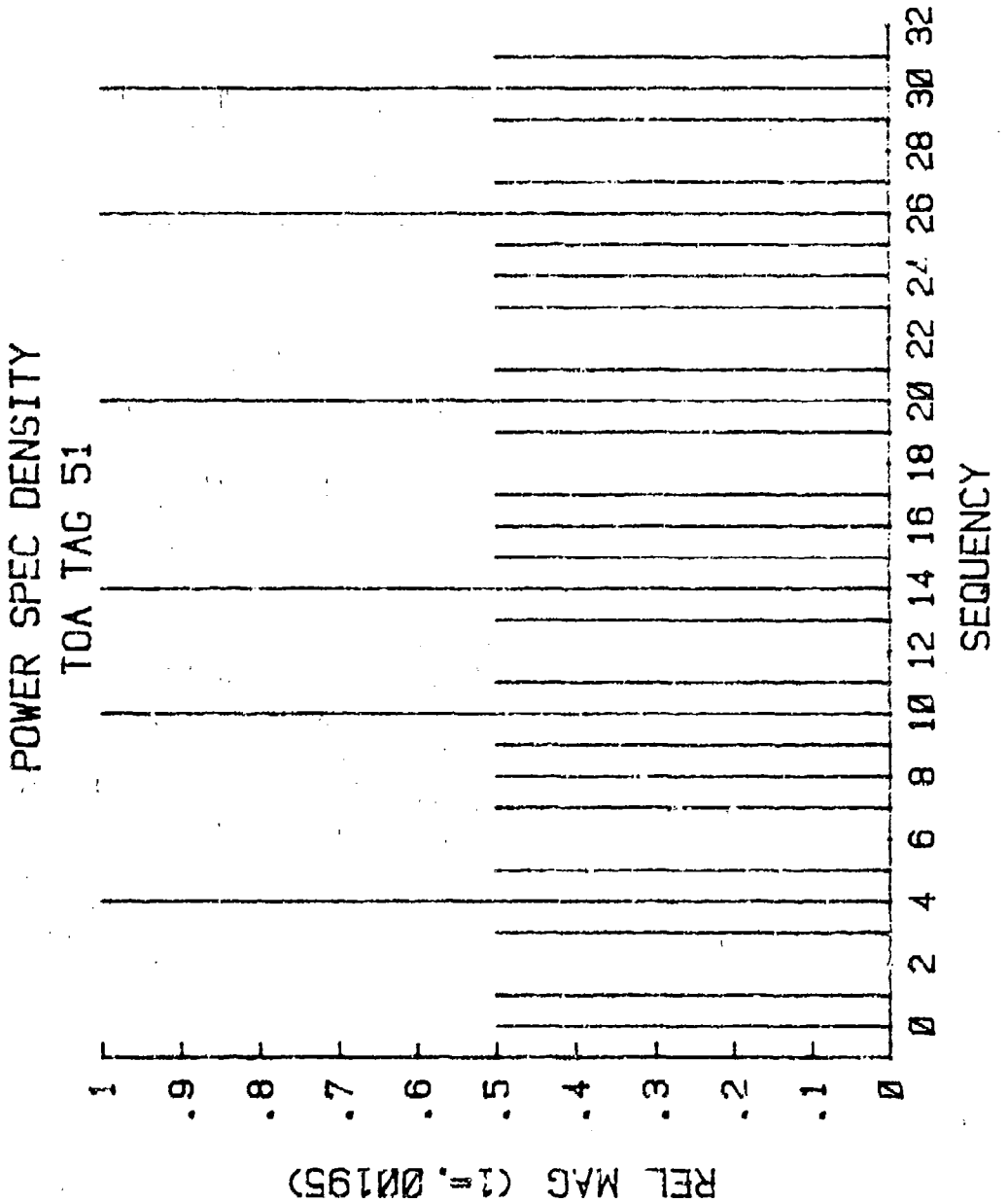

Figure D.43. PSD : TOA TAG 51.

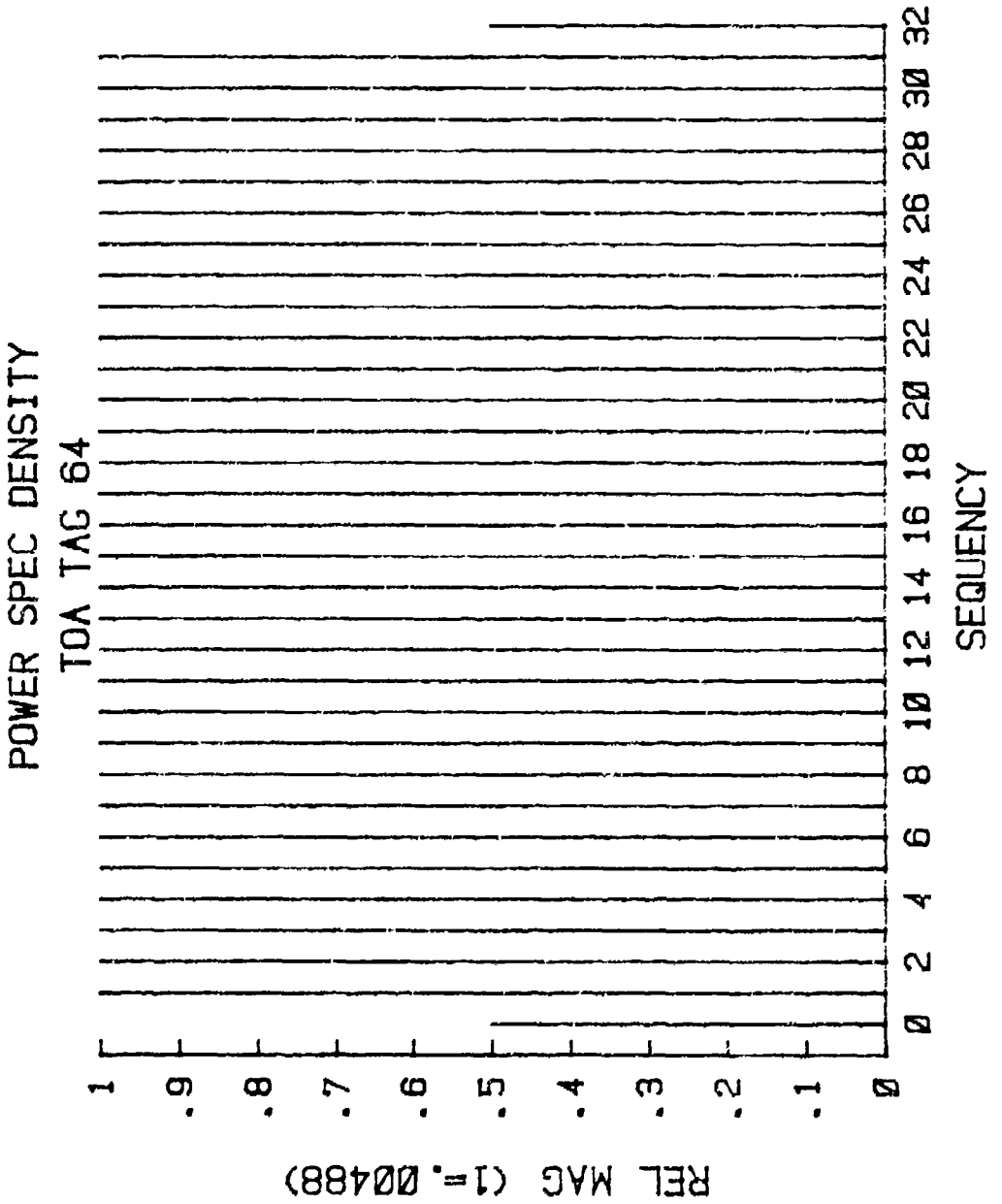

Figure D.44. PSD : TOA TAG 64.

APPENDIX E

ADDITIONAL PLOTS

These additional plots are referred to in the text.

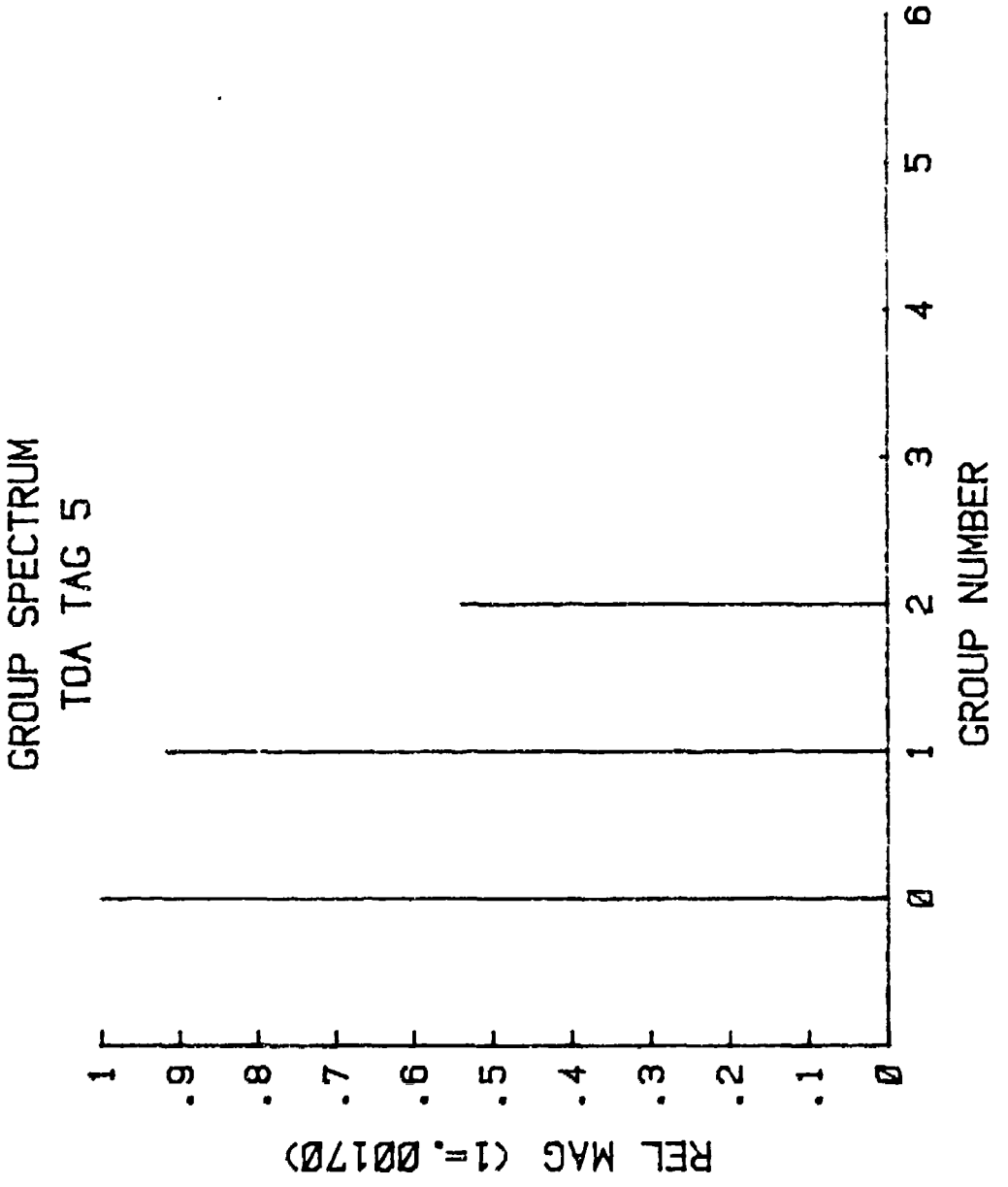

Figure E.1. GROUP SPECTRUM : TOA TAG 5.

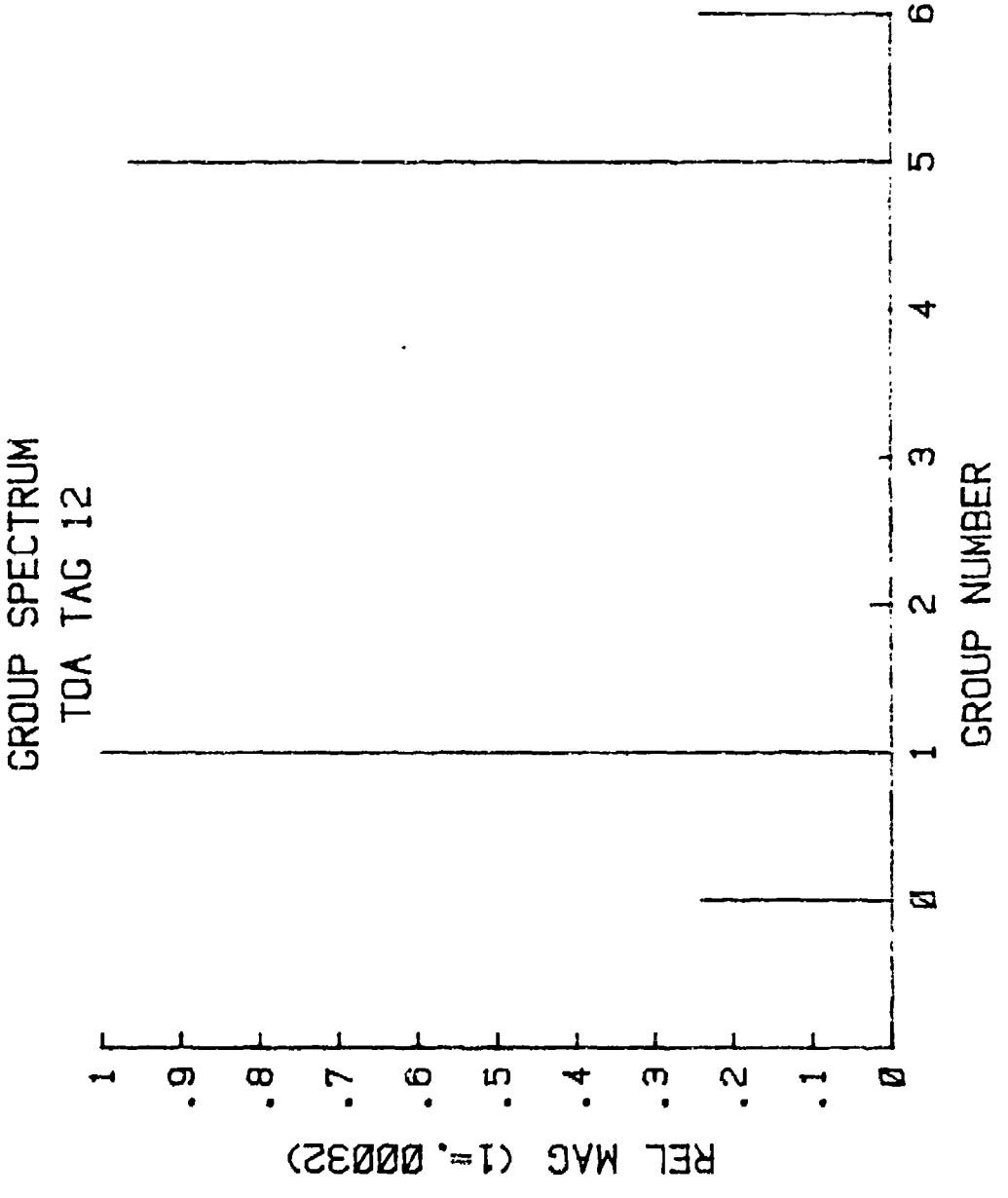

Figure E.2. GROUP SPECTRUM : TOA TAG 12.

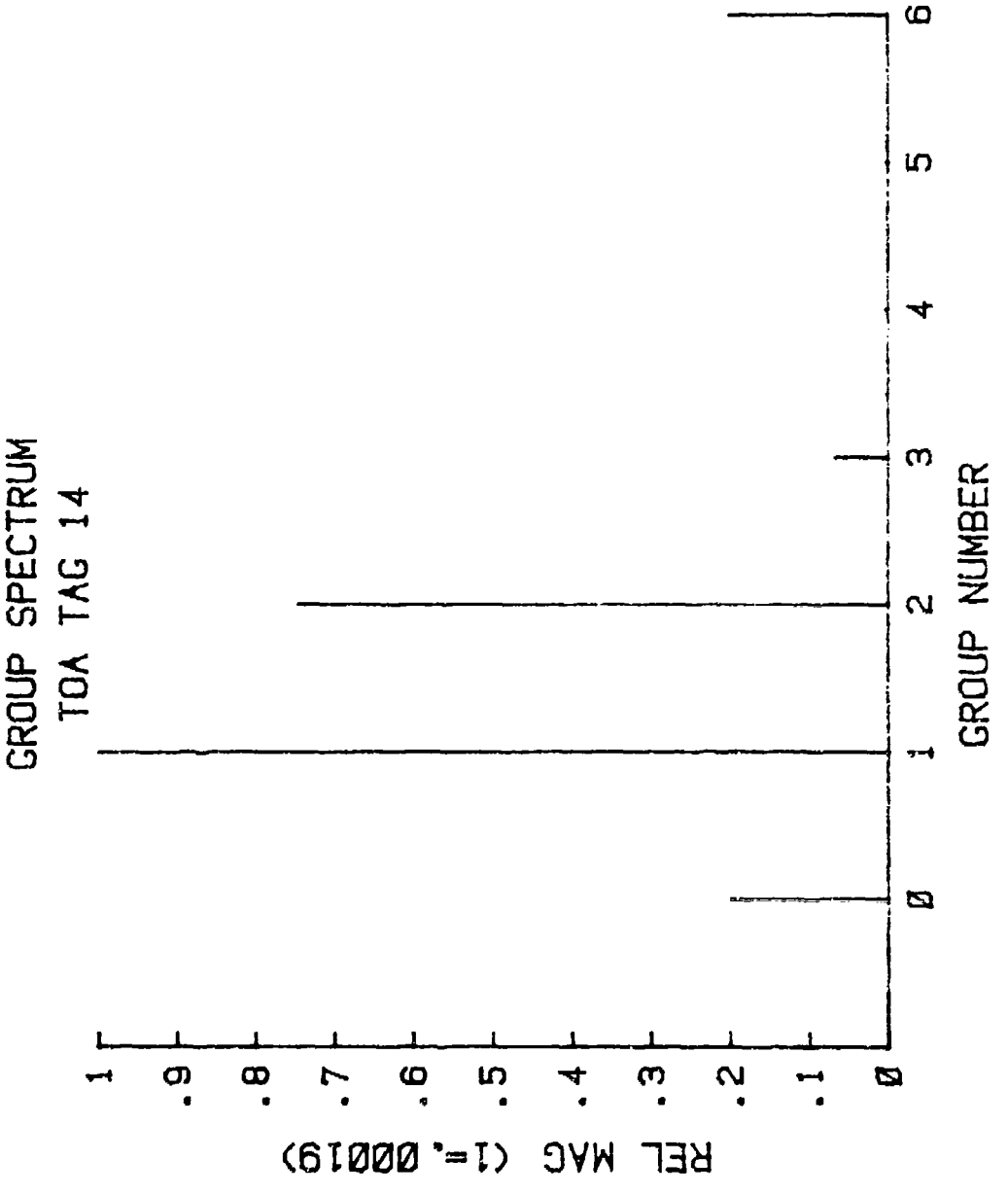

Figure E.3. GROUP SPECTRUM : TOA TAG 14.

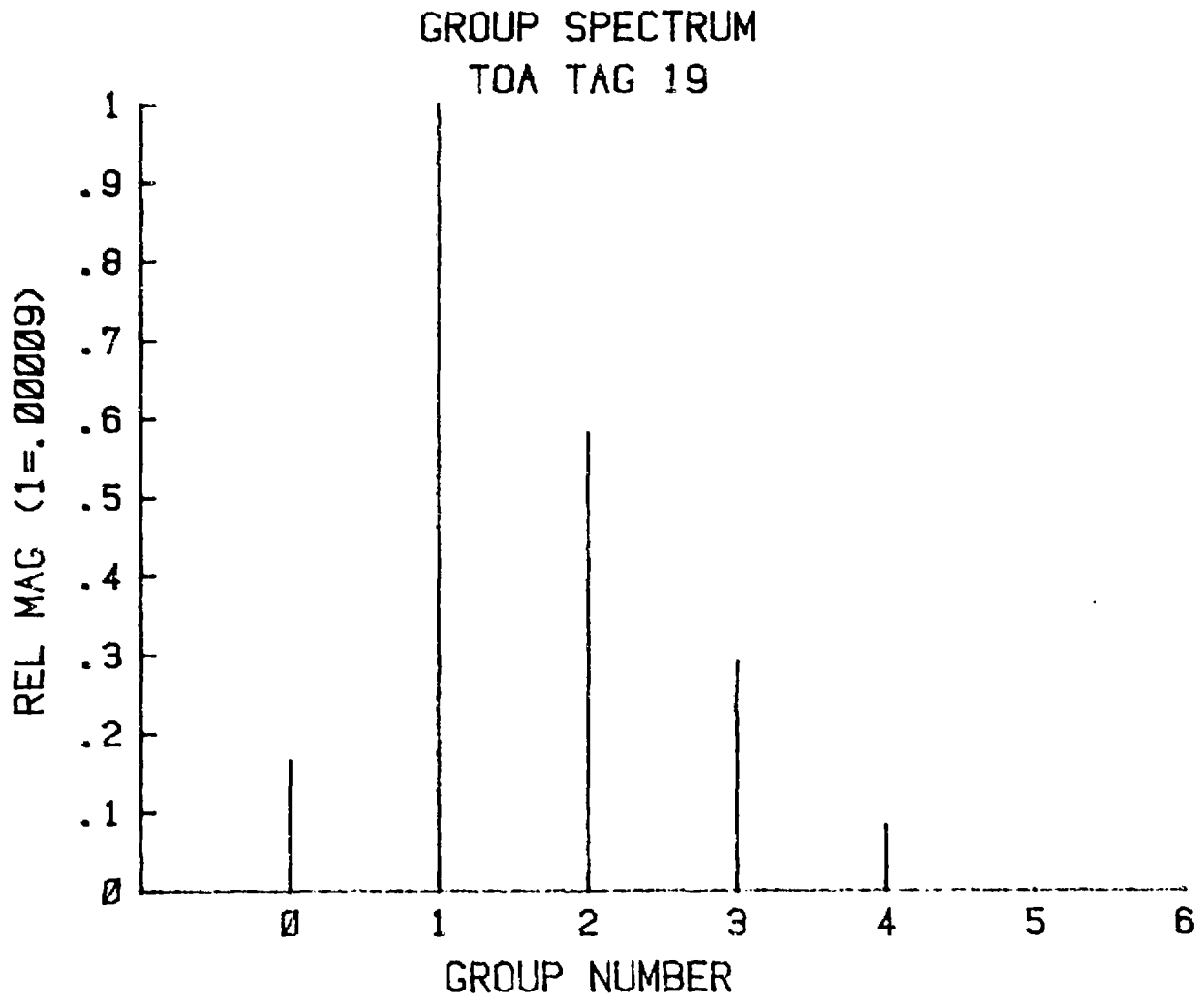

Figure E.4. GROUP SPECTRUM : TOA TAG 19.

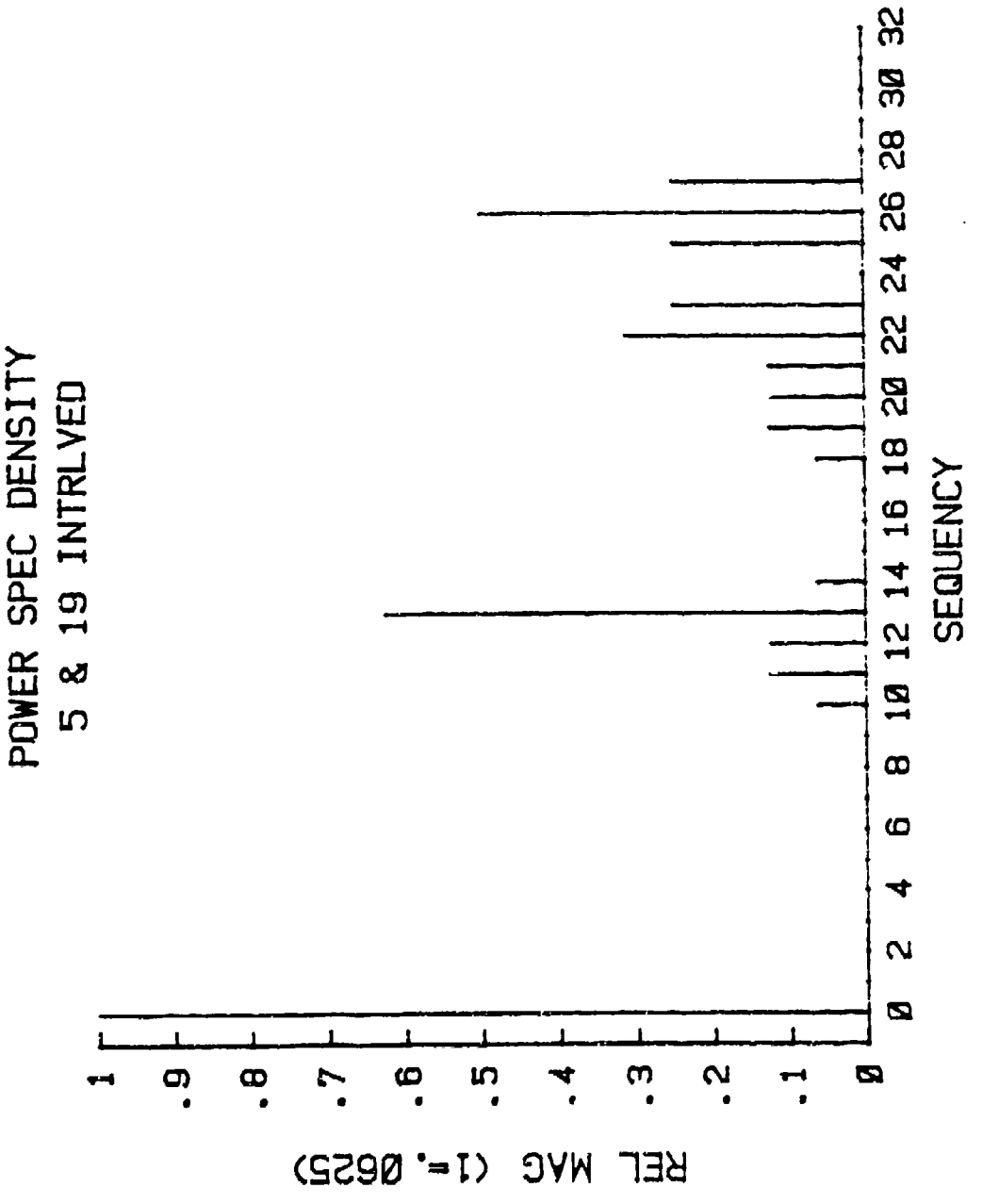

Figure E.5. PSD : TOA TAG 5 AND 19 INTERLEAVED.

LIST OF REFERENCES

1. Price, Alfred, Instruments of Darkness, p. 20, MacDonald and Jane's, 1977.

2. Fitts, Richard E. (editor), and others, The Strategy of Electromagnetic Conflict, United States Air Force Academy.

3. Flowers, Nick, "Cutlass-ESM High Speed Processing," Journal of Electronic Defense, May, 1983.

4. Wilson, Lonnie A., Electronic Support Measures Systems, Class handout from lecture course EE 4481, "Electronic Warfare Systems and Technology," Naval Postgraduate School.

5. Class notes from EE 4481," Electronic Warfare Systems and Technology," Naval Postgraduate School, Dr. Lonnie Wilson, Professor.

6. Schlesinger, Robert J., Principles of Electronic Warfare, Peninsula Publishing, 1961.

7. Wilson, Lonnie A., Electronic Warfare Systems, Class handout from lecture course EE 4481, "Electronic Warfare Systems and Technology," Naval Postgraduate School.

8. Naval Electronics Laboratory Center Technical Note TN3242A, Electromagnetic Warfare-- A Total Concept, by P.C. Fletcher, p. 3, 8 February 1977.

9. Klass, Phillip J., "New Procedures to Speed Electronic Warfare Work," Aviation Week and Space Technology, pp. 53-56, 13 July, 1981.

10. "British to Use Internal ECM Systems," Aviation Week and Space Technology, p. 74, 26 January, 1981.

11. "Belgium to Make Decision on ECM System for its F-16's," Aviation Week and Space Technology, p. 24, 5 April 1982.

12. "Airborne Jammer Enters Production," Aviation Week and Space Technology, pp. 68-69, 21 June, 1981.

13. Fiester, Clark G., "The Use of Embedded Computers in EW," Journal of Electronic Defense, p. 27-29, Vol. 6, No. 8, August, 1983.

14. Boyd, J.A., and other editors, Electronic Countermeasures, Peninsula Publishing, 1978.

15. Skolnik, Merrill I., Introduction to Radar Systems, McGraw-Hill, 1980.

16. Hoisington, D.B., Electronic Warfare, Naval Postgraduate School, April, 1980.

17. Collins, J.H., and Grant, P.M., "Signal Processing Pivotal to Next Generation ESM Receivers," Microwave Systems News, p. 104, April, 1981.

18. Hofmann, C.B., and Baron, A.R., "Wideband ESM Receiving Systems, Part I," Microwave Journal, December, 1980.

19. Brown, R.G., "Overview of Low Cost ECM Receiver Development," International Countermeasures Handbook, June, 1977.

20. Naval Research Lab Report Number 8247, Computers/Processors (For Electronic Warfare), by L.W. Lemley, August, 1978.

21. Davies, C.L., and Hollands, P., "Automatic Processing for ESM," Institution of Electrical Engineers Proceeding on Communications, Radar, and Signal Processing, Vol. 129, No. 3, June, 1982.

22. Whitehouse, Harper J., and Bromley, Keith, "Can Analog Signal Processing Survive the VHSIC Challenge?," Microwave Systems News, April, 1981.

23. Beauchamp, K.G., Walsh Functions and their Applications, Academic Press, 1977.

24. Paley, R.E., "A Remarkable Set of Orthogonal Functions," Proceedings of the London Mathematics Society, Vol. 34, pp. 241-279, 1932.

25. Harmuth, Henning F., Transmission of Information by Orthogonal Functions, Springer-Verlag, 1970.

26. S.J. Campanella and G.S. Robinson, "Digital Sequency Decomposition of Voice Signals," Proceedings of the Symposium on the Application of Walsh Functions, 1970.

27. Lackey, Robert B., "The Wonderful World of Walsh Functions," Proceedings of the Symposium on the Application of Walsh Functions, 1970.

28. G.S. Robinson, Properties of the Walsh and Fourier Spectra of Periodic Functions; The Development of a Unique Walsh-Fourier Spectrum, COMSAT LABS, Internal Memorandum, February 15, 1970, Clarkesburg, MD.

29. McGillem, Clare D., and Cooper, George R., Continuous and Discrete Signal and System Analysis, Holt, Rinehart, and Winston, 1974.

30. Cooper, George R., and McGillem, Clare D., Probalistic Methods of Signal and System Analysis, Holt, Rinehart, and Winston, 1971.

INITIAL DISTRIBUTION LIST

		No. copies
1.	Defense Technical Information Center Cameron Station Alexandra, Virginia 22314	2
2.	Library, Code 0142, Naval Postgraduate School, Monterey, CA 93943	2
3.	Associate Professor L.A. Wilson, Code 62Wi, Department of Electrical Engineering, Naval Postgraduate School, Monterey, CA 93943	1
4.	Professor John Bouldry, Code 73 Department of Electrical Engineering, Naval Postgraduate School, Monterey, CA 93943	1
5.	LCDR Larry W. Ward, USNR Patrol Squadron NINETY-THREE (93) Naval Air Facility Detroit Mt. Clemens, Michigan 48043	1